5-2013

Expression, Production, and Purification of Novel Therapeutic Proteins

Mckinzie Shea Fruchtl
University of Arkansas, Fayetteville

EXPRESSION, PRODUCTION, AND PURIFICATION OF NOVEL THERAPEUTIC PROTEINS

EXPRESSION, PRODUCTION, AND PURIFICATION OF NOVEL THERAPEUTIC PROTEINS

A dissertation submitted in partial fulfillment
of the requirements for the degree of
Doctor of Philosophy in Chemical Engineering

By

McKinzie S. Fruchtl
Hendrix College
Bachelor of Arts in Mathematics, 2008

May 2013
University of Arkansas

ABSTRACT

Interest in the production of recombinant proteins consisting of collagen binding domain (CBD) fused to a bioactive material has increased due to the targeting/attachment capabilities of CBD. For example, CBD fusions can be applied to the reversing of bone density loss and the repair of the eardrum, specifically, by choosing an appropriate fusion partner (parathyroid hormone or epidermal growth factor). The production of CBD fusions was examined using batch and fed-batch culturing of *Escherichia coli* to express the fusion proteins, and affinity chromatography to isolate the final product.

Different medium formulations, feeding strategies, and induction methods were tested in order to develop a production strategy lacking yeast extract or other difficult-to-validate materials. Lactose was also examined as an alternative inducer to IPTG due to its lower cost and toxicity. This induction strategy, in conjunction with alternative feeding methods and the use of a completely defined medium, was able to produce the desired fusion proteins in a comparable manner to IPTG-induced systems. Also, the affinity tag on the N-terminus of the protein and the collagen binding domain on the C-terminus of the protein both retained their activity throughout the fermentation and purification processes.

The second portion of this dissertation examined and utilized two different types of models to mathematically describe the biological system. The first model was able to describe the fermentation system with respect to changes in feed, volume, biomass, and carbohydrate concentrations. This type of modeling examined the entire physical fermentation system on a 'macro' scale. Unlike the second model, it disregarded what occurred on a cellular level.

The second model utilized metabolic flux analysis to track changes in metabolite concentrations and biomass during the expression of the target protein. Upon solving this model, the prediction of the intermediate fluxes proved to be accurate for glucose-fed experiments, as the simulated carbohydrate concentrations match those that were experimentally determined. With the inclusion of the models, the work described in this dissertation provided a link between experimentally observed phenomena and mathematical descriptions of biological systems.

This dissertation is approved for recommendation
to the Graduate Council.

Dissertation Director:

_____
Dr. Robert R. Beitle

Dissertation Committee:

_____
Dr. Edgar Clausen

_____
Dr. Ralph Henry

_____
Dr. Christa Hestekin

_____
Dr. Shannon Servoss

DISSERTATION DUPLICATON RELEASE

I hereby authorize the University of Arkansas Libraries to duplicate this dissertation when needed for research and/or scholarship.

Agreed _____
McKinzie S. Fruchtl

Refused _____
McKinzie S. Fruchtl

ACKNOWLEDGEMENTS

First and foremost, I would like to thank my advisor. Dr. Beitle is one of the most positive people I know. There were some experiments that I thought were complete failures, but he always managed to pull out the positive aspects. I don't know where I would be today if it weren't for him (and a happenstance meeting between his wife and my mother at a grocery store - so thanks to them too!). In all honesty, I couldn't have asked for a better mentor and friend in the research field and I can't fully express how grateful I am that I got the opportunity to work with him. I am one of the lucky ones!

I would also like to thank my committee members for their contributions to my work. Through the various update meetings, they were able to help troubleshoot portions of my work when I needed help and keep me on track.

Lastly, I thank my family and friends. It was a long five years and a rough road at times. They remained supportive and managed to see the light in every situation. I'm sure they got tired me ranting about lab issues and talking about mathematical modeling, but they smiled and nodded when I needed it most. They encouraged me to keep going and hang in there. I share my success with them.

TABLE OF CONTENTS

List of Figures

List of Tables

1. Overview

A novel therapeutic fusion protein has been shown to increase bone density and decrease hair loss. The fusion protein consists of parathyroid hormone (PTH) bound to collagen-binding domain (CBD). In this case, collagen-binding domain serves as a vehicle for attachment to tissues, while also increasing the half-life of the parathyroid hormone. In preparation for scale-up procedures, production and expression of this protein were investigated. Induction studies were carried out to find the conditions allowing for the greatest amount of recombinant protein expression.

To ease the purification process, a glutathione-S-transferase (GST) tail has been placed on the N-terminus of the PTH-CBD protein complex. Affinity chromatography was used to separate the target protein from the pool of bacterial proteins. After production and purification of GST-PTH-CBD, dynamic modeling was utilized to model the cultivation process and metabolic flux analysis was used to model the changes in metabolite concentrations during the expression of the target protein. Additionally, the model contains information about the effect of the inducer on the fermentation system as a whole.

2. Background

2.1 Bioprocessing and fermentation

Bioprocessing refers to the production of a commercially useful biomaterial from a biological process. In the context of this dissertation, it refers to the production of proteins via the fermentation process of a genetically engineered microbial strain. The proteins of particular interest have therapeutic applications and can be used in the biopharmaceutical industry. Because the success of any biopharmaceutical product depends on the ability to engineer large-

scale manufacturing protocols, there is a desire to increase production of these therapeutic proteins using bioprocessing methods (Tripathi et al., 2009).

For this work, fermentation refers to the breakdown of glucose under aerobic conditions by *Escherichia coli* to produce a variety of substrates. Of particular interest is the production of proteins. The goal of recombinant fermentation processes is to engineer cost effective production of target proteins by increasing yield in the smallest amount of materials and/or time (Tripathi et al., 2009). This is achieved by using a stable and highly productive fermentation process followed by cost effective recovery and purification of the product (Tripathi et al., 2009).

E.coli is perhaps the most widely used bacteria for the production of recombinant proteins (Babaeipour et al., 2008; Choi et al., 2006; Lee, 1996; Shiloach and Fass, 2005). Because of its simple structure, the vast information available on this species, and its inexpensive production methods, it is the microorganism of choice for the production of recombinant proteins (Choi et al., 2006; Kayser et al., 2005; Lee, 1996; Tripathi et al., 2009). *E. coli* is primarily used for cloning, genetic modification, and small-scale production specifically for research purposes (Ferrer-Miralles et al., 2009). However, the production of recombinant proteins in *E. coli* is most important because of its application in the pharmaceutical industry (Meadows et al., 2010). Demand for these products has increased because of their functionality in the therapeutic and diagnostic fields (Tripathi et al., 2009). Recombinant protein production from genetically modified organisms is also the largest sector of pharmaceutical biotechnology (Behme, 2009).

2.2 Media

The type of medium plays a very important role in the fermentation process, as some common medium components can inhibit growth if their concentration becomes too high. As reported by Lee et al., glucose concentrations at about 50 g/L can inhibit *E. coli* growth. Similarly, ammonia levels above 3 g/L, iron levels exceeding 1.15 g/L, zinc levels above 0.038 g/L, magnesium levels above 8.7 g/L and phosphorous levels greater than 10 g/L can all inhibit cellular growth (Lee, 1996; Shiloach and Fass, 2005). These numbers are important to consider when designing growth media because the optimal medium would use concentrations of nutrients that remain above the growth-limiting level (concentrations too low) and below the toxic level (concentrations too high), while not leading to wasteful expenditure (Faulkner et al., 2006).

There are three different types of media: defined, semi-defined, and complex. Defined media are used most often to achieve high cell densities (Lee, 1996). This is because each component is clearly defined and the concentration of these components can be tightly controlled throughout the culture process. Defined media are comprised mostly of different types of salts and some type of trace element solution (provides iron, zinc, copper, and other cofactors that cells need). Complex media, on the other hand, contain extremely nutrient rich components and the exact composition may be unknown. Examples of complex media are Luria-Burtani (LB) broth, peptone-based media, and media that may contain yeast extract and tryptone. The exact chemical make-up of these can vary from lot-to-lot, making scale-up and reproducibility more difficult than that of a fermentation protocol utilizing defined medium.

When growth or protein expression does not occur on a clearly defined medium, a combination of the two can be used. Semi-defined media may be used to increase product formation or decrease acetate production (Eiteman and Altman, 2006; Lee, 1996). For high cell density cultivations, it is important to use a medium that allows for higher growth rates while avoiding by-production formation (such as acetate). Though acetate formation is largely dependent on the strain of bacteria, it has been reported that acetate forms when the specific growth rate (dilution rate) exceeds 0.2 hr^{-1} and 0.35 hr^{-1} for growth on complex media and defined media, respectively (Han et al., 1992; Lee, 1996; Tripathi et al., 2009). These numbers are important to considering when designing a fermentation scheme. For batch cultivations, higher growth rates will decrease the ability for the media to sustain growth for longer periods of time. Acetate will also accumulate faster. Through the use of fed-batch fermentation, as discussed below, the culture can be maintained for a greater amount of time at a faster growth rate (Longobardi, 1994).

2.3 Fed-batch fermentation

In order to achieve high cell density cultures of *E. coli*, which result in high yields and productivity of recombinant proteins, fed-batch fermentation must be utilized. According to Tripathi et al., high cell density fermentation "is a major bio-process engineering consideration for enhancing the overall yield of recombinant proteins in *E. coli*" (Tripathi et al., 2009). Fed-batch processes are utilized to achieve higher cell concentrations while minimizing problems that can arise from high cell density cultivations, such as substrate or product inhibition, nutrient inhibition, or dissolved oxygen limitations in aerobic conditions (Ting et al., 2008). Fed-batch fermentation also provides an increase in productivity, which drives a decrease in manufacturing

cost (Longobardi, 1994). Without fed-batch fermentation, cell densities of *E. coli* may approach 15 g/l dry cell weight (DCW) on defined media, provided the nutrient concentrations remain below their inhibitory concentrations (Shiloach and Fass, 2005). In contrast, dry cell weights can approach over ten times this amount through the utilization of a feeding method during cultivation.

Fed-batch processing also permits control of the feed rate of glucose into the cultivation, which results in greater control on the growth rate of the culture (Ting et al., 2008). This helps control biomass accumulation at growth rates which do not cause the formation of acetic acid, a byproduct capable of inhibiting cell growth at concentrations as low as 2 g/l, depending on the strain (Shiloach and Fass, 2005). When acetate exceeds 5 g/l there is a definite negative impact on growth and most groups report on witnessing inhibition of growth when acetate reaches concentrations between 5 and 10 g/l (Tripathi et al., 2009; Yee and Blanch, 1993).

Different fed-batch feeding strategies also allow for different growth rates. The objective is to optimize the feeding strategy so that there is a balance between high growth rates and limiting factors that can arise as a result of these high growth rates. The control of the growth rate is important in fed-batch fermentation because it effects byproduct formation, cell productivity, and plasmid stability (Faulkner et al., 2006). Hence, the optimal feeding strategy would feed nutrient in at the same rate that the organism consumes the substrate (Kleman et al., 1991). Other considerations include the dosing of ammonia. It supplies nitrogen to the system while also maintaining the desired pH. In short, fed-batch processing allows one to monitor and adjust concentrations so that they remain supportive instead of inhibitory. A simple fed-batch fermentation schematic is shown in Figure 2-1. The system utilizes a simple stirred-tank reactor.

Volume accumulates due to the feeding of substrate during the fed-batch phase of the fermentation.

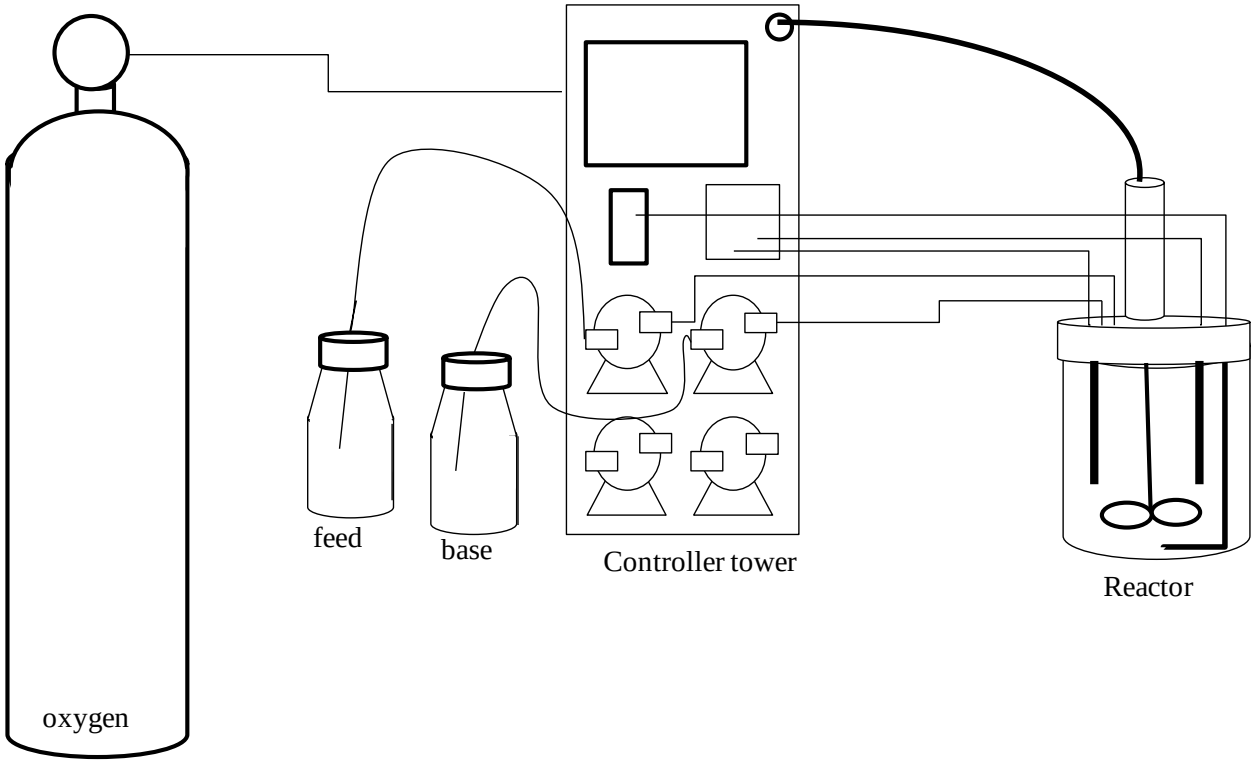

Figure 2-1. **Schematic of fed-batch fermentation set-up.** Based on signals from probes, the controller tower controls the flow of oxygen and base into the reactor. It also controls the flow of feed into the reactor using Applikon BioXpert software.

There are a few drawbacks of utilizing a fed-batch fermentation system. Due to the high number of cells that are in the reactor during fed-batch cultivation, the availability of dissolved oxygen can become an issue (Tripathi et al., 2009). At a certain point during fermentation, air alone may not contribute enough oxygen to the reactor to maintain growth. The solubility of oxygen in medium is low and decreases as the concentration of cells increase (Tripathi et al.,

2009). Pure oxygen would need to be supplied in this case, or the agitation speed would need to be increased.

For large scale fermentation processes, mixing may become an issue and can cause an inhomogeneous cellular environment. For example, cells close to injection ports during feeding will come in contact with a higher concentration of substrate than those farther away (Neubauer et al., 1995). Even though this contact may be higher for a short period of time, this can cause glucose oscillations. These oscillations can affect growth, acetate formation, and product stability. An example of this is discussed in Section 2.3.3.

Plasmid stability is also important to consider when performing fed-batch fermentation experiments. Due to the longer processing times and larger culture volumes, a higher number of generations of cells occur (Tripathi et al., 2009). The ability for the parent cell to propagate plasmids to daughter cells may become instable. This directly impacts the volumetric productivity of the culture. In order to avoid plasmid instability within the context of this dissertation, antibiotic pressure is utilized. However, the stability of antibiotics during the cultivation can decrease. In some cases, it may be necessary to add antibiotics to the culture during the cultivation to maintain the proper antibiotic pressure. If antibiotics are not desired to maintain selection, Zheng et al. (2008) found that adding tryptone may help. They found that cultures that were pulsed with tryptone (in the feed) enhanced the number of plasmid-bearing cells throughout the fermentation experiment. They also found that tryptone enhanced cell division. The disadvantage of this is that tryptone is a complex medium component.

Another important issue to consider is the formation of acetate. *E. coli* secretes approximately 10-30% of its carbon in the form of acetate during aerobic growth (Tripathi et al.,

2009). If cells cannot convert the glucose entering the reactor to a desirable product fast enough, the extra carbon often gets secreted as acetate. Problems that arise from this are described in detail in the next section.

2.3.1 Effect of acetate on the cellular system

Acetate, a harmful byproduct of fermentation, is produced via two pathways under aerobic conditions. When the conversion of the primary carbon source (glucose) to biomass and carbon dioxide is less than its uptake rate acetate excretion occurs (Kleman and Strohl, 1994). Acetate excretion from this build-up of glucose in the media is referred to as overflow metabolism (Akesson et al., 2001). Acetate excretion also occurs when there is a lack of dissolved oxygen in the medium (De Mey et al., 2007). Under this anaerobic condition, the formation of acetic acid is referred to as mixed-acid fermentation (Akesson et al., 2001). As previously stated, acetate can inhibit cell growth at concentrations as low as 2 g/l. High acetate levels can also lower biomass yield, negatively affect the maximum attainable cell density, and decrease the production of recombinant protein (Lee, 1996). Additionally, the build-up of acetate can have detrimental effects on the stability of intracellular proteins and cause the growth medium to acidify (De Mey et al., 2007). If the pH drops too low, cell lysis can occur.

As previously discussed, the rate of production of acetate is strain dependent and acetate production begins at a lower growth rate (0.2 hr^{-1}) when the medium is complex (nutrient-rich) as opposed to that when the medium is defined (0.35 hr^{-1}). To eliminate or reduce the build-up of acetic acid, there are two levels at which researchers have developed strategies: the genetic level and the bioprocess level (De Mey et al., 2007). At the genetic level, multiple research groups have looked at knocking out the genes that can lead to acetic acid excretion or

overexpressing genes that can cause a decrease in acetic acid formation. The strategies are based on the metabolism of *E. coli* and begin with changing the glucose uptake mechanism and the TCA cycle. The pyruvate branch point is also an important area to point out because the pyruvate concentration has an immediate influence on the excretion of acetate, according to De Mey et. al (2007). This branch point is also affected by the aforementioned pathway between glycolysis and the TCA cycle. From pyruvate, the genes directly affecting acetate production are examined for knockout or overexpression. Table 2.1 gives examples of genes that have been knocked out, overexpressed, inhibited, or stimulated and the effects that these actions had on acetic acid formation.

Another interesting approach using genetic modifications to reduce acetic acid concentrations was brought to light by Aristidou et al. (1995). They cloned the gene for acetolactate synthase (from *Bacillus subtilis*) in *E. coli*. This enzyme is capable of catalyzing pyruvate to non-acidic less harmful byproducts (compared to acetic acid). They reported a 220% increase in volumetric protein production and a 35% higher cell density using the acetolactate synthase modified strain.

Table 2-1. Summary of how changes on the genetic level affect acetic acid production. KO refers to knockout; OE refers to overexpression; I refers to inhibition; and Stim refers to stimulation. Table adapted from De Mey et al. (2007).

Pathway	Gene	Protein	Action	Result
Phospho-transferase pathway	ptsG	Glucose Specific Enzyme II	KO	Glucose uptake reduced; no acetate excretion
	arcA	Regulator of ptsG	KO	2x increase in ptsG
			OE	Glucose uptake decrease; decrease in acetate
Pyruvate branch point	pykF	Pyruvate kinase	KO	Glycolysis down regulated; decrease in acetate
	pykA pykF	Pyruvate kinase	KO	Major decrease in growth rate and acetate
	pdh	Pyruvate dehydrogenase	I	Decrease in growth rate; no acetate production
	ppc	Phosphoenolpyruvate (PEP) carboxylase	OE	Elimination of acetate production; growth is maintained; decrease in glucose consumption rate
			KO	Decrease is growth rate; undesirable metabolite production increases
	pck	PEP carboxykinase	KO	No acetate production from growth on high glucose concentrations
			OE	Slight raise in acetate production
	ppc pck	PEP carboxylase and PEP carboyxkinase	OE	Less growth; higher concentration of fermentative products
	pta	phosphotransacetylase	KO	Reduction in acetate; growth rate suffers; increase in lactate and formate
	ackA	Acetate kinase	KO	
	acs	Acetyl-CoA Synthetase	KO	No precise conclusion
			OE	Reduction in acetate; increase assimilation of acetate when sole carbon source
	poxB	Pyruvate oxidase	KO	Decrease in carbon to biomass; carbon needed for energy increased
	gltA	Citrate synthase	OE	Decrease in acetate; increase in formate and pyruvate
	aceA	Isocitrate lyase	Stim	Decrease in acetate by 13%
	icd	Isocitrate dehydrogenase	KO	Increase in citrate; not rate limiting step in Krebs cycle

Manipulation to reduce acetate at the bioprocess level mainly deals with media formulation and/or cultivation techniques. Many groups have reported on adding yeast extract to the media in order to reduce acetate accumulation during fermentation (Eiteman and Altman, 2006; Han et al., 1992; Tripathi et al., 2009). Yeast extract acts an alternative food source (nitrogen rich), so it slows the uptake rate of glucose, which decreases acetic acid formation. Panda et al. found that through the use of yeast extract, glucose uptake rate was lowered, but growth was not affected. It also helped maximize the volumetric productivity of the fermentation and produced less acetic acid (Panda et al., 2000). Reportedly, yeast extract also helps *E. coli* utilize acetate acid during carbon limitation (Tripathi et al., 2009). However, the addition of yeast extract would push the medium to a semi-defined medium, which is not desirable for the work in this dissertation. de Maré et al. (2005) examined the use of shifting temperatures in correspondence with oxygen changes to monitor the production of acetic acid. Decreasing the temperature helped control the oxygen consumption rate which in turn resulted in lower acetic acid concentrations. This may be due to slower glucose uptake and slower growth, but the group reported a 20% increase in cell mass using this technique.

To physically remove acetate from the culture broth, some groups have looked at utilizing dialysis-fermenters or macroporous ion-exchange resins (De Mey et al., 2007; Wong et al., 2009; Xue et al., 2010). These methods are successful at removing acetate, but sometimes essential nutrients are also removed. Additionally, these methods do not deal with the fact that acetate is still produced, thereby reducing the yield based on carbon utilization.

Another method that some research groups have employed makes use of the fact that acetate can provide both carbon and energy to the cells (Xue et al., 2010). In the presence of low

glucose concentrations, acetate is consumed and a diauxic growth pattern is observed (Xu et al., 2008). Namdev et al. showed that the "saw-tooth" pattern of dissolved oxygen percentage during fermentation correlated to the diauxic behavior of growth on acetate and glucose (Namdev et al., 1993). During growth on glucose, dissolved oxygen percentage was low, as demand was high. During the transition from growth on glucose, dissolved oxygen concentrations increased, as demand was low. Faulkner et al. made use of this phenomenon by starving the cultures at two different times during fermentation (Faulkner et al., 2006). This starvation caused acetic acid concentrations to decrease ten-fold.

In all of these cases, carbon is still being utilized to produce an unwanted byproduct. Other bioprocess methods that deal directly with preventing acetate excretion utilize various feed techniques based on mathematical predictions of nutrient demands to push carbon usage in the direction of desired product (De Mey et al., 2007).

With all of this in mind, the ideal fermentation system for the work in this dissertation would be one that utilizes a defined medium and one in which the feed rate is equivalent to the rate that biomass is produced from the feed source. One way of preventing acetate accumulation is to ensure that the specific growth rate of the culture does not exceed that at which acetate formation begins (Kim et al., 2004). Additionally, maintaining a low concentration of glucose in the media will help keep the acetate levels under the inhibitory concentration and cause recycle of acetate by its consumption.

2.3.2 Feed type

Most of the information above implies that glucose may be the only feed source for fed-batch fermentation processes. This is not the case. Though glucose is perhaps the most preferred feed source due to its ability to sustain such high growth rates in *E. coli*, many other groups report using glycerol as a feed source. For example, Korz et al. (1995) was able to achieve a cell density of 150 g/l utilizing glycerol as a feed source. One major draw to glycerol is that acetate is not produced in high quantities when glycerol is used as the feed source (Lee, 1996). Using glycerol as a source of carbon results in little to no flux to acetate secretion because glycerol uptake is much slower than glucose (Holms, 1986; Korz et al., 1995). This leads to reduction of the carbon flux to acetic acid (Lee, 1996). Kwon et al. (1996) utilized glycerol feed to aid in protein stabilization. They also found that glycerol-fed cultures produced 66% less acetate than those fed with glucose. It is important to note that they added peptone and casein acid hydrolysate to their media, so it was not completely defined. As previously reported, rich media components have an effect on acetic acid production (Section 2.3.1).

One major drawback is that glycerol is more expensive than glucose, but glycerol plays an important role in fed-batch fermentation when auto-induction techniques are desired because of the lift of catabolite repression. Lactose and glycerol can be taken up simultaneously. This idea is discussed in Section 2.4. Lastly, inhibition of growth can occur when the glycerol concentration exceeds 87 g/l (Dubach and Markl, 1992).

2.3.3 Strategies for the control of feeding

There are different types or methods of fed-batch fermentation. Each type relies on a different batch characteristic to indicate when the supplementation should begin. Using a direct feedback approach, the carbon source is monitored (Shiloach and Fass, 2005). Specific adjustments are made during the fermentation process depending on the carbon source concentrations to keep the carbon (glucose) concentrations as minimal as possible. This results in the inhibition of acetate accumulation.

On the other hand, an indirect feedback control system adjusts feeding through the online monitoring of dissolved oxygen, pH, or other parameters (Lee, 1996; Shiloach and Fass, 2005). pH-stat controlled fermentations start feeding after a spike in pH is witnessed by the controller. After the primary carbon source is depleted, the pH rises because of the excretion of ammonium ions (Kim et al., 2004). This phenomenon is shown in Figure 2-2. In this case, as the pH rises or falls, the feed rate changes. One advantage that this method has over an exponential feeding method is that direct feedback is not required to inhibit the accumulation of feeding substrate into the system. A decline in pH indicates that accumulation of substrate is occurring, as excess acetate is produced. This triggers the feed pump to stop pulsing substrate into the reactor. As previously mentioned, an increase in pH indicates that additional substrate should be fed into the reactor because the deamination of amino acids is occurring (to serve as energy source for the cell).

Kim et al. (2004) developed a feeding strategy that utilized the best characteristics of pH-stat and exponential feeding. Exponential feeding was carried out at growth rates of 0.1 and 0.3 hr^{-1} and after a pH change was observed (decrease in pH) or when glucose exceeded 20 g/L,

feeding was stopped. When pH began to climb, the group resumed feeding. They were able to achieve cell concentrations ranging from 63.5 g/l to 101 g/l while maintaining lower acetate concentrations as to compared to only pH-stat fermentations.

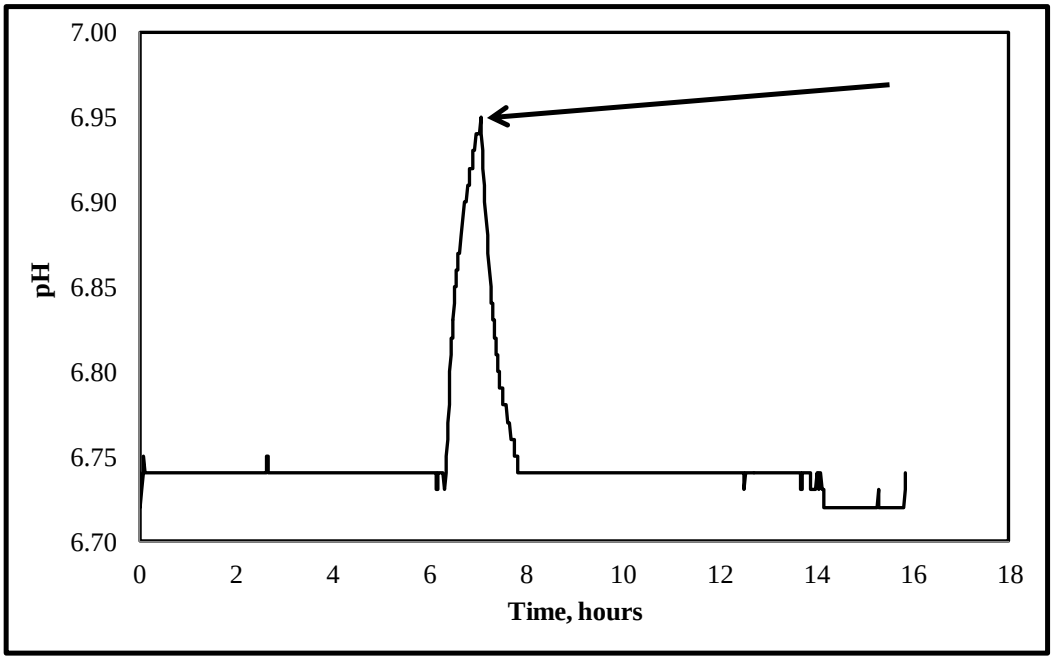

Figure 2-2. Example of pH profile during fed-batch fermentation. As indicated by the arrow, the spike in pH occurs because glucose was depleted from the reactor (at approximately 6.5 hours). At 7 hours feeding begins and the pH starts to decrease.

Similarly, a sharp spike in dissolved oxygen indicates that feeding should start in a DO-stat controlled fermentation. This is based on the principle that as substrates become limiting in cell cultures, growth slows. As a result, cellular respiratory activity slows and a spike in dissolved oxygen is witnessed (Chen et al., 1997). Figure 2-3 shows an example of a dissolved oxygen profile during a fed-batch fermentation.

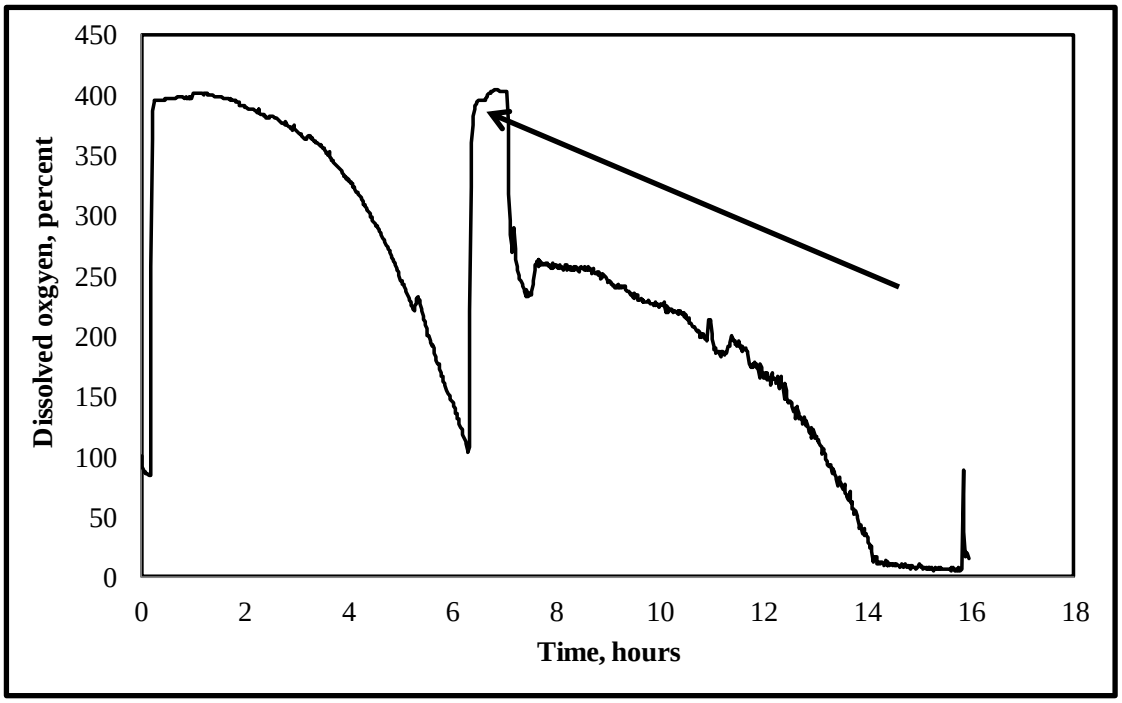

Figure 2-3. Dissolved oxygen profile during fed-batch fermentation. The spike at approximately six hours indicates that substrate has been depleted from the reactor (indicated by the arrow). After feed commences at 7 hours, the dissolved oxygen concentration decreases as growth begins to increase.

Chen et al. (1997) coupled pH and DO-stat controlled fermentations in an attempt to optimize cell growth. Using fermentation software, Chen et al. set up a system that triggered a feed pump every time the dissolved oxygen or pH rose above their desired set points. Similarly, the pump was deactivated when both the dissolved oxygen and pH dropped below the set points. They witnessed a 4-fold increase in cell concentration and improved plasmid yields 10-fold using this method.

The last classification of feed types contains methods in which feedback is not involved (non-feedback control). This group includes constant or pulsed feeding, increased feeding, or exponential feeding (Lee, 1996). These methods are simple in comparison to pH-stat or DO-stat.

pH-stat relies on detecting a tenth of a pH unit change and there can be a probe drift issue. Similarly, for DO-stat, the probe can drift with time and cause minor fluctuations to go unnoticed. In constant feeding, a predetermined amount of substrate is added at a constant rate to the system. This method does not require any feedback from the reactor or take into account any characteristics of the growth environment. Because the growth demands will eventually overcome the amount of substrate fed, the specific growth rate decreases during cultivation.

Pulsed feeding involves adding an amount of substrate into the reactor. After this period, substrate addition is paused and may resume at a later time. The down side of pulsed feeding is that it can cause glucose oscillations. Lin and Neubauer (2000) found that while these oscillations inhibit overgrowth of plasmid-free cells, they negatively affect product yield and stability. These glucose oscillations can also be present in types of fed-batch fermentation. If the uptake of glucose exceeds the local mass transfer of glucose, cells may be starved for a short period of time (Neubauer et al., 1995). As discussed previously, this is especially important when scaling-up processes because mixing may become an issue.

In increased feeding, a step-wise feeding strategy may be employed. This helps compensate for the decrease in specific growth rate, as witnessed in a constant feeding strategy. Lastly, a constant specific growth rate can be targeted using an exponential feeding strategy (Lee, 1996). An exponential fed-batch fermentation method commonly used to pre-determine the amount of glucose that should be fed into the reactor to achieve a certain growth rate was proposed by Korz et al. and Lee et al. (Korz et al., 1995; Lee, 1996):

$$M_s(t) = F(t)S_F(t) = \left(\frac{\mu}{Y_{X/S}} + m\right)X(t)V(t) = \left(\frac{\mu}{Y_{X/S}} + m\right)X(t_F)V(t_F)\, exp^{\mu(t-t_F)} \quad (2.1)$$

where M_s is the mass flow rate (g/h) of the substrate, F is the feeding rate (l/h), S_F is the concentration of the substrate in the feed (g/l), μ is the specific growth rate (1/h), $Y_{X/S}$ represents the biomass on substrate yield coefficient (g/g), m is the maintenance coefficient (g/g h), and X and V represent the biomass concentration (g/l) and cultivation volume (l), respectively. The yield coefficient for *E. coli* on glucose is generally taken to be 0.5 g/g. The maintenance coefficient is often 0.025 g/g h (Korz et al., 1995). This equation has been widely adapted for fed-batch fermentation processes, as exponential feeding allows cells to grow at a constant rate (Kim et al., 2004).

For most fermentation experiments, the feeding strategy does not change after induction of the protein. However, Wong et al. (1998) report on the effect of post-induction feeding strategies. This group tested pH-stat, constant, exponential, and linearly increasing the feed after induction occurred. They found that after induction, the dry cell weight was not a function of the feeding strategy. Before induction, the dry cell weights did depend on the strategy employed to add nutrients to the system. However, the amount of protein varied depending on the strategy used after induction. This may be important to consider if production levels or growth begin to significantly decline after induction.

2.4 Expression and production

To increase production of recombinant proteins it is important to maximize the number of cells that can properly express the protein (Aucoin et al., 2006). This maximum production can be inhibited by strong promoters because of the increased metabolic burden placed on the cell. The resulting protein production can inhibit cell growth or cause cell degradation. Therefore, it is important to separate the growth phase and the protein production phase (Aucoin et al., 2006).

For the control of the synthesis of the target protein, the DNA for the inducible promoter is placed 5' to the target protein's genetic code (Aucoin et al., 2006). Thus, when the promoter is induced, the production of the target protein is also triggered by the physical change in the cell's environment. Hence, a distinct production period occurs that can be tracked separately from a growth period.

The solution to this problem is to use a promoter that can be induced by a chemical or temperature change. Inducing the promoter activates the production of the desired protein. This decreases the likelihood of proteases degrading the target protein during cell growth (or in the case of toxic proteins, inhibiting further growth). Examples of common chemical inducers include isopropyl-β-D-thiogalactopyranoside (IPTG), lactose, and arabinose. Some promoters are thermally inducible, meaning that a drop or increase to a particular temperature will activate the promoter, and hence activate the production of the target protein. For example, 30°C may be used for a pre-induction growth temperature and the temperature may be shifted to 36 to 42° for protein expression (Harder et al., 1993).

2.4.1 *Lac* operon

The *lac* operon is used to control therapeutic protein synthesis in the context of the work for this dissertation. It is typically induced with IPTG, but because of its high cost and toxicity to humans, IPTG is not desired for large scale production (Gombert and Kilikian, 1998; Menzella et al., 2003; Neubauer et al., 1992). As an alternative, induction with lactose can cause recombinant protein expression. A promoter that can be activated by IPTG will also be activated in the presence of lactose, but lactose can be metabolized by cells whereas IPTG cannot. Thus,

after induction with IPTG, the concentration of the inducer remains constant whereas the lactose concentration may change if it is used as an inducer.

Three structural genes make up the *lac* operon: *lacZ*, *lacY*, and *lacA* (Santillan and Mackey, 2008). They are responsible for the production of β-galactosidase, lac permease, and a transacetylase, respectively. The cleavage of lactose to yield glucose and galactose is performed by β-galactosidase. Lac permease is a transmembrane protein that is responsible for the uptake of lactose by the cells. Transacetylase transfers an acetyl group (from coenzyme A) to a hydroxyl group on galactose. Additionally, β-galactosidase and lac permease both play an active role in the regulation of the *lac* operon, as described below.

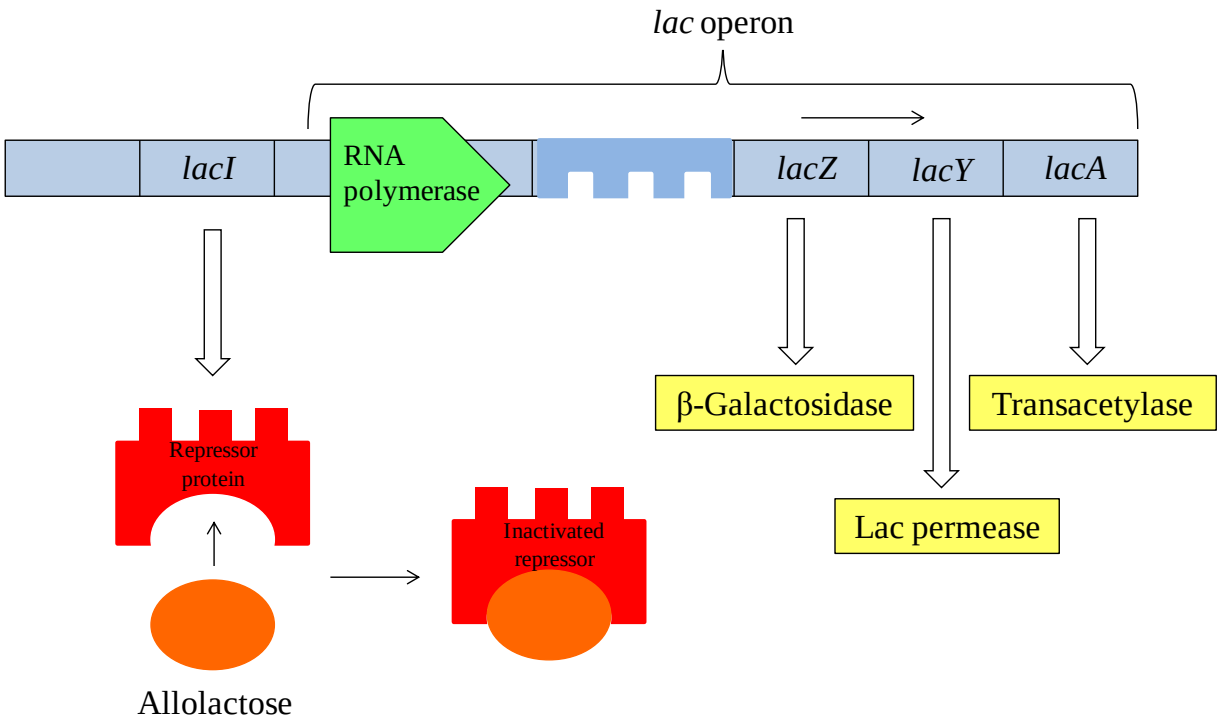

Figure 2-4. Cartoon of *lac* operon showing genes and protein products with repressor molecules. The yellow indicates protein products and the red represents repressor molecules. Adapted from http://www.blc.arizona.edu/Marty/411/Lectures/Figures/Lac_Operon_rep.GIF.

Repression of the *lac* operon is controlled by lacI (Santillan and Mackey, 2008). Under a different operon, *lacI* codes for the *lac* repressor. The repressor inhibits the transcription of *lac* operon genes by binding an operator. This repressor is inactivated when it is bound to allolactose (a byproduct of lactose metabolism). A positive feedback loop exists in this system (Santillan and Mackey, 2008; Santillan and Mackey, 2008; Santillan, 2008; Santillan, 2008; van Hoek, M. J. A. and Hogeweg, 2006; van Hoek, M. J. A. and Hogeweg, 2007). This loop gives rise to bistability of the *lac* operon. Bistability occurs when there are two stable equilibria for the operon that exist for certain inducer concentrations: induced and repressed (van Hoek, M. J. A. and Hogeweg, 2007). As lac permease and β-galactosidase are produced, there is an increase in the rate of lactose uptake. This in turn causes an increase in lactose metabolism which increases the concentration of allolactose. Since allolactose decreases the activity of the repressor, there is an increase in *lac* operon activity. This results in an increase in production of lac permease, β-galactosidase, and transacetylase. A schematic of the *lac* operon with its repressor molecules and protein products is given in Figure 2-4.

The *lac* operon can be downregulated by glucose. The concentration of extracellular glucose effects the production of an activator that upregulates gene expression by increasing the affinity of mRNA polymerase to the lac promoter. As the concentration of extracellular glucose increases, the intracellular production of cyclic adenosine monophosphate (cAMP) decreases. cAMP binds to a receptor (cAMP receptor protein) to form the CAP complex. This complex binds DNA upstream from the lac promoter and increases the affinity of mRNA polymerase to the lac promoter. Thus, a decrease in cAMP leads to a decrease in the CAP complex, which causes a decrease in affinity of mRNA to the lac promoter. This phenomenon is known as

catabolite repression. In a separate mechanism, external glucose also decreases the efficiency of lac permease to transport lactose into the cell (Santillan and Mackey, 2008).

2.4.2 Simple induction strategies

For simple batch cultures, the chemical inducer is typically added at the mid-exponential growth phase of the culture. At this point, there are many cells in the culture to be induced, but there is still opportunity for growth of new cells. Though, induction towards the end of the log phase or during the stationary phase can affect product solubility and influence expression levels (Berrow et al., 2006). For fed-batch experiments, the induction technique varies. Since overall yield of the product depends on the overall biomass concentration and the product yielded from each cell, high cell density cultivations coupled with satisfactory induction techniques should be developed to increase overall yield (Gombert and Kilikian, 1998). In order to balance cell growth and maintain specific cellular protein yield, the induction strategy should take the following into account: level of gene expression, toxicity of product (either concentration of product or the product itself), localization of the induced product, and the degradation characteristics of the product (Tripathi et al., 2009).

There are multiple methods used to induce high cell density cultures. Some of these are as simple as inducing at a particular optical density (similar to shake flask or batch cultivations). Others may involve pulsing the inducer into the system at different times or adding multiple types of inducer. An examination of specific methods follows.

Examples of simple induction methods are briefly summarized. Fan et al. (2005) induced a high cell density culture when the OD_{600} reached 95 units by increasing the temperature by ten degrees. After two hours, the temperature was decreased by three degrees. Similarly, Shin et al.

(1997) induced fed-batch cultivations with IPTG when the cell concentration reached 70 to 80 g/L. Kweon et al. (2001) induced a fed-batch culture with IPTG when the cell mass had reached its highest and ended the fermentation experiment three hours later. This group also tested protein production using different ratios of lactose and IPTG as inducers. They found that lactose alone only produced 55% of protein that IPTG produced and increasing the ratio of IPTG to lactose caused protein expression to increase. Another relatively simple, but unique idea was set forth by Sandén et al. (2003). They induced fed-batch cultures at certain growth rates to examine the effect the growth rate had on the culture. They used IPTG to induce cultures when $\mu = 0.5\ h^{-1}$ (during exponential feeding) or when $\mu = 0.1\ h^{-1}$ (after they switched to constant feeding). The group found that experiments with higher feed rates gave a higher production of target protein.

Similar to this work, Ramchuran et al. (2005) was interested in examining lactose induction versus IPTG induction and their effects on recombinant protein production. They induced all cultures at the same given cell mass concentration, but varied the length of the induction period depending on the inducer used (3 hours for IPTG, 6 hours for lactose). They determined that lactose was a viable choice for prolonging the production phase as compared to IPTG.

After a thorough examination of studies performed on lactose induction, it is apparent that the optimal timing of induction is dependent on the desired product. Neubauer et al. (1992) found that the yield of recombinant protein increased if lactose was added when the glucose concentration was low. This group found that "lactose, when added during the transition from the exponential to the stationary phase, can induce overexpression" of recombinant protein.

Interestingly, waiting an hour after this transition to induce cultures caused a decrease in their target protein expression (Donovan et al., 1996; Neubauer et al., 1992). These experiments showed that induction with lactose when glucose is nearly depleted is optimal for their target protein expression. It is important to keep in mind that they did not examine induction with lactose in a fed-batch fermentation scenario.

On the fed-batch scale, Gombert and Kilikian (1998) induced cultures with lactose 20 minutes prior to the end of the fed-batch fermentation stage. Inducing cultures this way allowed induction to start when growth rates were still high. This group also pulsed lactose into the system three different times after the conclusion of the fed-batch phase. In order to test Neubauer's hypothesis about induction timing, for some experiments, the first lactose pulse was added when glucose was depleted. For others, lactose was added 20 minutes prior to glucose exhaustion. After comparing these two methods, a higher target protein concentration was achieved when lactose was added prior to glucose exhaustion. They also found that residual lactose concentrations played an important role in the decrease in yield of target protein as increasing the amount of lactose pulsed into the fermenter (to 5.7 g/g DCW as opposed 4.3 g/g DCW) caused a decrease in product concentration. In experiments where they added 1.2 to 2.3 g lactose/g cell, they stated that the lactose concentration wasn't high enough to cause protein expression. Throughout their experiments, growth did not appear to be affected by the switch from the fed-batch phase to the induction phase, but they also pulsed yeast extract into the system in the runs that were most successful at producing recombinant protein.

Menzella et al. (2003) also examined using lactose as an inducer for fed-batch fermentation experiments. This group induced cells after the OD_{590} reached 120 units. They

used a pre-determined feed rate based on the substrate balance equation previously discussed to reach that particular OD. To induce the culture, a 35% lactose solution was fed into the reactor using a DO-stat method to avoid acetate accumulation. This method is very similar to that of Gombert and Kilikian (1998). The Gombert group pulsed lactose into the system when they noticed a sharp rise is dissolved oxygen. The DO-stat method of feeding lactose into the reactor essentially feeds after the oxygen levels rise above a certain level. However, Menzella et al. (2003) followed the feeding lactose with the feeding of a 35% glucose solution into the system. They found that increasing the lactose concentration above 0.8 mM did not increase the amount of protein produced. The fastest rate of lactose feeding corresponded to the highest volumetric yield of target protein. From this, they concluded that the lactose was used both as a carbon source and inducer very efficiently.

Hoffman et al. (1995) used a feeding medium to induce cultures with lactose on defined media. In their experiments, the feeding solution contained 600 g/l glucose as a carbon substrate supplemented with 50 g/l lactose for induction. Using this technique of inducing, they found that the growth rate slowed, but that it was still higher than what they found for cultures grown on complex media and induced with IPTG or lactose (as batch addition). The induction period lasted for 5-12 hours and resulted in a 12-fold increase in volumetric productivity as compared to the results they achieved for batch cultures.

2.4.3 Auto-induction

Another induction technique is referred to as auto-induction. According to Xu et al. (2012), auto-induction is defined as "automatic induction of recombinant protein expression by inducing compounds such as lactose already present in either complex or chemically defined media at the beginning of cultivation." When the preferred carbon sources are exhausted, auto-induction can occur. This is based on diauxic growth of cells on lactose after the preferred carbon sources are gone. Most auto-induction mediums contain mixtures of glucose, glycerol, and lactose (Blommel et al., 2007; Li et al., 2011). After initial consumption of glucose, metabolism shifts to consume lactose and glycerol. Auto-induction techniques allow for the shift from an un-induced state to an induced state to be controlled by the host organism (Blommel et al., 2007). Auto-induction is an option with respect to this dissertation since lactose can be used to induce the *lac* operon. As long as lactose is added to the media prior to the start of cultivation or prior to depletion of the primary substrate (glucose), auto-induction of the culture will occur.

It is important to note that most strategies utilizing auto-induction require the use of yeast extract or other undefined components. Studier (2005) published his findings on auto-induction in 2005. In his paper, Studier reports on significant concentrations of target protein expressed without the required inducer when cultures were grown using certain complex media. He developed a strategy for auto-inducing shake flasks using media that contains a soluble enzymatic digest of casein, yeast extract, and a variety of salts, minerals, and amino acids. Since then, Studier's media recipe has been commercialized by EMD Biosciences as the "Overnight Express Autoinduction System" (Grabski et al., 2005). This system contains three different types of media for auto-induction of cultures, two of which are complex. The remaining type is

defined, but it is recommended for Se-Met labeling of proteins for further use with x-ray crystallography studies, not necessarily for enhancing the production of protein without adding an inducer (Grabski et al., 2005).

Auto-induction of shake flasks is a fairly straightforward procedure, as all medium components and inducer are present at the start of cultivation. For auto-induction of fed-batch fermentation experiments, the feeding of glucose can interfere with this induction technique. In most fed-batch fermentation experiments, the feeding of glucose into the reactor begins as the glucose in the media initially is consumed. This would not allow for the consumption of lactose to occur, so perhaps induction will not take place. Also, as previously discussed, the build-up of glucose in the media can inhibit the action of the lac operon, so induction would not occur or it would be significantly haltered. This is where the use of an alternative feed source would come into play. Glycerol can be used to maintain growth. Additionally, *E. coli* does not preferentially consume glycerol over lactose. Thus, the lactose may have a chance at acting as an inducer once the glucose is depleted during the batch phase.

However, a different set of batch-scale experiments by Kim et al. (2007) showed that lactose induction results in an 8-fold increase in protein compared to auto-induction and a 20-fold increase in yield compared to IPTG. Though, auto-induction increased yield 3-fold compared to simple IPTG induction while also decreasing costs. First cells were grown up in media containing glycerol as a carbon source. After depletion of glycerol, primary induction was performed by adding IPTG and lactose to final concentrations of 1 mM IPTG and 0.2% lactose. Six hours later, a portion of this culture was used to inoculate fresh medium containing 2% lactose as a sole carbon source and fermentation continued for 18 hours. Glycerol was used as

the initial carbon source to prevent by-product formation that occurs from glucose metabolism. Lactose was added when glycerol was depleted because they assumed that the cells would more readily take up lactose if no other source of carbon was present and IPTG was used as a pre-inducer to "pre-activate" the cells. They found that this IPTG/lactose primary induction method with growth on lactose for 18 hours after induction increased the yield of protein as compared to growth on auto-induction media or induction with IPTG alone. It is important to note that the media this group used contained casein hydrolysate and yeast extract. These results indicate that a simple auto-induction technique may not be sufficient when inducing high cell density cultivation.

Work by Kotik et al. (2004) suggested that lactose pulsing with auto-induction can increase product formation. The initial media used casein hydrolysate, salts, and lactose. They fed the system exponentially with glycerol and supplemented the feed with one gram of lactose every 2 hours. Volumetric productivity increased 100-fold compared to shake flasks with LB. In their work, they conclude that "intermittent addition of lactose during fed-batch growth was sufficient for a long-lasting and efficient production of [protein]."

2.5 Dynamic modeling and metabolic flux analysis

Mathematical modeling is often used to estimate and predict protein production given a set of changing conditions. This modeling is refered to as dynamic modeling in this dissertation. Dynamic modeling takes into account the concentration of inducer by incorporating equations that represent how concentrations of regulatory molecules change during the induction process. In this case, the bistability of the *lac* operon can be modeled using a set of differential equations that describe the regulation of the operon. The following two equations are representative of those that are utilized for this type of modeling (Chen et al., 1991; Cheng et al., 2001; Kremling et al., 2001; Wong et al., 1997):

$$\frac{d[mRNA_i]}{dt} = \alpha k_i^{synthesis}[G_i] - (k_i^{degradation} + \mu)[mRNA_i] \tag{2.2}$$

$$\frac{d[protein_j]}{dt} = k_j^{synthesis}[mRNA_i] - (k_j^{degradation} + \mu)[protein_j]; i = j \tag{2.3}$$

In these equations, k and μ represent rate constants for synthesis and degradation of proteins and the specific growth rate, respectively. [mRNA], [G], and [protein] represent the concentrations of messenger RNA, gene for repressor protein, and recombinant protein product, respectively. In the first equation, α represents the dosing of IPTG (or lactose), since the production of recombinant protein is IPTG dose dependent. In both equations, the first term represents the increase in formation due to production. The second term represents the decrease in concentration due to degradation and dilution due to growth. As the number of cells increase, the concentration on a per cell basis decreases. Therefore, the growth rate is taken into account. Similar mass balance equations can be written to describe cyclic-AMP, mRNA, enzyme concentrations, and repressor RNA concentration. It is important to include all of these mass balances because each one affects the final concentration of the target protein.

These equations work for batch fermentations and can potentially be used for fed-batch cultivations. However, there is an additional set of equations that describe the growth characteristics and by-product formation for fed-batch fermentation processes. This type of modeling does not provide any information on production formation, but can accurately describe other physical conditions in the fed-batch reactor. As described by many groups the equations below represent the change in feed, volume, cell mass, acetate, and glucose that occur during the fermentation process (Chen et al., 1995; Cockshott and Bogle, 1999; Jenzsch et al., 2006; Levisauskas and Tekoris, 2005; Mohseni et al., 2009; Roeva et al., 2007; Roeve and Tzonkov, 2006; Xu et al., 2008). The groups also report on utilizing Monod kinetics to incorporate the inhibition of growth by certain by-products in the growth rate term.

$$\text{Volume equation: } \frac{dV}{dt} = F(t) \tag{2.4}$$

$$\text{Cell mass equation: } \frac{dX}{dt} = \left(\mu - \frac{F(t)}{V(t)}\right) * X \tag{2.5}$$

$$\text{Acetate equation: } \frac{dA}{dt} = \left(qA_g - qA_c\right) * X - \left(\frac{F(t)}{V(t)}\right) * A \tag{2.6}$$

$$\text{Glucose equation: } \frac{dG}{dt} = \left(\frac{F(t)}{V(t)}\right) * (G_F - G) - qGc * X \tag{2.7}$$

The feed equation that this type of model typically incorporates is the same as the equation given in Section 2.3.3 where feed rate is based on the specific growth, feed composition, and other constants that describe reactor conditions. The change in volume depends on the feeding strategy and since the feed rate changes with time for exponential feeding, the change in volume can be defined by the feed rate. In some cases, if the sample size at a specific time is large, this size can be account for by subtracting it from the feed equation. In

the case of this dissertation, the volumes of the samples taken are negligible with respect to the volume of the broth in the reactor. For constant-volume cultivations, the cell mass equation is usually denoted by μ*X. For fed-batch experiments, dilution occurs due to the addition of substrate. Hence, the cell mass equation for a fed-batch experiment includes a term for dilution due to feeding/volume changes.

For changes in carbohydrate concentrations, the dilution due to volume changes is again taken into account. For determination of acetic acid, the amount re-consumed by the cells is subtracted from the amount generated from the cells. Since these amounts are calculated on a per cell basis, the sum is multiplied by the cell mass. Here, the amount of acetate consumed is represented by the Monod equation and the amount generated follows Tessier-type kinetics since the amount generated depends on the concentration of glucose:

$$qA_c = qA_{cmax} \times \frac{A}{A+K_A} \tag{2.8}$$

$$qA_g = \left(\frac{G}{G+K_A}\right)^{Kx} \tag{2.9}$$

For glucose, the saturation constant, the maximum uptake rate, and information about acetic acid concentrations are used to calculate the amount consumed. Since cells can consume acetic acid, Monod-type noncompetitive inhibition kinetics is used. In the equations above, the amount of consumed glucose is denoted by qGc, with qGc defined as follows:

$$qG_c = \left(\frac{qG_{max}}{1+\frac{A}{K_G}} \times \frac{G}{G+K_G}\right) \times X \tag{2.10}$$

Notice that these equations do not contain any information about inducer concentration or any pathways that are involved in the induction process. For a fermentation process in which the yield of product is constant (with respect to time), these equations may be used. However, since lactose is examined as an inducer for this dissertation, it is desirable to add an equation that describes lactose uptake in the presence of other substrates. In order to do this, the glucose equation is modified and is represented in the following equation:

$$\frac{dL}{dt} = \left(\frac{F(t)}{V(t)}\right) * \left(L_f - L\right) - qLc * X \tag{2.11}$$

The same concept follows for lactose as it did glucose. Lactose uptake can be inhibited by glucose. qLc contains the information for Monod non-competitive inhibition kinetics, along with the maximum uptake rate of lactose:

$$qL_c = \left(\frac{qL_{max}}{1+\frac{G}{K_L}} \times \frac{L}{L+K_L}\right) \times X \tag{2.12}$$

All of the variables with their units and a description are given in Table 2.2.

Table 2-2. Variables, units, and description of variables used for dynamic modeling of a fed-batch fermentation process.

Variable	Units	Description
F(t)	l/hr	Feed rate
V(t)	liter	Volume
X(t)	grams	Cell mass
A(t)	g/l	Acetate concentration
G(t)	g/l	Glucose concentration
L(t)	g/l	Lactose concentration
μ	1/h	Specific growth rate
Gf	g/l	Glucose concentration in feed
X0	grams	Cell mass at time of feed start
V0	liter	Volume at time of feed start
$Y_{c/g}$	g/g	Yield of cells on glucose
qA_g	g/gh	Acetate generated during fermentation
qA_c	g/gh	Acetate reutilized or consumed
qG_c	g/gh	Glucose consumption rate
Lf	g/l	Lactose added
qL_c	g/gh	Lactose consumption rate
qA_{cmax}	g/gh	Maximum uptake of acetate
qG_{cmax}	g/gh	Maximum uptake of glucose
qL_{cmax}	g/gh	Maximum uptake of lactose
K_G	g/l	Saturation constant for glucose
K_L	g/l	Saturation constant for lactose
K_A	g/l	Saturation constant for acetate
K_X	--	Exponent fit to data for generation of acetate from glucose

It is also important to note the need for a maintenance coefficient. In most cases, the set-point for the growth rate in the feed profile is not the growth rate that the culture achieves. This can cause major discrepancies between the experimental observations and the simulated data. Typically, after modeling the feed profile, volume, and cell mass, one can determine when and if a maintenance coefficient will be needed (depending on the simulation of cell mass compared to data obtained from the fermentation experiments).

While dynamic modeling examines the fed-batch system on the macro-scale, one method commonly used to optimize *E. coli* production on the micro-scale is metabolic flux analysis (MFA). Metabolic flux analysis allows for the assessment and prediction of metabolite concentrations and rates of reactions during the cellular metabolism process using a constraints-based approach. Knowledge is gained about how metabolic fluxes are utilized by cells and how cells optimize their growth rates by tracking the movement of carbon throughout the system (Varma and Palsson, 1994a). As previously discussed, in order to produce high concentrations of bacterial cells, fermentation processes are utilized. For bacterial fermentations, the products are typically the cells themselves, but they can also be metabolites that the cells produce during the fermentation process. In order to tightly control this process, the medium that the cells are grown is monitored and controlled. Glucose and other carbon sources can be added for nutritional purposes. Additionally, since *E. coli* grows aerobically, the rate of oxygen into the fermentation tank is controlled.

MFA utilizes mass and energy balance principles (Meadows et al., 2010). A substance that is put into the system must leave the system in some form or another. The rate at which this occurs is referred to as the pathway flux (Koffas et al., 1999). In some fermentation processes, glucose is put into the system as a feed source. The carbon from glucose may leave the system in the form of protein, amino acids, cellular components, or secreted products. Hence, MFA tracks the rates at which these types of metabolites form during cellular metabolism in a fermentation process using data about stoichiometry, cell components, and growth kinetics (Pramanik and Keasling, 1997). Using this constraints-based approach, the objective function is a metabolic process, such as the production of biomass (cell mass). Constraints are determined by the underlying cellular processes that occur which may limit the behavior of a particular cell

and its growth rate. These constraints determine a solution space, and an objective function is then optimized using linear programming methods. Overall, metabolic flux models incorporate stoichiometry of metabolic pathways, requirements for growth during metabolism, and corresponding optimality principles to predict the flux distribution and growth of the cell under particular conditions of the cellular environment (Varma and Palsson, 1994a). After the model is solved, it can be used to accurately describe the time course of growth and product secretion (proteins, metabolites, cellular components), in addition to predicting the effects of eliminating or altering genes in the bacteria's genetic profile.

Many researchers use isotopic labelling to monitor metaoblic processes. Using these methods, stable isotope measurements can be used to gain information about fluxes. For example, Antoniewicz et al. (2007) used ^{13}C-labeled glucose for feeding cultures. After feeding with natural glucose, they used the labeled glucose to track uptake and distribution to other molecules. For labeled experiments, fluxes must be obtained using nuclear magnetic resonance (NMR) or mass spectrometry (MS). Then, the data with information about fluxes and molecular requirements can be fitted with computer modeling (Sauer, 2006). The difference between the fit and the data is minimized to get a better description of the fluxes. However, it is not necessary to use isotopic labeling to perform MFA on bacterial systems.

In order to use metabolic flux analysis, mass balance equations for each metabolite must be written. The concentration of each substrate is equal to the difference between the amount generated from the metabolic precursor and the amount used as a metabolic precursor to some other component. Under non-steady state conditions, information about the accumulation of metabolites must also be contained. Mathematically, this can be written as $\boldsymbol{A} \cdot \boldsymbol{r} = \boldsymbol{x}$ where **A** is

a matrix that contains all of the stoichiometric information, **r** is a vector that contains the information about transport and reaction fluxes, and **x** is a vector that contains metabolite concentration data (Covert et al., 2001). Note that **A** will be a large matrix comprised mostly of zeroes and ones depending on the stoichiometry of the set of reactions that are to be modeled. Under balanced growth conditions and due to the fact that the reactions are fast between metabolic substrates (milliseconds to seconds) compared to growth (hours or days), the system can be assumed to be operating under steady-state conditions. Hence, $\boldsymbol{A} \cdot \boldsymbol{r} = \mathbf{0}$.

To minimize the number of possible solutions, many constraints can be used. For example, the fluxes must be a positive number and since they exist in a single direction, **r** must be greater than or equal to zero. Data about substrate yields can also be used to further constrain the flux vector. Lastly, linear programming is used to optimize a desired objective. For example, the objective may be to maximize biomass. If this is the case, then linear programming would be used to maximize biomass with respect to the constraints defined for the fluxes and the information contained in the stoichiometric matrix. The resultant outcome would be the actual fluxes calculated with the biomass output.

As summarized by Stephanopoulos (1999), there are many other applications for metabolic flux analysis:

(1) improvement of yield and productivity of products native to host

(2) production of products that are new to the host cell

(3) improvement of cellular properties (i.e. prevention of overflow metabolism or the ability to withstand certain fermentation conditions)

(4) identification of substrates/enzymes as therapies for disease control

(5) use and production of intermediates for pharmaceuticals.

For example, Lee et al. (1997) utilized metabolic flux analysis to optimize glucose uptake while minimizing acetate production from glucose. Through the use of models, they found that supplementing media with citrate will optimize glucose uptake through glycolysis, the TCA cycle, and the HMP pathway while reducing acetate production. Similarly, Sauer et al. (1999) used metabolic flux analysis to examine how genetic and environmental changes affect the carbon physiology in *E. coli*. These groups performed the analysis without using an isotopically labeled carbon source.

Even with the advantages of protein production using *E. coli* rather than mammalian hosts, it is important to expand computational models of *E. coli* to increase understanding, design, and related processes in the industrial scale-up conditions (Meadows et al., 2010). This will aid in the large scale production of biopharmaceutical products with respect to time and cost effectiveness. Also, perturbing a system after it has been solved can lend valuable information about the importance of a metabolite or process in metabolism. If the resultant outcome does not change, then the perturbation had no effect on the system and the perturbed metabolite, input, etc. had little importance in the scheme of the system.

For this dissertation, lactose was examined as an induction source. In the absence of glucose, it can also be used as a carbon source. Upon modeling this type of system, it will be necessary to include information about metabolic pathways that involve both glucose and lactose metabolism. The same applies to the use of glycerol as a feed source. In the absence of glucose,

glycerol provides the necessary source of carbon and the pathways/reactions that describe glucose metabolism can also be incorporated into the model.

2.6 Purification

A major task for the pharmaceutical industry is to achieve highly purified and well-characterized production of recombinant proteins (Terpe, 2003). In order to separate and purify the target protein from the pool of proteins expressed during the fermentation process, fast protein liquid chromatography (FPLC) is a common strategy that is utilized. The column typically used in this system contains a cross-linked resin that has ligands attached to its surface depending on the protein of interest. The total soluble lysate is loaded to the column. During the loading step, the protein of interest interacts with the ligands on the surface of the resin. This interaction causes the target protein to adsorb to the resin or causes the protein to slow its progress through the column. After the total protein pool passes over the column, the column is washed to elute loosely bound or contaminant proteins. Then, elution of the target protein follows. This occurs by loading the elution buffer to the column. The buffer typically contains a species that interferes with the binding of the target protein to the column resin. The purified sample is then collected and further analyzed.

One type of FPLC is referred to as affinity chromatography due to the attraction between the target protein and the biospecific surface ligands. In order to create interactions between surface ligands and target proteins, the genes encoding for the target protein will often be genetically altered prior to expression and production. In this process, the DNA encoding for the additional tag or affinity tail is fused to a gene of interest. Then, when the target protein is expressed during fermentation, the tag is expressed with it resulting in the affinity tag – target

protein complex. Purification tags have been used to facilitate purification in affinity, ion-exchange, hydrophobic, covalent, and metal-chelating separations (Sassenfeld, 1990).

There are several advantages to using affinity tags to facilitate the purification of a particular protein. Some tags can increase the solubility of the target protein and also add stability to the protein. For some proteins, there is also a minimal effect on the tertiary structure and the biological activity of the target protein (Terpe, 2003). The affinity tails can also allow for simple and accurate assay of the affinity tag – target protein complex during purification (Sassenfeld, 1990; Terpe, 2003). Affinity tails are also extremely versatile and affinity chromatography usually results in a product that is 90-99% pure (Terpe, 2003). Tails can be added at the N-terminus or the C-terminus of the protein and can be expressed in many different cellular systems – bacterial, yeast, and mammalian (Terpe, 2003). One disadvantage of using affinity tags is that the column resin often costs more than that not using a biospecific ligand. Secondly, the fact that the protein must have a tag added on to the tail end can be a disadvantage in some cases because removal of the tail must occur prior to any additional work.

The affinity tail of interest for this project is glutathione-S-transferase (GST). This enzyme is 26 kDa in size. Fusion proteins with a GST tail can be purified by passing the cellular lysate over a column containing immobilized glutathione (Terpe, 2003). In order to elute the fusion protein, reduced glutathione is used after the total protein pool has passed through the column. The last step to achieve a final target protein in its active, therapeutic form is to cleave the tag from the target protein. With GST, this is performed by using thrombin or Factor Xa (Sassenfeld, 1990; Terpe, 2003). These enzymes cleave the peptide bond between the GST tag and the target protein.

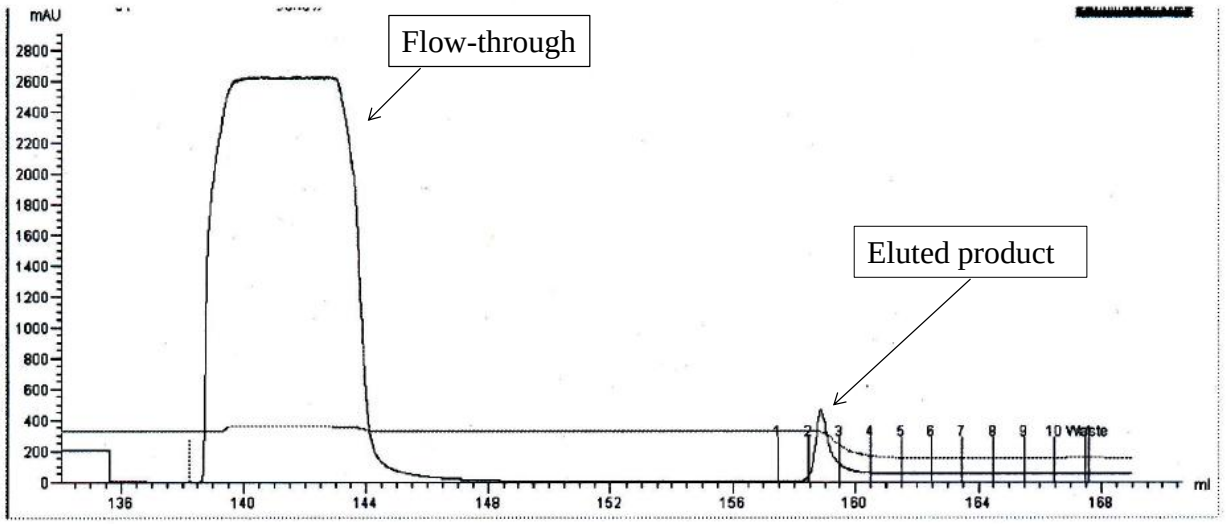

Figure 2-5. A typical chromatogram for chromatography utilizing a GST-tagged protein. A change in buffer causes the elution of target proteins by disrupting the binding affinity between the target protein and substrates in the buffer.

2.7 Medically relevant CBD-fusions as test cases for dissertation

For the work in this dissertation, an important group of therapeutic molecules was under investigation. Expression levels of collagen binding domain fusion proteins are low, so these types of fusion proteins are good candidates for developing methods that increase therapeutic protein production.

Recent investigations have shown that biomaterials play an important role in tissue engineering (Hannachi Imen et al., 2009). In order to enhance tissue regeneration both synthetic and biological materials have been used (Shi et al., 2011). Commonly used synthetic matrix materials used include polypropylene and polytetrafluoroethylene (Shi et al., 2011). Though these materials show an increase in the rate of tissue regeneration, they can cause infections and

adhesions because they are nonabsorbable (Shi et al., 2011). On the other hand, biological materials that have previously been used come from donors. The issue with this is that the materials can vary due to differences in each donor. Hence, it is a necessity to find novel biomimetic or bioactive materials that can enhance tissue regeneration without the use of synthetic materials and without the reliance on donors (Hannachi Imen et al., 2009). Substances that exhibit these characteristics include growth factors. Growth factors are recognized by cells and can activate cellular regeneration, but they cannot be delivered by ordinary drug delivery systems because of their limited target specificity and short half lives *in vivo* (Nozomu et al., 1998).

Making up approximately 30% of whole-body protein content, collagen is the most abundant protein in mammals (Chen et al., 2010; Matsushita et al., 1998). It is the major protein component in connective tissues and bone. Collagen has been used in tissue engineering because of its ability to provide structural stability in addition to its ability to increase cellular attachment (Shi et al., 2011). To overcome the complications stated above, growth factors that are to be used as therapeutic proteins have been fused to collagen binding domains (CBD) and produced in *E. coli*. This reduces both problems of specificity and short half-lives because collagen binding domain can be used as an "anchoring unit" for *in vivo* applications (Toyoshima et al., 2001). It specifically targets collagen and the resulting vehicle is a non-diffusible, longer lasting fusion protein. It has been shown that growth factors and cell binding peptides fused to biomaterial carriers can achieve biomolecular recognition of cells in addition to interacting with surrounding tissues (Hannachi Imen et al., 2009). Also, after the fusion of a growth factor to CBD, recombinant proteins exhibited collagen binding activity in addition to maintaining growth factor activity and its concentration at the target site (Shi et al., 2011).

It has been found that collagenase from *Clostridium histolyticum* has broader substrate specificity and can hydrolyze collagen at diverse sites (Toyoshima et al., 2001). This suggests that utilizing CBD from this source would have broader clinical applications. In designing a CBD fusion protein it is important to keep in mind that only proteins that act in or from the extracellular space can be used as the functional domain. Thus, the product may have to be directly injected into affected tissue or used as an ointment (Nozomu et al., 1998).

2.7.1 PTH-CBD

Parathyroid hormone (PTH) or parathyroid hormone related peptide (PTHrP) has the ability to increase bone density after administration (Liu et al., 2007). Hyperparathyroidism is correlated with bone loss because of its ability to remove calcium from bones to maintain extracellular calcium concentrations. According to Fu et al. (2005), "PTH has an anabolic effect on bone formation by stimulating renal calcium readsorption, phosphate excretion, and bone remodeling." Administration of PTH actually has the ability to enhance bone density (Sakon et al., 2010). The hormone binds to receptors on osteoblasts. This action increases the longevity of osteoblast activity, thus causing bone gain.

Parathyroid hormone also enhances epidermal cell proliferation, which can promote hair growth. However, because of its short half-life (approximately 4 minutes), an anchoring unit such as CBD is necessary for delivery of PTH to target cells. Indeed, a PTH-CBD fusion protein can be used to promote bone and hair growth and to prevent cancer metastasis to bone among other things (Sakon et al., 2010). This action is shown in Figure 2-6.

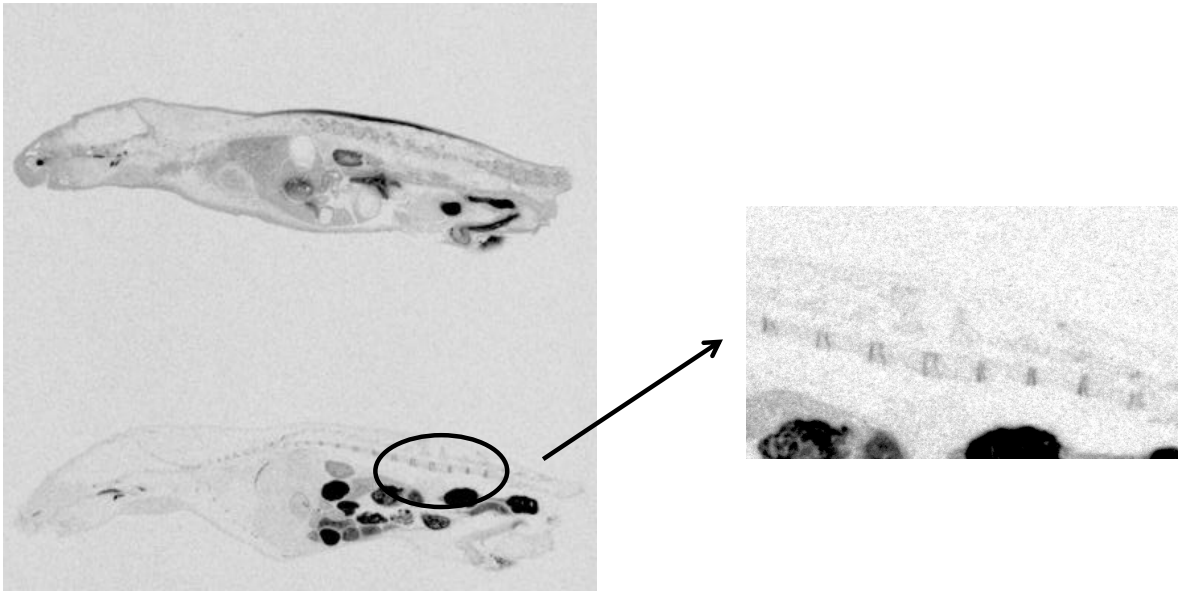

Figure 2-6. Translocation of PTH-CBD after subcutaneous injection in mice. The top image is taken 1 hour after injection in the back of the animal. The bottom image is taken 12 hours after the injection. In this image, PTH-CBD has translocated to the skeletal system. The enlargement on the right shows PTH-CBD in the vertebral column 12 hours after injection. (Images generously provided by Dr. Joshua Sakon, Department of Chemistry, University of Arkansas).

2.7.2 EGF-CBD

Epidermal growth factor (EGF) has the ability to stimulate the proliferation of the epidermis and other epithelial tissues *in vivo*. In cell culture systems, it has the increased ability to stimulate the growth of a wide variety of cells (Carpenter et al., 1982). Specifically, its applicability to quickly heal ruptured ear drums is under current investigation (collaborator's laboratory). Because of these characteristics, it is a candidate for fusion with CBD to act as a biomaterial for tissue engineering purposes.

3. Specific aims

This dissertation seeks to address important aspects of bioprocessing, namely the expression, production, and purification methods of novel therapeutic proteins through experiments that combine fermentation, purification, and metabolic flux analysis techniques. A novel therapeutic protein, parathyroid hormone fused to collagen binding domain, has been of recent interest due to its applications for therapeutic purposes. The collagen binding domain (CBD) allows for efficient uptake of parathyroid hormone. The effects of this uptake include decreased hair loss and decreasing losses in bone density, thus reversing or subduing the side effects of current cancer treatments (chemotherapy). In order to enhance purification of PTH-CBD, a glutathione S-transferase tail is attached to the PTH-CBD complex. This allows for easier purification of the protein complex using affinity chromatography. Metabolic flux analysis is used to model the system and the chemical induction of the therapeutic protein complex. This aids in the development of media and induction strategies

The broad goal of this experimental program was to gather information on production of PTH-CBD in a manner in which scale-up work is plausible in order to increase availability of the protein complex for therapeutic purposes. This involved investigating defined mediums that allow for high cell density cultivations while increasing protein expression, monitoring induction techniques that will incorporate good manufacturing practice applications, and investigating certain aspects of GST affinity chromatography. An overview of the direction of experiments is given in Figure 3-1, with specific aims given below.

Specific objectives include the following scientific aims:

Aim 1. Increase expression of PTH-CBD by modifying and testing mediums appropriate to fed-batch fermentation processes.

Aim 2. Test various induction techniques to further enhance expression of the therapeutic protein.

Aim 3. Investigate the use of fast protein liquid chromatography with a glutathione-S-transferase (GST) affinity column for the purification and recovery of the therapeutic protein.

Aim 4. Mathematically model the cellular system using techniques consistent with metabolic flux analysis.

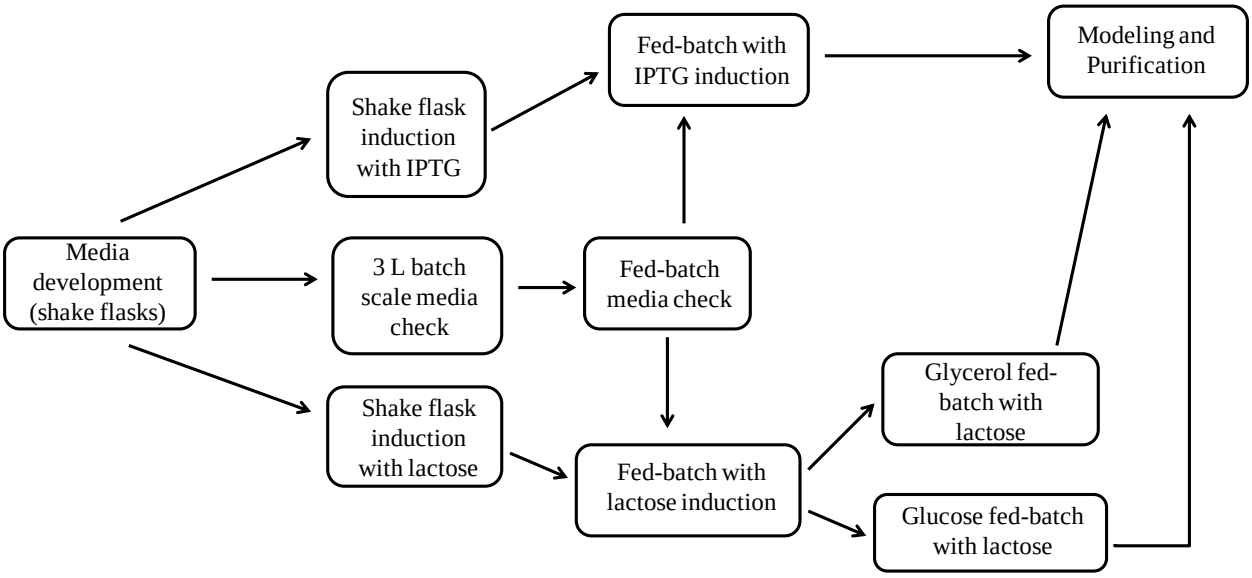

Figure 3-1. Flow chart of how experiments proceeded.

The work in this dissertation lays the foundation for increasing production of therapeutic proteins by investigating fed-batch fermentation, media enhancement, induction techniques, and GST purification. Such advances are of great interest to the pharmaceutical and biotechnology

industries due to the increase in recombinant protein expression and use thereof in therapeutic applications.

It also thoroughly examines the use of lactose as an alternative to IPTG as an inducer. The body of literature for IPTG induction is far more mature than that for lactose. Within the literature for lactose induction, fed-batch fermentation with lactose is rarely discussed. A search of **fed-batch fermentation "IPTG induction"** within Google Scholar yields 629 results, whereas the search with **"lactose induction"** yields 94 results. It is also difficult to find work on lactose induction with fed-batch fermentation utilizing completely defined media.

4. Materials and Methods

4.1 Strains and plasmids

Chemically competent *E. coli* BL21 (DE3) was purchased from Novagen. This strain was used as the host for all fermentation experiments. For long term storage, *E. coli* DH5α was used. For plasmid preparations, *E. coli* chemically competent Top10 cells from Invitrogen were used. Competent cells were transformed with recombinant pGEX plasmid provided by Dr. Joshua Sakon (Department of Chemistry, University of Arkansas). This plasmid, pCHC305, contains the genetic information for the recombinant protein GST-PTH-CBD (383 amino acids), as depicted in Figure 4-1.

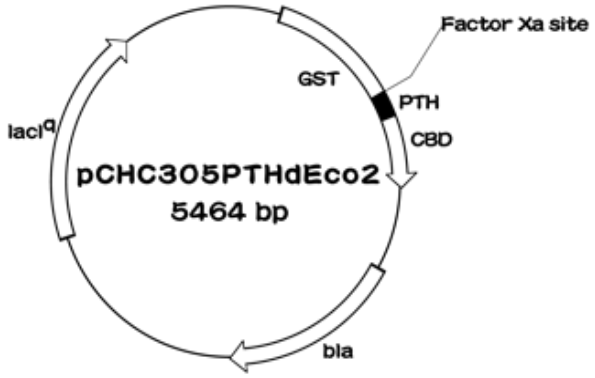

Figure 4-1. Plasmid map of pCHC305. There is a Factor Xa recognition site between the tag and PTH-CBD. This allows for cleavage of the tag after purification using Factor Xa.

For transformation of cells with plasmid, the heat shock method was used. Competent cells were placed on ice after removal from storage at -80°. After the cells thawed, 1-2 µl of plasmid DNA was added and mixed by gently tapping the tube. After incubation on ice for 30 minutes, the tube was placed in a 42° thermocycler for approximately 45 seconds. This was followed incubation on ice for two minutes. Next, 0.5 ml of S.O.C. medium (Invitrogen) was

added to the tube. It is comprised of (per liter): 20 g tryptone, 5 g yeast extract, 10 mM NaCl, 2.5 mM KCl, 10 mM $MgCl_2$, 10 mM $MgSO_4$, 20 mM glucose. The cells were incubated at 37° for three hours at 200 rpm. Cells were then spread on Luria-Bertani (LB) plates supplemented with 150 μg/ml ampicillin and incubated overnight at 37°. After colony formation, colonies were picked for fermentation experiments and for storage in glycerol at -20° and -80°.

4.2 Media

LB was used for all plates and seed cultivations. For seed cultivations, a colony was picked off of a plate and put in a 5 ml falcon tube containing LB and 150 μg/ml ampicillin. These were incubated overnight at 37° and shaken at 250 rpm. Since it was desired to use a completely defined media for fed-batch cultivations, modified minimal salts (M9) media was investigated and compared to LB with respect to growth and recombinant protein production. As described by Babaeipour, et al. (2008), the composition of M9 per liter of water is as follows: 10 g glucose, 15 g of K_2HP0_4, 7.5 g of KH_2P0_4, 2 g of citric acid, 2.5 g of $(NH_4)_2S0_4$, 2 g of $MgSO_4$-$7H_20$, and 1 ml of trace element solution. A 5X stock was made of the salts solution. The trace element solution contains, per liter of 1 M hydrochloric acid, the following: 2.8 g of $FeSO_4$-$7H_20$, 2 g of $MnCl_2$-$4H_20$, 2.8 g of $CoCl_2$-$7H_20$, 1.5 g of $CaCl_2$-$2H_20$, 0.2 g of $CuCl_2$-$2H_20$, and 0.3 g of $ZnSO_4$-$7H_20$. Glucose solutions and trace element solutions were sterilized separately and added to the final 1X media.

4.3 Shake flask cultivations

For experiments performed in 250 ml shake flasks, 50 ml of media were inoculated with 5 ml of overnight seed culture. For 1 L shake flasks, 250 ml of media were inoculated with 20 ml overnight seed culture. Media were supplemented with 150 μg/ml ampicillin in every shake

flask experiment. In shake flasks that were induced, the inducer (isopropyl-beta-D-thiogalactospyranoside (IPTG) or lactose) was added at the mid-exponential phase of growth (at an optical density (OD) between 0.6 and 0.8 units (at 600 nm). Samples were taken throughout the fermentation process to track protein expression and growth (via OD_{600}).

In order to find an optimal medium for the production of recombinant protein, a number of experiments were performed to test different media conditions. To examine the effect of glucose on growth and protein expression, a set of flasks containing only LB was compared to a set of flasks containing LB supplemented with 10 g/l glucose. Each flask was inoculated with the same volume of overnight seed culture. Samples were taken every hour to track growth and protein expression.

A similar experiment was performed to compare *E. coli* growth and protein expression on M9 medium, M9 medium supplemented with amino acids, and LB. The amino acids chosen to supplement M9 were not arbitrarily chosen, but calculated using a basis of one gram of target protein produced. The frequency of a particular amino acid in the primary sequence can be used to calculate the overall concentration of that particular amino acid in the protein. Using this information, the amount of a particular amino acid required for the production of one gram of recombinant protein can be calculated, as shown in Table 4-1. Based on the higher amounts of lysine, aspartic acid, glycine, and leucine required, the medium was supplemented with these amino acids. It was also supplemented with serine because serine has the ability to produce other amino acids during metabolism. Amino acids were solubilized in water and filter sterilized. 250 mM each of lysine, glycine, and serine were kept as stock solutions. Leucine

and aspartic acid stocks were 125 mM and 50 mM, respectively. Cultures were induced with lactose or IPTG.

Table 4-1. Amino acid composition of GST-PTH-CBD with the amount of each required to make one gram of protein.

Monomer		MW	Frequency	Percentage	Mass	mmol/g protein	Grams of aa reqd for 1 gram of protein
Ala	A	89	15	3.92	1335	0.342	0.030
Arg	R	174	15	3.92	2610	0.342	0.059
Asn	N	132	18	4.70	2376	0.410	0.054
Asp	D	133	27	7.05	3591	0.615	0.082
Cys	C	121	4	1.04	484	0.091	0.011
Gln	Q	146	9	2.35	1314	0.205	0.030
Glu	E	147	27	7.05	3969	0.615	0.090
Gly	G	75	31	8.09	2325	0.706	0.053
His	H	155	10	2.61	1550	0.228	0.035
Ile	I	131	26	6.79	3406	0.592	0.078
Leu	L	131	36	9.40	4716	0.820	0.107
Lys	K	146	31	8.09	4526	0.706	0.103
Met	M	149	13	3.39	1937	0.296	0.044
Phe	F	165	13	3.39	2145	0.296	0.049
Pro	P	115	22	5.74	2530	0.501	0.058
Ser	S	105	21	5.48	2205	0.478	0.050
Thr	T	119	13	3.39	1547	0.296	0.035
Trp	W	204	6	1.57	1224	0.137	0.028
Tyr	Y	181	25	6.53	4525	0.570	0.103
Val	V	117	21	5.48	2457	0.478	0.056
Total:			383	100	50772		
Number of peptide bonds:			382		6876		
Protein molecular weight:					43896		

To determine the an optimal amount of amino acids that should be added to the M9, experiments were performed that compared the addition of amino acids to a final concentration of 5 mM and 10 mM. Ammonium hydroxide was utilized to pH the M9 modified with amino acids (as the amino acids dropped the pH below the physiological value). The approximate pH for shake flask experiments was 6.8.

To track the consumption of glucose and lactose, 1 liter shake flasks with M9 modified with amino acids, 10 g glucose, and 10 g lactose were inoculated with seed cultures as described above. Samples were taken throughout the cultivation and supernatants were saved for later analysis.

4.4 Batch cultivations

In order to further test the medium formulation prior to fed-batch fermentation, batch fermentation was utilized. M9 supplemented with glucose and amino acids was used for all batch fermentation experiments. No substrates were added to the media during cultivation with the exception of ammonium hydroxide for pH control and inducer. IPTG, lactose, and a combination of the two were used. The goal of the batch cultivations was to monitor growth under different inducer substrates. For IPTG induction, 10mM IPTG was used. For lactose induction, 15 grams of lactose was added per liter of medium. For induction using both lactose and IPTG, 5 mM ITPG was used with 7.5 g/l lactose. Appropriate amounts of ampicillin and anti-foam were added to the medium prior to cultivation.

To prepare for the fermentation process, a single colony of *E. coli* BL21 pCHC305 was transferred from a plate to a 5 ml culture tube. After overnight growth in a 37° C incubator, 100 ml of M9 medium were inoculated. After six to eight hours, the 100 ml culture was spun-down at 4750 rpm for 25 minutes and resuspended in 50 ml of fresh M9 medium. This was used to inoculate 1 liter of medium (as previously described) in a 3 L Applikon bioreactor (Foster City, CA). The bioreactor was equipped with BioXpert Advisory software from Applikon. The reactor was also outfitted with an Applisense pH probe and dissolved oxygen probe. The pH was maintained at approximately 6.8 (with a range of 6.75 to 7) during the cultivation using 7 M

NH_4OH. The culture was stirred at 750 rpm until it became necessary to adjust the stir rate (to 1000 rpm) to maintain the proper dissolved oxygen concentration. Adjustments in oxygen delivery were made as necessary during the process to ensure that the dissolved oxygen concentration did not drop below 35%. The temperature was maintained at 37° C using a heating jacket and cooling loop. Optical densities were monitored using a Bugeye optical density probe (BugLab, Foster City, CA) and a DU800 Beckman Coulter spectrophotometer (Brea, CA). A linear correlation for the Bugeye response to the actual OD as measured by the spectrophotometer was determined for each individual experiment. Figure 4.2 shows a few examples of these linear correlations.

4.5 Fed-batch cultivations

After shake flask and batch cultivations were performed to select an appropriate medium, fed-batch fermentations were run. M9 supplemented with 5 mM amino acids and 10 mg/l thiamine was used for fed-batch fermentation runs. This was also supplemented with 1 ml anti-foam to control foaming and 150 μg/ml ampicillin to maintain selection. Additional anti-foam was added during cultivation when the foam reached a level approximately 2 inches from the top of the reactor. Unless specified, the feed for all fed-batch fermentation experiments was comprised of the following, per liter water: 500 g glucose, 20 g $MgSO_4$-$7H_20$, and 5 ml trace element solution. The glucose solution and salt solution were sterilized separately. The reactor was outfitted as described in Section 4.4.

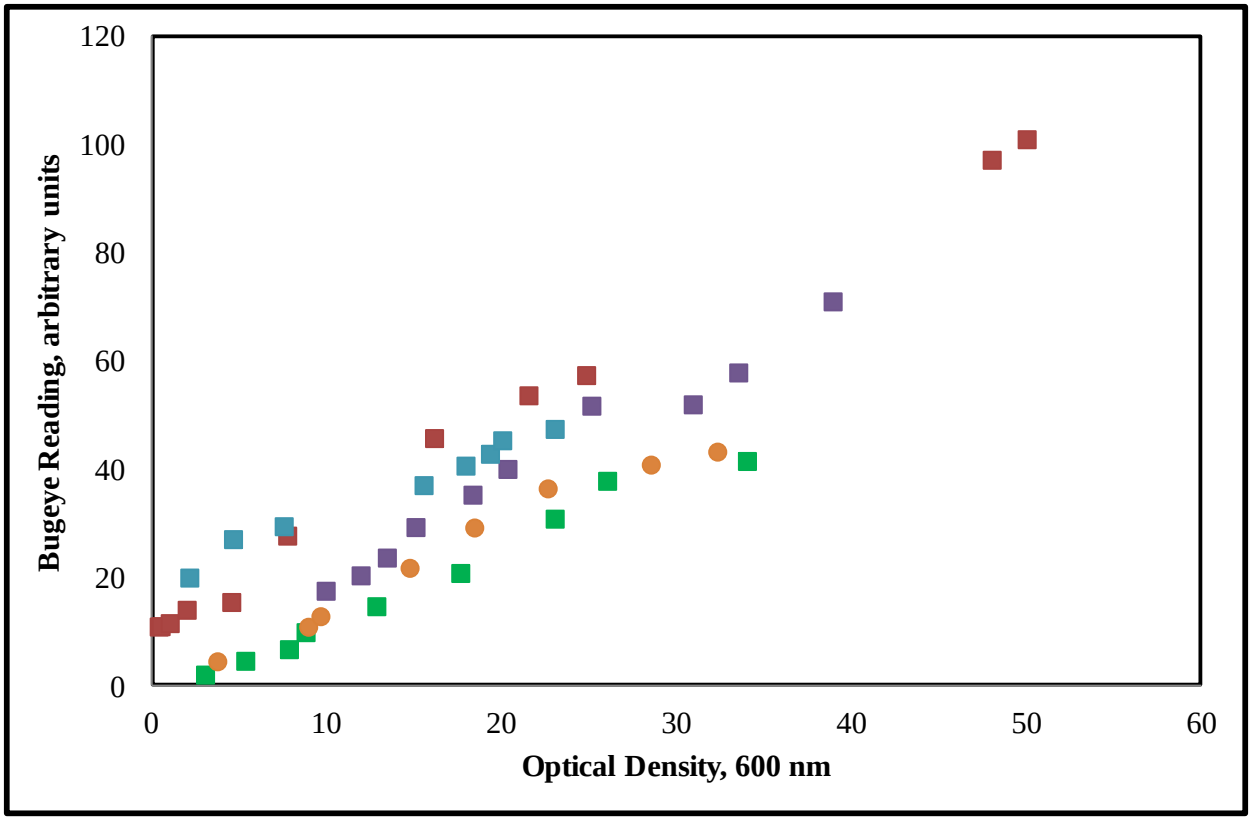

Figure 4-2. Linear correlations between optical density and Bugeye output are used to determine the growth curve for the entire fermentation experiment in terms of optical density. A conversion factor between optical density and dry cell weight is used to calculate the grams of cells produced during the experiment. The average R^2 value for the correlation between the OD and Bugeye output is 0.98.

Each fermentation experiment can be broken down into a batch phase and a feeding phase. In the batch phase, the culture used only the carbon sources provided in the medium at the start of the cultivation. During this phase, no nutrients were fed to the reactor. After approximately 7 - 8 hours, the feeding phase began. The exact timing depended on the lag phase of the culture and how quickly the culture grows on the initial carbon substrate. As previously described, a rise in pH indicated that there is no carbon present in the system. Similarly, a sharp decline in oxygen indicated that feeding should start. In the fed-batch experiments, these two events occurred at the same time and were witnessed by the Applikon advisory software. After

observing that these two events occurred between 7 to 8 hours after inoculation, it was determined that feeding should start at some time in that range. For experiments where a four hour (long) lag phase is observed, feeding began at 8 hours. For experiments with shorter lag phases (2.5 hours), feeding began around 7 hours after initial inoculation.

The feeding profile used for fermentation experiments was based on that proposed by Korz et al. (1995) and Lee et al. (1997) and was previously described. A feeding profile was programmed into the Applikon software that mimics the exponential feed based on substrate concentrations. The actual programming information is depicted in Figure 4-3, with a thorough discussion following.

No	Statement	Begin	End
1	---------- 1. group ----------	0:00	0:02
2	#set the constant values		
3	mu=0.2		
4	Yxs=0.5		
5	Sin=500		
6	X0=5		
7	V0=1.1		
8	mult1=(mu*X0*V0)/(Yxs*Sin)		
9	feed=0		
10	FDPUMP=0		
11	FDSTEP=1		
12	FDWAIT=7		
13	---------- 2. group ----------	0:02	
14	#STEP 3: feed mode, calculate the current feed value		
15	IF FDSTEP=3		
16	mult2=mu*((TIME-FDTIME)/60)		
17	feed=mult1*exp(mult2)*1000/60		
18	FDCHECK=0		
19	FDPUMP=feed		
20	IF FDPUMP<0.1		
21	FDPUMP=0.1		
22	FDCHECK=1		

No	Statement	Begin	End
23	ENDIF		
24	ELSE		
25	#STEP 2; inoc done, wait for start of feed		
26	IF FDSTEP=2 AND TIME>=FDTIME		
27	FDSTEP=3		
28	ELSE		
29	#STEP 1 check for inoccolation		
30	IF INOC=1 AND FDSTEP=1		
31	INOCTM=TIME		
32	FDTIME=INOCTM+FDWAIT*60		
33	FDSTEP=2		
34	ENDIF		
35	ENDIF		
36	ENDIF		
37	---------- 3. group ----------		
38	LevelIO=0	0:00	4:32
39	LevelIO=1	4:33	4:59
40	LevelIO=0	5:00	
41			
42			
43			
44			

Figure 4-3. Image of program utilizing exponential feeding algorithm.

For this program, there were three separate groups of information. The program ran the information in group one during the first two minutes of the fermentation experiment. This essentially set the initial conditions. In lines three through 7 in the example given above, the conditions were set to run an exponential feeding profile: $\mu = 0.2\ hr^{-1}$, $Y_{x/s} = 0.5$ g/g, $S_{in} = 500$ g/liter, $X_0 = 5$ g DCW, and $V_0 = 1.1$ liters. Line 8 describes the coefficient for the feed rate equation:

$$F(t) = \frac{\mu}{Y_{x/s} \times S_{in}} \times X_0 \times V_0 \times e^{\mu t} \tag{4.1}$$

The only term that depends on time is the exponential term. Thus, the rest of the equation can be calculated at the beginning of the run, as these values will not change. This coefficient was defined as mult1 in the program. Lines 9 and 10 set the initial conditions for the feed - start at flow rate of 0 ml/min. The FDSTEP term in line 11 set the step for the feed program - start at step one. FDWAIT in line 12 told the program how long to wait before feed should start. In this case, feed started after 7 hours of wait (batch) time. The second group starts on line 15, but the first step of the second group starts on line 29. This portion of the program ran from two minutes after the start of the experiment to the end of the fermentation run. Step 1 of group 2 identifies that inoculation has been performed. If inoculation has been performed (based on an offline variable that the user defines) and if the feed step is set to step 1, then the program calculated the exact time that the feed should start. For this example, feed started after 422 minutes because the inoculation variable was triggered after 2 minutes and the user defined FDWAIT as 7 hours. Then, the program advanced to feed step 2 (line 22). Step 2 of the program waited until the run time of the fermentation exceeded the 422 minutes that was calculated in step 1. After the program time exceeded the FDTIME, step 3 commenced (on line 15). Step 3 of group 2

performed all of the calculations for the feeding amount of this program. Mult2 calculated the value in the exponential term. It took into account the elapsed time and the user-defined growth rate. In line 17, the program compiled data from mult1 and mult2 to get a feed rate in terms of ml/min.

The system utilized a variable-speed pump to exponentially add substrate to the fermenter at a constant rate per minute (since the program calculates an amount to feed every minute). The minimum amount that the Masterflex® pump could add to the system is 0.1 ml/min (using the tubing with the smallest diameter available). Lines 20 through 22 of the program accounted for the pump sensitivity issue. If the program calculated a feed rate lower than 0.1 ml/min, the profile corrected for this and 0.1 ml/min was actually fed into the reactor. This check was in place until the program calculated a feed rate greater than 0.1 ml/min. This means that the substrate was fed on a constant-feed system for about 4 hours at the beginning of the fed-batch period. After this constant-feeding period, exponential feeding began.

The third and final group in the example program contains the information that triggered a built-in pump. Once activated, inducer was added to the system. It turned on and turns off at user-defined times. A value of zero indicates that the pump was turned off for that given period while a value of 1 indicates that the pump was on. In the example in Figure 4-3, the level pump was turned on when the elapsed time was 4 hours and 33 minutes and remained on until 4 hours and 59 minutes.

To maintain that this feeding strategy kept the cultivation substrate limited, the exponential feeding profile was initially regulated so that feeding stayed between 0.1 and 0.3 ml/min. For this particular experiment everything in the profile algorithm remained the same,

with the exception of a regulatory loop. As shown in Figure 4-4, once the algorithm calculated that the feed should be a value greater than 0.3 ml/min, this value was divided by 0.3 so that the value fed into the reactor returned to 0.1 ml/min. Once the calculated value exceeded 0.9 ml/min, it was divided by 0.9 to again return it to 0.1 ml/min. This regulatory group is written in lines 24-32 in the algorithm. After the initial experiment using this profile, all other feeding experiments used the exponential feeding algorithm that was previously described.

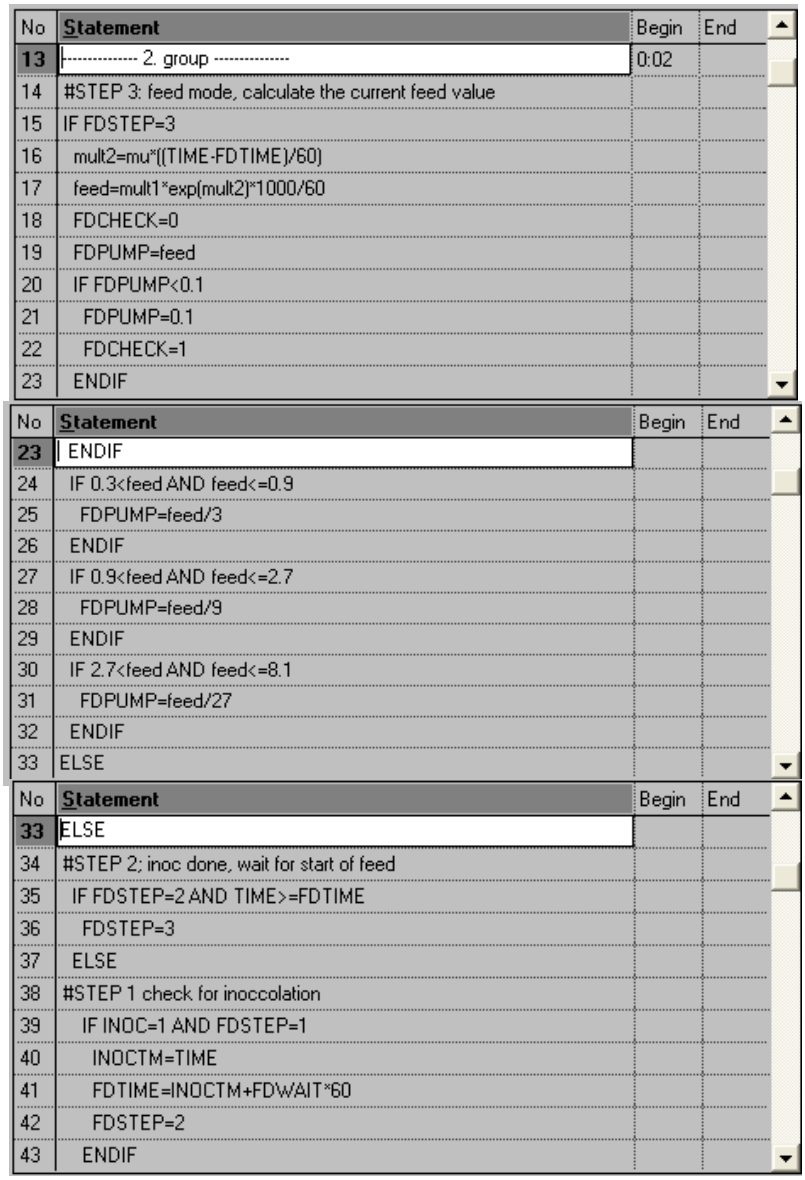

No	Statement	Begin	End
13	---------- 2. group ----------	0:02	
14	#STEP 3: feed mode, calculate the current feed value		
15	IF FDSTEP=3		
16	mult2=mu*((TIME-FDTIME)/60)		
17	feed=mult1*exp(mult2)*1000/60		
18	FDCHECK=0		
19	FDPUMP=feed		
20	IF FDPUMP<0.1		
21	FDPUMP=0.1		
22	FDCHECK=1		
23	ENDIF		

No	Statement	Begin	End
23	ENDIF		
24	IF 0.3<feed AND feed<=0.9		
25	FDPUMP=feed/3		
26	ENDIF		
27	IF 0.9<feed AND feed<=2.7		
28	FDPUMP=feed/9		
29	ENDIF		
30	IF 2.7<feed AND feed<=8.1		
31	FDPUMP=feed/27		
32	ENDIF		
33	ELSE		

No	Statement	Begin	End
33	ELSE		
34	#STEP 2; inoc done, wait for start of feed		
35	IF FDSTEP=2 AND TIME>=FDTIME		
36	FDSTEP=3		
37	ELSE		
38	#STEP 1 check for inoccolation		
39	IF INOC=1 AND FDSTEP=1		
40	INOCTM=TIME		
41	FDTIME=INOCTM+FDWAIT*60		
42	FDSTEP=2		
43	ENDIF		

Figure 4-4. Image of program utilizing regulatory algorithm to keep feed rates below 0.3 ml/min during the fermentation process.

To examine an alternative feeding method, glycerol feed was used for a few experiments. The media composition (M9 with amino acids) was kept the same with the exception of the addition of 2 g/l glycerol to prime the cultivations for feed on glycerol or in the case of auto-induction, as described below. The molar concentration of carbon in the glycerol feed was the same as that in the glucose feed and the feed profile was kept the same. All other component concentrations (trace elements, magnesium salts) were also kept the same. Some of these cultivations were auto-induced and 10 g/l of lactose was added to the initial cultivation media. One set of experiments examined using 15 g lactose to induce the culture 12 hours after inoculation (5 hours after feeding on glycerol). Another set examined auto-induction with pulsing 10 g lactose into the system 14 hours after inoculation (when initial lactose is depleted).

Fermenter cultivations that were not auto-induced were induced with lactose or IPTG. For experiments in which lactose was added at the time of feed start, the level pump on the Applikon system was utilized. By adding a couple of lines to the feed profile, the level pump can be turned on or off at a designated time (previously discussed). The appropriate amount of lactose was solubilized in 50-60 ml of milliQ water (to inhibit crystallization) and filter sterilized. The solution was placed in a sterile bottle and attached to the reactor with the appropriate tubing. The level pump was programmed to be equal to one for a thirty minute period at the time that was desired for induction. A value of one turns the pump on; a value of zero returns the pump to the off state. For IPTG-induced cultures, a 250 mM stock of IPTG was made and kept in a -20 freezer until use. Final concentrations of IPTG in the reactor for induction were 5 mM and 10 mM.

Multiple fed-batch experiments were performed. Table 4-2 displays the induction technique, with respect to inducer concentration, type, and time or indicator for induction. Each fermentation experiment was run until there was a decrease in growth or until a specified time after induction. They typically lasted for approximately 24 hours. Samples were taken throughout the run at specified times. The culture broth was spun down for 35 minutes at 4750 rpm and 2° C. Supernatants were filtered and stored at -20° C. Cell pellets were also stored at -20° C.

Table 4-2. Summary of fed-batch fermentation experiments with respect to induction type, concentration of inducer, length of induction period, and feed type. Duplicates of each run were performed, unless specified by an asterisk.

Type of inducer	Concentration of inducer	Induction time or indicator	Length of induction, hours	Feed
Lactose	10 g/l	11 hours after inoculation	14	glucose (st)
Lactose	10 g/l	12 hours after inoculation	12	glucose
Lactose*	10 g/l	auto-induction	25	glucose
Lactose	10 g/l	at time of feed start	12	glucose
Lactose	10 + 10 g/l	auto-induction with pulse at 12 hours	22 + 10	glucose
IPTG	5 mM	OD ≈ 65	5	glucose
IPTG	10 mM	OD ≈ 65	5	glucose
Lactose	10 g/l	auto-induction	21	glycerol
Lactose	15 g/l	induction at time of feed start	10	glycerol
Lactose*	10 + 10 g/l	auto-induction with pulse at 14 hours	21 + 7	glycerol

4.6 Lysate preparation

Cell pellets were retrieved from the freezer and placed on ice. For pellets from 5 ml of culture broth, 2 ml phosphate buffered saline (PBS: 8 g NaCl, 0.2 g KCl, 1.44 g Na_2HPO_4, 0.24 g KH_2PO_4 in 1 liter) with 5 mM ethylenediaminetetraacetic acid (EDTA) was used to resuspend the pellet. The ratio of PBS to pellet (determined by culture volume) was kept constant. After

resuspension in buffer, cells were lysed via sonication and spun down at 4750 rpm for 35 minutes. Lysates were stored at -20° C.

4.7 Analytical Assays

4.7.1 Cell growth and fermentation conditions

As previously discussed, cell growth was monitored using an online optical density probe and a spectrophotometer (at 600 nm). To determine dry cell weight, analysis was performed throughout the fermentation experiments using a Mettler-Toledo MJ33 moisture analyzer. One ml of culture broth was spun down at 14000xg for 2 minutes. The pellet was washed twice with milliQ water and pipetted onto the moisture analyzer. Samples were dried at 60° C until constant weight was achieved. Calibrations were made between optical densities (taken by the spectrophotometer) and dry cell weights. Wet cell weights were taken by either spinning down the entire culture for 1.5 hours at 4750xg and weighing cell mass or by pre-weighing 50 ml culture tubes. A given amount of culture was pipetted into the tube and spun down. The difference in the weight of the tube before and after centrifugation was divided by the volume of broth in the tube to get weight per volume (g/ml). Final volumes of culture were known, so total weight could be calculated. Fermentation conditions such as dissolved oxygen concentration, pH, stir rate, and temperature were monitored and logged by the Applikon advisory software program.

4.7.2 Carbohydrate determination

Glucose concentrations were determined using a glucose hexokinase kit (Sigma, St. Louis, MO). Acetic acid concentrations were determined using an enzyme-based kit by

Boehringer Mannheim/R-biopharm (Darmstadt, Germany). To determine lactose and glycerol concentrations, a Waters high pressure liquid chromatography unit was used. Samples were loaded onto a BioRad Aminex HPX-87N carbohydrate column at a flow rate of 1 ml/min, with milliQ water as the mobile phase. Standards of lactose and glycerol were also loaded to determine elution times, and to determine the peak area that corresponds with the standard concentrations.

4.7.3 Protein analysis

Total protein concentration was determined using a Bio-Rad *DC*™ protein assay kit, with bovine serum albumin (BSA) as a standard. Target protein concentrations were determined using the densitometry technique with sodium dodecyl sulfate-polyacrylamide gel electrophoresis (SDS-PAGE). Standards and samples were mixed with 5X sample buffer (9 ml 8 M urea, 0.242 g Tris-HCl, 0.8 g SDS, bromophenol blue (pH = 8)). Equal concentrations of protein were loaded into the wells of a 12.5% SDS-PAGE gel. Gels were run at a constant voltage of 250 V for 35-40 minutes, depending on the migration of the ladder marker. After completion, gels were incubated with staining solution (250 ml methanol, 0.055 g Commassie Blue, 250 ml de-ionized water, 50 ml acetic acid) and left overnight on a shaker. After staining period, gels were de-stained with de-staining solution (850 ml de-ionized water, 75 ml acetic acid, 75 ml methanol). Following the de-staining process, gels were photographed or scanned and densitometry was performed using ImageJ software. An example of this process is given in Figure 4-5. On the top left is a representative gel with a molecular weight ladder and three different concentrations of BSA. Using the ImageJ software, each rectangular lane is selected and plotted. The resultant plot is given on the right hand side. Each peak corresponds to a band

on the gel. Then, the peak can be selected and ImageJ will calculate the area under the curve. The outcome for this example is shown on the bottom left side. Peak areas obtained for proteins in lysates were compared to those obtained for BSA standards. Typical coefficients of determination (R^2) for BSA standards and peak areas were greater than 0.98.

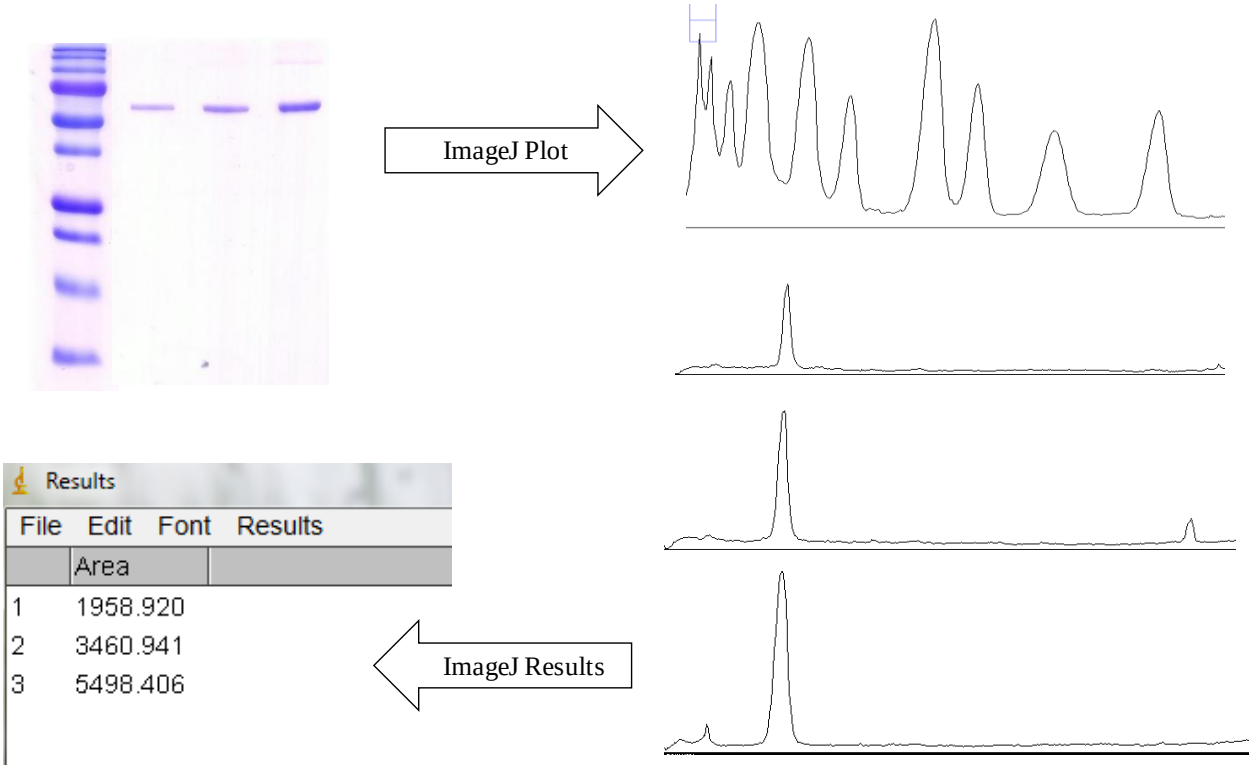

Figure 4-5. Analysis of SDS-PAGE gel using densitometry. The coefficient of determination for the trend between BSA concentration and peak area is 0.99.

To qualitatively compare target protein concentrations between samples, western blotting was performed. Samples were analyzed on 12.5% SDS-PAGE gels and immunoblotted using antibodies specific to GST. For western blotting, Protran BA 85 nitrocellulose membranes were used (Whatman, Piscataway, NJ). After soaking western blot papers and sponges in cold towbin buffer, transfer occurred at 100 V, constant 350 mA, for 70 minutes using a Bio-Rad transfer apparatus. The primary antibody, polyclonal anti-GST antibody (GE Healthcare, Piscataway, NJ), was incubated overnight at 4°C with the membrane after transfer. The secondary antibody

utilized was anti-goat IgG (whole molecule) alkaline phosphatase (Sigma, St. Louis, MO). After three hour incubation period at 4°C, visualization procedure was performed. Visualization was completed using nitroblue tetrazolium (NBT) and 5-bromo-4-chloro-indolyl phosphate (BCIP) until protein bands appeared.

4.8 Fast protein liquid chromatography (FPLC)

Cellular lysates were purified using a FPLC system from ÄKTA Amersham Pharmacia Biotech. Prior to purification, cell lysates were filtered through a 0.20 μm filter. GSTrap FF columns from GE Healthcare (Piscataway, NJ) were equilibrated with PBS loading and binding buffer, pH=7.3. Lysates were loaded at 0.5 ml/min. Washing after loading was performed at a flow rate of 1 ml/min with PBS. After 5 to 10 column volumes (CV) of washing (until the baseline returned to zero), elution using 50 mM Tris-HCl with 10 mM reduced glutathione was performed. If a peak was absent, the concentration of reduced glutathione was increased to 25 mM. Fractions were collected and stored at -20° C for further analysis.

4.9 Activity analysis

In order to assess the activity of the collagen binding domain, purified GST-PTH-CBD was incubated for thirty minutes at room temperature on a collagen sheet. For control experiments, green fluorescent protein (GFP) and PBS were incubated on separate collagen sheets. After brief washing period with Towbin buffer (without methanol), the binding of GST-PTH-CBD and/or GFP to the collagen sheets was visualized using the western blot protocol. The primary antibody was incubated for an overnight period. The secondary antibody was incubated with the collagen sheet for three hours. The secondary antibody was visualized using

NBT and BCIP, as described previously for a pre-determined amount of time as to reduce over-development of the sheet.

4.10 Dynamic modeling

For reasons discussed in Section 6.1, it was decided that the following equations would be used to dynamically model the fed-batch fermentation system (refer to Table 2-2 for the description of variables):

$$\frac{dF}{dt} = \mu F(t) \tag{4.2}$$

$$\frac{dV}{dt} = F(t) \tag{4.3}$$

$$\frac{dX}{dt} = \left(\mu - \frac{F(t)}{V(t)}\right) X \tag{4.4}$$

$$\frac{dA}{dt} = \left(\left(\frac{G}{G+K_A}\right)^{Kx} - \left(A_{cmax} \times \frac{A}{A+K_A}\right)\right) X - \left(\frac{F(t)}{V(t)}\right) A \tag{4.5}$$

$$\frac{dG}{dt} = \left(\frac{F(t)}{V(t)}\right) * (G_F - G) - \left(\frac{qG_{max}}{1+\frac{A}{K_G}} \times \frac{G}{G+K_G}\right) X \tag{4.6}$$

$$\frac{dL}{dt} = \left(\frac{F(t)}{V(t)}\right) * \left(L_f - L\right) - \left(\frac{qL_{max}}{1+\frac{G}{K_L}} \times \frac{L}{L+K_L}\right) X \tag{4.7}$$

These equations are representative of the fed-batch fermentation system with respect to feed, volume, cell mass, acetate, glucose, and lactose. MATLAB was also used to solve this system of equations. The values for the saturation constants were not known, so an initial guess was used. Then, the program was designed so that MATLAB would reduce the least squares difference between the experimentally determined measureables and the simulation output. This difference

was minimized by changing the saturation constants. In MATLAB, this routine was performed using the 'fminsearch' built-in function. To simulate the system of differential equations, the built-in ordinary differential equation (ODE) solver ODE15s was used. There are a number of different solvers built-in to MATLAB and this particular solver is efficient at solving stiff systems (where one component has an extremely small time step). The MATLAB code for this model is provided in Section 9.7.

After solving this initial system, other equations were examined to model acetate, glucose, and lactose in an attempt to obtain a better description of the relationship between these three variables. For acetate, the following equations were examined in addition to the equation above:

$$\frac{dA}{dt} = \frac{1}{Y_{\frac{A}{X}}} * \mu X - \left(\frac{F(t)}{V(t)}\right) A \tag{4.8}$$

$$\frac{dA}{dt} = \left(\frac{G}{G+K_A} - (A_{cmax} \times \frac{A}{A+K_A})\right) X - \left(\frac{F(t)}{V(t)}\right) A \tag{4.9}$$

Equation 4.8 is one that is typically used in the literature to model acetic acid concentrations for fed-batch fermentation (Mohseni et al., 2009; Roeva et al., 2007). However, this equation does not take into account the possibility of the re-consumption of acetic acid when other carbon sources become limiting. In this case, acetic acid is constantly excreted from the cells (given by $Y_{A/X}$). Due to the widespread nature of this equation occurring in reported models for fed-batch fermentation, it was decided to examine its usage in the context of this dissertation. Equation 4.9 is similar to the original equation proposed in the initial model. However, it no longer contains the exponent for Tessier-type kinetics, but it still contains information about glucose and the effect that glucose may have on acetate production.

For glucose, two equations were used, where the previous equation took into account the decrease in glucose uptake due to the presence of acetate:

$$\frac{dG}{dt} = \left(\frac{F(t)}{V(t)}\right) * (G_F - G) - \frac{1}{Y_{\frac{S}{X}}} * \mu X \tag{4.10}$$

$$\frac{dG}{dt} = \left(\frac{F(t)}{V(t)}\right) * (G_F - G) - \left(\frac{qG_{max} * G}{G + K_G}\right) X \tag{4.11}$$

Equation 4.10 takes into account the addition of glucose into the reactor due to feeding and subtracts the amount of glucose that is consumed by the cells ($Y_{S/X}$). However, this equation assumes that consumption of glucose (yield of cells from substrate) is constant throughout the entire fermentation process. It also does not take into account the presence and consumption of other carbohydrates. Equation 4.11 follows the same Monod-type equation, but in this equation, it is assumed that acetate does not affect glucose uptake.

For lactose, one additional equation was examined:

$$\frac{dL}{dt} = \left(\frac{F(t)}{V(t)}\right) * \left(L_f - L\right) - \left(\frac{qL_{max} * L}{L + K_L}\right) X \tag{4.12}$$

Equation 4.12 mirrors Equation 4.11, but for lactose consumption instead of glucose consumption. The underlying assumption in this equation is that lactose is not affected by glucose concentrations.

A combination of these equations was used in an attempt to "optimize" the model for the fed-batch experiments performed. A number of iterations of the simulation were performed to gain a better understanding of the relationship between the carbohydrates and their saturation coefficients.

4.11 Metabolic flux analysis

As discussed in Section 2.5, metabolic flux analysis is used to gain access to information about the processes that occur within the cell by tracking the movement of carbon throughout the system. For the system examined in this dissertation, the pathways of three major metabolic processes were examined: glycolysis, tricarboxylic acid cycle, and hexose monophosphate pathway (Figure 4-6). The incorporation of lactose and glycerol into the system was also considered (Figures 4-7 and 4-8).

A balance equation can be written for each component in the system. For example, for the metabolic map given in Figure 4-6, the balance around glucose 6-phosphate can be written as $x_2 = r1 + r33 - r2 - r3 - r4$. Here, x_2 represents glucose 6-phosphate, *r1* and *r33* both feed into glucose 6-phosphate from glucose and lactose, respectively, and *r2*, *r3*, and *r4* all pull from glucose 6-phosphate (hence the subtraction from the overall concentration of glucose 6-phosphate). This information can be compiled into matrix form where each balance equation represents a row in the matrix. Mathematically, all information about the system can be written in the form of $\boldsymbol{A} \cdot \boldsymbol{r} = \boldsymbol{x}$ where **A** is a matrix that contains all of the stoichiometric information, **r** is a vector that contains the information about transport and reaction fluxes, and **x** is a vector that contains metabolite concentration data (Covert et al., 2001).

It is important to note that a couple of assumptions have been made about the system. First of all, it is assumed that all intermediates exist in a "pseudo-steady state" environment, and hence no accumulation occurs (Kauffman et al., 2003). Secondly, the steady state assumption is also used for the production of cellular components. Here, the concentration of the required components is based on the cellular composition and the demands of precursors for the

production of biomass and protein. This is discussed in detail below. The last set of information comes from the experimentally determined concentrations of certain metabolites (lactose, glucose, acetate, etc.) and information about biomass production.

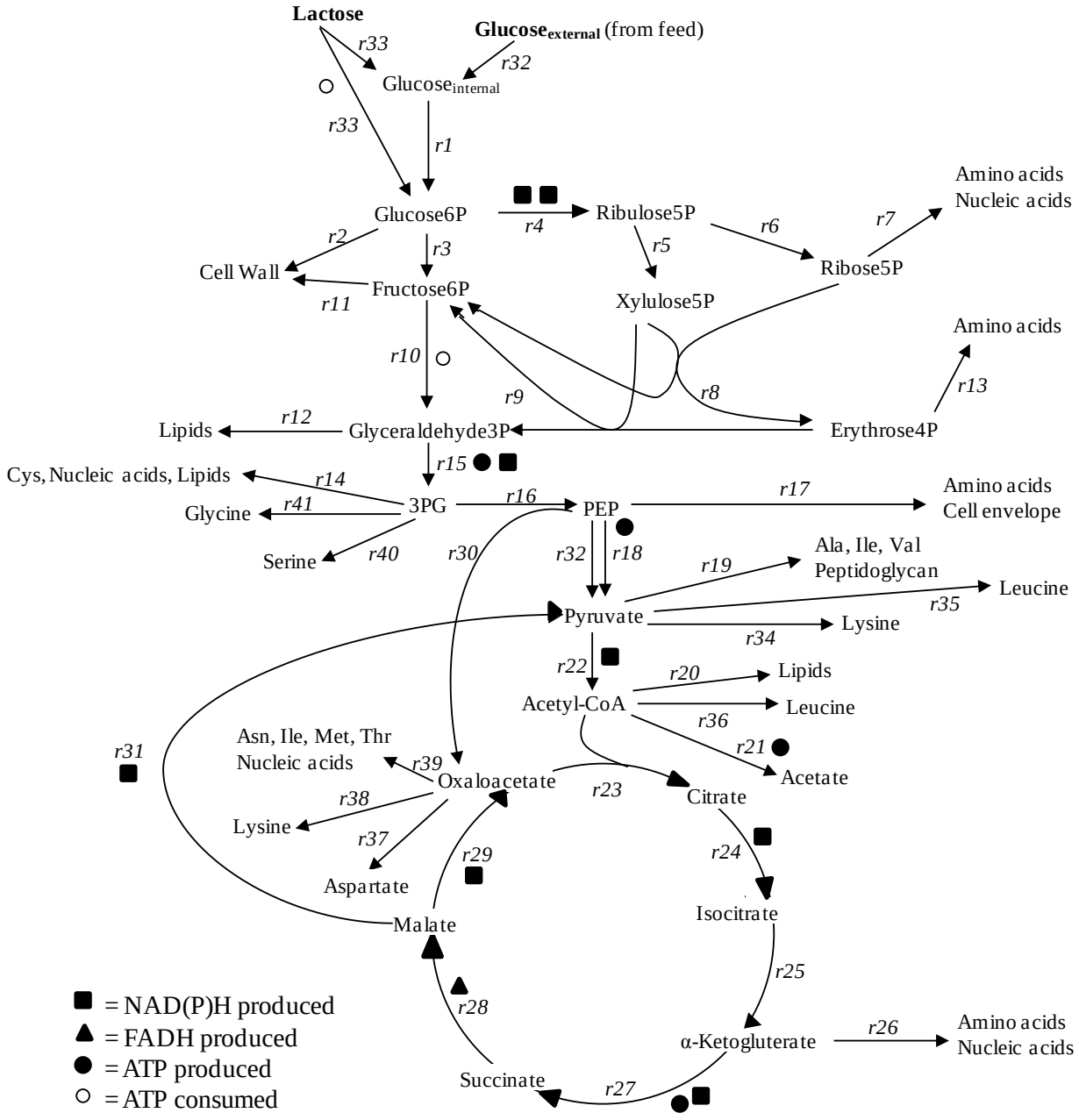

Figure 4-6. Metabolic network incorporating the consumption of lactose in addition to the feeding of glucose.

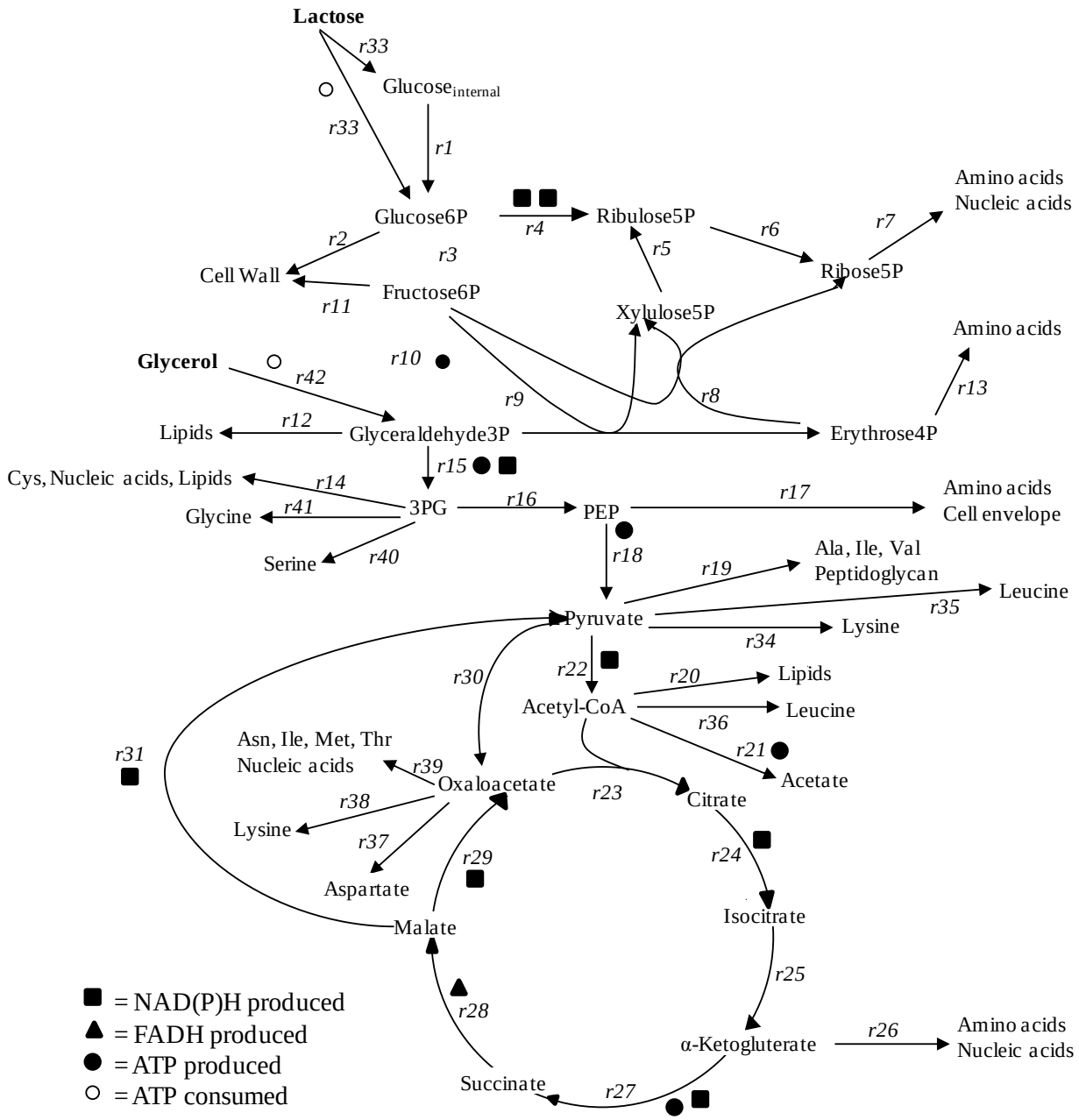

Figure 4-7. Metabolic pathways incorporating induction with lactose and glycerol feed.

Figures 4-6, 4-7, and 4-8 give the metabolic pathways that were examined using metabolic flux analysis. The significant differences between the three maps is the incorporation of glycerol and the absence of other carbohydrates. In the absence of glucose and lactose, gluconeogenesis occurs. With glycerol feed, the HMP pathway fluxes were reversed in order to

make glucose from glycerol. It is also important to reverse these fluxes so that the necessary precursors can be synthesized from other HMP pathway components (e.g. amino acids and nucleic acids from ribose 5-phosphate). Upon glycerol uptake, an ATP molecule is required for the phosphorylation of glycerol and ultimate synthesis of glyceraldehyde 3-phosphate. The map in Figure 4-7 was used when lactose was still present in the system and glycerol was used as the feed source. Figure 4-8 is representative of the fluxes when lactose was no longer present in the media and glycerol was used as a feed source. With this system, there are two possible scenarios. One involves simply removing the internal glucose flux and lactose flux from the map in Figure 4-7. The other possibility is that the carbon from the glycerol flux is stored as glycogen. An additional ATP molecule is required for this step. The pathway representing this phenomenon is indicated by the dashed oval in Figure 4-8.

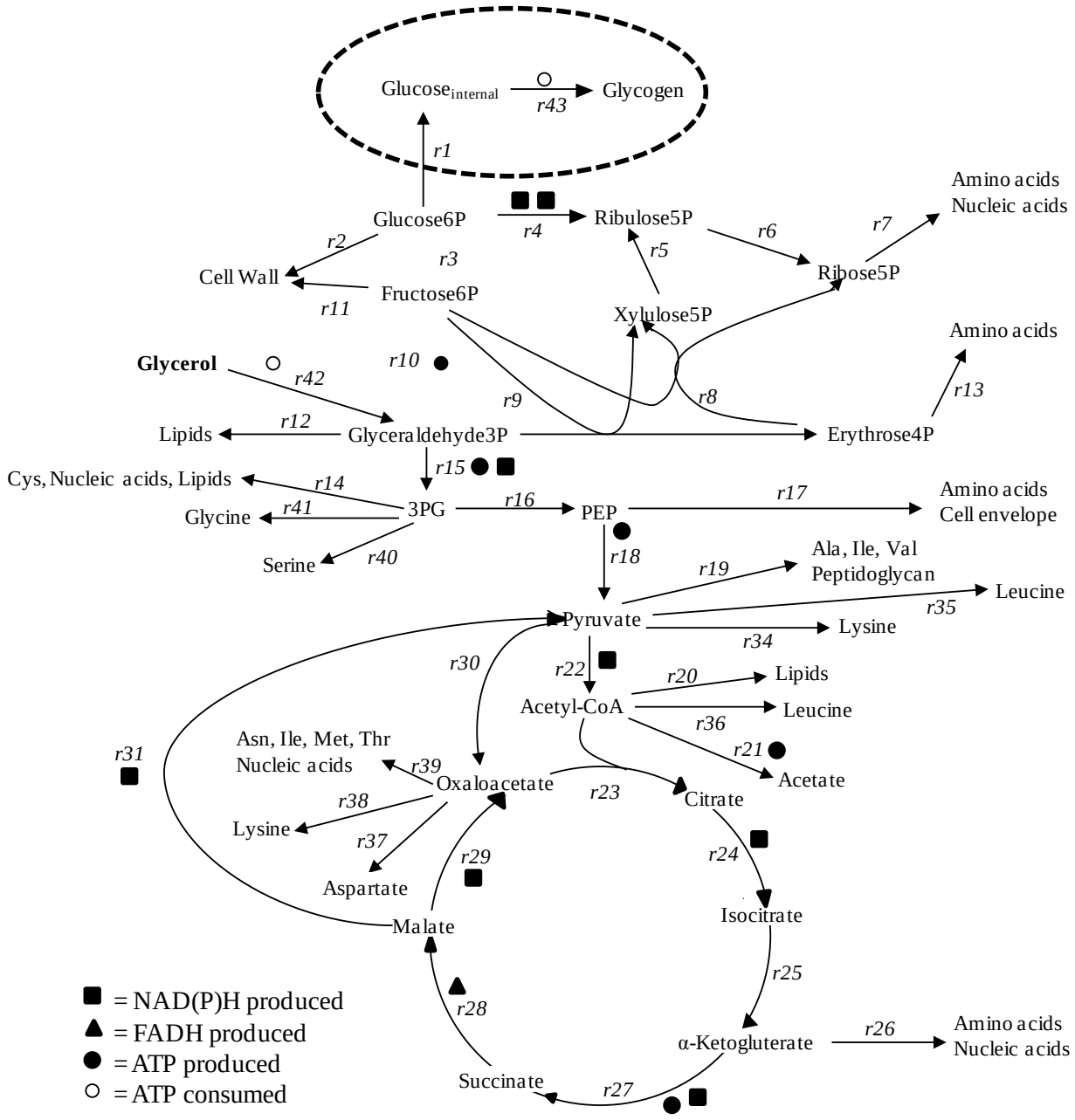

Figure 4-8. Flux pathway when glycerol is the only carbohydrate fed into the system and present in the media (after lactose has been depleted).

The corresponding chemical reactions are given in the Appendix (9.5), but the mathematical representation of these reactions is given below.

Intermediates:

$x1 = r32 + r33 – r1$		Balance on internal glucose
$x2 = r1 + r33 – r2 – r3 – r4$		Balance on glucose 6-phosphate
$x3 = r4 – r5 – r6$		Balance on ribulose 5-phosphate
$x4 = r6 – r7 – r8$		Balance on ribose 5-phosphate
$x5 = r5 – r8 – r9$		Balance on xylulose 5-phosphate
$x6 = r3 + r8 + r9 – r10 – r11$		Balance on fructose 6-phosphate
$x7 = r8 – r9 – r13$		Balance on erythrose 4-phosphate
$x8 = 2* r10 + r9 + r42 – r12 – r15$		Balance on glyceraldehyde 3P
$x9 = r15 – r16 – r14 – r40 – r41$		Balance on 3-phosphoglycerate
$x10 = r16 – r17 – r18 – r30 – r32$		Balance on phosphoenol pyruvate
$x11 = r31 + r32 + r18 – r19– r22 – r34 – r35$		Balance on pyruvate
$x12 = r22 – r20 – r21 – r23 – r36$		Balance on acetyl-CoA
$x13 = r23 – r24$		Balance on citrate
$x14 = r24 – r25$		Balance on isocitrate
$x15 = r25 – r26 – r27$		Balance on α-ketoglutarate
$x16 = r27 – r28$		Balance on succinate
$x17 = r28 – r29 – r31$		Balance on malate
$x18 = r29 + r30 – r23 – r37 – r38 – r39$		Balance on oxaloacetate
Precursors:		
$x19 = r7$	$= \rho 7*D$	AA, NA from ribose 5-phosphate
$x20 = r13$	$= \rho 13*D$	AA from erythrose 4-phosphate
$x21 = r17$	$= \rho 17*D$	AA, Cell envelope from PEP
$x22 = r19$	$= \rho 19*D$	AA, peptidoglycan from pyruvate
$x23 = r20$	$= \rho 20*D$	AA, Lipids from AcCoA
$x24 = r26$	$= \rho 26*D$	AA, NA from α-ketoglutarate
$x25 = r39$	$= \rho 39*D$	AA, NA from oxaloacetate
$x26 = r14$	$= \rho 14*D$	AA, NA, Lipids from 3PG
$x27 = r12$	$= \rho 12*D$	Lipids from glyceraldehyde 3P
$x28 = r11$	$= \rho 11*D$	Cell wall from fructose 6-phosphate
$x29 = r2$	$= \rho 2*D$	Cell wall from glucose 6-phosphate
$x30 = r34$	$= \rho_{Lys\_PYR}*D$	Lysine from pyruvate
$x31 = r35$	$= \rho_{Leu\_PYR}*D$	Leucine from pyruvate
$x32 = r37$	$= \rho_{Asp\_OA}*D$	Asparate from OA
$x33 = r38$	$= \rho_{Lys\_OA}*D$	Lysine from OA
$x34 = r36$	$= \rho_{Leu\_AcCoa}*D$	Leucine from acetyl-CoA
$x35 = r40$	$= \rho_{Ser\_3PG}*D$	Serine from 3-phosphoglycerate
$x36 = r41$	$= \rho_{Gly\_3PG}*D$	Glycine from 3-phosphoglycerate
$x40 = 2*r4 + r24$	$= 18*D$	NADPH balance
Measureable components:		
$x37 = r21$	$= C_{acetate}*(D/X)$	Balance on acetate
$x38 = r32$	$= C_{glucose}*(D/X)$	External glucose uptake
$x39 = 2*r33$	$= C_{lactose}*(D/X)$	Lactose uptake (breakdown)
$x41 = r42$	$= C_{glycerol}*(D/X)$	Balance on glycerol

For the intermediates given above, $x_i = 0$ due to the pseudo-steady state assumption (no accumulation of metabolic intermediates). In order to calculate the precursor pool demands for cell maintenance along with production of target protein, one must have information about the requirements for cell growth. This information, along with the metabolic precursors from which the amino acids, dNTP's, etc. are derived, was compiled and is given in Table 4-3. The information about the type and amount of precursor required for the target protein is given in Table 4-4. This information was calculated from the amino acid composition (Table 4-1).

Assuming that P is the mass percentage of target protein production to total cell mass, the calculation of precursor demand (given by ρ) can be written as the following:

$$\rho = P*\rho_P + (1-P)*\rho_{c\_p} + \rho_{c\_o} \quad (4.13)$$

In this equation, ρ_P represents the precursor demand from target protein expression (sum of the demands for the target protein amino acids); ρ_{c_p} represents the precursor demand from proteins for cellular composition (sum of the demands for amino acids); and ρ_{c_o} represents the precursor demand for other cellular components (non-protein sum). As an example, consider that the percentage of target protein is 10 and examine the requirements for 3-phosphoglycerate (3PG). Then, the precursor demand is:

$$\rho = P*\rho_P + (1-P)*\rho_{c\_p} + \rho_{c\_o} = 0.1*1.275 + 0.9*0.874 + 0.6164 = 1.5305 \quad (4.14)$$

The values for ρ_i are given in Tables 4-3 and 4-4 for each metabolic precursor. These calculations were performed for all of the metabolic precursors and are shown in Section 9.6. The precursor values were multiplied by the dilution rate (growth rate - D) to get the final amounts needed for protein expression and cell growth. This information was contained in the

accumulation vector because these minimal amounts of metabolites are required for cell maintenance and protein expression.

Unlike other metabolic flux models, information about the addition of the amino acids in the media was contained in this model. As shown in Figures 4-6 and 4-7, pyruvate, acetyl-CoA, 3-phosphoglycerate, and oxaloacetate are all metabolic precursors for certain amino acids that were contained in the media. Thus, these precursors were not in as high demand for production of certain amino acids. This information was included by considering the fluxes of these amino acids (Lys, Leu, Asp, Gly, Ser) separate from the total amino acid flux. Then, since the concentration of the amino acid was known, this information was added in the **x** vector. Consider, for example, the flux of leucine from acetyl-CoA. The individual precursor demand for leucine was subtracted from the total precursor demand because the demand was not as high due to the presence of leucine in the media. The same logic followed for the other amino acids in the media. Since leucine and lysine are produced from two different metabolic precursors, these amino acids appear two times as a component in the system (each component from their different metabolic precursors).

Additionally, since the final amount of product was known, the amount of each amino acid (C_i) required for production was calculated by multiplying the amount required per gram protein ($C_{i\_protein}$, Table 4-4) and adding this to the product of the amount required for cell maintenance (C_{i_cell}, Table 4-3) and grams of biomass:

$$C_i = C_{i\_cell}*\text{Biomass} + C_{i\_protein}*\text{Protein}_{total} \quad (4.15)$$

The information about carbohydrates and biomass also helped constrain the system.

Table 4-3. Synthesis of monomers from metabolic precursors (based on stoichiometry) (Chassagnole et al., 2002; Pramanik and Keasling, 1997; Varma et al., 2004)**.**

Monomer	mmol/g cell	G6P	F6P	Gly3P	R5P	E4P	3PG	PEP	PYR	AcCoA	OA	KG
Ala	0.488								0.488			
Arg	0.281											0.281
Asn	0.229										0.229	
Asp	0.229										0.229	
Cys	0.087						0.087					
Glu	0.250											0.250
Gln	0.250											0.250
Gly	0.582						0.582					
His	0.090				0.090							
Ile	0.276								0.276		0.276	
Leu	0.428								0.856	0.428		
Lys	0.326								0.326		0.326	
Met	0.146										0.146	
Phe	0.176					0.176		0.352				
Pro	0.210											0.210
Ser	0.205						0.205					
Thr	0.241										0.241	
Trp	0.054				0.054	0.054		0.054				
Tyr	0.131					0.131		0.262				
Val	0.402								0.804			
Sum	5.081				0.144	0.361	0.874	0.668	2.750	0.428	1.447	0.991
ATP	0.165				0.165		0.165					
GTP	0.203				0.203		0.203					
CTP	0.126				0.126						0.126	
UTP	0.136				0.136						0.136	
dATP	0.0247				0.0247		0.0247					
dGTP	0.0254				0.0254		0.0254					
dCTP	0.0254				0.0254						0.0254	
dUTP	0.0244				0.0244						0.0244	
Lipid A	0.129			0.129			0.129					
Lipid B	0.258									2.1156		
Lipo A	0.0157	0.0157	0.0157									
Lipo B	0.0235	0.0353			0.0235		0.0235	0.0235		0.329		
Pep A	0.0276		0.0552					0.0276	0.0276	0.0552	0.0276	0.0276
Pep B	0.0552								0.0552			
Glyc	0.154	0.154										
1 C	0.0485						0.0458					
Orn	0.0593											0.0593
Sum	1.5007	0.205	0.0709	0.129	0.7534	0	0.6164	0.0511	0.0828	2.4998	0.3394	0.0869
Total	6.582	0.205	0.071	0.129	0.897	0.361	1.490	0.719	2.833	2.928	1.786	1.078

Table 4-4. Metabolic costs for production of GST-PTH-CBD.

Monomer	mmol/g cell	G6P	F6P	Gly3P	R5P	E4P	3PG	PEP	PYR	AcCoA	OA	KG
Ala	0.342								0.342			
Arg	0.342											0.342
Asn	0.410										0.410	
Asp	0.615										0.610	
Cys	0.091						0.091					
Glu	0.205											0.205
Gln	0.615											0.615
Gly	0.706						0.706					
His	0.228				0.228							
Ile	0.592								0.592		0.592	
Leu	0.820								1.640	0.820		
Lys	0.706								0.706		0.706	
Met	0.296										0.296	
Phe	0.296					0.296		0.592				
Pro	0.501											0.501
Ser	0.478						0.478					
Thr	0.296										0.291	
Trp	0.137				0.137	0.137		0.137				
Tyr	0.570					0.570		1.140				
Val	0.478								0.956			
Sum	8.725				0.365	1.003	1.275	1.869	4.236	0.820	2.905	1.663

After compiling all of this information, the system was solved for **r** using linear programming methods. Since there was an optimization call in this part of the model, the built-in MATLAB function 'linprog' was used. For this routine, the optimization statement, stoichiometric matrix, and accumulation vector are inputs. The output is the resultant fluxes with information about convergence and the number of iterations that were performed before the optimal set of fluxes was found. This function optimizes biomass production by optimizing the values for the fluxes that lead to biomass synthesis. The following fluxes from Figure 4-6 were optimized: *r2, r7, r11, r12, r13, r14, r17, r19, r20, r26, r34, r35, r36, r37, r38, r39, r40,* and *r41*. The result is a vector that contains the intermediate fluxes the optimized the fluxes listed above. This particular function constrains the possible outputs in a manner that all fluxes must be

greater than or equal to zero. This aided in reducing the solution space for the minimization routine.

The resultant fluxes for this model gave a final snapshot of the system with regard to concentrations and production of biomass components. Only the final concentrations for acetate, glucose, lactose, glycerol, and biomass were used in the calculations that helped determine the fluxes. For many of the experiments, modeling the system using only the final concentrations for carbohydrates and biomass was not sufficient to describe the system as a whole due to the early elapsed time in which the stationary phase of the fermentation system was reached. In this case, it was interesting to examine the change in the fluxes from time point to time point by using the experimental data taken from the experiment. Once again, by optimizing the fluxes from metabolic precursors to cell wall components, the overall biomass formation was optimized. The same fluxes were optimized as those in the overall snapshot model (described in the previous paragraph). These fluxes contribute to the formation of amino acids, cell wall, lipids, nucleic acids, cell envelope, and peptidoglycan. The precursors that are required for cell formation and protein production were calculated the same way as before.

After performing the optimization routine, the output was the resultant fluxes that allowed for optimization of the biomass. Here, **A** was the same stoichiometric matrix as before and **x** contained information about the intermediates (concentration is zero), the precursor information, and concentrations determined from the experiments. However, unlike before, the accumulation vector contained information about the fluxes of carbons at each time step were used. For example, samples were taken at 16, 18, 20, and 22 hours for the 12 hr lactose-induced experiment. The concentration changes of lactose and glucose (or glycerol) between each time

point were calculated on a mM/hr basis. The biomass was also averaged and the acetate production was calculated. For this step-by-step analysis, the dilution factor was not required for calculation of the concentrations due to the averaging of the concentrations over the time interval at which the samples were taken (one or two hours depending on the experiment).

As a test to the validity of the model, the next experimental concentration can be compared with the simulated concentration by using the flux information and methods comparable to Euler's method:

$$C_{i+1} = C_i + r_i * \Delta t * \text{Biomass} \tag{4.16}$$

Here, multiplying the flux for glucose or glycerol, acetate, or lactose from the simulation by the time step and the averaged biomass (2 hours in most cases) and adding this product to the initial concentration yielded information about the new concentration. The MATLAB code for the generation of the metabolic flux analysis is given in the Appendix (Section 9.8).

After solving for the fluxes, the ATP balance was used to calculate the yield of cells from ATP. This provided useful information about the effect that different inducers and feed sources have on the biomass production from ATP. The balance equation for ATP depended on the fermentation experiment that was modeled. For example, the breakdown of lactose to glucose 6-phosphate through galactose metabolism requires a molecule of ATP. Similarly, glycogen synthesis and the synthesis of glyceraldehyde 3-phosphate from glycerol both require ATP. However, the contribution of NAD(P)H and FADH to ATP synthesis did not depend on the experimental method. For each experiment, the following balances exist:

$$\text{NAD(P)H} = 2*r4 + r15 + r22 + r24 + r27 + r29 + r31 \tag{4.17}$$

$$FADH = r28 \quad (4.18)$$

$$ATP = -r10 + r15 + r18 + r21 + r27 \quad (4.19)$$

$$ATP_{total} = ATP + 1.3*(2/3)*FADH + 1.3*NAD(P)H \quad (4.20)$$

For lactose in the media, *-r33* should be added to the ATP equation. For glycerol feed, *-r42* should be added. Lastly, in the case that glycogen is synthesized, *-r43* should be added to the equation. Also, for glycerol-fed experiments, the reversal of fluxes through glycolysis and the HMP pathway will cause production of ATP so r10 would not be subtracted, but added. The coefficient of 1.3 represents the number of ADP molecules that are phosphorylated per electron pair transferred to oxygen during respiration. Also, it is assumed that one molecule of FADH is equivalent to 2/3 molecule of NADH. The requirement of ATP for the synthesis of glucose 6-phosphate from glucose is not considered because it is added into the model as a biosynthetic demand (Holm's table). Using these balances, the resultant yield for biomass from ATP in gram cell/mol ATP were calculated using Equation 4.21:

$$Y_{x/ATP} = (1000*D)/ATP_{total} \quad (4.21)$$

5. Results and discussion

5.1 Shake flask cultivations

A number of experiments were performed to examine the effects of media on the growth of *E. coli* harboring plasmid pCHC305. From this point on, the bacterial strain will simply be referred to as pCHC305 and target therapeutic protein will be referred to as GST-PTH-CBD. Figure 5-1 shows results from the study of growth on LB and its dependency on glucose. As shown in Figure 5-1, LB supplemented with glucose allowed for slightly higher optical densities. Though, this increase was not significant, as the growth rate for both cultures was equivalent. However, LB supplemented with glucose did not enhance therapeutic protein production as evident by similar band intensities of protein near the target molecular weight in Figure 5-2. Equal concentrations of total protein were loaded to each lane in the SDS-PAGE gel. GST-PTH-CBD runs at approximately 44 kDa on a 12.5% gel. It is interesting to note that the length of the induction period also did not have an effect on protein production when cells were grown in LB or LB supplemented with glucose and induced with IPTG. This indicated that there was a basal expression level of target protein in the absence of inducer.

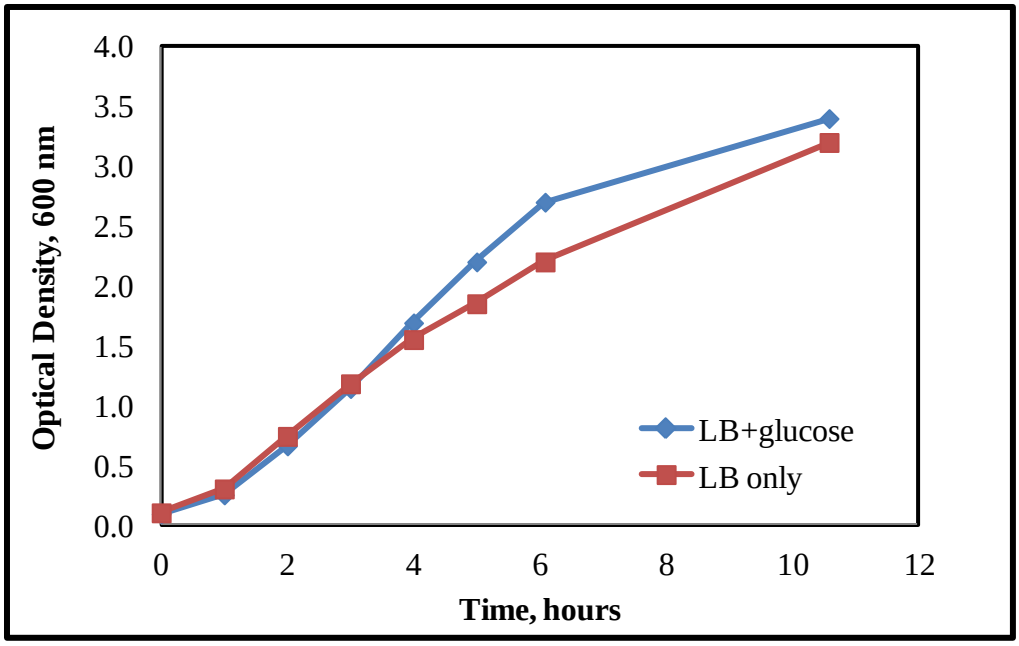

Figure 5-1. Comparison of growth on LB or LB + glucose. Growth chart indicates that LB supplemented with glucose allowed for slightly higher optical densities of pCHC305 when grown in LB.

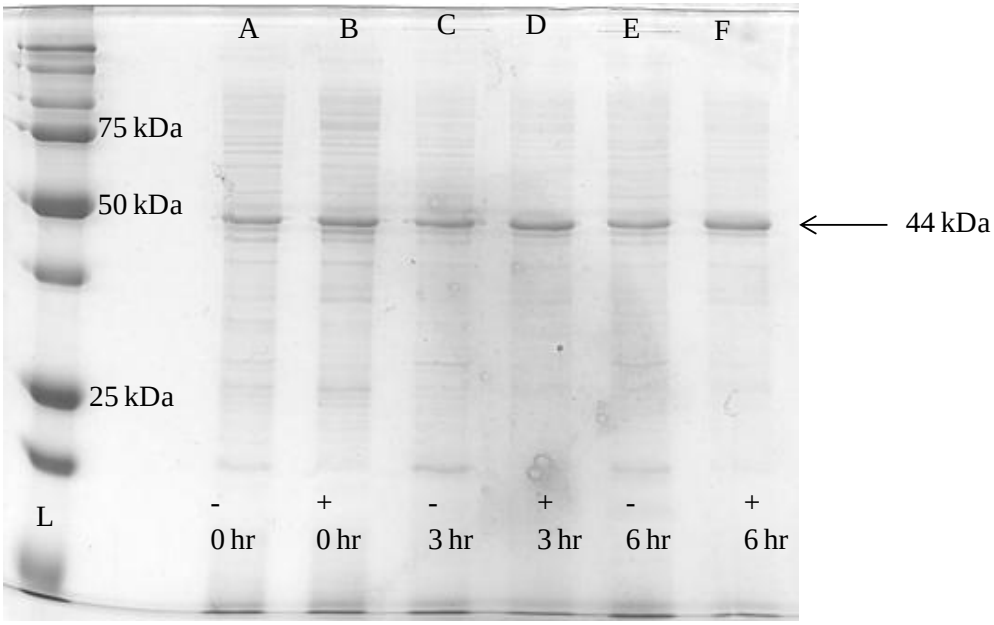

Figure 5-2. Comparison of protein expression on LB or LB supplemented with glucose. SDS-PAGE gel shows protein expression with and without glucose present in the medium. Negative sign indicates lack of glucose; positive sign indicates presence of glucose. Sign is followed by the time (after induction).

While growth curves are important to consider when choosing a proper medium, protein expression on the medium is perhaps more important. The next step was to test the expression of GST-PTH-CBD when using a defined medium, such as M9 supplemented with glucose. To examine the expression of GST-PTH-CBD on M9 supplemented with glucose, lysates from cells grown on M9 + 10 g/l glucose or LB were loaded to a 12.5% SDS-PAGE gel. The same concentration of protein was loaded to each lane in order for direct comparison of target protein production. As indicated by the intensity of the band in lane 4 at 44 kDa in Figure 5-3, M9 + glucose allowed for higher expression of GST-PTH-CBD (compared to lysates from cells grown on LB). For the remainder of this dissertation, M9 + glucose will refer to M9 supplemented with 10 g/l of glucose.

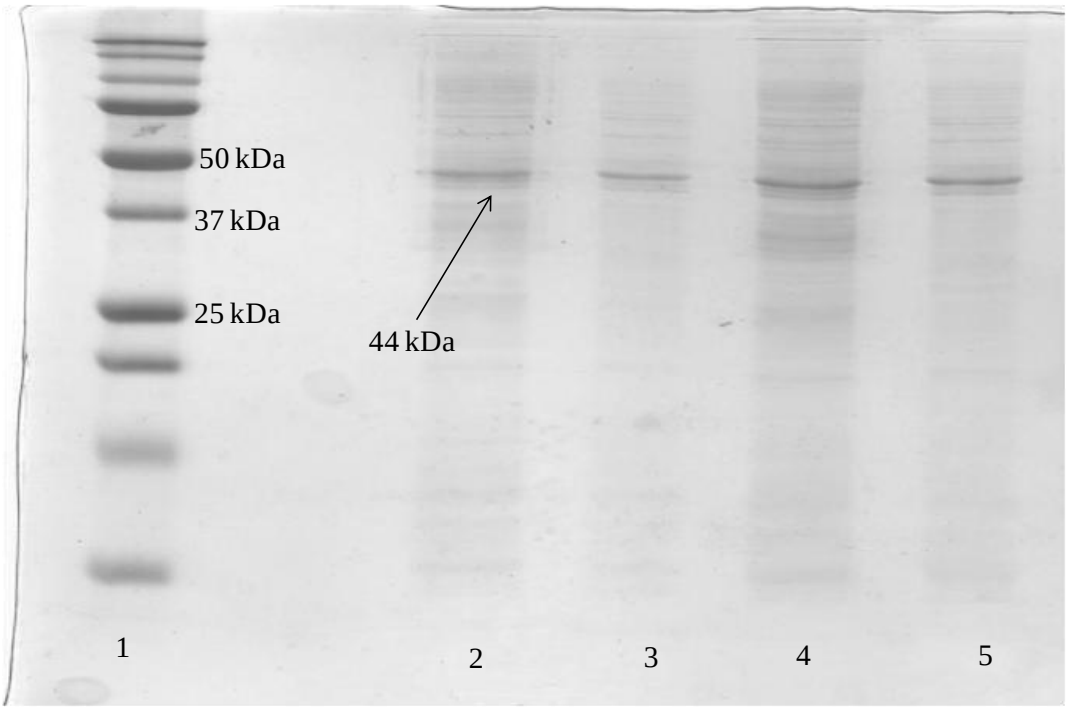

Figure 5-3. Comparison of GST-PTH-CBD expression from cells grown on LB or M9. Lane 1 – molecular weight standard; 2 – pre-induction, M9 + glucose; 3 – pre-induction, LB; 4 – post induction, M9 + glucose; 5 – post induction, LB.

Since M9 + glucose was found to be a viable choice as a growth medium for pCHC305, induction experiments were carried out to determine the effect that lactose or IPTG had on the expression of GST-PTH-CBD. Induction was carried out with 10 g/l lactose or 10 mM IPTG at an optical density between 0.6 and 0.8 units. As shown by the western blot in Figure 5-4, the greatest amount of target protein was expressed two hours after induction with IPTG because the band at 44 kDa is much more intense for this lysate. Qualitatively, expression amounts seemed to taper as the length of the induction period increases. Even though higher optical densities were achieved when lactose was the inducer (data shown below), a higher amount of target protein was expressed when IPTG was used.

It is also in this western blot that an intense band representing degraded protein is apparent. This lower band runs at approximately 26 kDa on a SDS-PAGE gel and interacts with the antibodies used for the western blot procedure. It was determined by mass spectrometry that this lower band is glutathione-s-transferase (GST). This is this tag used for the target protein. It is conjectured that the GST portion of the protein is released from the ribosome before the remaining portion of the protein is translated. This phenomenon is referred to as ribosomal pause. The appearance of this band could also be due to proteases cleaving the site between GST and PTH-CBD during cultivation.

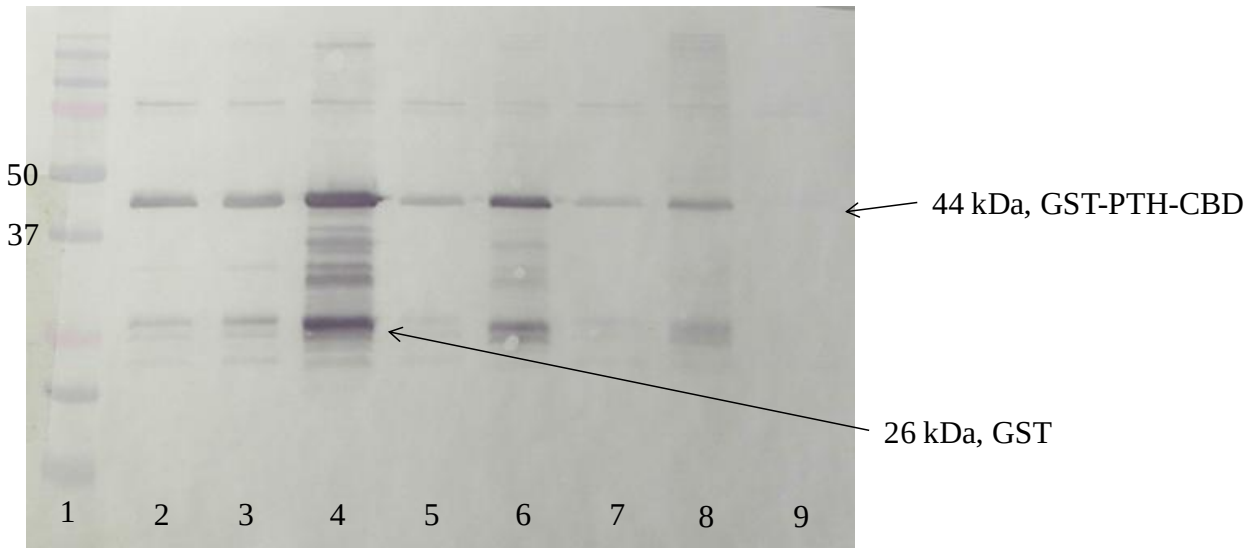

Figure 5-4. Western blot of lysates from lactose or IPTG induction with M9 + glucose media. Lane 1 – molecular weight standard; 2 – pre-induction, IPTG; 3 – pre-induction, lactose; 4 – 2 hr post IPTG; 5 – 2 hr post lactose; 6 – 4 hr post IPTG; 7 – 4 hr post lactose; 8 – final, IPTG; 9 – final, lactose. Basal amount of target protein is present prior to induction.

To further increase therapeutic protein expression, M9 + glucose was supplemented with amino acids. Growth on M9 + glucose supplemented with amino acids and thiamine was also investigated. As shown in Figure 5-5, using M9 + glucose or M9 + glucose supplemented with amino acids (with or without thiamine) extended the time at which the culture reached the stationary phase of growth. Additionally, cultures grown on M9 + glucose supplemented with amino acids achieved higher optical densities than those grown on M9 + glucose without amino acids.

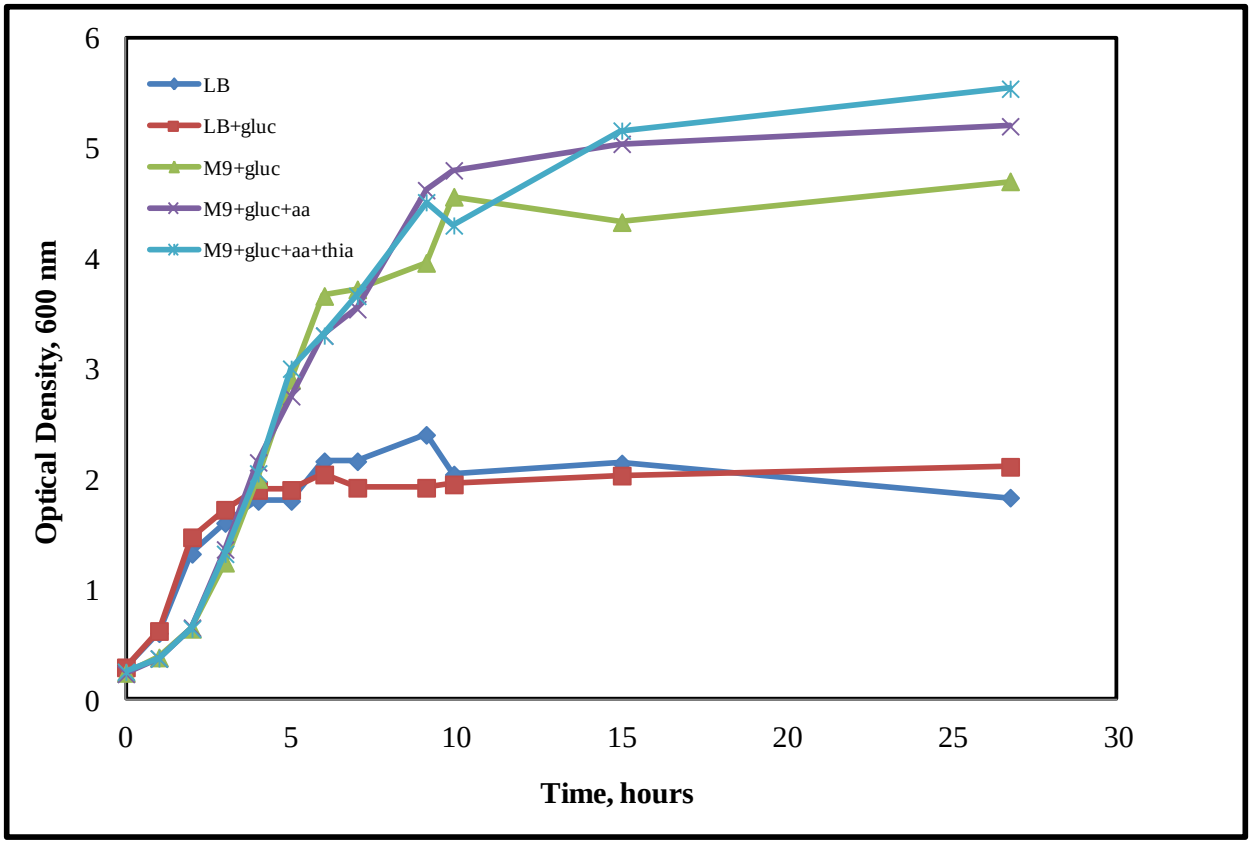

Figure 5-5. Growth curve comparison of LB versus M9 + glucose supplemented with amino acids. Cultures grown on M9 supplemented with amino acids achieved over two times the optical densities as those grown on LB by extending the time at which the stationary phase of growth is reached. For reasons discussed below, the concentration of the additional amino acids was 5 mM for this experiment.

Next, the effect of different amino acid concentrations on growth was examined. Shake flask cultivations were performed with M9 + glucose supplemented with 0, 5, or 10 mM of amino acids. Lysine, aspartate, glycine, serine, and leucine were added to final concentrations of 5 or 10 mM in M9 + glucose. Samples were again taken during cultivation to track protein expression and growth. The inducer (lactose or IPTG) was added at the mid-exponential phase of growth (between 0.6 and 0.8 optical density units). This was typically 3-4 hours after inoculation. Figure 5-6 shows growth dependency on inducer type and/or amino acid concentration.

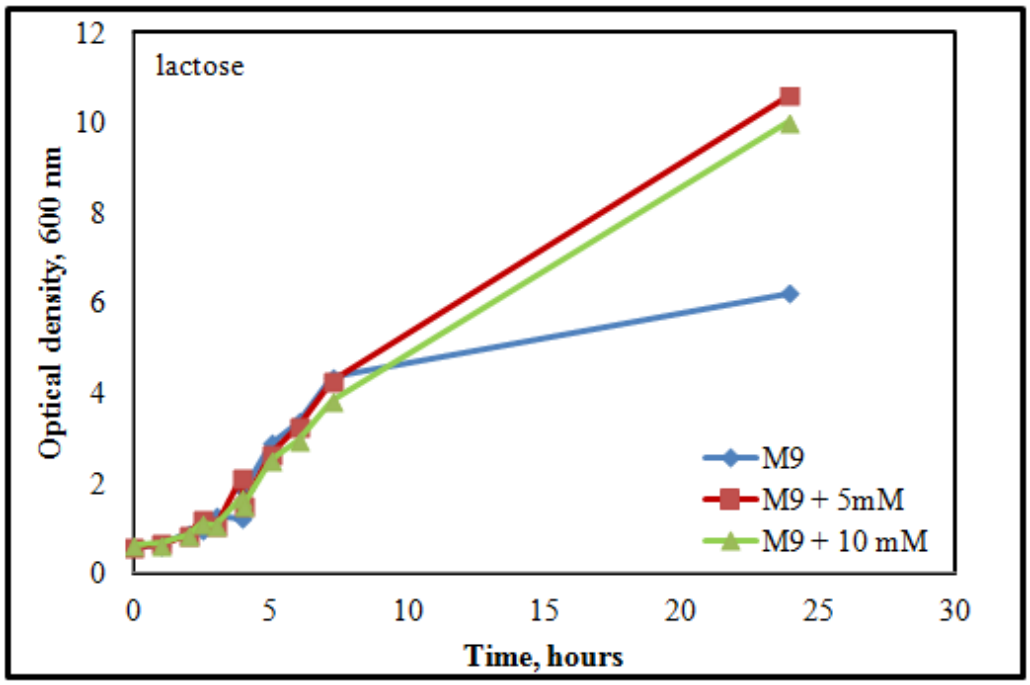

(a)

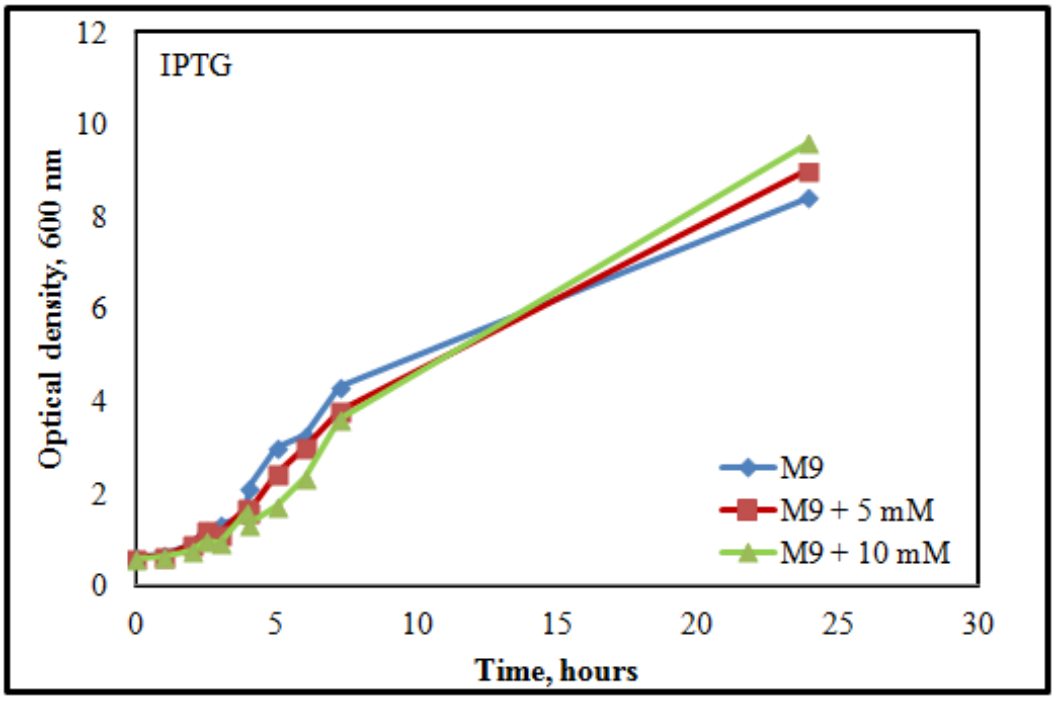

(b)

Figure 5-6. Growth characteristics of induced cultures grown on M9 supplemented with different concentrations of amino acids. (a) Cultures were induced with lactose. Shake flasks supplemented with amino acids reached higher optical densities than that without the addition. (b) Cultures were induced with IPTG. In both figures, M9 was supplemented with 10 g/l glucose.

In the end, similar results were achieved - shake flasks supplemented with amino acids had higher final optical densities, especially when lactose was used as the inducer. It is important to note that cultures induced with lactose and supplemented with amino acids achieved higher optical densities than those induced with IPTG. This was also important because the lactose-induced cultures were able to sustain growth for a longer period of time. This is likely due to the fact that lactose can act as a carbon source for *E. coli*.

Western blots were also performed to examine expression in M9 + glucose supplemented with amino acids based on inducer type. Western blots with lysates from cells taken at four hours after induction are shown in Figure 5-7. Figure 5-8 depicts lysates from cells taken 22 hours after inoculation.

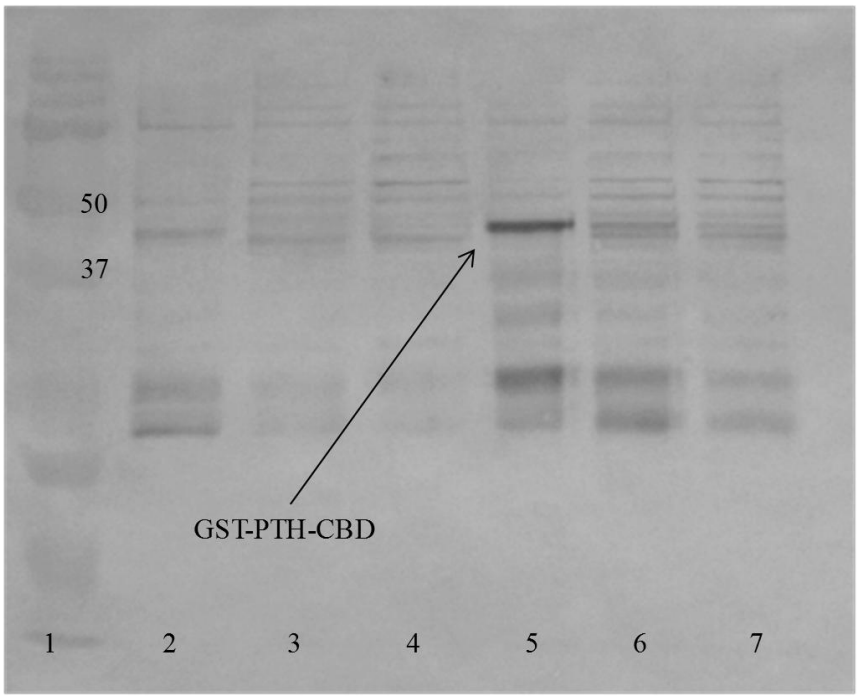

Figure 5-7. Western blot of lysates from cells grown on M9 + glucose supplemented with different concentrations of amino acids induced with IPTG or lactose for four hours. Lane 1 – molecular weight standard; 2 – M9 + glucose, lactose; 3 – M9 + glucose + 5 mM amino acids, lactose; 4 – M9 + glucose + 10 mM amino acids, lactose; 5 – M9 + glucose, IPTG; 6 – M9 + glucose + 5 mM amino acids, IPTG; 7 – M9 + glucose + 10 mM amino acids, ITPG.

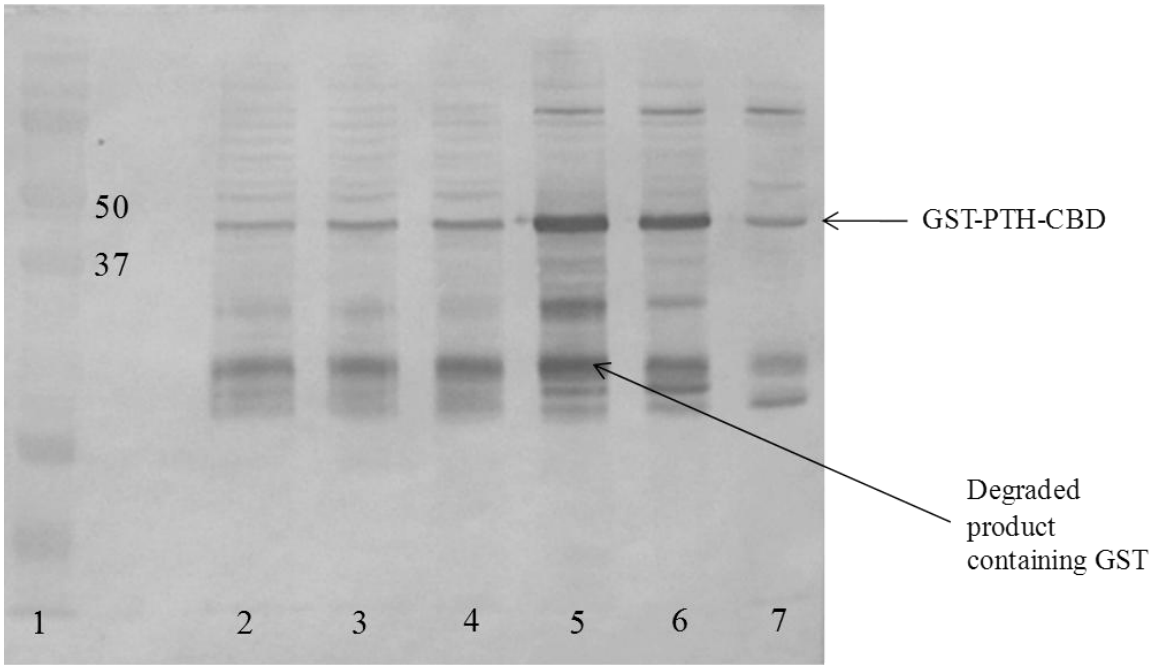

Figure 5-8. Western blot of lysates from cells grown on M9 + glucose supplemented with different concentrations of amino acids induced with IPTG or lactose for 22 hours. Lane 1 – molecular weight standard; 2 – M9 + glucose + 10 mM amino acids, IPTG; 3 – M9 + glucose + 5 mM amino acids, IPTG; 4 – M9, IPTG; 5 – M9 + glucose + 10 mM amino acids, lactose; 6 – M9+ glucose + 5 mM amino acids, lactose; 7 – M9, lactose.

It is evident through the intensity of the band at appropriate molecular weight in these two western blots that M9 + glucose supplemented with amino acids greatly enhanced GST-PTH-CBD expression when lactose is used was the inducer. But, for this case to hold true, the induction period must last for approximately 22 hours. After an induction period of four hours, there was an increase in target protein expression only in the IPTG induced sample with M9 + glucose only. Amino acids did not aid in the production of target protein when IPTG was used as the inducer, and at an induction period of four hours, lactose did not act as an inducer. This result could be due to catabolite repression, as previously discussed in Section 2.4.1. At four hours, glucose was still present in the culture broth, so lactose uptake was repressed.

As shown in Figure 5-8, pCHC305 grown on M9 supplemented with 10 mM amino acids and induced with lactose expressed the greatest amount of GST-PTH-CBD. This sample also had the highest concentration of degraded product, as the intensity of lower bands in lane 5 was greater. Additionally, the amount of sodium hydroxide that was needed to increase the pH of the medium supplemented with 10 mM amino acids to 6.8 caused some of the salts to precipitate. It is for these reasons that it was decided to use a 5 mM amino acid concentration to supplement M9 in further experiments.

Since amino acids appear to aid in protein expression when lactose is used as an inducer, experiments were performed to see if auto-induction would work for shake flasks. This could automate the induction process, as everything is in the medium prior to cultivation. Shake flask experiments were carried out to monitor the difference between auto-induction and manual induction. Unlike work done by others, there were no undefined components added to the medium, for the auto-induction experiment. M9 + glucose was used, with the only addition being lactose and amino acids. After analysis of the samples taken from shake flasks, it was determined that auto-induction did not have an effect on protein expression. The samples with lactose initially present and lactose manually added at the mid-exponential phase did not exhibit any significant increases. This finding makes sense with the analysis of carbohydrate concentrations portrayed in Figure 5-9. HPLC results indicated that the lactose concentration did not change throughout the cultivation, and after 25 hours, there was still glucose present in the medium. Although, as shown in Figures 5-7 and 5-8, induction via lactose must have occurred between 4 and 22 hours after induction. At some point when the glucose concentrations decreased, catabolite repression decreased to allow induction with lactose.

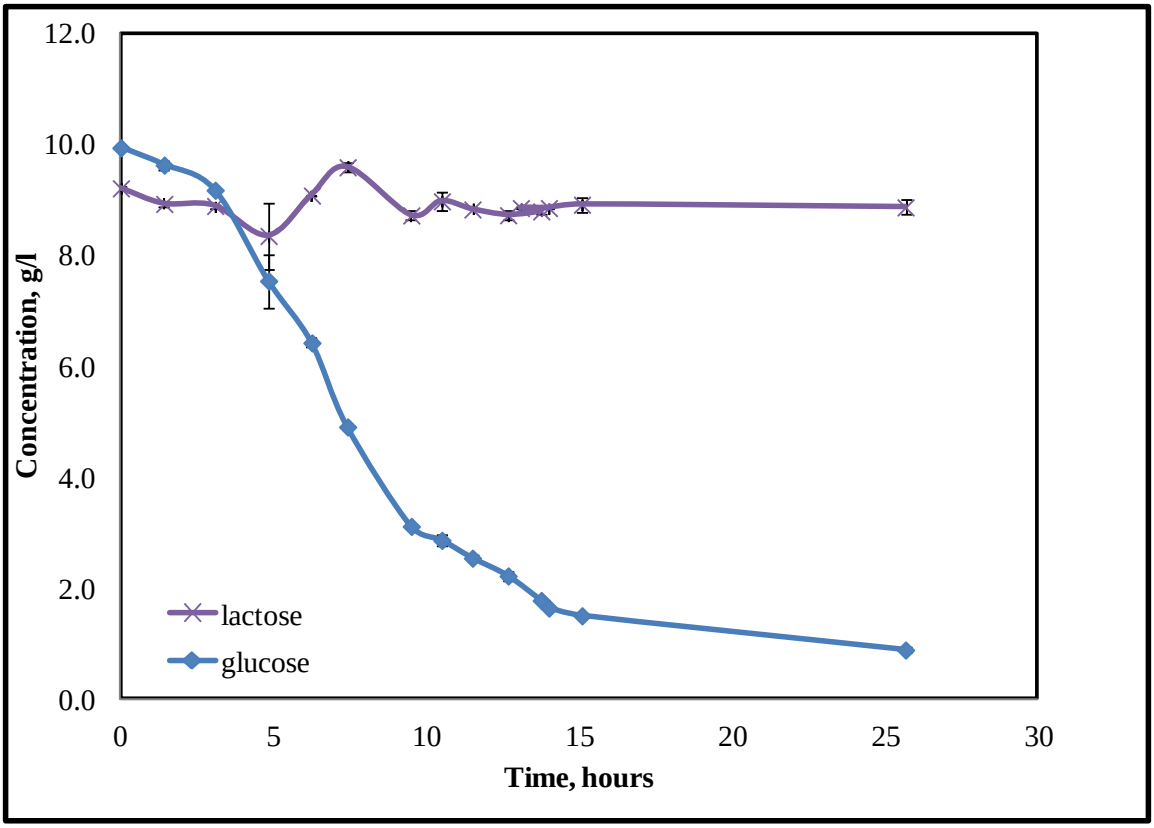

Figure 5-9. HPLC analysis of glucose and lactose for auto-induction in shake flasks. Initial concentrations of glucose and lactose were 10 g/l. Lactose concentrations did change during the 25 hour cultivation period.

After completion of shake flask experiments, it was determined that M9 + glucose supplemented with 5 mM amino acids would be used to examine protein expression and pCHC305 growth on the 3L production scale. It was also established that lactose can be used as an inducer in conjunction with the supplemental amino acids to express GST-PTH-CBD.

5.2 Batch cultivations

As discussed in Section 4.4, batch fermentation was used to test the medium formulation on a larger scale with different inducers. Figure 5-10 is a compilation of growth data from batch fermentation experiments. Each experiment was run in duplicate and the average growth data was plotted with respect to time.

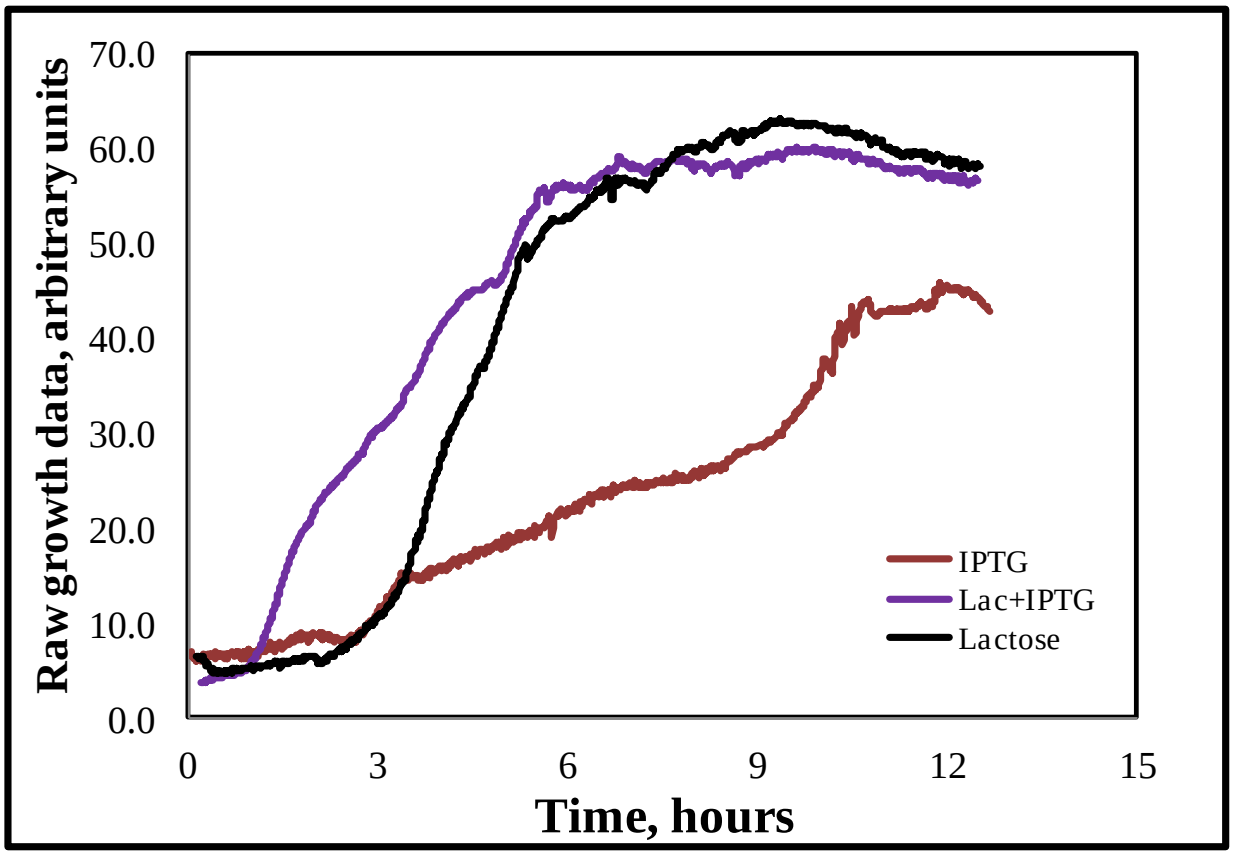

Figure 5-10. Growth data for batch fermentations with different inducers.

As shown above, IPTG negatively affected growth of batch cultures when added at a concentration of 10 mM. Decreasing the amount of IPTG to 5 mM and adding lactose to the culture did not have any apparent effect on growth as compared to cultures that were induced only with lactose. For these reasons, lactose was further examined as an induction source.

5.3 Fed-batch cultivations

As discussed in Section 2.3, fed-batch fermentation is used to achieve high cell density cultivations. For this work, an exponential feeding strategy was employed. This strategy and feeding profile development was thoroughly discussed in Section 4.5. To calculate product per gram cell basis (product yield), the concentration in terms of mg/l (found by densitometry) was divided by the value for the dry cell weight per liter (as determined by moisture analyzer). The value of mg/g DCW takes into account the denseness of the culture to give target protein concentration on a per gram cell basis. When reporting data for fermentation experiments, dry weight is often used because it accounts for difference in moisture content. For downstream processing (centrifugation, purification, etc.), the amount of product per cell is important to consider because of the amount of cells that must be processed. This type of calculation can also relate production of target protein to its volumetric productivity. For example, the goal for recombinant fed-batch fermentation is to produce a large number of cells. However, if a low number of cells is produced, but the target protein per cell is high, then the volumetric productivity is high. While this information is useful, it is also important to consider the total amount of product produced for a given experiment.

In many industrial applications, it may be desired to produce a certain amount of product. In this case, it is not as important to consider the amount of cells required to produce this product because this cost is ultimately passed down to the end-user. Needless to say, the results for protein expression are given in both units.

5.3.1 Cultures fed with glucose as major carbon source

5.3.1.1 Lactose induction after inoculation

The first fed-batch experiment utilized a feeding profile that exponentially delivered feed at rates between 0.1 and 0.3 ml/min. The growth rate for the profile was set at 0.2 hr^{-1}, which is within range of suggested growth rates for exponentially feeding *E. coli* cultures. This method is henceforth referred to as the saw-tooth method because of its characteristic feed profile. The cultivation was completely glucose limited, as glucose assays indicated that there was no glucose left in the culture broth. It was also induced with lactose 11 hours after inoculation. Figure 5-11 represents the growth curve for this type of cultivation. The final dry cell weight for this fermentation type was 50 grams. The average total dry cell weight of two runs is plotted versus time.

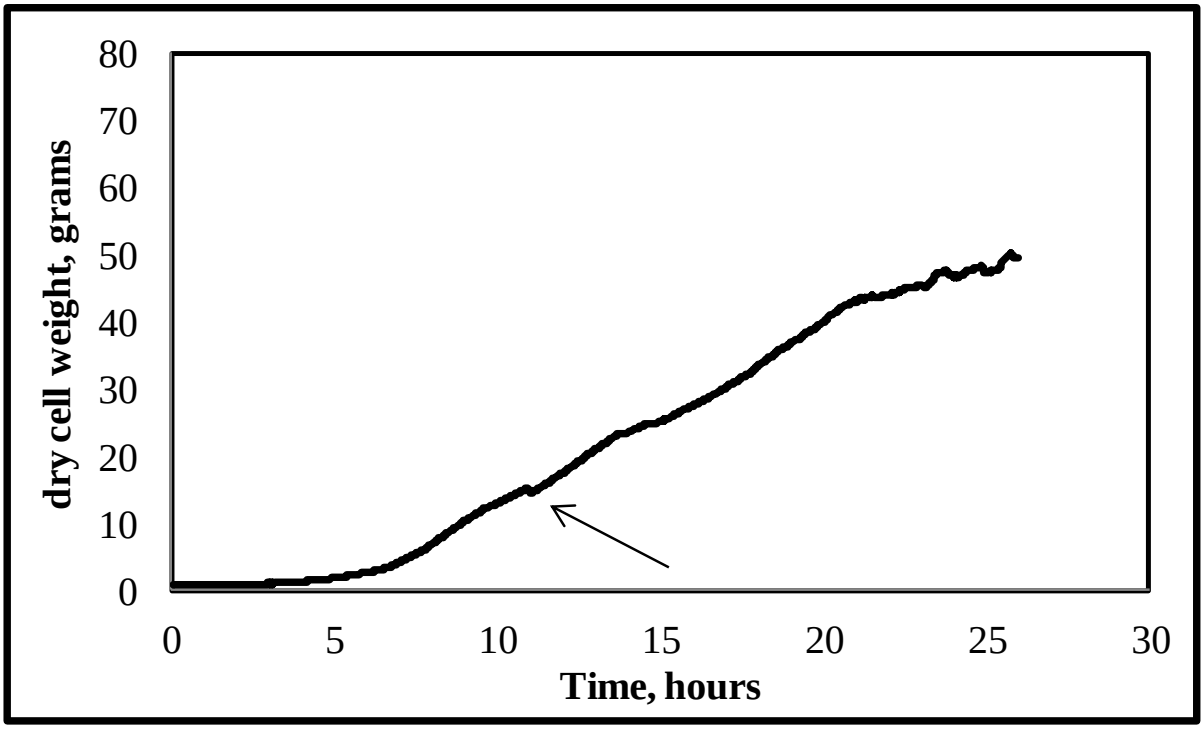

Figure 5-11. Growth curve for saw-tooth feeding method with induction at 11 hours with lactose. The arrow indicates when induction occurred.

Next, protein expression was examined. As shown in Figure 5-12, western blotting was performed to qualitatively compare expression levels at different times after induction. Densitometry was performed on 12.5% SDS-PAGE gels in order to quantify GST-PTH-CBD expression. Results are given in Figure 5-13, with the feed profile also displayed. In Figure 5-13 (a), the values for mg/g DCW is plotted versus time. Total product yield is plotted in Figure 5-13 (b).

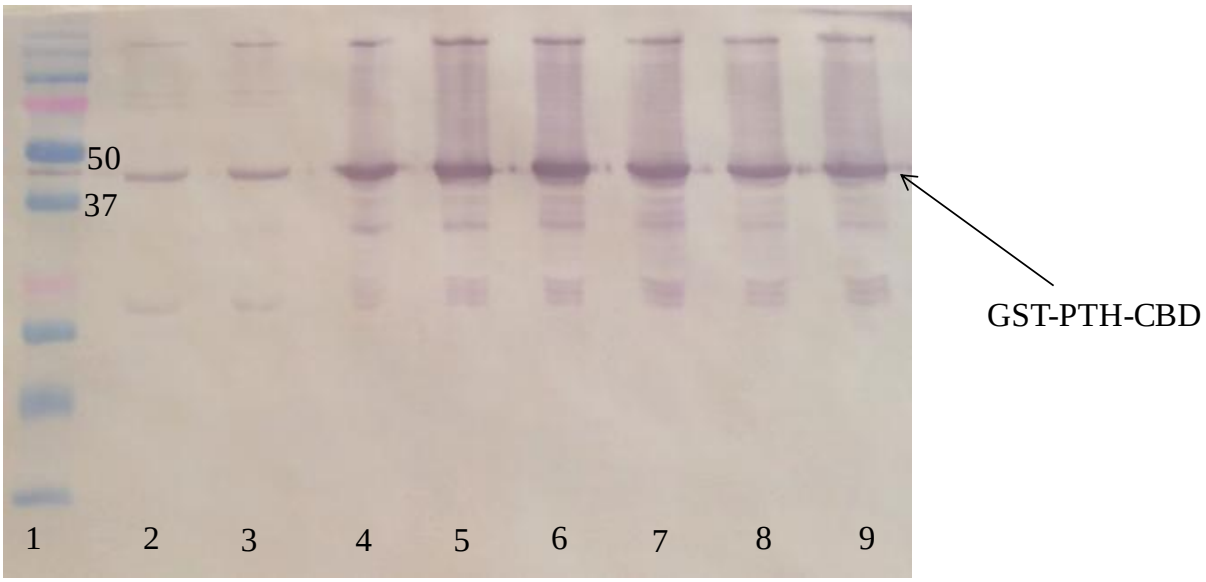

Figure 5-12. Western blot of lysates from saw-tooth feeding method. Lane 1 – molecular weight standard; 2 – pre-induction; 3 – 2 hours after induction (13 hr elapsed); 4 – 4 hr post (15 hr elapsed); 5 – 6 hr post (17 hr elapsed); 6 – 8 hr post (19 hr elapsed); 7 – 10 hr post (21 hr elapsed); 8 – 12 hr post (23 hr elapsed); 9 – 14 hr post (25 hr elapsed).

Qualitatively, the maximum amount of protein expressed occurred after 12 hours of induction (lane 7 in Figure 5-12). This conclusion was drawn due to the decreasing intensity of the target band after 12 hours of induction. This qualitative description matched the results found from densitometry. After densitometry, it was determined that the maximum amount of product was expressed at the 12 hour mark. From the findings from this experiment, the

remaining cultivations were stopped 12 hours after induction when lactose was used as an inducer.[***]

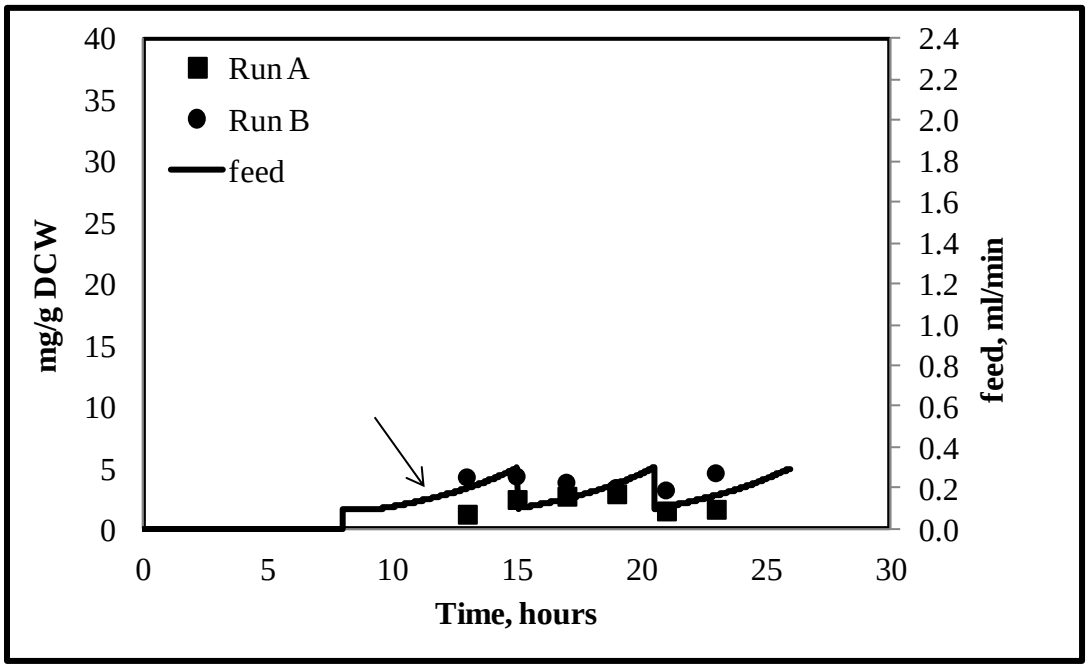

(a)

[***]For the figures in the remainder of the results section, all graphs have identical data ranges to allow for a visual interpretation when possible to aid in comparison. The arrow also indicates the time at which the culture was induced, when applicable.

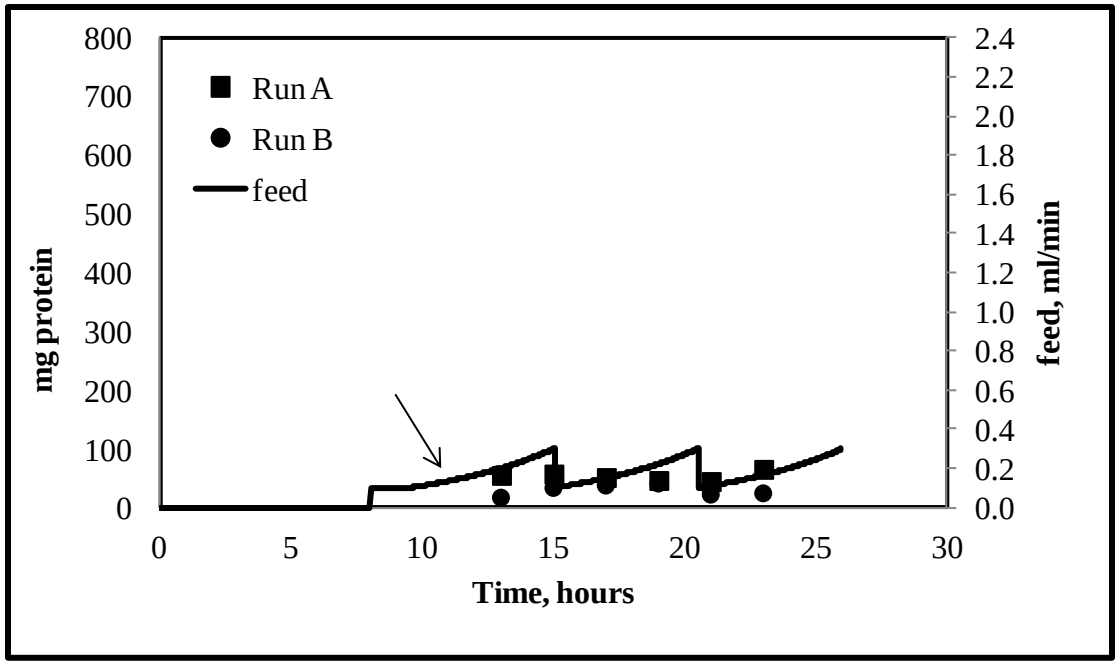

(b)

Figure 5-13. Protein yield and feed profile versus time for saw-tooth method. (a) Protein concentrations are given on a per gram cell basis to take into account changes in volume and cell density. (b) Protein concentration is in terms of total amount of product produced during the fermentation experiment.

As can be seen from Figure 5-13, the formation of product did not depend on the elapsed time. There was constant yield of product from cells, regardless of the substrate concentration, induction period, or cell density. Additionally, as previously stated, this feeding strategy allowed for completely limiting the substrate, which is desired to keep acetic acid concentrations low. These concentrations are given in Figure 5-14. In comparison to later runs, this feeding strategy was perhaps too limiting when it comes to substrate delivery because the glucose concentrations in exponential feeding experiments with no control is also zero. Nonetheless, approximately 41 mg of GST-PTH-CBD was produced with a final cell mass of 50 g and very little acetate produced.

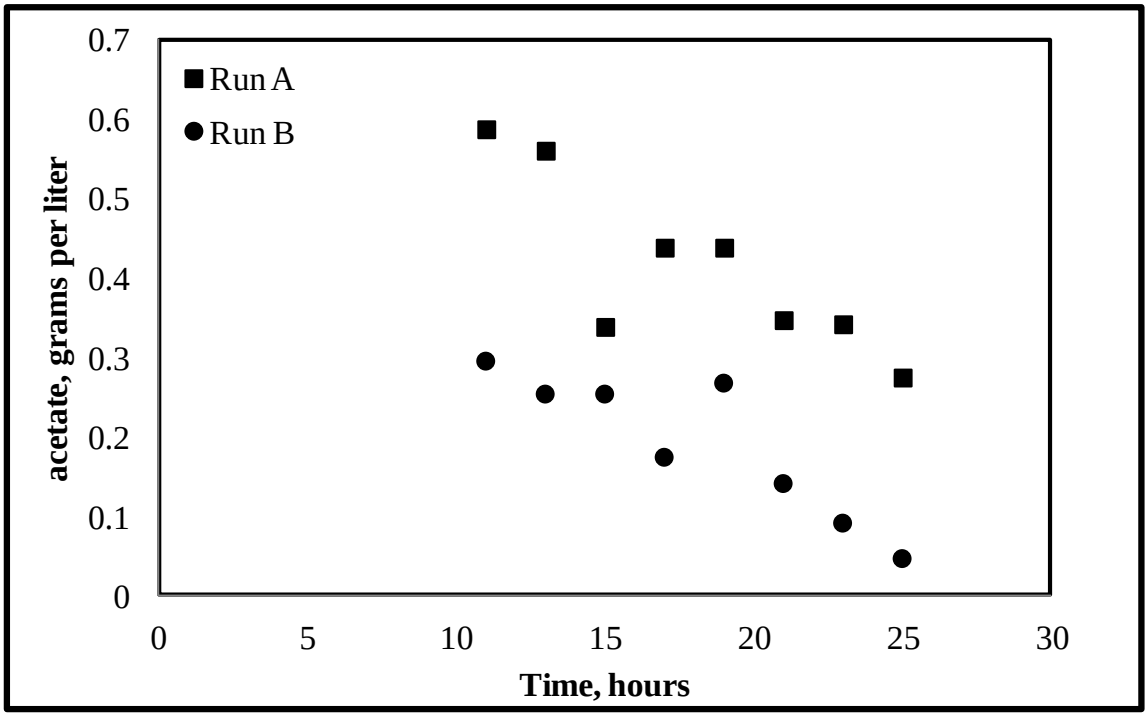

(a)

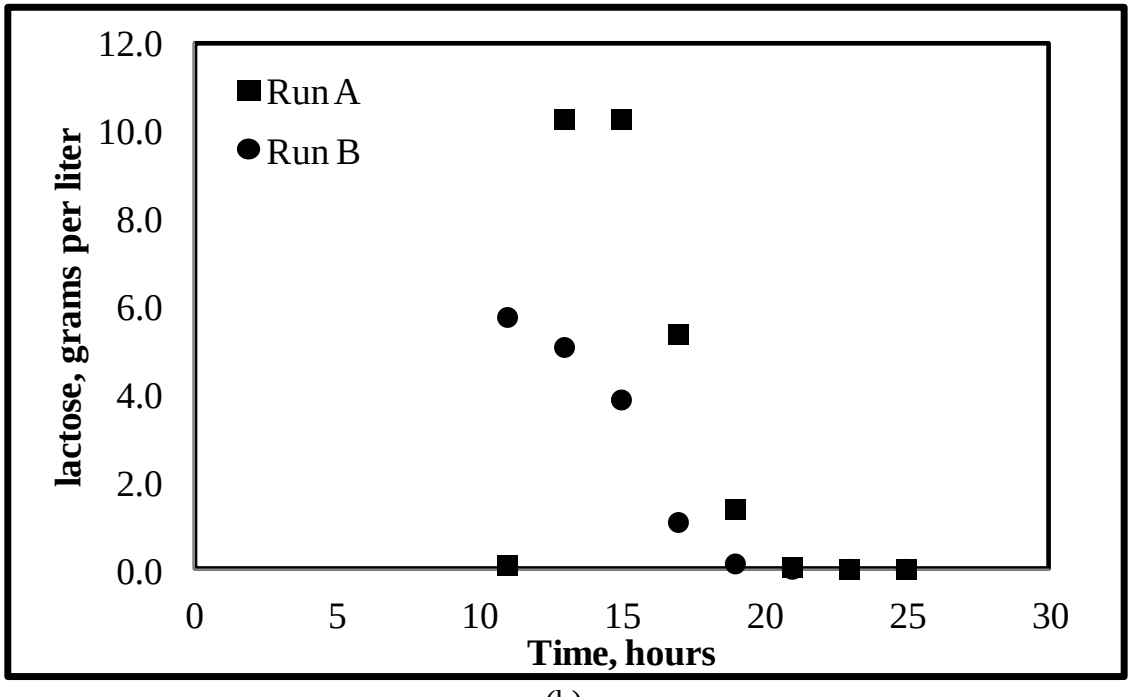

(b)

Figure 5-14. Carbohydrate concentrations versus time for saw-tooth feeding strategy. (a) Acetic acid; (b) Lactose was introduced to the reactor 11 hours after inoculation to give a final concentration of 10 g/l.

In an attempt to push the final cell mass to larger values, the next feeding strategy was exponential with no adjustment or control. The growth rate was kept at 0.2 hr^{-1} and initial un-induced fed-batch experiments proceeded. Four experiments were completed to monitor accumulation of glucose in the culture broth with respect to cultivation time. The glucose concentrations of these non-induced samples remained zero until the very end of the cultivation. After 24 hours, accumulation of glucose at low concentrations began (less than two grams). Because of these results, it was decided that the feeding strategy used for future fed-batch experiments would be an exponential feeding profile with no regulatory loop and a growth rate set at 0.2 hr^{-1}. It allows for limiting the substrate in fed-batch cultivations without compromising the final total cell mass. On average for the un-induced runs, the final wet cell weight was 191 g/l with a dry cell weight of 47 g/l. Growth values were averaged and plotted versus time. These data are shown in Figure 5-15.

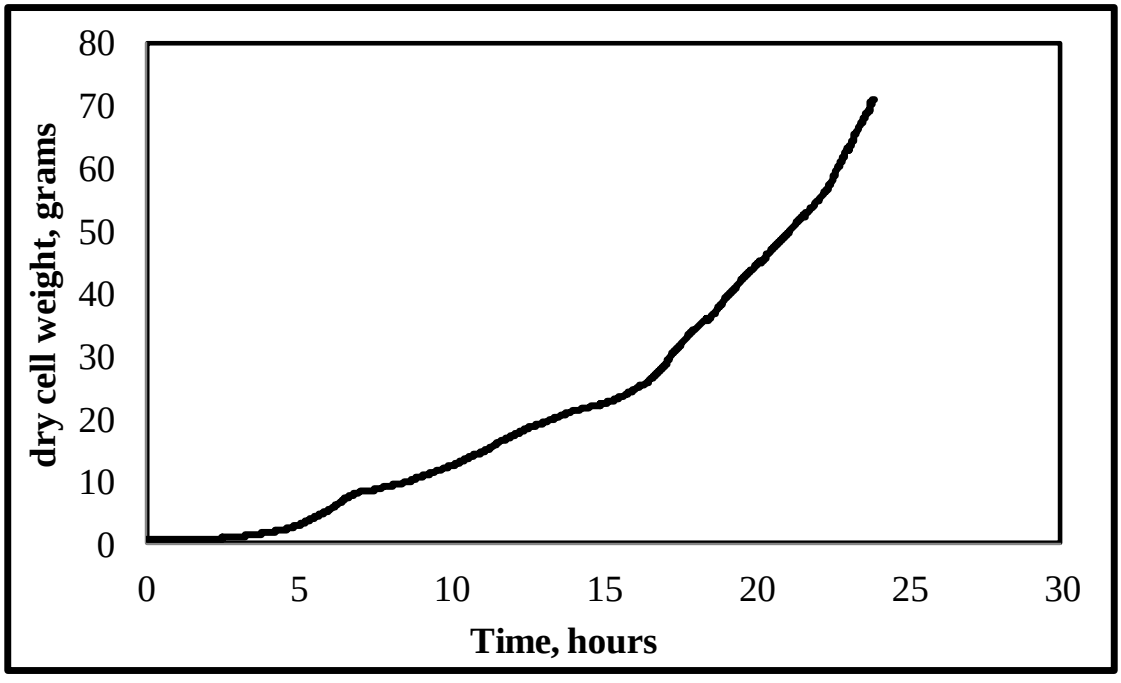

Figure 5-15. Growth curve for fermentations that were un-induced using an exponential feeding method with the growth rate set to 0.2 hr^{-1}.

The next set of experiments utilized an exponential feeding profile with a growth rate set to 0.2 hr^{-1} and was induced with lactose 12 hours after inoculation.

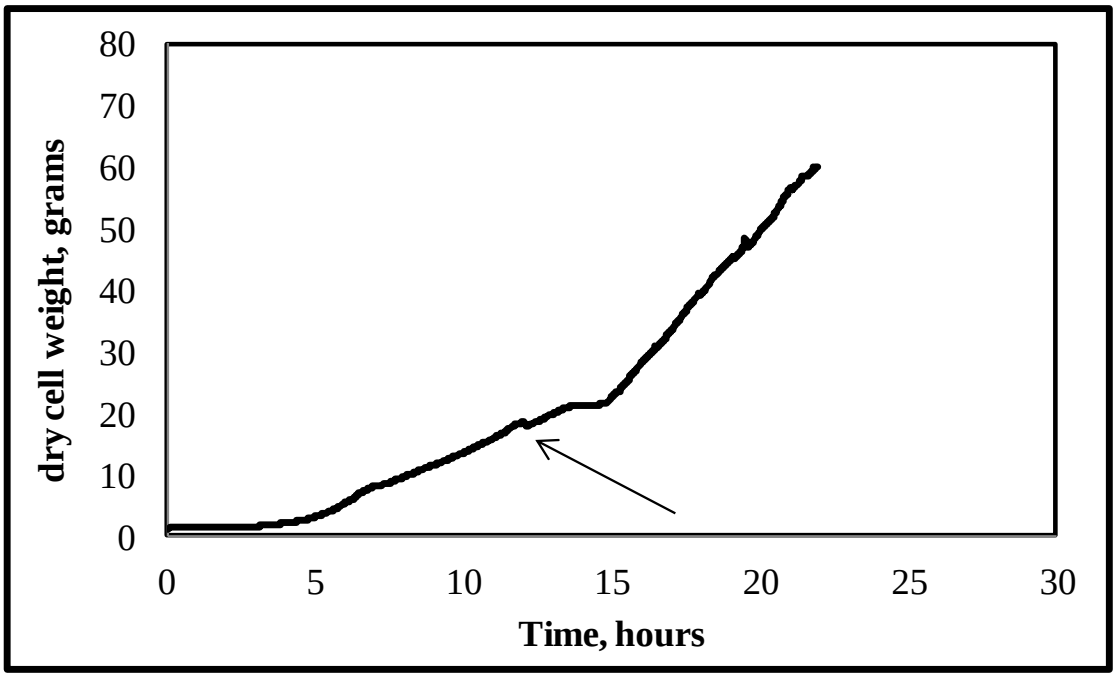

Figure 5-16. Growth profile for fermentation experiments induced with lactose 12 hours after inoculation. The final total dry cell weight was 60 grams. The induction period lasted for approximately 12 hours.

The final cell mass for the exponential feeding strategy under induction with lactose was 60 grams (shown in Figure 5-16). With respect to growth, the final cell mass was not as high as that for the un-induced control experiments, but was 10 grams higher than the final cell mass for the saw-tooth experiments. Protein yield (mg protein/g cell) was also higher than the yield from the experiments using the saw-tooth feeding profile. As shown in Figure 5-17 (a), the concentration of protein produced per gram cell tripled. For the saw-tooth method, the average protein yield was about 3 mg/g DCW, but for the exponential method the yield was almost 10 mg/g DCW. The total concentration ranged from 300 to 500 mg depending on the time at which

the fermentation was stopped, as shown in Figure 5-17 (b). These values increased due to the increase in volume. On a per cell basis, the average expression of product was constant throughout the experiment.

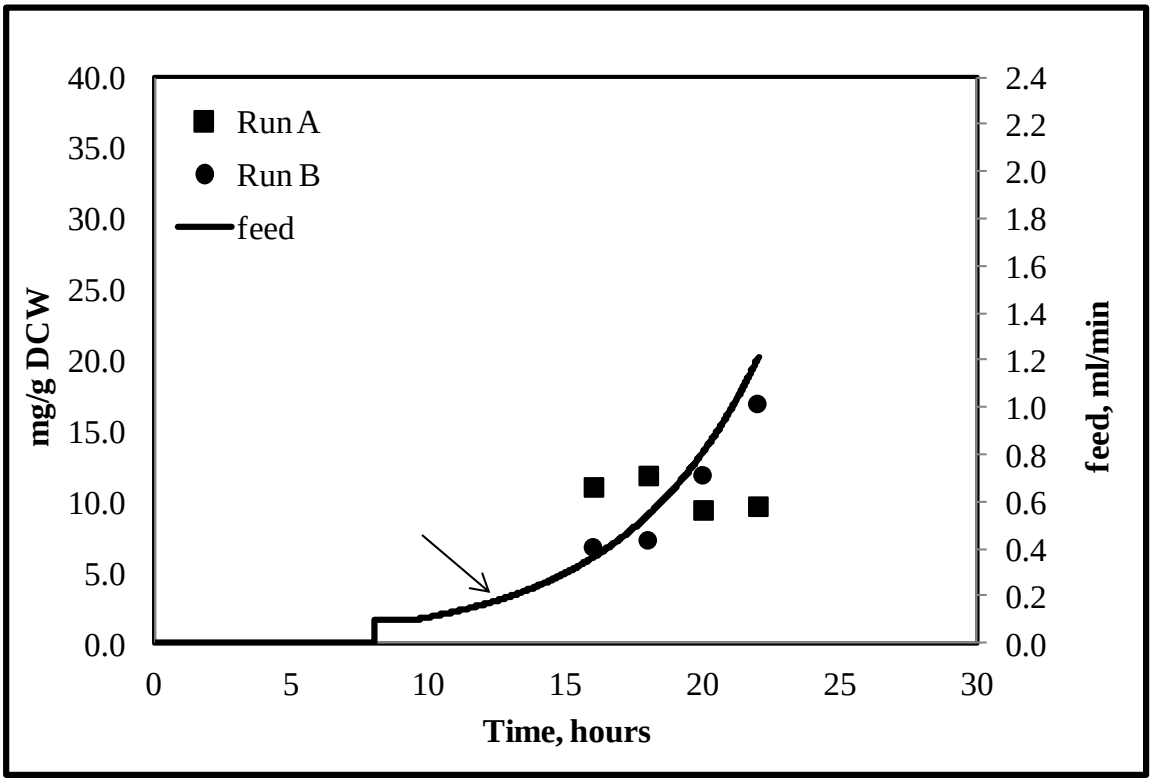

(a)

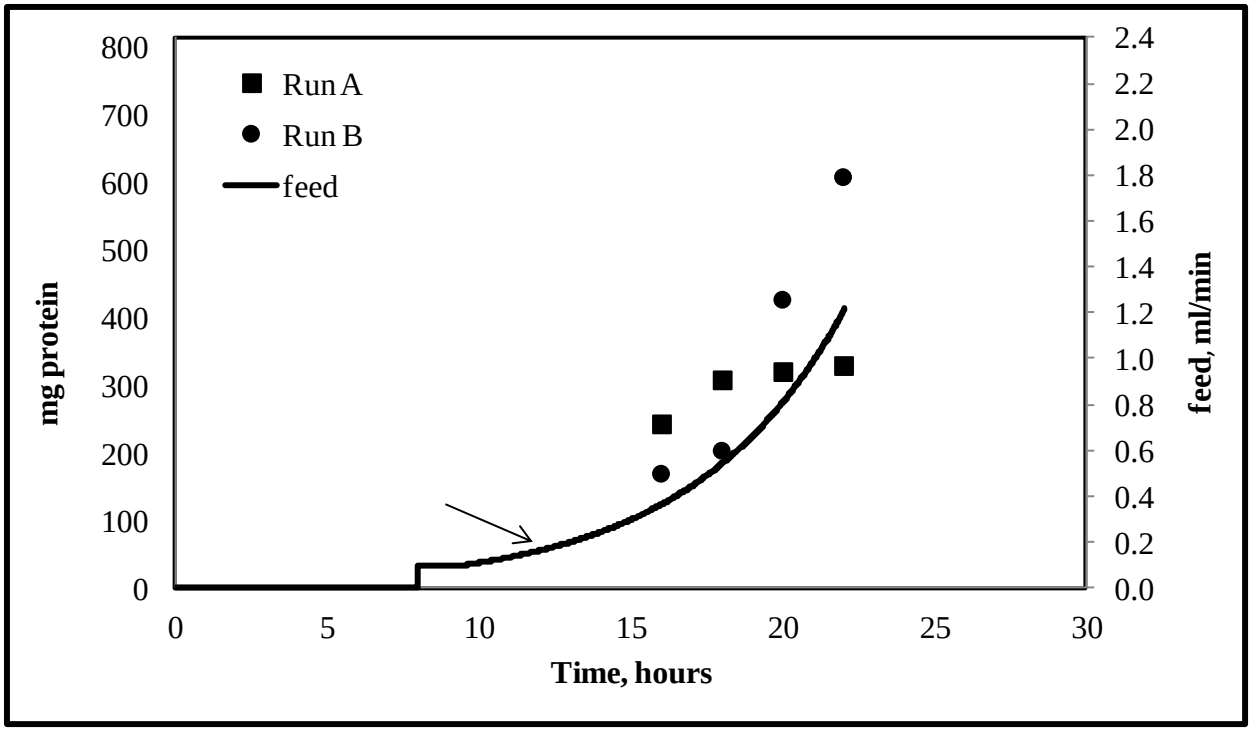

(b)

Figure 5-17. Protein concentrations for fermentations induced 12 hours after inoculation with exponential feeding strategy. (a) Concentrations are given using a per gram cell basis; (b) Total concentrations are calculated based on densitometry and given in milligrams.

The carbon analysis for this set of experiments (shown in Figure 5-18) yields much information about the uptake and accumulation of substrates. Unlike the un-induced test runs, glucose for this set of induced cultivations began to accumulate approximately 12 hours after feeding started. This, in turn, caused accumulation of acetic acid because the glucose consumption rate was lower than the rate at which glucose was pumped into the system (see Section 2.3.1). Unlike the previous shake flask experiments, the lactose concentration decreased even though glucose was present in the media. This indicates that *E. coli* was utilizing both sugars simultaneously. Additionally, acetic acid concentrations began approaching inhibitory values for one of the experiments, but growth did not appear to be stunted by this accumulation.

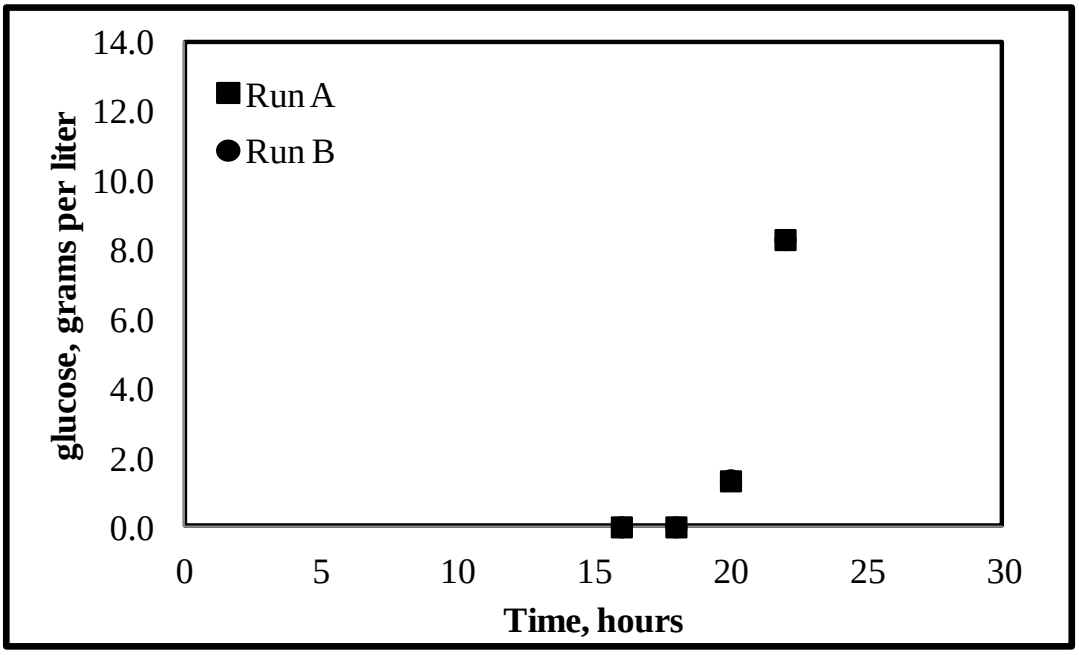
14.0
12.0
10.0
8.0
6.0
4.0
2.0
0.0
glucose, grams per liter
Run A
Run B
0
5
10
15
20
25
30
Time, hours

(a)

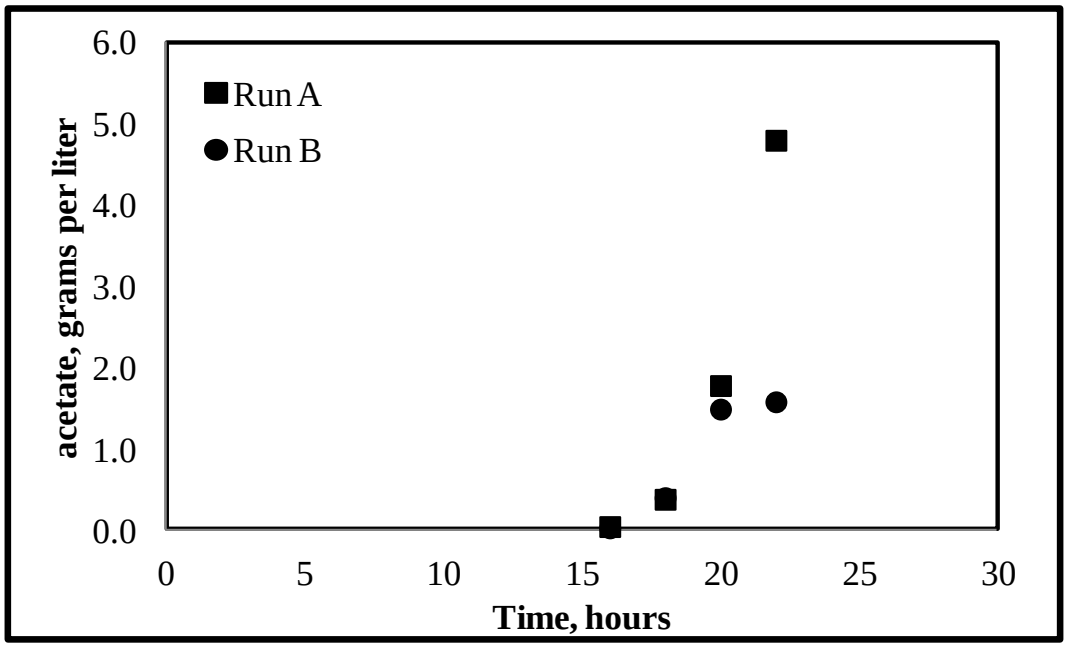
6.0
5.0
4.0
3.0
2.0
1.0
0.0
acetate, grams per liter
Run A
Run B
0
5
10
15
20
25
30
Time, hours

(b)

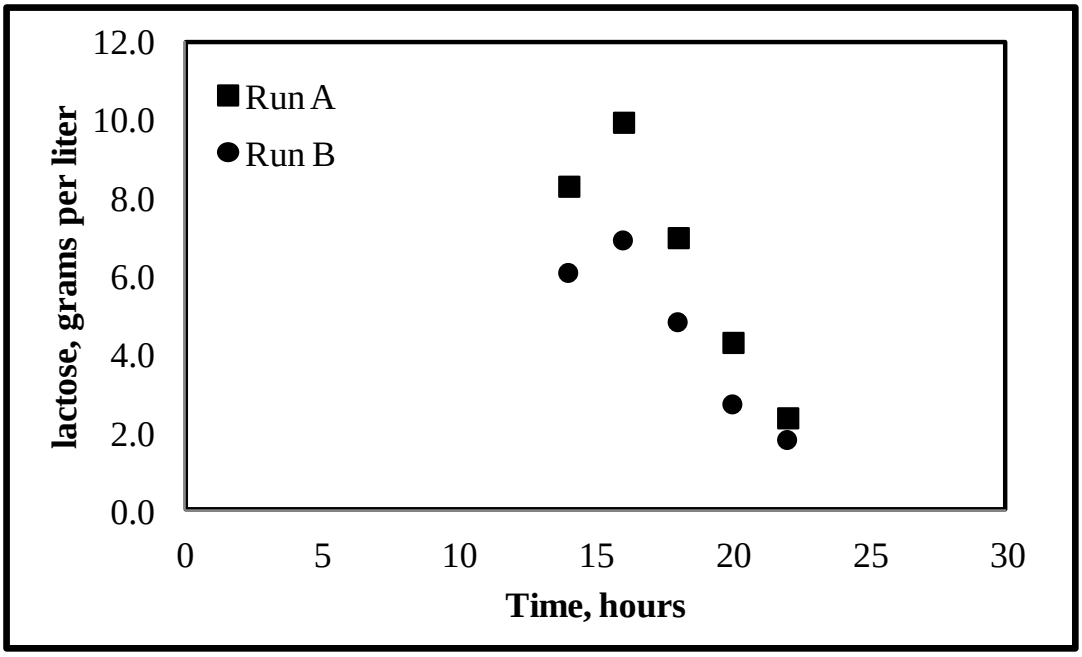

(c)

Figure 5-18. Carbon analysis for cultures induced with lactose 12 hours after inoculation with the exponential feeding strategy. (a) Glucose concentration versus time. Glucose began to accumulate after 20 hours of cultivation (12 hours after feeding started); (b) Acetic acid concentration versus time. Acetate began accumulating 18 hours after inoculation; (c) Lactose concentration versus time. Lactose was added 12 hours after inoculation. Data from two experiments is given.

Since the previous experiment indicated that *E. coli* pCHC305 utilized glucose and lactose concurrently, the length of induction can be extended by adding lactose earlier on in the cultivation period. Additionally, adding lactose when the concentration of glucose is low may extend the ability of lactose to act as an inducer. Hence, the next set of experiments examined the induction of pCHC305 at the time of feed start. The feeding profile here was the same as before - exponential feeding with the growth rate set to 0.2 hr^{-1}.

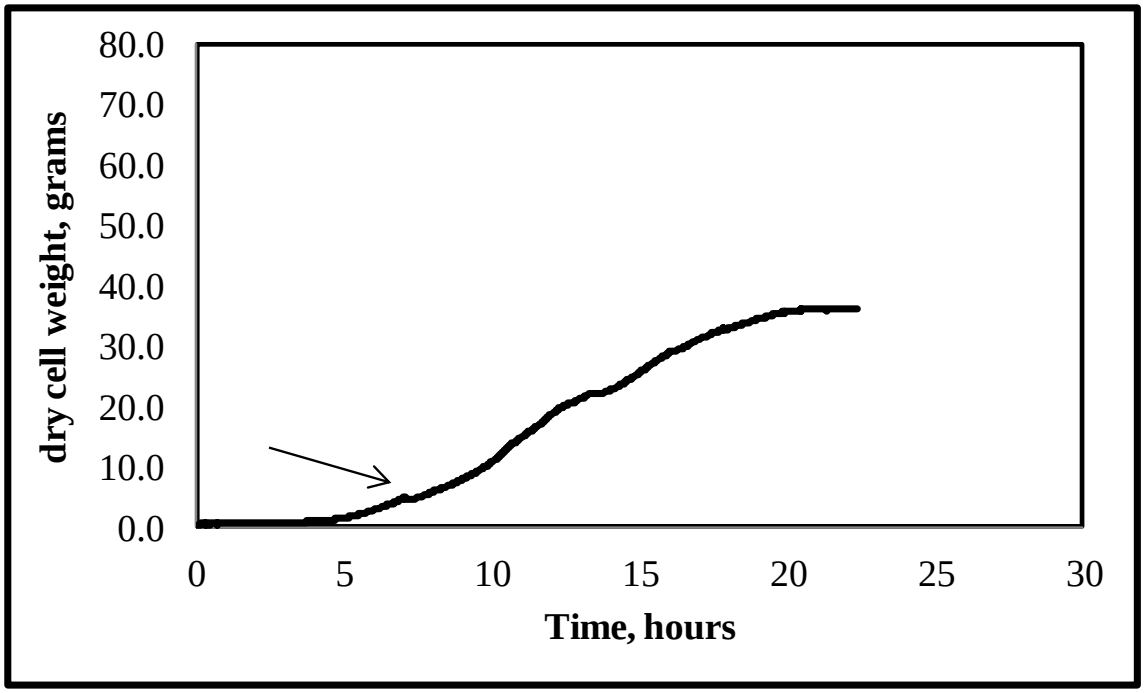

Figure 5-19. Growth curve for cultivation induced when feed started. The final cell mass was approximately 41 grams.

As shown in Figure 5-19, adding lactose earlier in the cultivation period appeared to decrease the maximum attainable cell mass. The final cell mass was 41 grams. In the experiment where lactose was added 12 hours after cultivation, the final mass was 60 grams. Additionally, there did not appear to be a significant difference in the yield of GST-PTH-CBD. The yield of product remained around 10 mg/g DCW with a total amount around 200 mg. While this is a significant increase over the saw-tooth method, there was not an increase in expression with regard to inducing the culture 12 hours after inoculation. In fact, inducing the culture 12 hours after inoculation achieved higher total amounts of protein simply because of the increase in the production of cells.

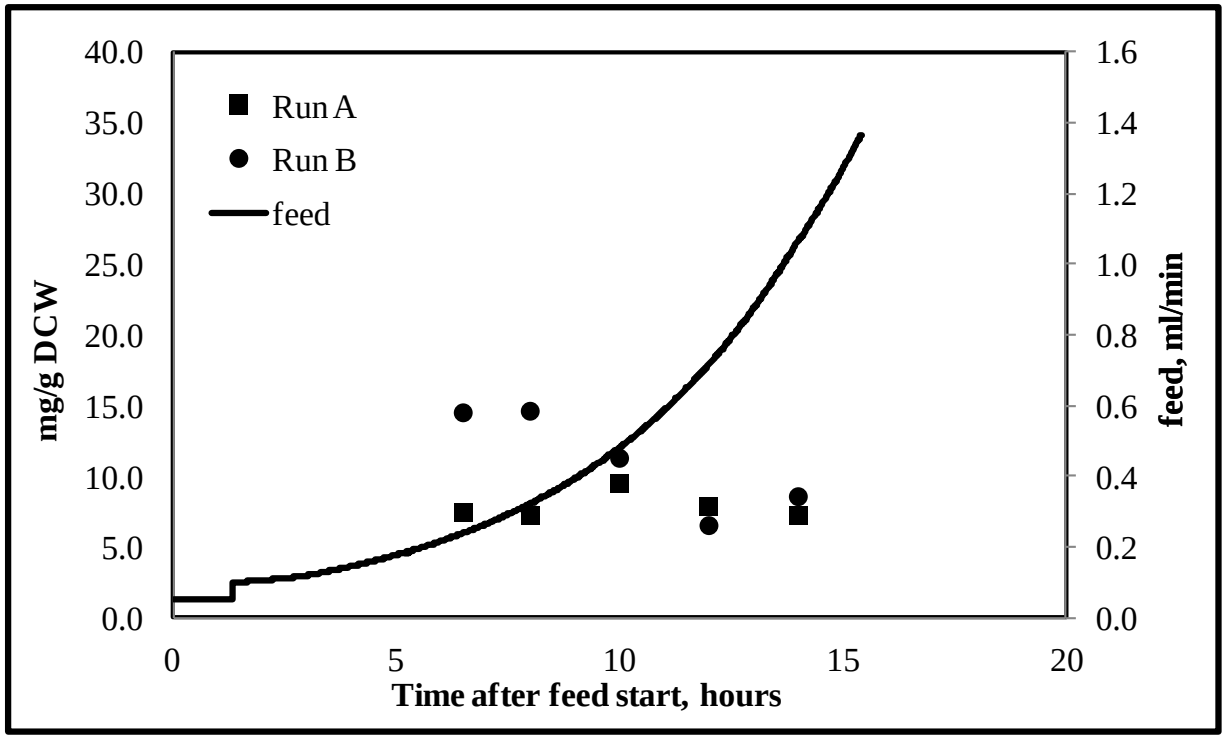

(a)

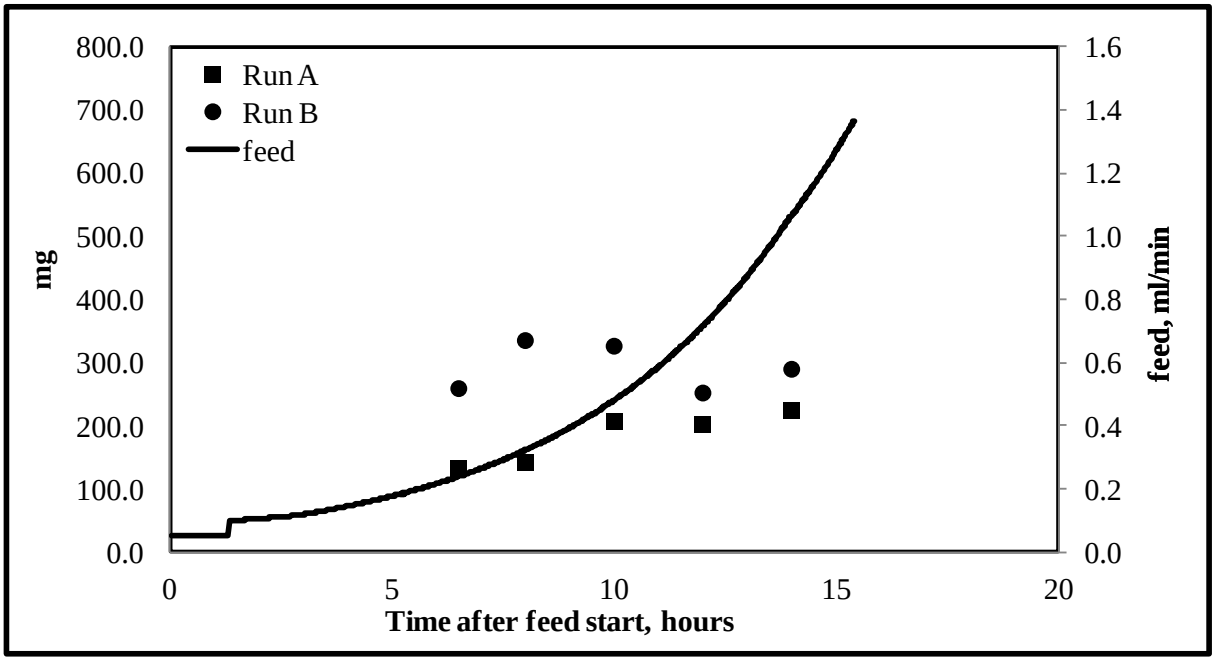

(b)

Figure 5-20. Protein concentrations with respect to time for cultivations induced with lactose at the time of feed start. (a) Concentration of protein on a per gram cell basis; (b) Total protein concentrations determined by densitometry.

When lactose was introduced into the system 12 hours after inoculation, glucose began to accumulate approximately 12 hours after feed start. For this set of experiments, lactose was used to induce the culture when the feed started and glucose began to accumulate six hours after feed start (Figure 5-21 (a)). Since glucose accumulated six hours earlier, lactose introduced into the system at an earlier time point must affect glucose uptake. However, the glucose concentrations remained low during the fermentation experiment, so it was still consumed by the cells.

Alternatively, a slower growing system will not take glucose up as fast, which can also result in lower numbers of cells and accumulation of glucose earlier in the fermentation experiment. The glucose numbers here were not as high as those for the lactose induced 12 hours after inoculation. Because of the accumulation of glucose, acetate also began accumulating at approximately 7 hours after feed start. These acetate numbers, as shown in Figure 5-21 (b), did not reach inhibitory values. Thus, it is not thought that the accumulation of acetic acid caused the low number of cells at the end of cultivation.

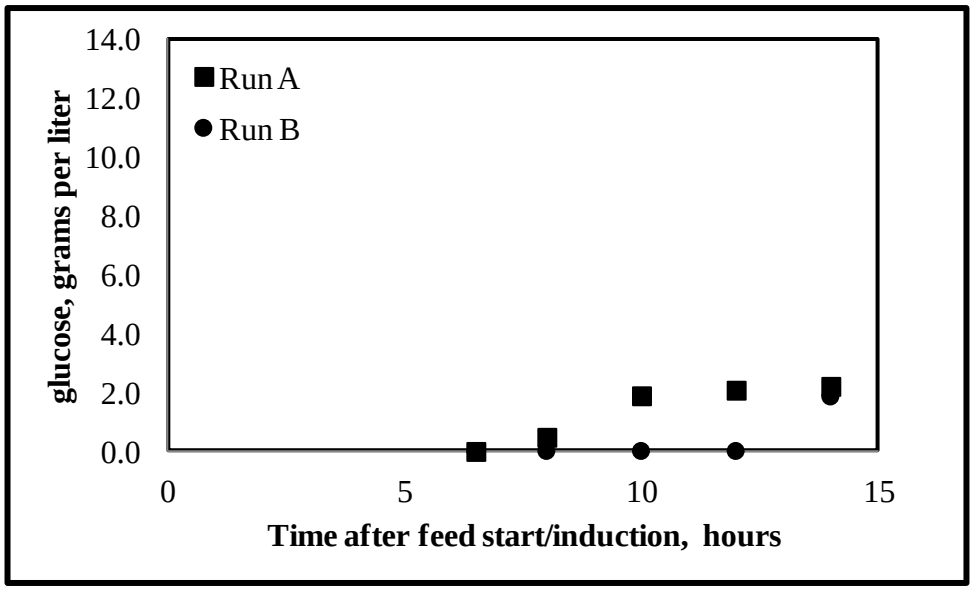

(a)

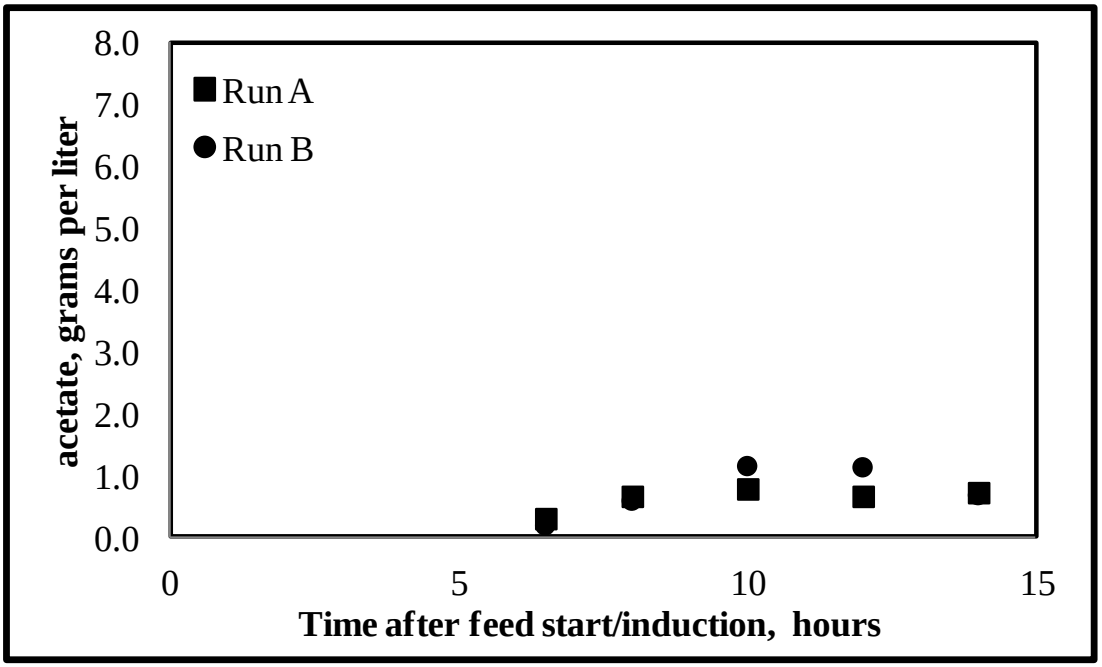

(b)

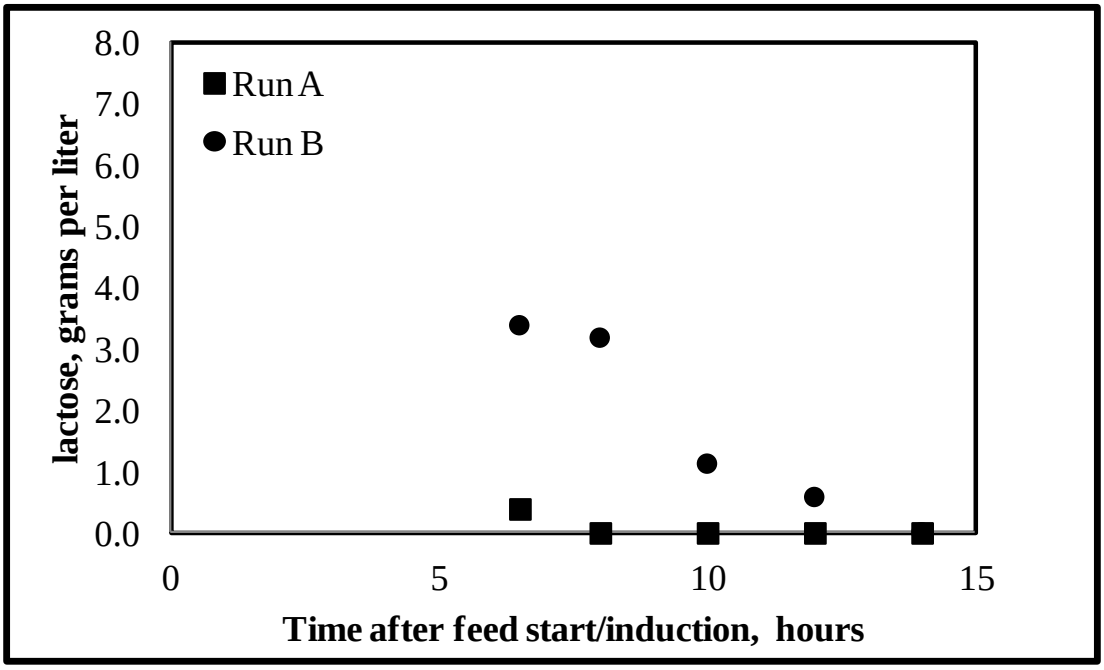

(c)

Figure 5-21. Carbon analysis for cultivations induced with lactose when feed started. (a) Glucose started to accumulate 6 hours after feed start; (b) acetic acid began to accumulate 7 hours after feed start; (c) lactose was depleted 14 hours after induction.

This specific characteristic of acetic acid concentration during fermentation has been reported by others. Shiloach et al. (1996) compared different bacterial strains for acetic acid consumption and inhibition. For BL21, they found that acetic acid concentrations peaked around 2 g/l. For two hours after the peak, the concentration remained constant. This was followed by a decrease in acetic acid concentration. This outcome is very similar to the trend that is shown in Figure 5-21 (b). Shiloach et al. proposed that the reasoning for this was because BL21 reacts to lower acetic acid concentrations. As a result of these low concentrations, the cells reduce their glucose uptake so acetate can be consumed.

To summarize the fed-batch fermentation experiments that utilized lactose induction at different times with different feed profiles, Table 5-1 provides a list of experiments with their respective results. As shown below, lactose induction 12 hours after inoculation provided the greatest number of cells and the highest yield of protein per gram cell. However, the protein numbers for amount produced per cell were comparable to those for fermentations that were induced when the feed started (7 to 8.4 hours after inoculation). Of these three types of fermentation, lactose induction 12 hours after inoculation was best at total protein production. It is important to note that for the remaining results, $Y_{P/X}$ describes the protein yield in terms of mg product/g cell (dry weight).

Table 5-1. Summary of experiments performed with lactose induction (NOT auto-induction) with glucose feed. To indicate the saw-tooth feeding profile, st is used. Other cultivations were fed exponentially.

Method	Final DCW	Average mg	Maximum mg	Average $Y_{P/X}$	Maximum $Y_{P/X}$
Lactose 11 hrs after inoc (st)	50	40.8	44.9	2.97	3.23
Lactose 12 hrs after inoc	60	327	463	9.92	11.3
Lactose at feed start	41	192	220	9.44	10.9

5.3.1.2 Auto-induction with lactose

The next method examined for production of GST-PTH-CBD was auto-induction. The introduction of a secondary carbon source when the primary substrate is limited can cause a shift in metabolism after the depletion of the primary source. In this case, the introduction of the secondary carbon source pushed the cells to consume lactose, thus causing induction. This shift was completely controlled by the cells, as 10 g/l of lactose was added to the media prior to the start of cultivation.

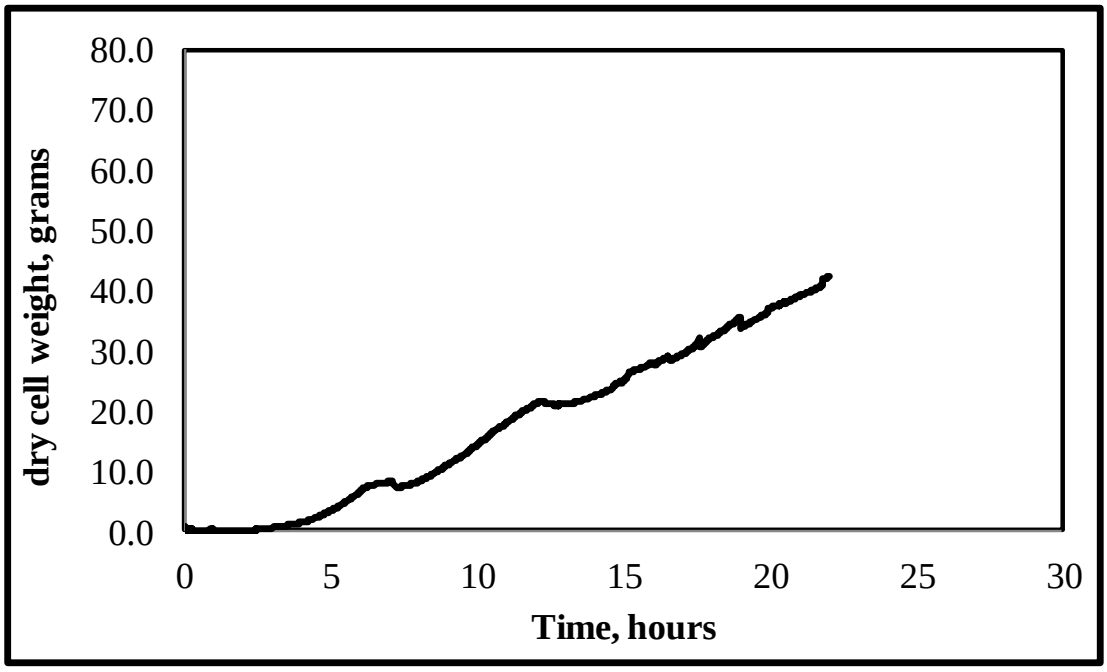

Figure 5-22. Growth curve of auto-induced cultivations indicates that the final dry cell weight was approximately 43 grams.

As shown in Figure 5-22, the cultivation never reached the stationary phase and the final dry cell weight was 43 grams. This dry cell weight was very close to the one achieved for the fermentation experiments that were induced at the time of feed start (41 grams). The dips in the growth curve towards the end of the cultivation are caused by changes in oxygen flow. The

Bugeye optical density probe is sensitive to these changes, hence the reason for taking optical density measurements by an external source throughout the cultivation.

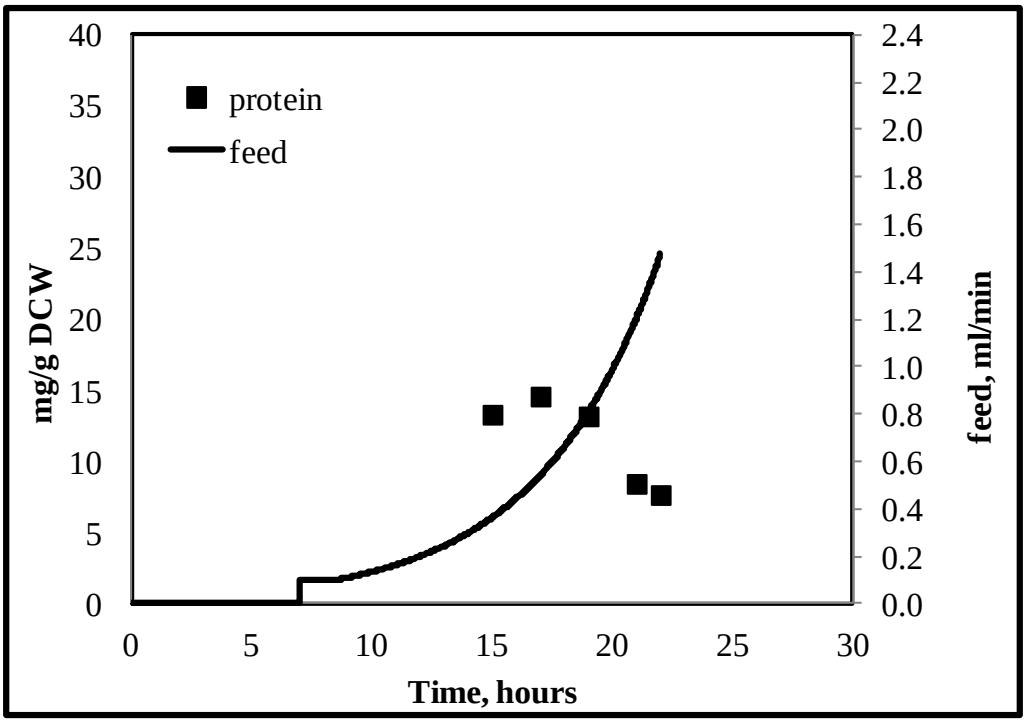

(a)

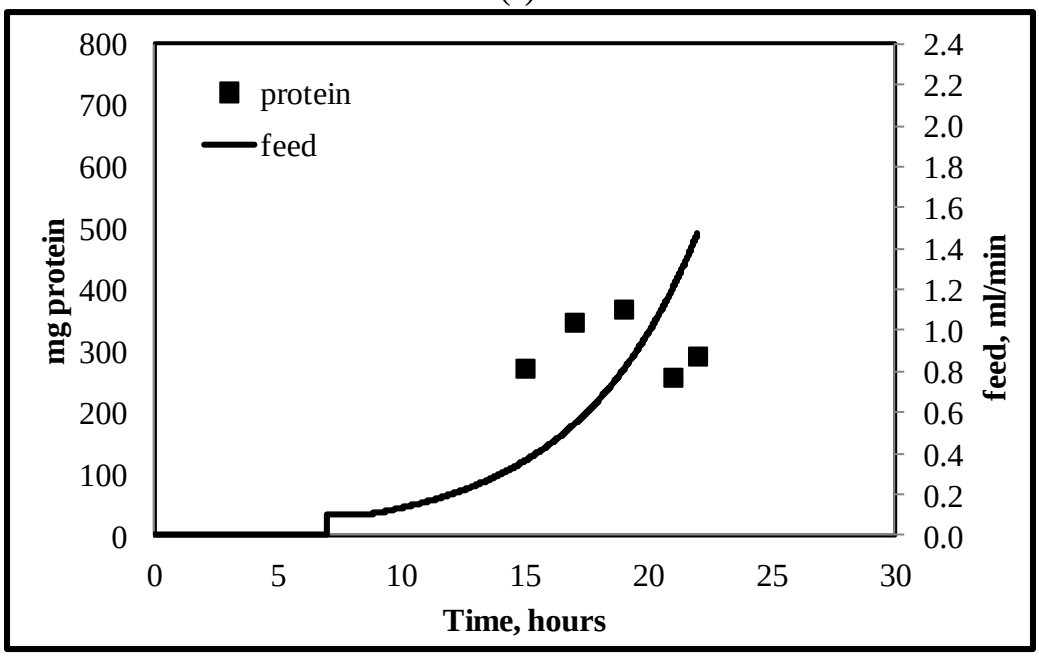

(b)

Figure 5-23. Protein concentrations with respect to time for auto-induced cultures. (a) Product yield; (b) Total protein concentrations.

As indicated in Figure 5-23 (a), the yield of product decreased after 20 hours. This would be expected if no additional production of protein occurred and there was a significant increase in cell growth after 20 hours, but Figure 5-22 does not indicate any significant increases in growth. However, the growth chart doesn't indicate that the stationary phase has been reached, so this small increase could account for the decrease in protein per gram cell. On average, 11.4 mg protein per gram DCW was produced and 310 mg of total protein was produced throughout the experiment (Figure 5-22 (b)). In comparison to previous runs, auto-induction produced the highest concentration of protein on a per gram cell basis, but one of the lowest cell masses at the end of cultivation.

The glucose concentrations and acetic acid concentrations remained fairly steady during the fermentation experiment. Both substrates began to accumulate at 14 hours after inoculation, as shown in Figure 5-24. However, the acetic acid concentration never exceeded the inhibitory limit for cell growth and again, this wasn't considered to be the cause for the lower cell concentration.

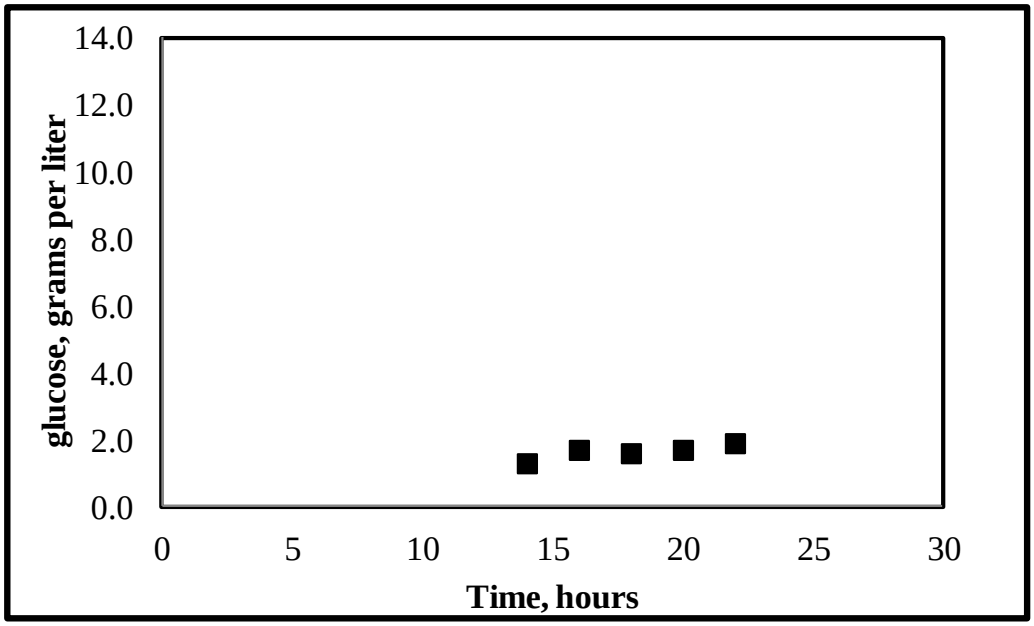

(a)

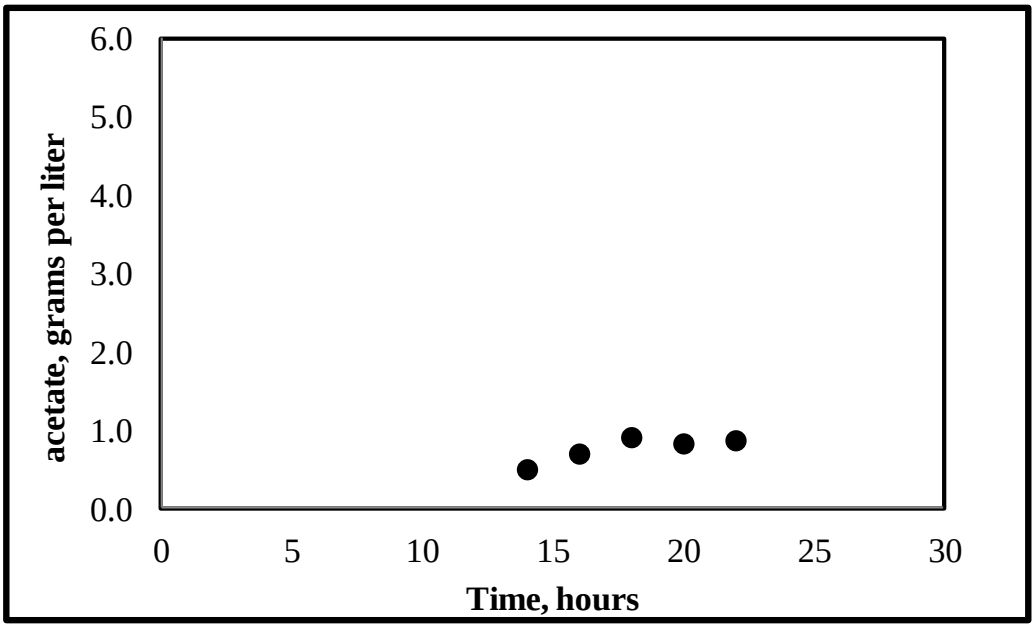

(b)

Figure 5-24. Carbohydrate concentrations for auto-induced fed-batch fermentation experiment. (a) Glucose concentration; (b) Acetic acid concentration.

So far, it appears that lactose not only has an effect on the protein production, but also has an effect on the final cell mass. To recap, when lactose was added 12 hours after induction,

the final cell mass was 60 grams. When lactose was added when the feed started (between 7 and 8.4 hours), the final cell mass was 41 grams. Auto-induction gave a final cell mass of 43 grams. When lactose was added earlier on in the fermentation, the cell mass was negatively affected.

After 15 hours of cultivation, the lactose concentration in the medium was less than 0.3 g/l. Because of this, the goal of the next set of experiments was to examine protein production and cell growth using auto-induction with an additional pulse of lactose into the reactor. This pulse was added at the 12 hour mark, as to inhibit depletion of lactose in the reactor.

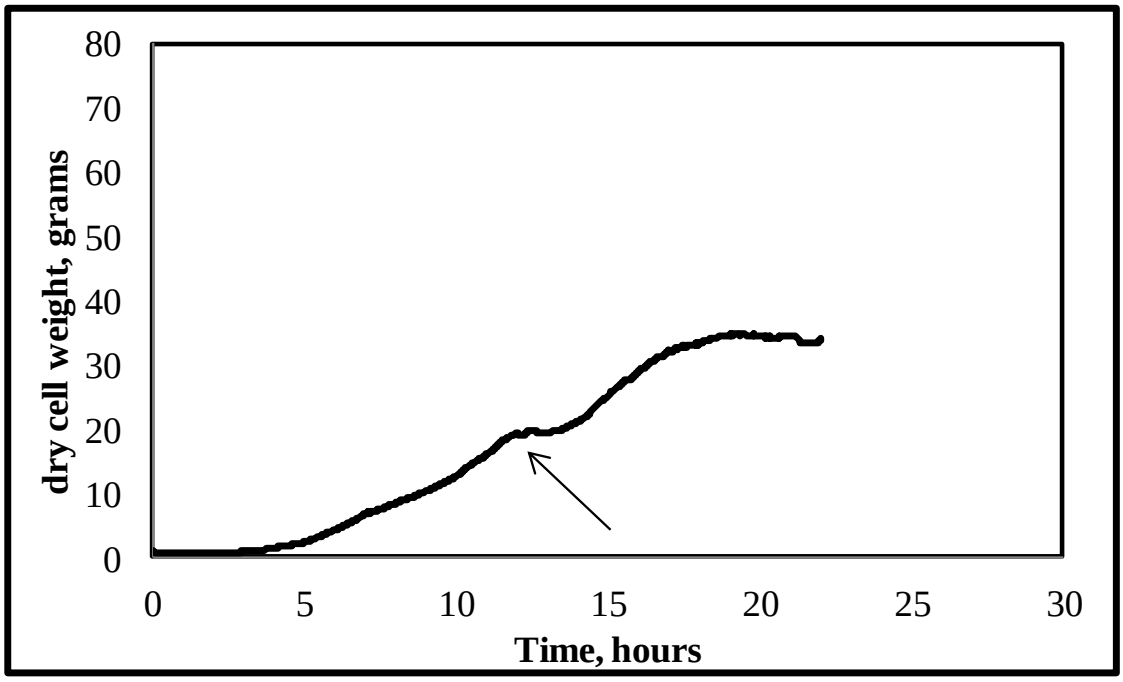

Figure 5-25. Cell growth from auto-induced fermentation with lactose pulse.

The final cell mass for the auto-induced cultures with an additional lactose pulse 12 hours after inoculation was 33 grams, as shown in Figure 5-25. This was the lowest amount of cells produced from a fed-batch fermentation so far. Even though the cell mass suffered, product yield actually increased and was the highest produced from any of the fed-batch fermentation

experiments so far (Figure 5-26). On average, 13.9 mg of protein were produced per gram of cell, giving an average of 301 mg of total protein. The protein numbers were comparable to auto-induction without pulsing, but the cell mass was almost 10 grams lower. Once again lactose inhibits growth but not uptake of glucose by the cells.

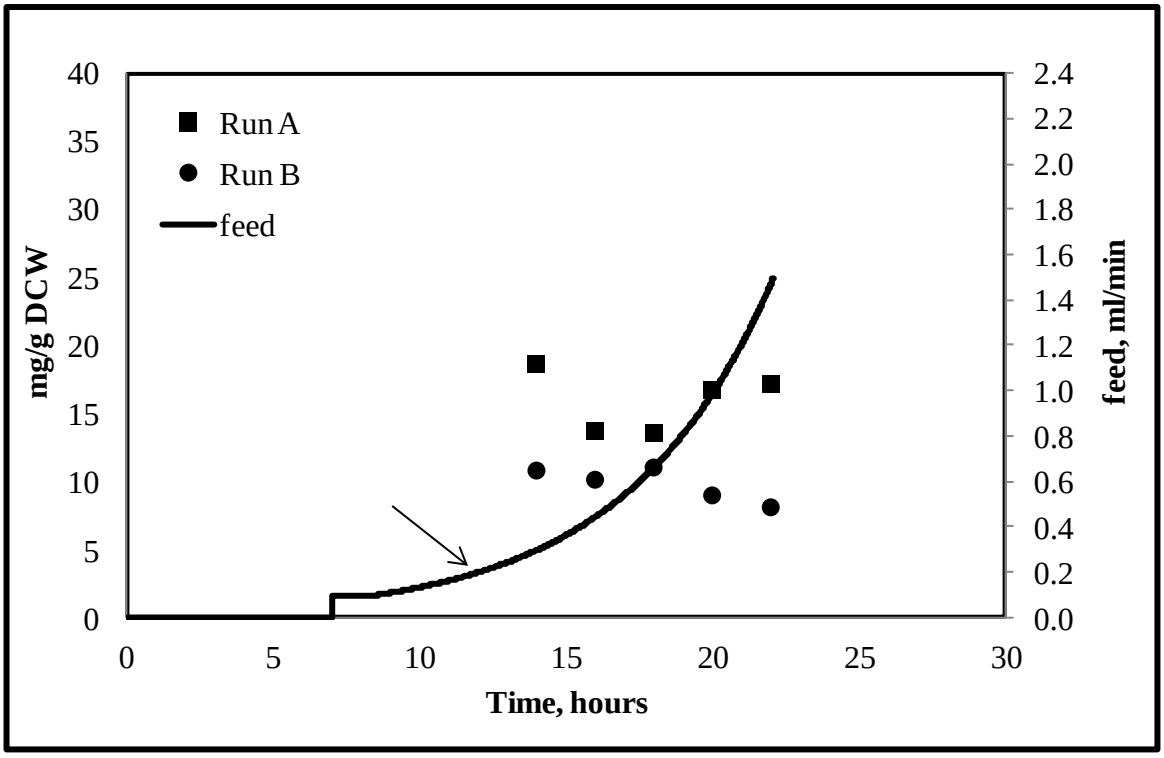

(a)

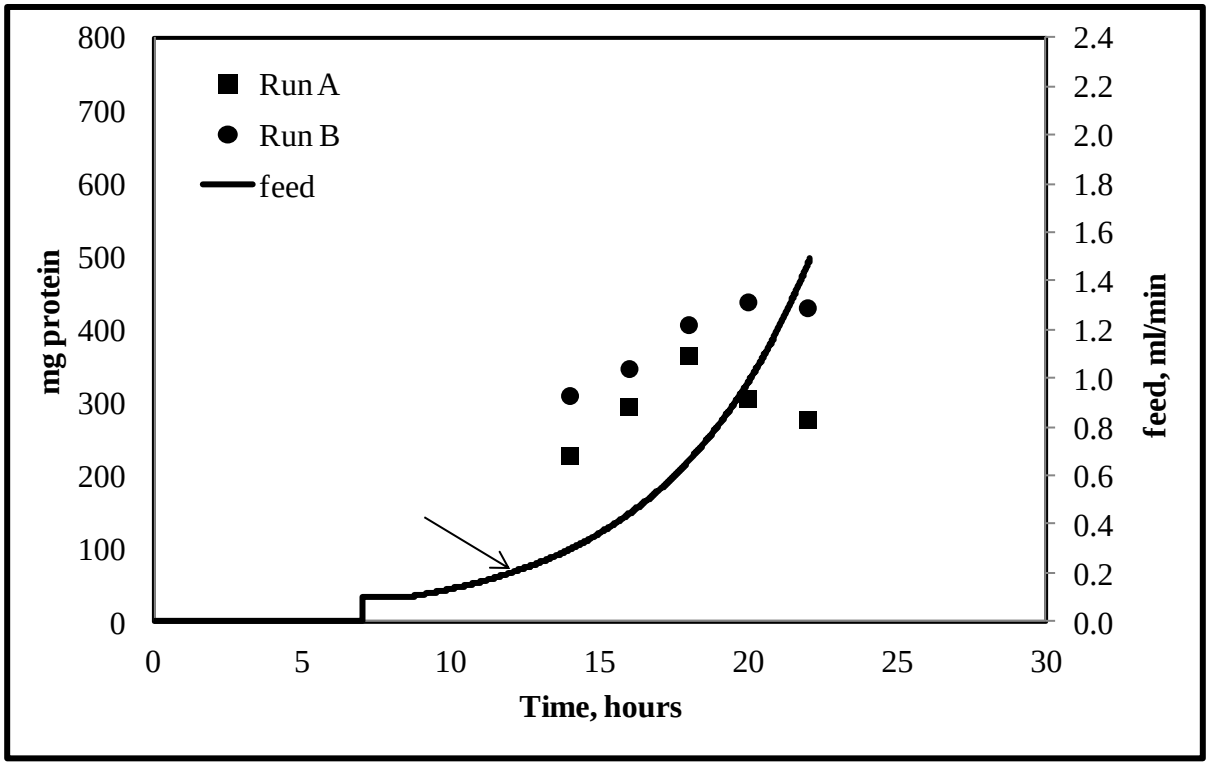

(b)

Figure 5-26. Protein concentrations with respect to time for auto-induction with additional pulsing of lactose. (a) mg protein per gram cell; (b) total mg of protein during fermentation.

Additionally, the average yield of protein per gram cell was fairly constant. It did not appear that protein production depended on the elapsed time of cultivation and the protein produced per gram of cell remains around 14 mg throughout the experiment.

As shown in Figure 5-27, glucose and acetate began to accumulate after 15 hours of fermentation. Concentrations of both substrate increased until approximately 18 hours of fermentation, then stay steady for the remainder of the cultivation. The final concentrations were 1.9 g/l and 1.1 g/l for glucose and acetate, respectively.

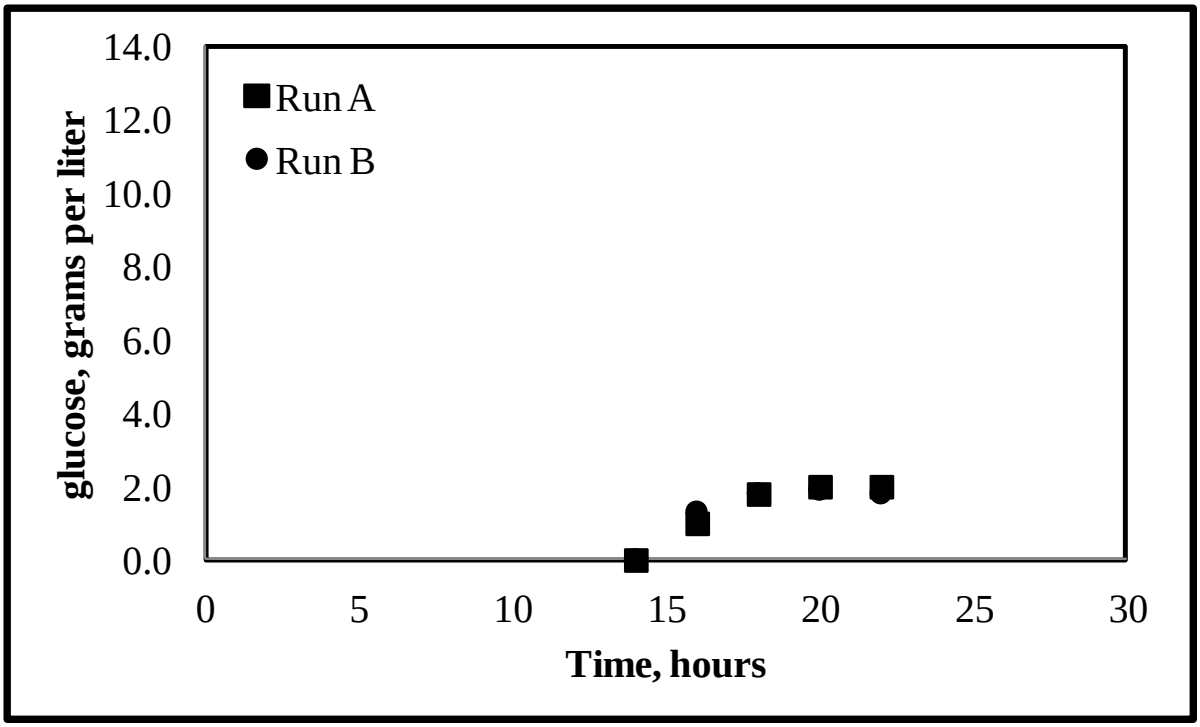
14.0
12.0
10.0
8.0
6.0
4.0
2.0
0.0
glucose, grams per liter
Run A
Run B
0
5
10
15
20
25
30
Time, hours

(a)

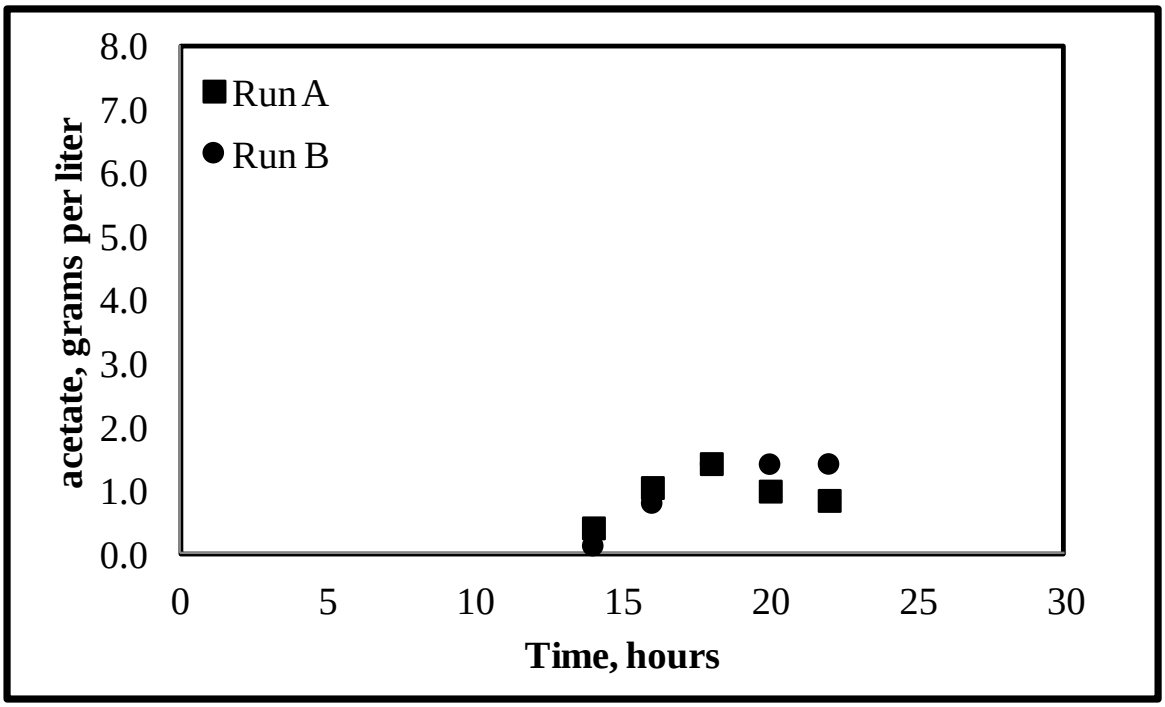
8.0
7.0
6.0
5.0
4.0
3.0
2.0
1.0
0.0
acetate, grams per liter
Run A
Run B
0
5
10
15
20
25
30
Time, hours

(b)

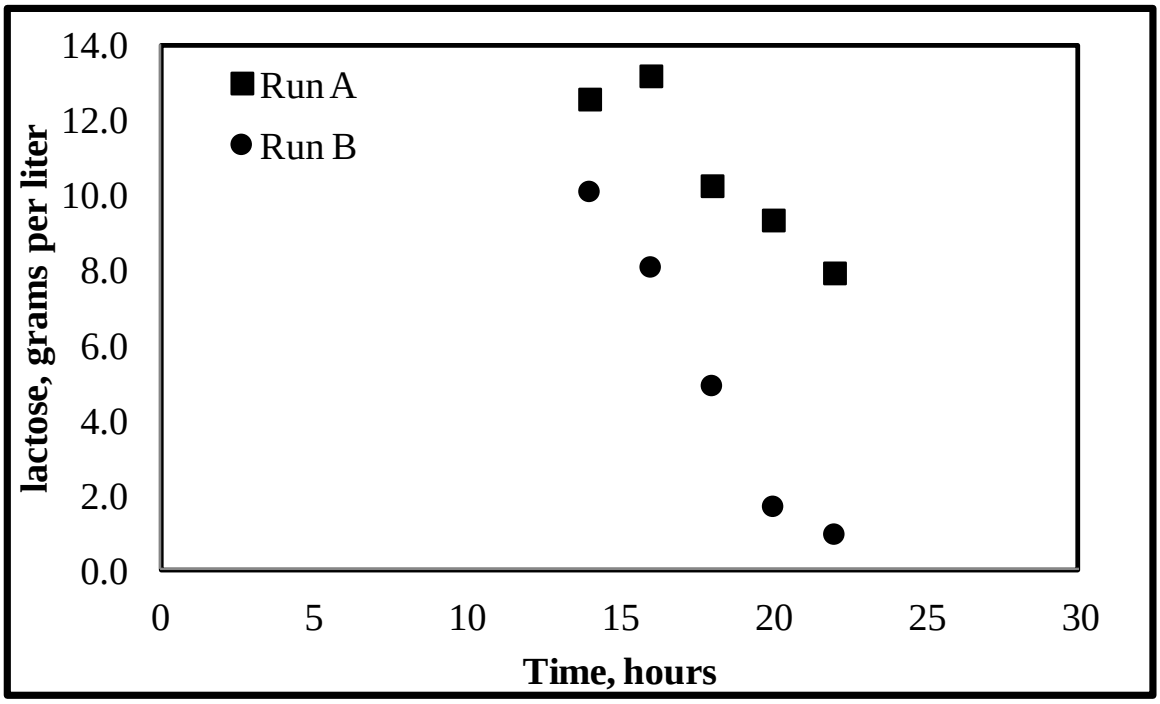

(c)

Figure 5-27. Carbohydrate concentrations for auto-induction with lactose pulse. (a) Glucose accumulated after 15 hours of cultivation; (b) Acetate accumulated after 15 hours of fermentation; (c) Lactose was still present in media at the end of cultivation.

The lactose concentration was over 10 g/l after the pulse of lactose into the system, indicating that there was lactose still remaining in the reactor prior to the pulse. These results are consistent with the results for the auto-induced culture. After 15 hours of inoculation, there was still lactose remaining in the system. The lactose concentration for both experiments seemingly linearly decreased to concentrations of 1 and 8 g/l after 22 hours of cultivation. While this difference is large, the general trend of lactose consumption was the same for both experiments.

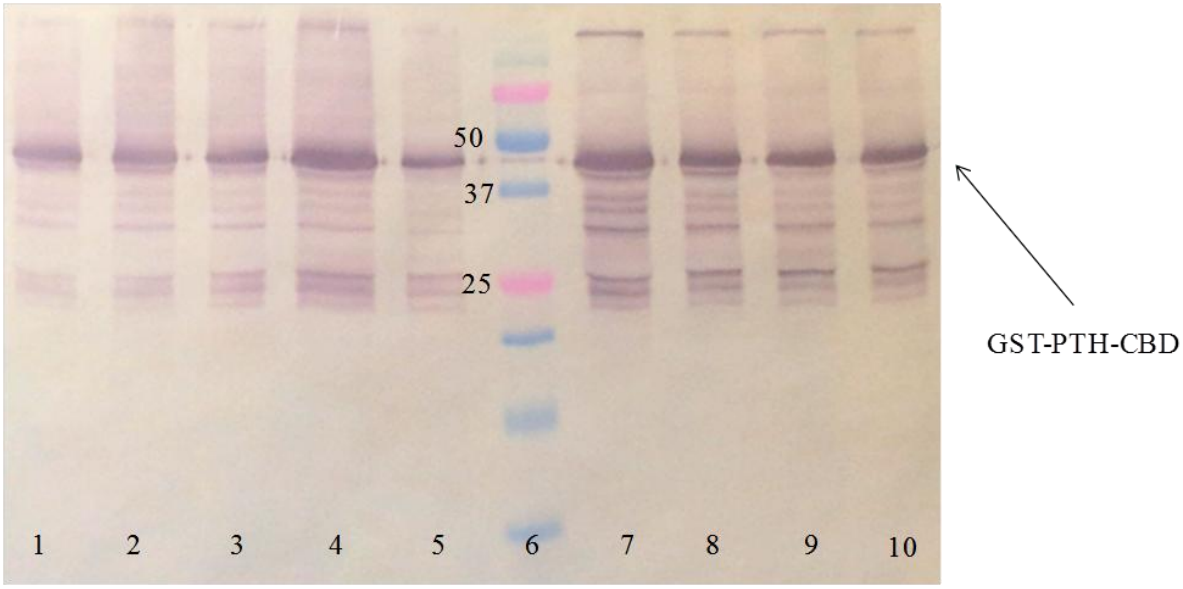

Figure 5-28. Western blot of lysates from auto-induced fed-batch cultures with lactose pulsed into the reactor 12 hours after inoculation. Lane 1 – 2 hours post induction, run A; 2 – 4 hr after induction, run A; 3 – 6 hours after induction, run A; 4 – 8 hr post, run A; 5 – 10 hr post, run A; 6 – molecular weight ladder; 7 – 4 hr post, run B; 8 – 6 hr post, run B; 9 – 8 hr post, run B; 10 – 10 hr post, run B. Times of induction are given with respect to time after the pulse into the system. For example, 6 hours post would be 18 hours after inoculation since the pulse was added 12 hours after inoculation.

As shown by the western blot in Figure 5-28, intense bands representing target protein are present in samples of lysates taken throughout the fermentation experiment. The lysates are from two separate experiments. In run A (left of the molecular ladder), the highest concentration of target protein was produced 8 hours after the pulse of lactose into the system. On the other hand, for run B (right of the molecular ladder), the highest concentration of target protein was produced after only 4 hours of induction with respect to the pulse of lactose. However, the average amount of product remains somewhat constant according to the densitometry results given in Figure 5-26 (b).

5.3.1.3 IPTG induction

To establish a comparison for the lactose-induced runs, experiments were set up for IPTG induction. One set was induced with IPTG to a final concentration of 5 mM. The second set was induced with IPTG to a final concentration of 10 mM. In both cases, the desired induction period was five hours. To induce the maximum number of cells, IPTG was added to the reactor 19 hours after inoculation and the experiment was stopped 24 hours after inoculation. Glucose was utilized as the feed in both cases.

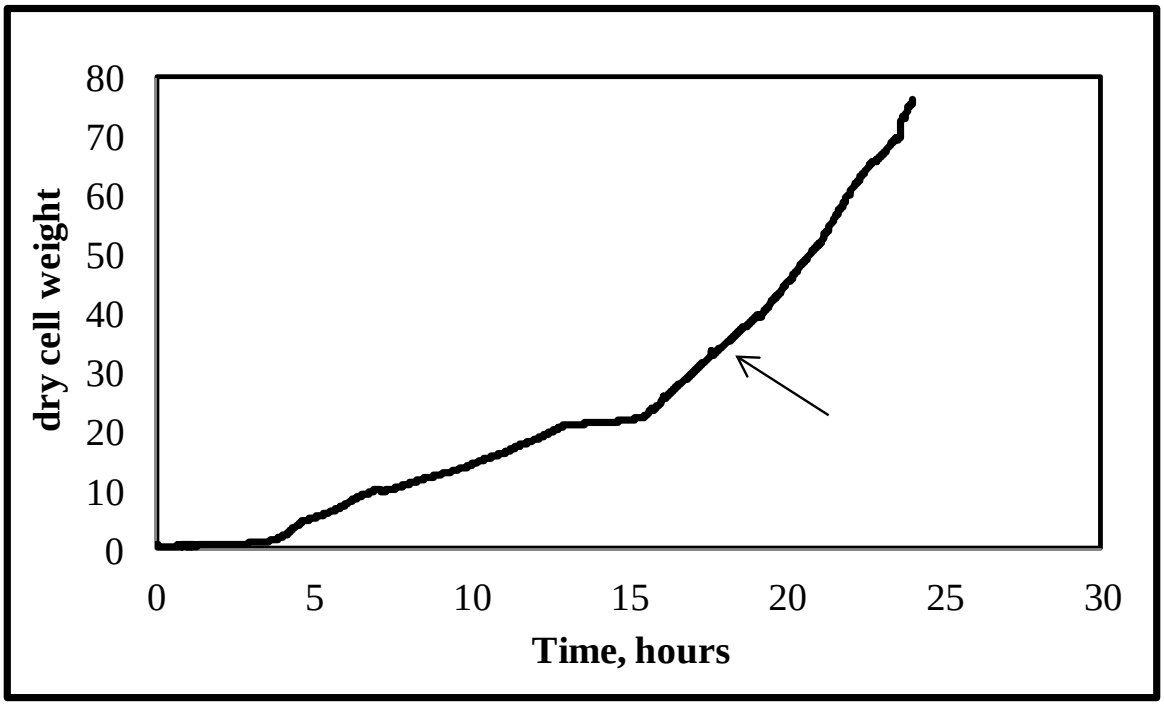

Figure 5-29. Growth curve for 5 mM IPTG-induced culture.

The final dry cell weight for cultivations induced with 5 mM IPTG exceeded previous experiments. With a final dry cell weight of 76 grams (Figure 5-29), these cultivations surpassed the 12 hour lactose cultivations by 16 grams. Additionally, the stationary phase of growth was

not achieved, even after 24 hours of cultivation. Thus, on the fed-batch level, IPTG did not affect cell growth. This result was not expected. As shown previously (Figure 5-10), IPTG negatively affected growth on the batch scale. Also, others reported on growth inhibition by IPTG. Kilikian et al. (2000) found that cell yield from glucose using lactose as an inducer was four times higher than the cultures that were induced with IPTG. Contrary to what Kilikian et al. (2000) and Kosinski et al. (1992) report, there was no apparent metabolic burden from IPTG induction on the fed-batch scale. Also, protein expression with IPTG did occur, so protein production from IPTG did not place any apparent burden on cell growth.

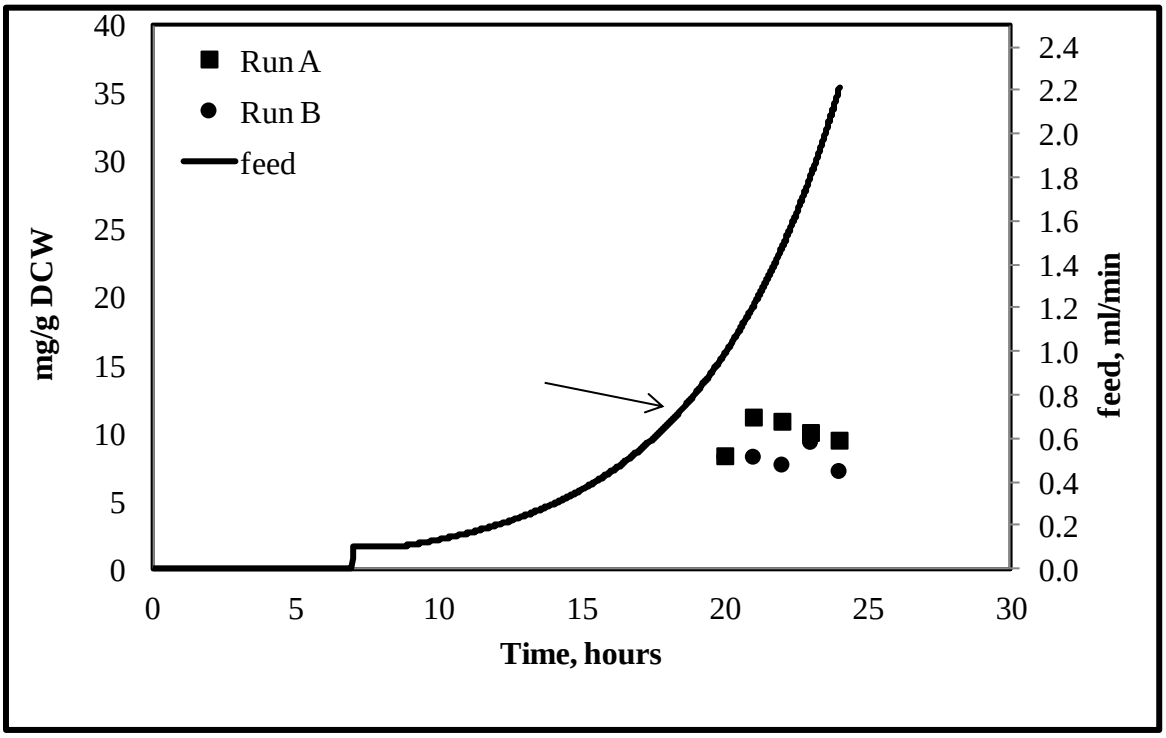

(a)

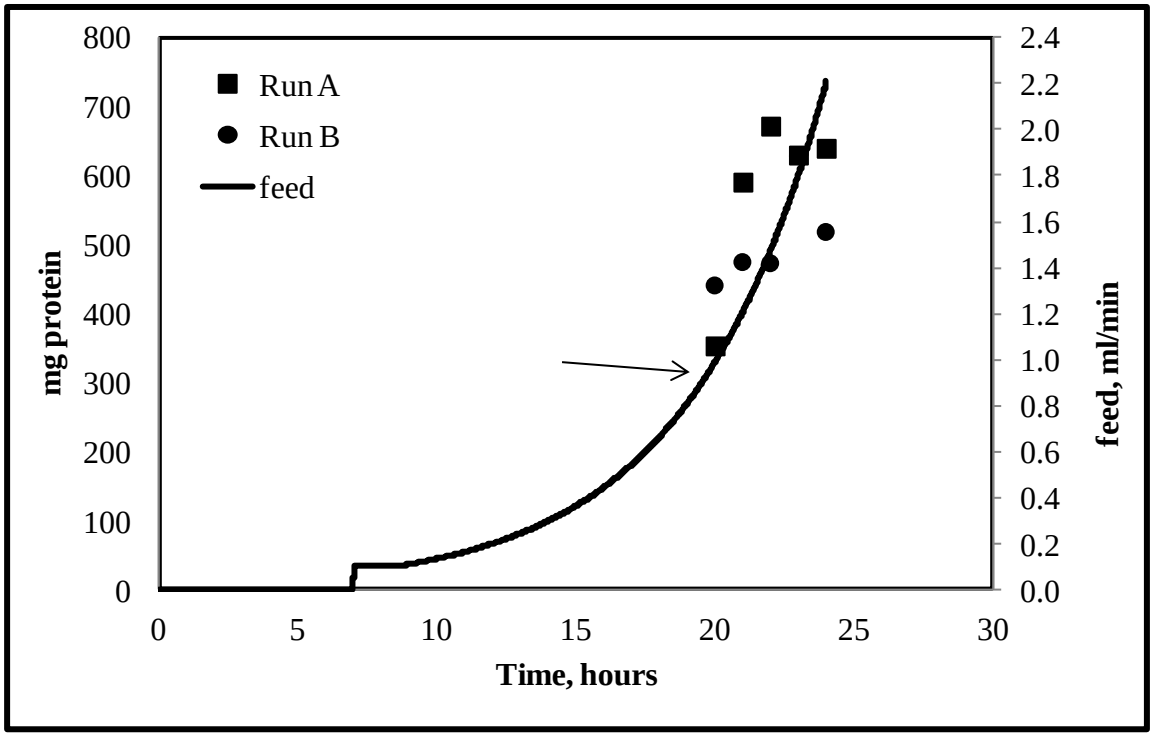

(b)

Figure 5-30. Protein concentrations with respect to time for 5 mM IPTG-induced cultivations. (a) Protein expression on a per gram cell basis; (b) Total amount of protein expressed during cultivation with IPTG induction.

As shown in Figure 5-30 (a), the average product yield was approximately 9 mg. This yield was actually lower that that achieved from auto-induced cultures and comparable to that achieved from simple lactose induction. Though, the yield of protein per cell remained constant for both experiments, which is a similar characteristic to most of the lactose-induced experiments previously discussed. **On a per gram cell level, auto-induced cultures on defined medium surpassed protein production from IPTG-induced cultures.** However, 5 mM IPTG induction surpassed lactose induction and auto-induction with regard to **total protein** expression. This is due to the higher cell densities that were attained using IPTG as an inducer. The average total amount of protein expressed under IPTG induction was approximately 540 mg (Figure 5-30 (b)). The maximum amount of total protein approached 700 mg and was expressed 4 hours after IPTG induction.

As shown in Figure 5-31 (a), glucose accumulated at 20 hours. The accumulation of glucose was 13 hours after the feed started. This was the same for cultures induced with lactose 12 hours after inoculation. However, the auto-induced cultures began to accumulate glucose only 14 hours after inoculation (7 hours after feed start). The cultures induced when the feed commenced also began accumulating glucose 7 hours after feed start. It is also important to note that in all of the cultivations were glucose started accumulated at 7 hours after feed start, the average concentration of glucose never exceeded 2.5 g/l. When glucose didn't start to accumulate until later on in the cultivation (13 hours after feed start), the amount of accumulated glucose was much higher. It reached almost 10 g/l in cultures induced with lactose 12 hours after inoculation and almost 12 g/l for 5 mM IPTG-induced experiments. This indicates that uptake or accumulation of glucose is affected by the time at which lactose is added to the system. The earlier lactose is added, the earlier that glucose will began to accumulate, but the lower the accumulated amount will be. For lactose added later or not at all (as in the IPTG-induced case), glucose accumulation occurred later on in the fermentation, but at higher concentrations.

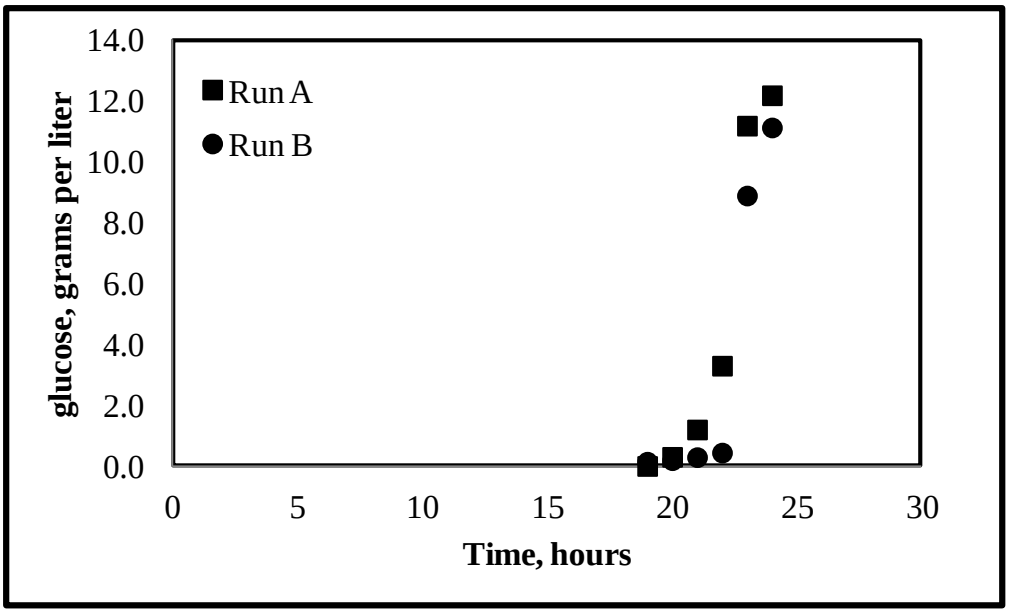

(a)

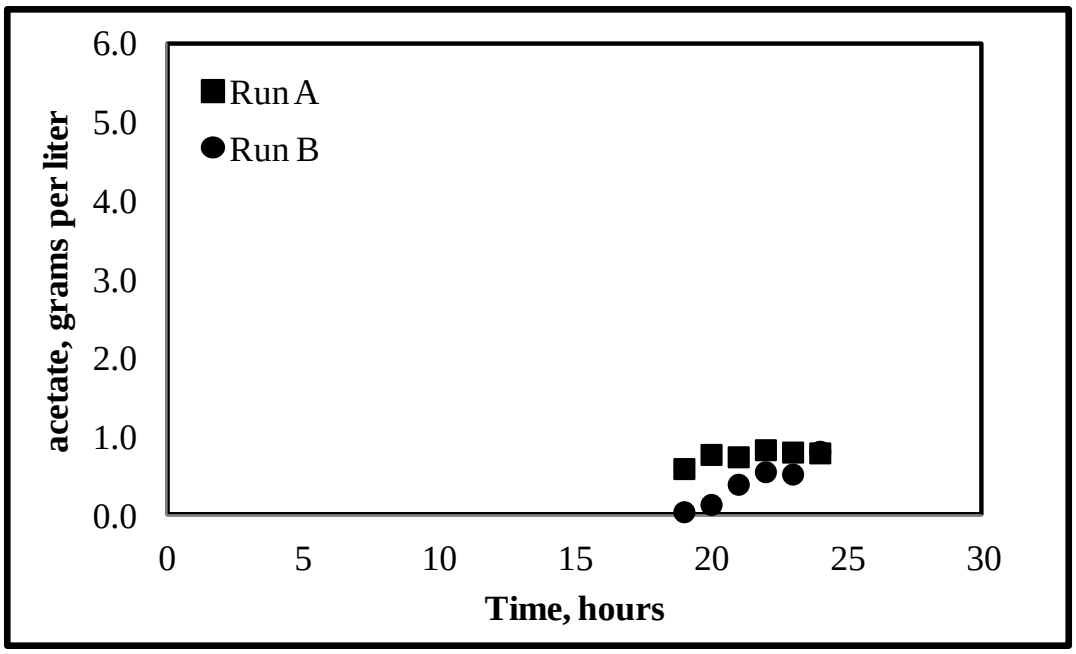

(b)

Figure 5-31. Carbohydrate analysis for 5 mM IPTG-induced cultures. (a) Glucose concentrations; (b) Acetic acid concentrations. Data from two different experiments is given.

As previously witnessed, acetic acid began to accumulate approximately when glucose began accumulating. Once again, the amounts of acetic acid accumulation (Figure 5-31 (b)) did not exceed the inhibitory value. In fact, the concentration of acetic acid remained under one gram per liter even though glucose accumulated in high amounts.

Next, induction with 10 mM IPTG was examined. It was suggested that 10 mM IPTG be used to induce protein expression with this particular construct, so this experiment was performed as a baseline comparison for lactose-induced runs in the same manner that the 5 mM IPTG-induced experiments were conducted. The growth for 10 mM IPTG-induced runs was very similar to that for 5 mM IPTG induction and is shown in Figure 5-32. Because these fermentations never reached the stationary phase, it can be conjectured that the fermentation could be induced at a later time to produce even more protein. Also, 10 mM IPTG-induced

experiments suffered slightly with growth as compared to 5 mM IPTG-induced experiments (70 versus 76 grams).

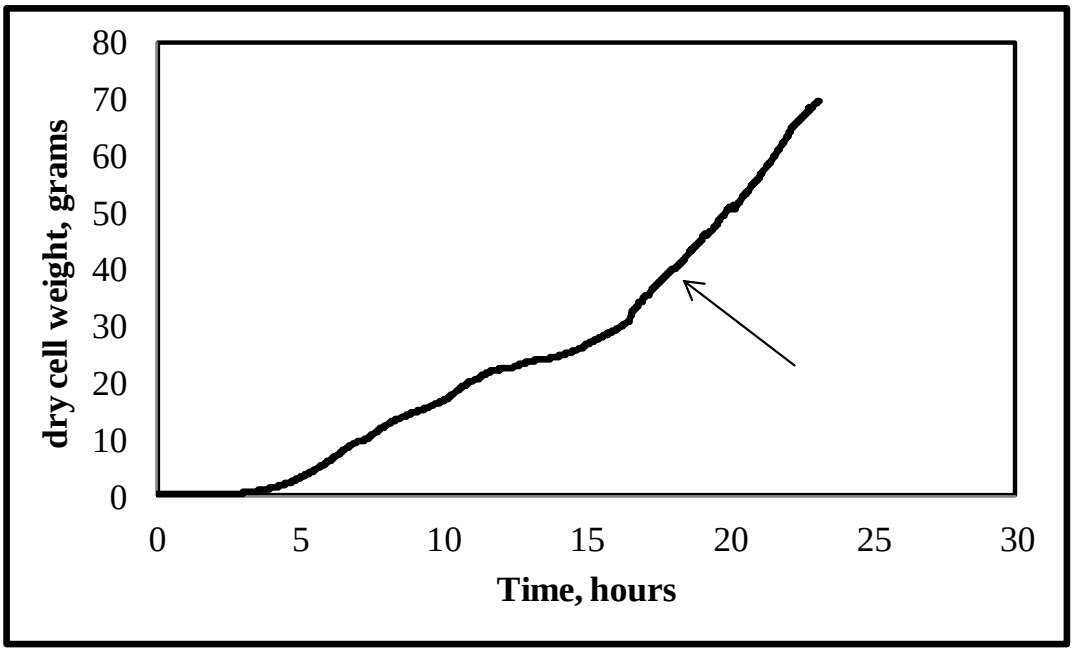

Figure 5-32. Growth curve for 10 mM IPTG-induced cultures.

The protein concentrations are given in Figure 5-33 for 10 mM IPTG induction. The average product yield was 12.1 mg. Not unlike before, the 10 mM IPTG-induced experiments exhibited constant yield of protein per cell. This yield was higher than the 5 mM IPTG induced cultures, but still lower than the auto-induced cultures discussed above. Once again**, on a per cell basis, auto-induction with lactose on defined medium produced more protein than IPTG induction.** However, as shown in Figure 5-33 (b), the total amount of protein produced exceeded all experiments previously discussed. The average total amount of protein was approximately 600 mg. The maximum amount expressed was almost 800 mg and again occurred four hours after induction.

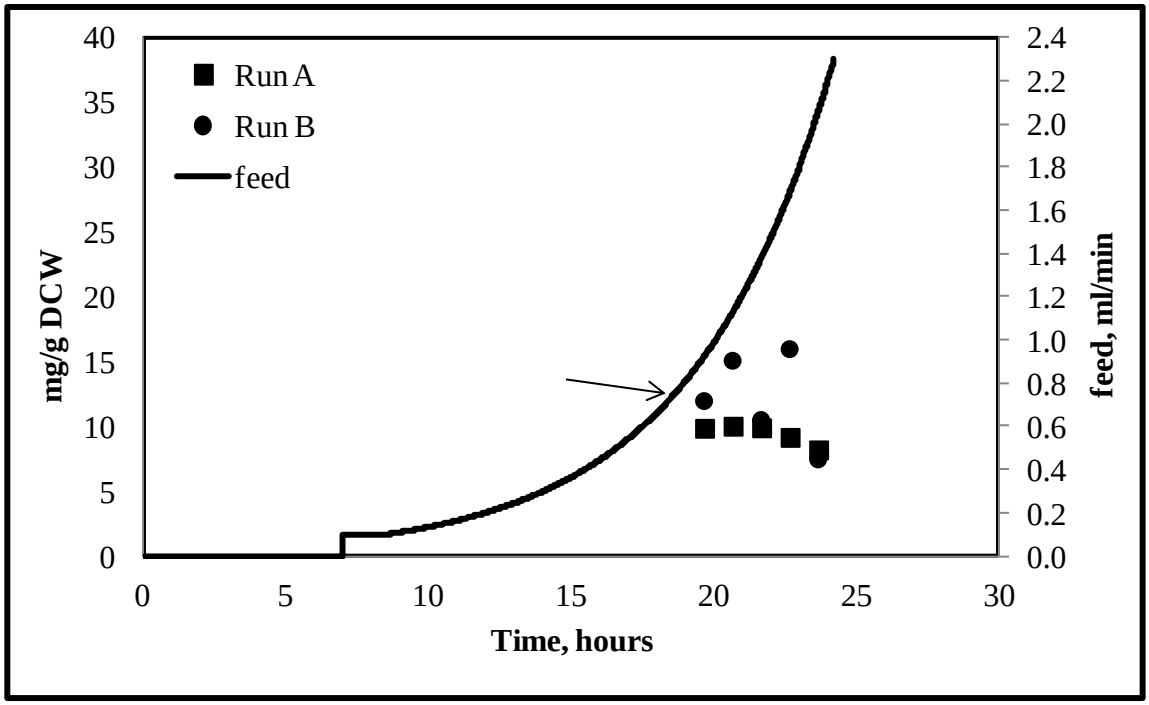

(a)

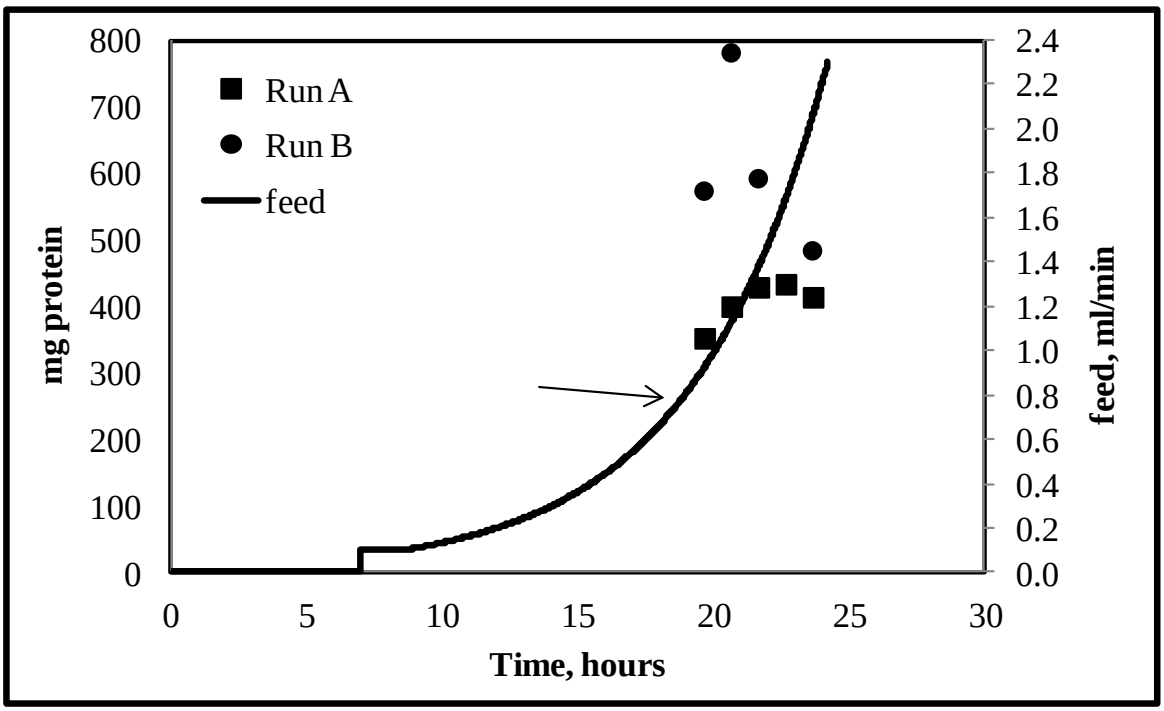

(b)

Figure 5-33. Protein concentrations with respect to time for 10 mM IPTG-induced cultures.

The carbohydrate analysis for the 10 mM IPTG-induced experiments mimicked that for the 5 mM IPTG-induced experiments. Glucose accumulated approximately 20 hours after inoculation, as shown in Figure 5-34 (a), to almost 12 g/l for both experiments. This was the same time and concentration at which glucose accumulated for the 5 mM IPTG induction experiments. Similarly, acetic acid accumulated to 1 g/l, which is well below the value thought to inhibit cell growth (Figure 5-34 (b)).

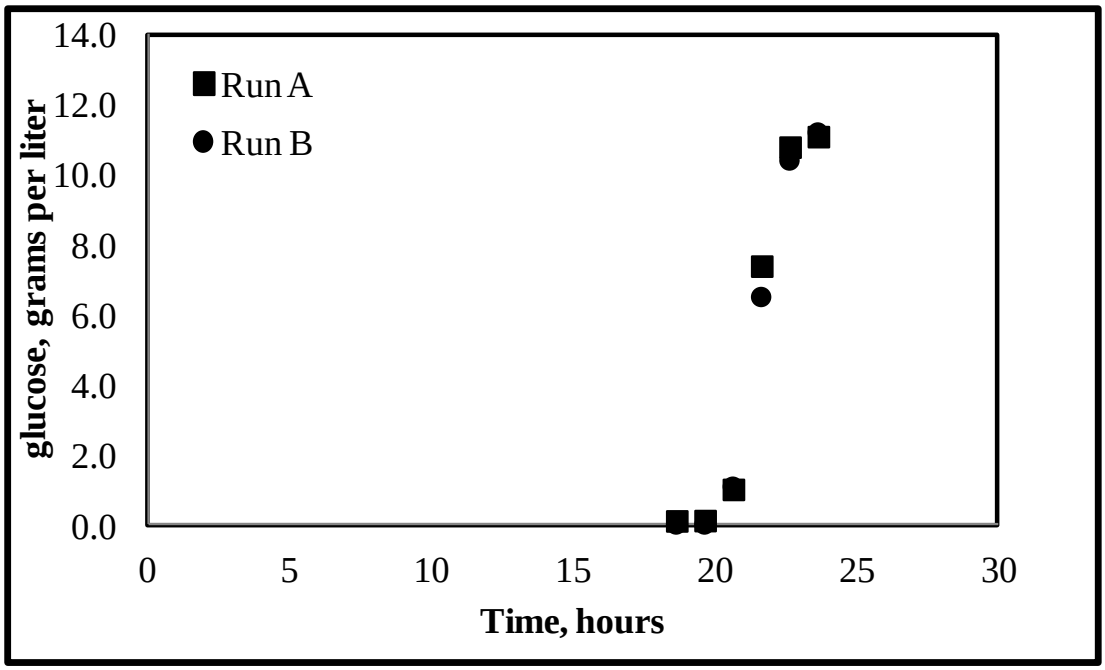

(a)

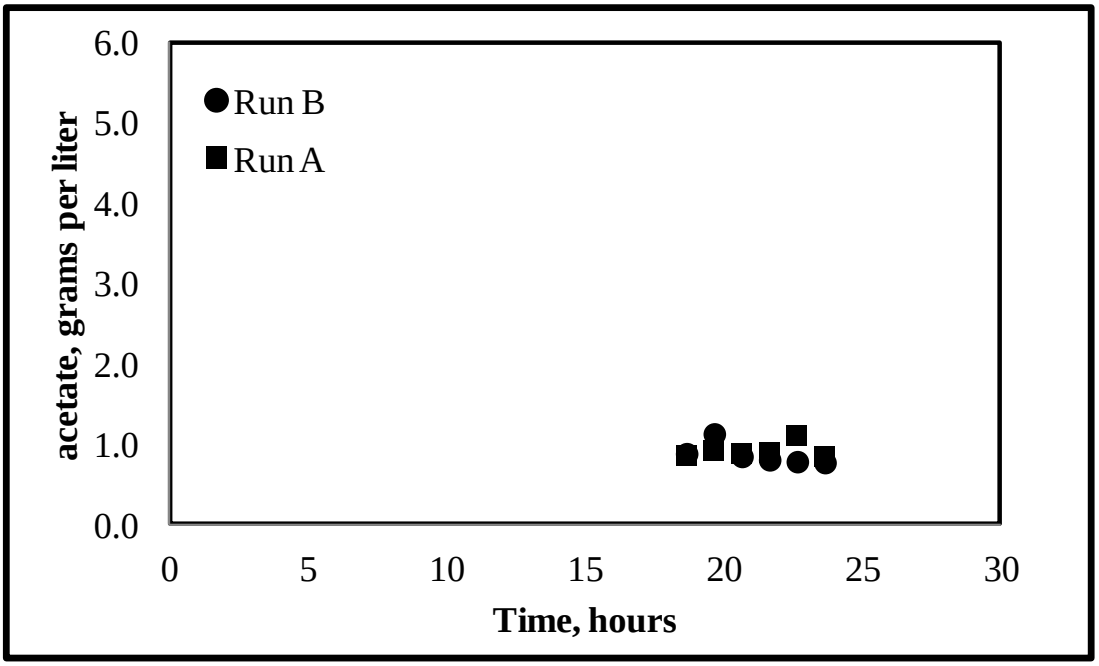

(b)

Figure 5-34. Carbohydrate analysis for cultures induced with 10 mM IPTG. (a) Glucose accumulated after 20 hours of inoculation (13 hours after feed start); (b) Acetic acid remained around 1 g/l between 18 and 24 hours after inoculation. Data from two different experiments is given.

In order to summarize all of the fed-batch fermentation experiments with glucose as a feed source, Table 5-2 shows the final characteristics of each experiment with respect to cell mass and protein expression.

Table 5-2. Summary of all fed-batch experiments using glucose as a feed source. A-I refers to fed-batch experiments that utilized an auto-induction technique.

Method	Final DCW	Average mg	Maximum mg	Average $Y_{P/X}$	Maximum $Y_{P/X}$
Lactose 11 hrs after inoc (st)	50	40.8	44.9	2.97	3.23
Lactose 12 hrs after inoc	60	327	463	9.92	11.3
Lactose at feed start	41	192	220	9.44	10.9
Lactose A-I	43	308	369	11.4	14.6
Lactose A-I with pulse	33	301	358	13.9	16.3
5 mM IPTG	76	542	629	9.06	9.72
10 mM IPTG	70	611	725	12.1	13.2

According to Table 5-2, IPTG-induction yielded the highest amount of total protein. This finding is due to the fact that higher cell densities were achieved using IPTG as an inducer. However, experiments that utilized an auto-induction technique yielded the highest amount of protein per gram of cell. It is also important to note that IPTG did not have an effect on growth on the 3L fed-batch scale, as it did on the batch scale. Since batch cultures were also induced with 5 mM and 10 mM IPTG, this was not expected. However, for batch cultivations, induction occurred when the optical density was less than 6 units. For fed-batch cultivations, induction occurred when the optical density was between 65-70 units. This is a 10-fold difference in cell density and on a per cell basis, the cells in the batch cultivations witnessed higher local IPTG concentrations. Since the amount of IPTG added is based only on volume (not on cell density), this local concentration difference may account for the differences in IPTG affecting growth. Also, as shown in the growth curves for fed-batch experiments utilizing lactose, lactose inhibited the production of biomass, but not the uptake of glucose on the fed-batch scale.

5.3.2 Cultures fed with glycerol as major carbon source

5.3.2.1 Lactose induction after inoculation (at feed start)

To investigate the ability of lactose to act as an inducer in the absence of glucose, fed-batch experiments were performed with glycerol feed. The first experiment utilized a pulsing of 15 grams of lactose into the system when the feed commenced. 15 grams of lactose was used instead of 10 g/l to see if the higher amount of lactose increased the amount of product with no substrate inhibition due to the presence of glucose in the system. The initial concentration of lactose after the pulse was approximately 14 g/l. As shown in Figure 5-35, the final dry cell

weight barely reached 20 grams. This was the lowest final dry cell weight observed amongst all of the experiments thus far.

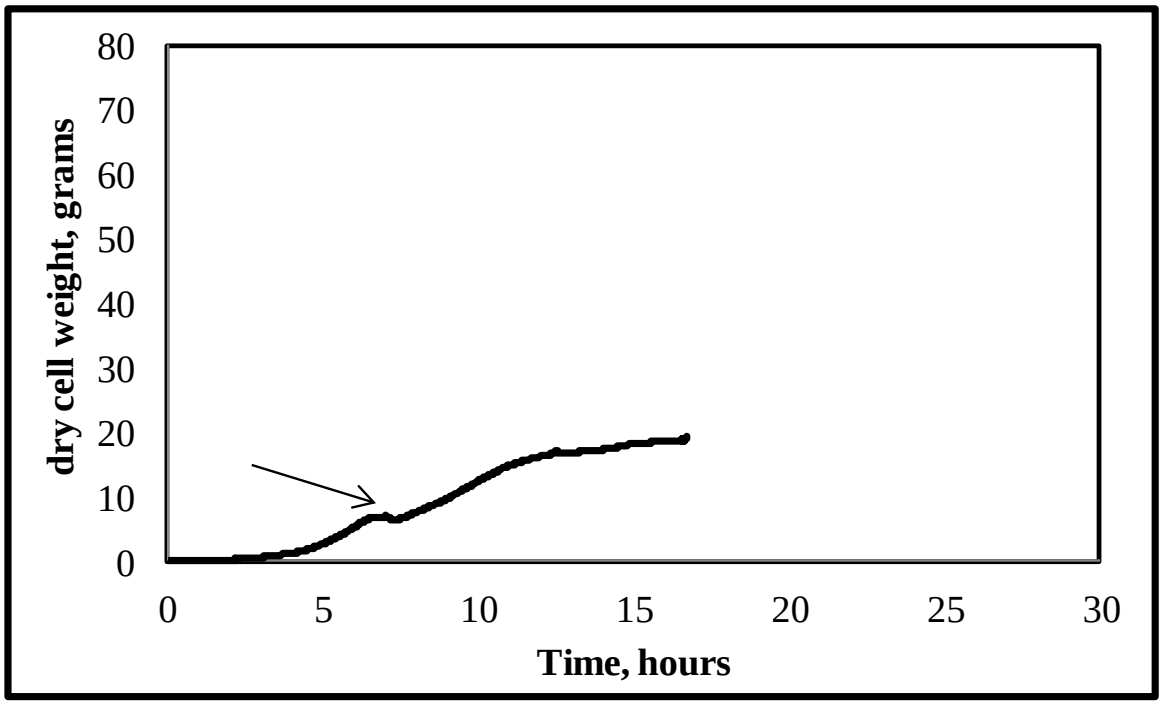

Figure 5-35. Growth chart for glycerol-fed cultivations with 15 grams lactose added at feed start.

Even though the final cell mass was low, the product yield was comparable to that achieved in the experiments that were auto-induced and pulsed with lactose. The average yield per gram cell was 13.7 mg/g DCW (shown in Figure 5-36 (a)). This was one of the highest numbers reached for yield of product per gram cell. Also, the yield of product actually increased during the fermentation experiment. In previous experiments, the yield remained somewhat constant or oscillated during the experiment. The maximum yield achieved in this run was 16.2 mg/g DCW. The highest maximum yield was achieved in the auto-induced pulsed with lactose experiment at an average value of 16.3 mg/g DCW. Thus, protein yield numbers from glycerol-fed auto-induced experiments mimicked those achieved from auto-inducting cultures using glucose as the feed substrate with an extra lactose pulse.

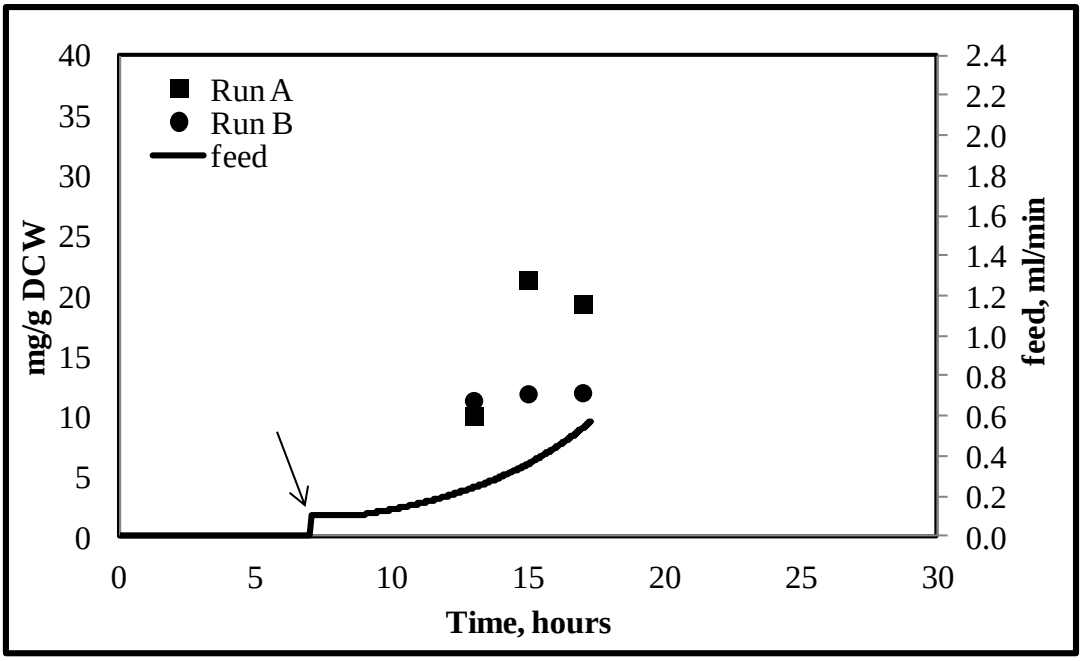

(a)

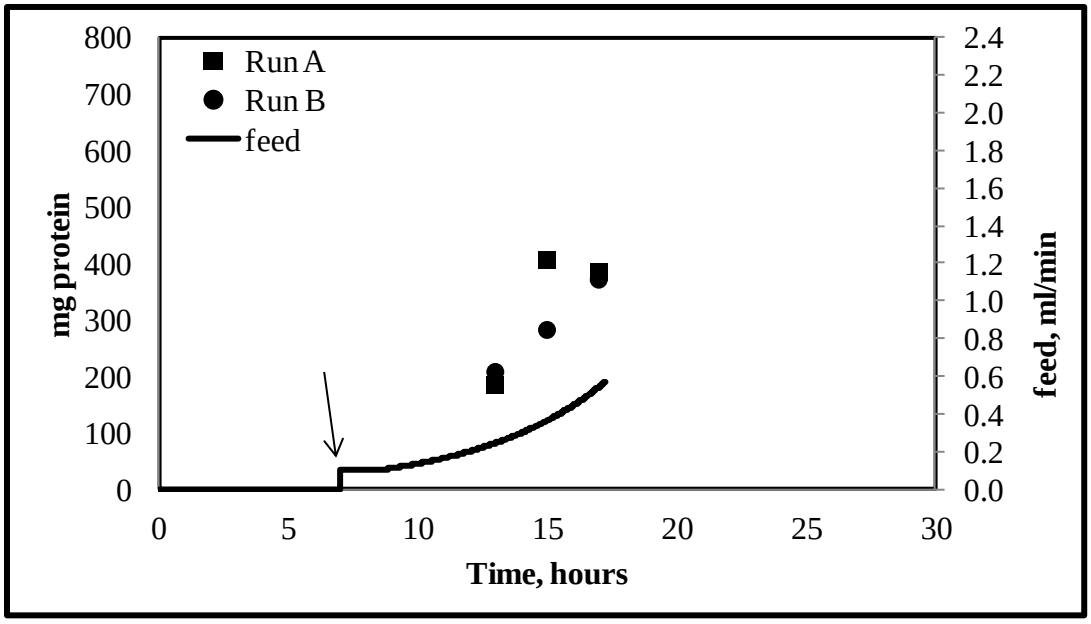

(b)

Figure 5-36. Protein concentration with respect to time for glycerol-fed cultivations with 15 grams of lactose added at feed start. (a) Protein produced per gram cell; (b) Total protein production.

Due to the low number of cells produced during cultivation, the total product numbers also suffer. The greatest amount produced on average was approximately 308 mg, with an average of 244 mg protein. This was on the lower end of the numbers for total product yield.

Table 5-3. Comparison of results for fermentations induced with lactose when feed started with respect to type of feed.

Feed	Average mg	Maximum mg	Average $Y_{P/X}$	Maximum $Y_{P/X}$	Final DCW
Glucose	192	220	9.44	10.9	41
Glycerol	244	308	13.7	16.2	19

With the exception of using 15 grams (14 g/l) lactose instead of 10 g/l lactose, the two experiments can be directly compared with respect to type of feed used. Table 5-3 summarizes the results from glucose or glycerol-fed fermentations with the inducer added at the time of feed start. Even though the final dry cell weight for the glycerol-fed experiments was less than half of that for the glucose-fed experiments, the results for protein production are higher. The average yield increased from 9.44 to 13.7 mg/g DCW. Similarly, the average total amount of product increased from 192 to 244 mg. Hence, using glycerol feed with 15 grams of lactose increased protein production compared to glucose-fed fermentations when the lactose was added at the time of feed start.

As shown in Figure 5-37(a), 15 grams of lactose was completely consumed by 17 elapsed hours. Also, glycerol accumulation began after 14 hours of fermentation. By the end of the fermentation, glycerol exceeded concentrations of 12 g/l. The low growth characteristic cannot be attributed to the accumulation of glycerol because glycerol accumulated at much higher concentrations in the next type of fermentation and the growth for those experiments is much better.

The acetic acid concentration in this type of fermentation did not exceed 0.4 g/l (Figure 5-37(b)) and was oscillatory in nature. It first began accumulating when glycerol began to accumulate. However, the glycerol accumulated in an exponential manner for both experiments, while acetate decreased at the next time point. This was followed by an increase. Because of the low concentration of acetic acid, the low density of cells cannot be attributed to growth inhibition by acetate. However, it was not expected that acetic acid will accumulate in glycerol-fed cultivations. The reasoning for this accumulation is discussed in detail in the next section.

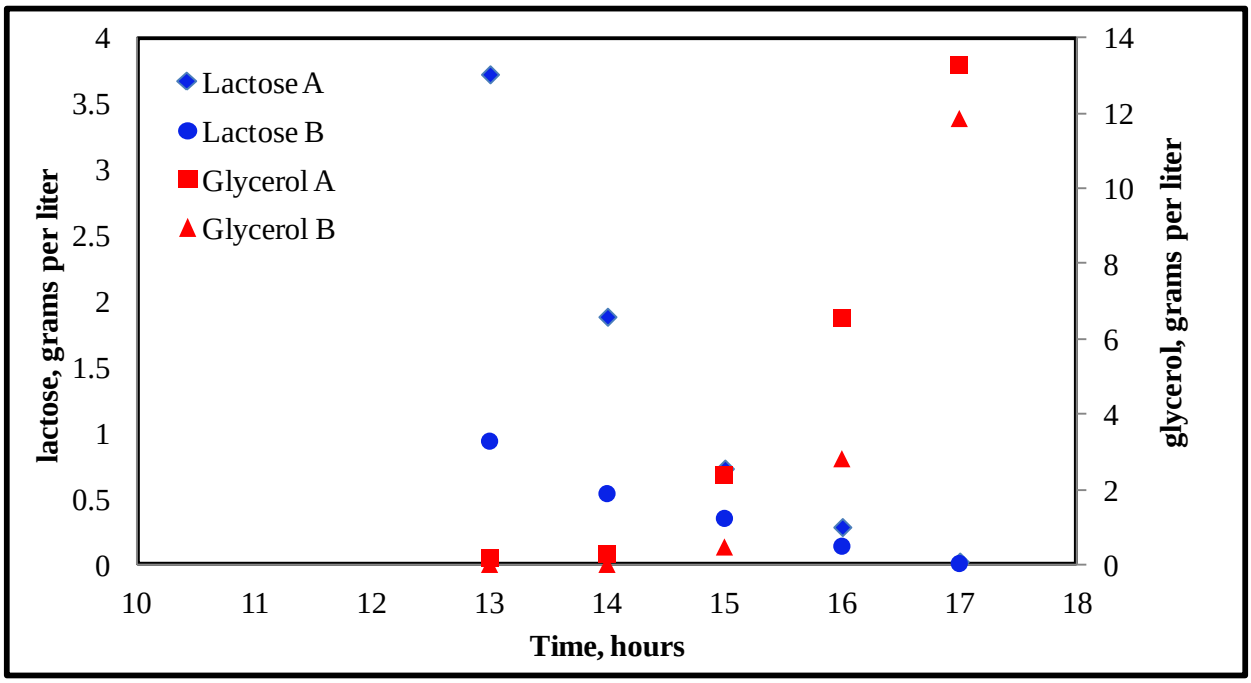

(a)

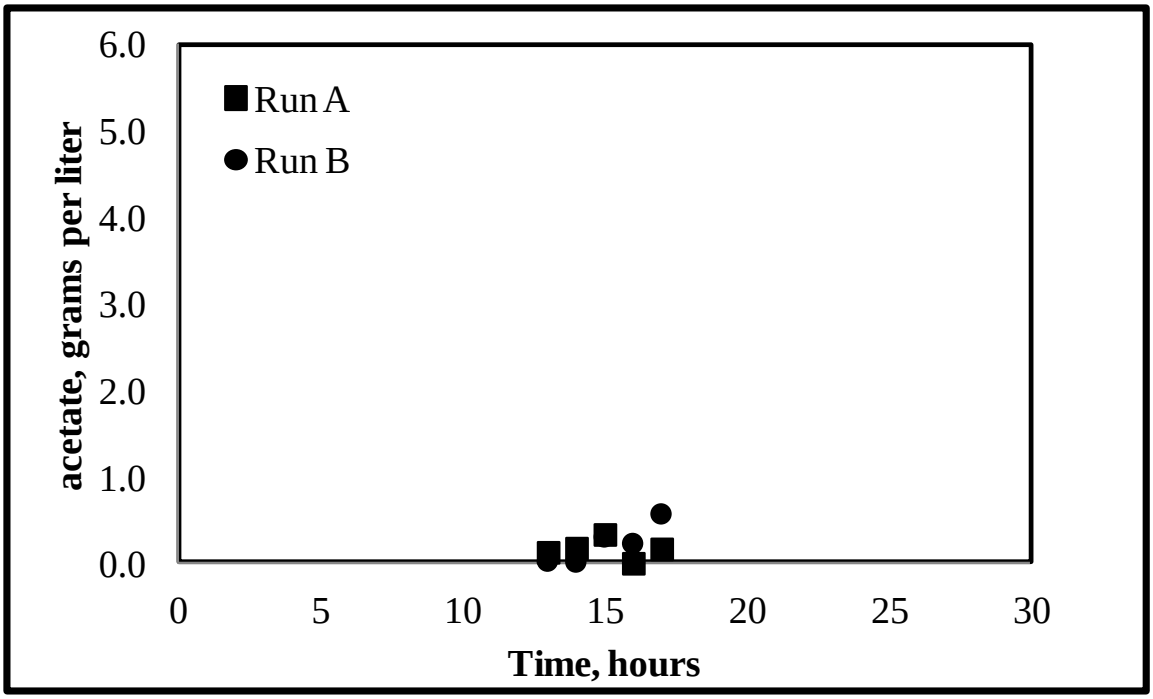

(b)

Figure 5-37. Carbon concentrations with respect to time for glycerol-fed cultivations induced with 15 grams of lactose at feed start. (a) Lactose and glycerol concentrations during fermentation; (b) acetic acid concentrations during cultivation.

It is important to note that there were only three data points for the protein concentrations for these experiments because foam became an issue with glycerol-fed fermentations that were induced when the feed began. On multiple occasions, disregarding the high concentration of anti-foam in the reactor, the culture broth foamed out of the reactor through the condenser exhaust tube. This event happened after 17 hours of fermentation on each occasion. It could be conjectured that higher amounts of protein would have been produced if the fermentation experiment had lasted for longer than 17 hours. However, 17 hours of fermentation time did allow for a ten hour induction period which is consistent with previous experiments. Also, since the stationary phase had been reached almost five hours prior to foaming-out, cell growth probably would not have benefited from additional fermentation time.

From a cost stand point, the cost of production of these two experiments is also comparable. About six cents separates the cost per mg/g DCW of product, with the lower amount coming from the glucose-fed experiment. The cost analysis is discussed for each experiment in detail in Section 5.4.

5.3.2.2 Auto-induction with lactose

The next set of experiments examined auto-induction with glycerol. Lactose was added prior to inoculation at a concentration of 10 g/l. As shown in Figure 5-38, the final dry cell weight was approximately 35 grams. This was almost double the dry cell weight from the fermentations using glycerol feed and induction with lactose at feed start, but half as much as the glucose-fed IPTG-induced fermentation experiments.

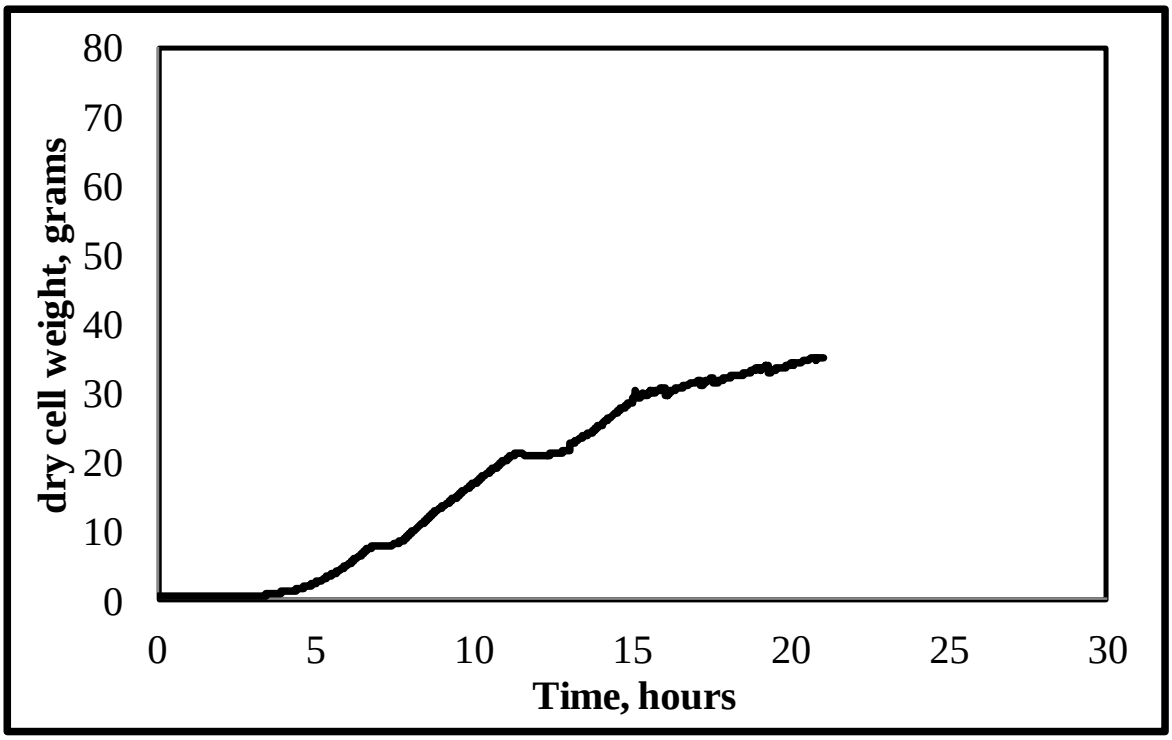

Figure 5-38. Growth chart for auto-induced cultures with glycerol feed.

Even though the final cell mass did not exceed experiments previously performed, protein yield exceeded any fermentation thus far. As shown in Figure 5-39 (a), the production of protein remained somewhat constant throughout the fermentation experiment at an average value of 20.2 mg/g DCW. (The next highest is 13.9 mg/g DCW and was achieved in the auto-induced glucose-fed experiments with an extra pulse of lactose.) The total protein numbers increased linearly (Figure 5-39 (b)) during the experiment due to the fact that the stationary phase never completely leveled off or remained constant, as shown in Figure 5-38. The average maximum total amount of protein produced was 522 mg, with an overall average amount of 426 mg.

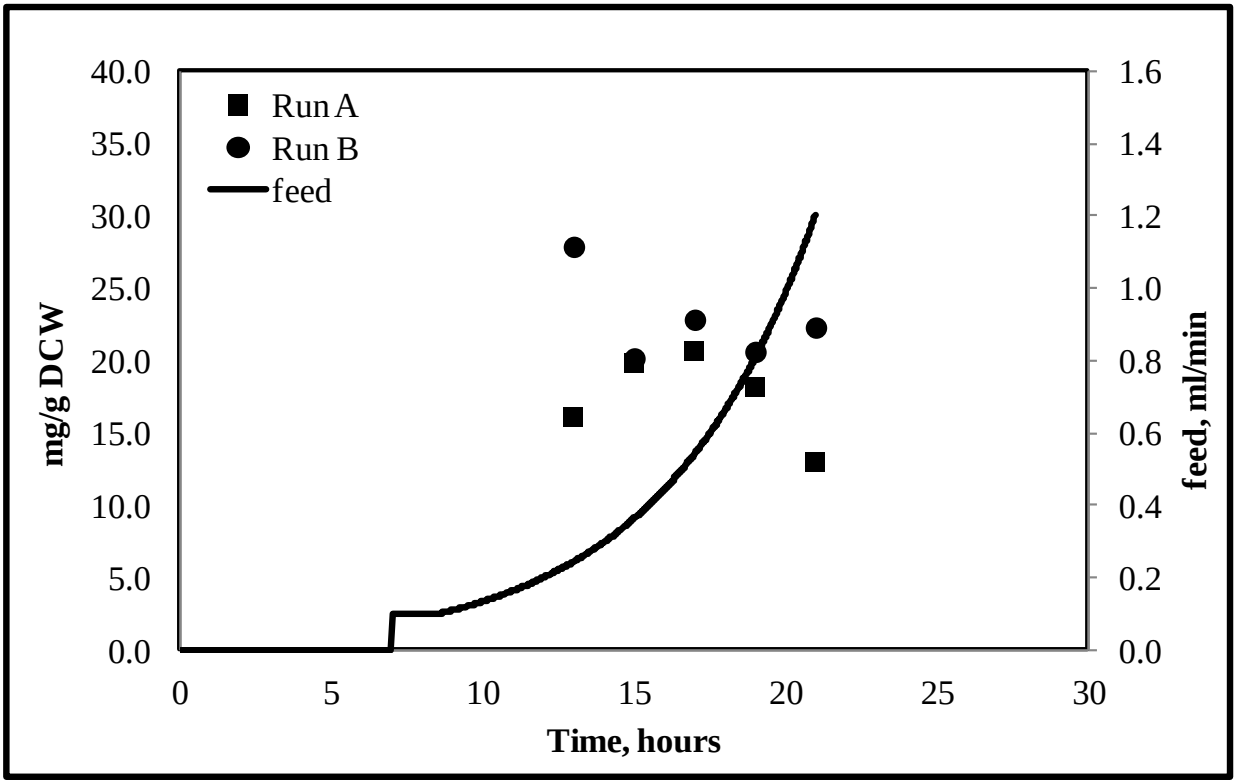

(a)

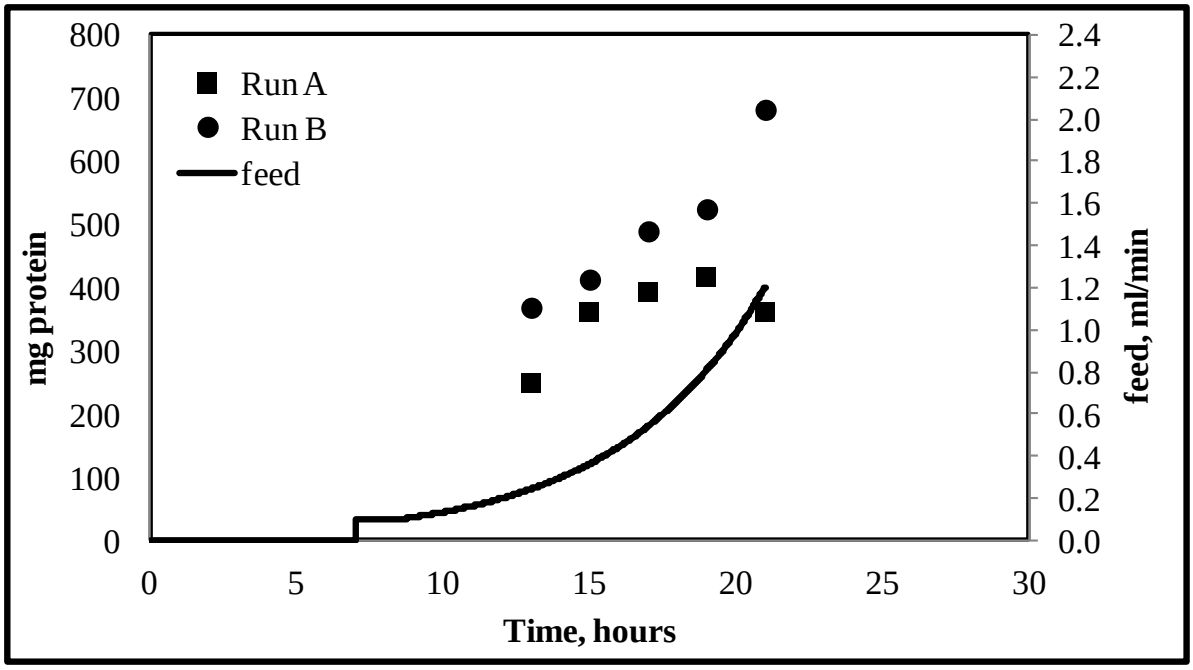

(b)

Figure 5-39. Protein concentrations with respect to time for auto-induced cultures with glycerol feed.

For cultures auto-induced with lactose, direct comparison of results is feasible since the only difference between the two sets of experiments is the feed type. Table 5-4 summarizes the important results with respect to protein production and final dry cell weight based on the feeding substrate. For glucose-fed auto-induced cultures, the final dry cell weight was slightly higher. However, the glycerol-fed auto-induced cultures produced almost two times the amount of GST-PTH-CBD than the glucose-fed fermentations. Though, unlike before, the cost of producing 1 mg/g DCW using auto-induced glycerol-fed cultures was double that of auto-induced glucose-fed cultivations. As discussed later in Section 5.4, this cost is still extremely low compared to cultures that were induced with IPTG ($0.185 and $0.36 versus $5.97).

Table 5-4. Comparison of auto-induced experiments with respect to feed type.

Feed	Average mg	Average maximum mg	Average $Y_{P/X}$	Maximum $Y_{P/X}$	Final DCW
Glucose	308	369	11.4	14.6	43
Glycerol	426	522	20.2	22.0	35

In these experiments, the lactose was completely depleted by 15 hours. Glycerol also accumulated 15 hours after inoculation, as shown in Figure 5-40(a). The glycerol concentration at the 17 hour mark was similar to that in the 17 hour sample from the previous glycerol-fed fermentation with lactose added at feed start. But, since this fermentation experiment lasted four hours longer, the final glycerol concentration exceeded 50 g/l. The highest concentration of substrate accumulated in the glucose-fed experiments was approximately 12 g/l. It is clear through these experiments that the cells do not consume glycerol as efficiently as they consume glucose with the feed profile that was in use. This was expected due to the lower growth rates and lower biomass yields that are typically found in the literature when using glycerol feed (compared to glucose feed). Also, glycerol could have become inhibiting over a certain amount, though the concentration here did not exceed the reported inhibitory value. Glycerol accumulated at concentrations greater than 10g/l around 17 hours after inoculation. This was approximately when the stationary phase of the culture is reached (Figure 5-38).

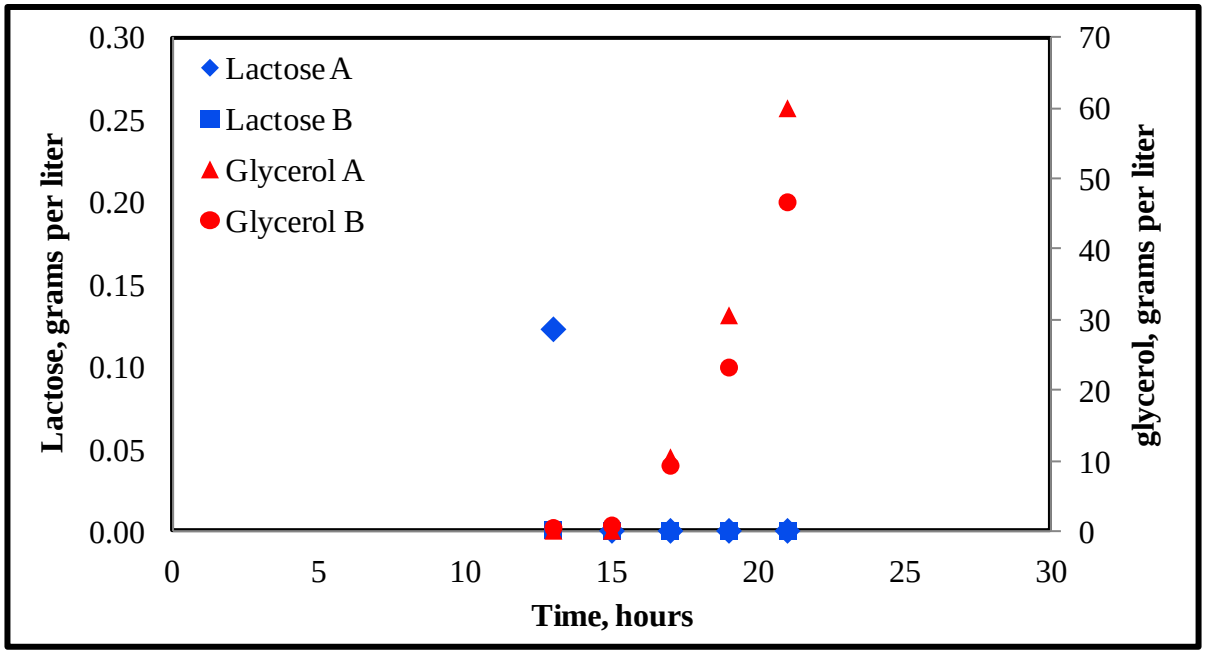

(a)

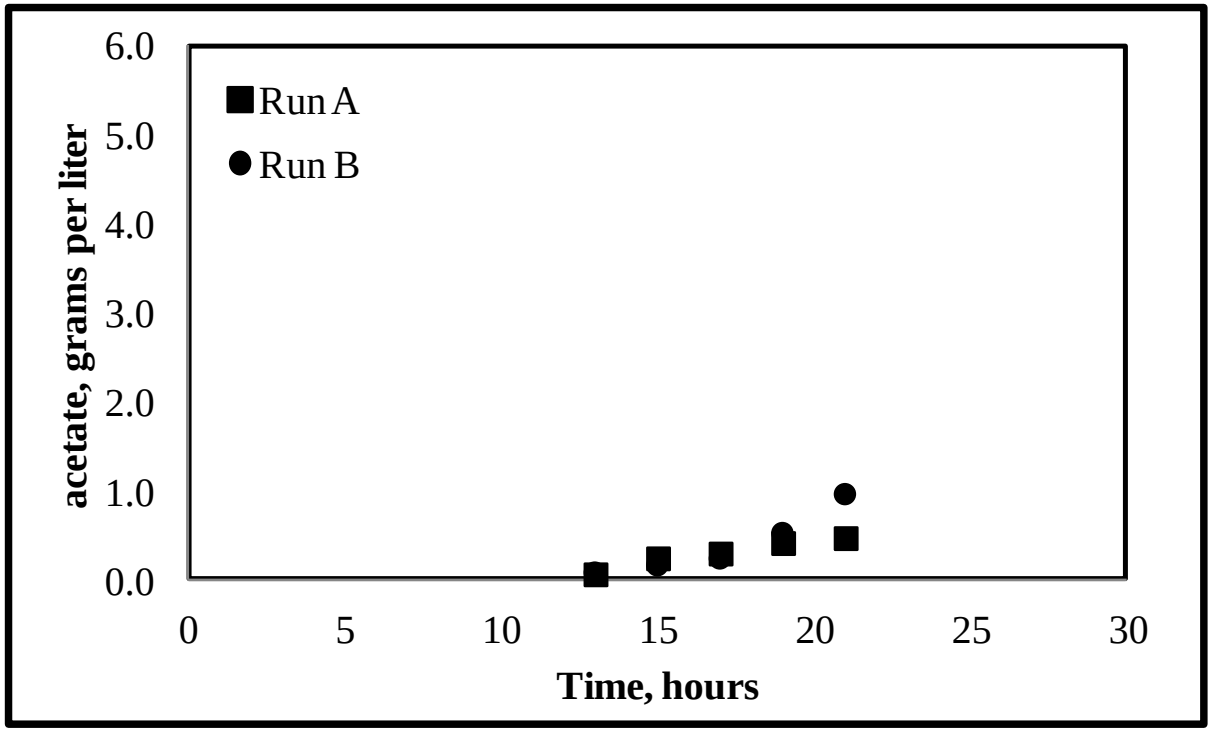

(b)

Figure 5-40. Carbon concentrations. (a) Lactose and glycerol concentration; (b) Acetic acid concentration during fermentation experiment.

Additionally, lactose was completely consumed by 15 hours of cultivation. Thus, the next experiment examined the pulsing of lactose into the system 14 hours after inoculation to avoid completely depleting lactose from culture broth.

Unlike the previous experiment where there was no more than 0.4 g/l produced, acetate accumulated at a concentration over 1 g/l (Figure 5-40 (b)). The appearance of acetate also occurred prior to the accumulation of glycerol. As stated before, acetic acid does not typically accumulate for experiments fed with glycerol. Other groups found this same phenomenon for fed-batch fermentation experiments. Garcia-Arrazola et al. (2005) and Macaloney et al. (2007) found that acetic acid was excreted when the specific growth rate reached a critical value. Recall that for defined media, acetate synthesis will begin at a growth rate of 0.35 hr^{-1}. While it is not probable that this growth rate is achieved during glycerol-fed fermentations with glycerol feed, Korz et al. (1995) found that the critical growth rate for acetate synthesis from glycerol is 0.17 hr^{-1}. If the growth rate exceeds this value, acetic acid accumulates regardless of the accumulation of glycerol.

In the experiments performed by Korz et al. (1995), glycerol is exponentially fed to the reactor in a manner such that the concentration of glycerol remains undetectable during the feeding portion of the experiment. But, at the end of the experiment, over 3 g/l of acetate is detected. Similarly, Macaloney et al. (1997) found that acetate was excreted after the growth rate surpassed a critical rate. In one experiment, they kept the feed rate low enough as to not surpass the critical growth rate and no acetate accumulated during the feeding phase of the fermentation. When they increased the feed as to cause glycerol accumulation, acetic acid began accumulating as well. It is important to note that Macaloney et al. utilized yeast extract and tryptone, so the

media was not completely defined. However, Garcia-Arrazola et al. (2005) utilized a completely defined media and found similar results.

It can be concluded that acetate does accumulate when glycerol is used as the carbon source if a certain critical growth rate is reached. Though, the concentration of acetate that accumulated for this experiment was low compared to the concentration that must be reached to cause inhibition of growth.

The final fermentation that was performed utilized auto-induction with an additional pulse of lactose into the system 14 hours after inoculation. Ten grams of lactose was added prior to inoculation. As shown in Figure 5-41, the final cell mass never exceeded 20 grams. The growth for this experiment was comparable to the glycerol-fed fermentations with lactose added at the time that feeding began. The stationary phase was reached early on in the cultivation - only 12 hours after inoculation. The fermentation was carried out for nine additional hours and a slight increase in growth was witnessed towards the end of run. However, the final dry cell weight was still among the lowest dry cell weights achieved for a fed-batch fermentation experiment.

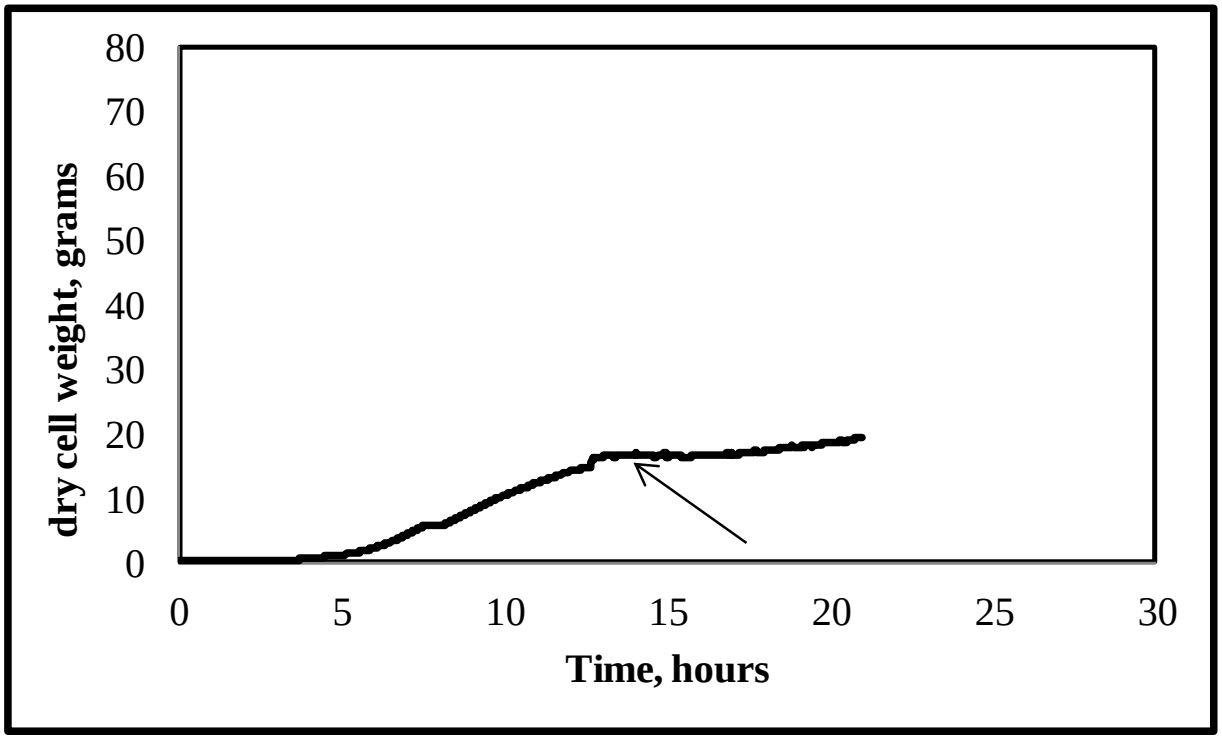

Figure 5-41. Growth curve for auto-induced cultures with lactose pulsed into glycerol-fed fermentation at 14 hours.

The trends for product yield are interesting for auto-induction with a pulse and glycerol feed. As shown in Figure 5-42 (a), an increase in product formation was witnessed from 13 to 17 hours after inoculation. After this point, a decline in product occurred. This was the only experiment where the increase in product yield per gram of cells was followed by a sharp decline. This would make sense if there was a sharp increase in the number of cells and constant product formation because the division of product by a larger number would decrease product per gram cell. As previously discussed, a slight increase towards the very end of the experiment occurred, but it was not significant enough to decrease the product yield as such.

At its maximum, 16.3 mg/g DCW of target protein was made. On average, 12.1 mg/g DCW of GST-PTH-CBD was produced. This was the same per gram cell yield as that for

cultures induced with 10 mM IPTG. Due to the lack of accumulation of cell mass, the total protein numbers were quite low. With the exception of the total protein from the saw-tooth cultivations, they were the lowest achieved in all fermentation experiments. 177 mg of GST-PTH-CBD was produced, as shown in Figure 5-42 (b). On average, approximately 150 mg of protein was made during each cultivation experiment.

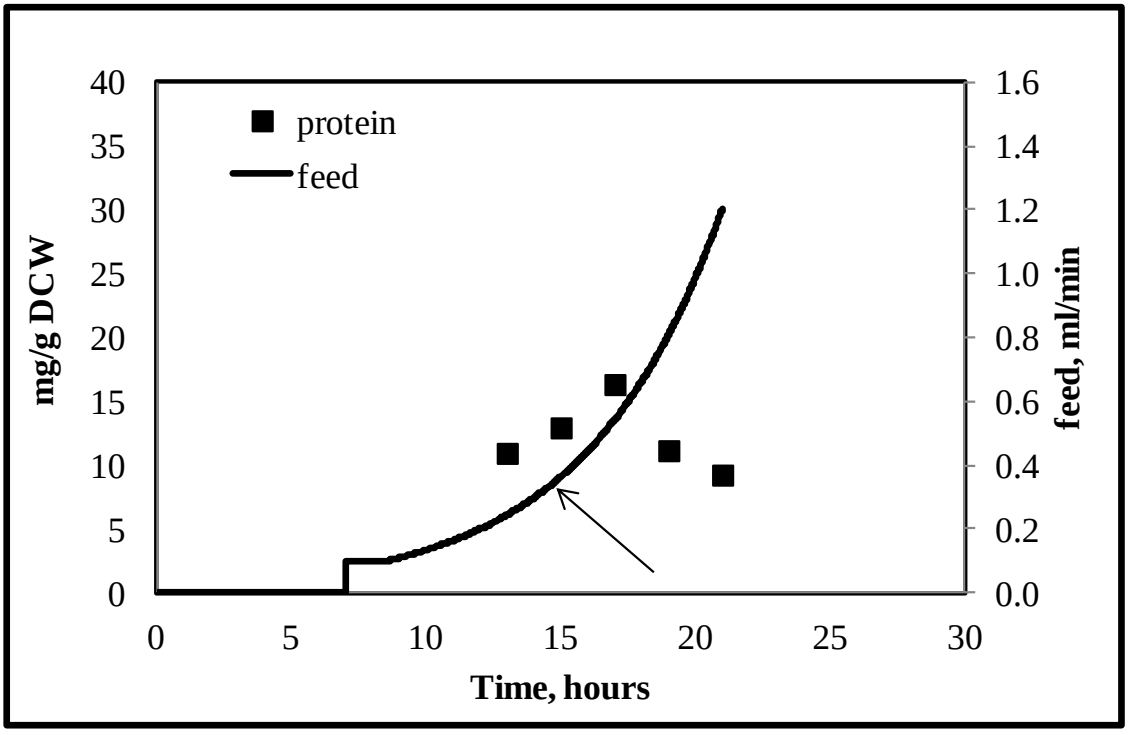

(a)

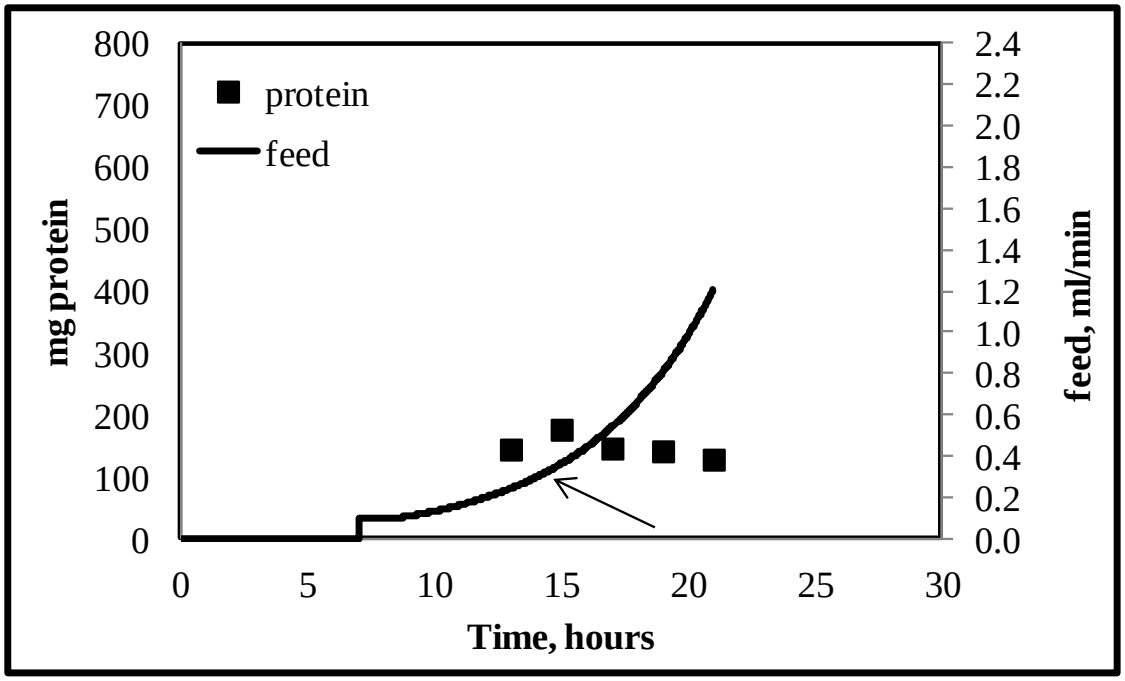

(b)

Figure 5-42. Protein concentrations for glycerol-fed auto-induced cultures with lactose pulsed into system at 14 hours.

For this experiment, glycerol uptake was drastically different (shown in Figure 5-43(a)). Accumulation of glycerol had already begun at the 12 hour elapsed mark and eclipsed 70 g/l by the time the fermentation ended. This value was close to that identified as a growth-inhibiting value. In the preceding experiment, glycerol accumulation did not begin until after 15 hours of cultivation. The final concentration was also lower - approximately 50 g/l.

The additional pulse of lactose into the system at 14 hours helped maintain a non-zero concentration of lactose during the experiment. Though, after the pulse, the concentration dropped below 2 g/l by the next hour. The acetic acid profile was also different for this experiment (Figure 5-43 (b)). Unlike previous experiments, the concentration appeared to

decrease as glycerol accumulated. Towards the end of the fermentation, it leveled off and then decreased drastically in the final sample taken.

As before, the accumulation of glycerol at such a high amount shows how inefficiently the cells uptake glycerol when the same exponential feed profile used for glucose feed is used for feeding glycerol. It could be that this high concentration of glycerol becomes the inhibitory factor for growth. This could account for the stationary phase being reached at 12 hours after inoculation.

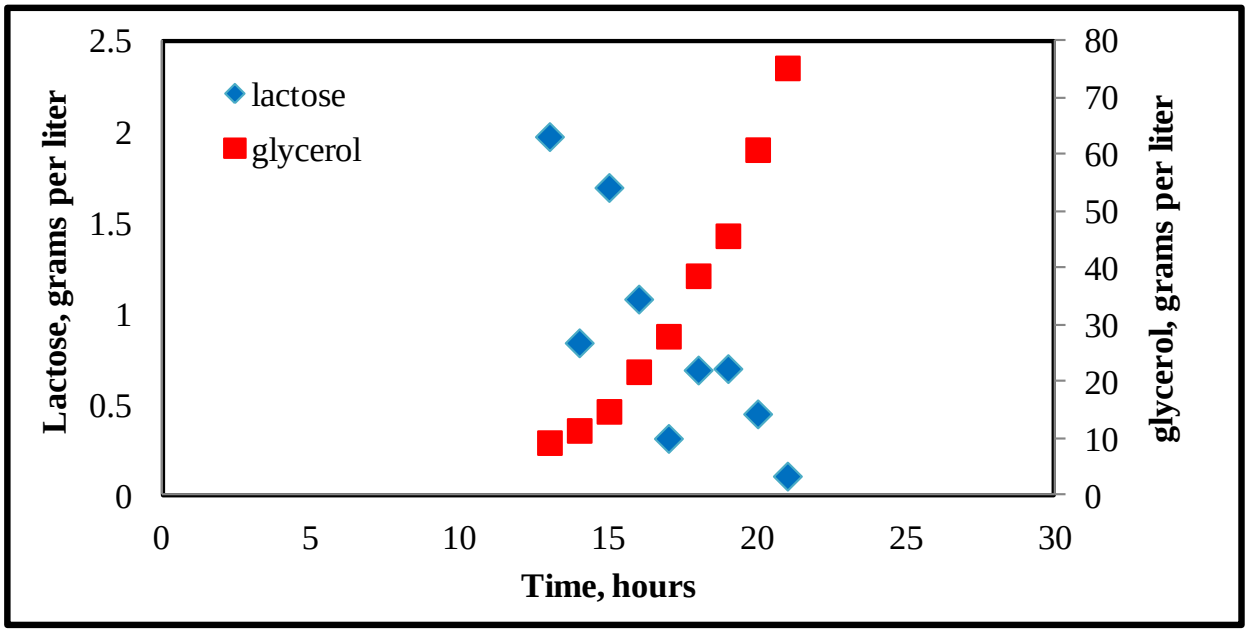

(a)

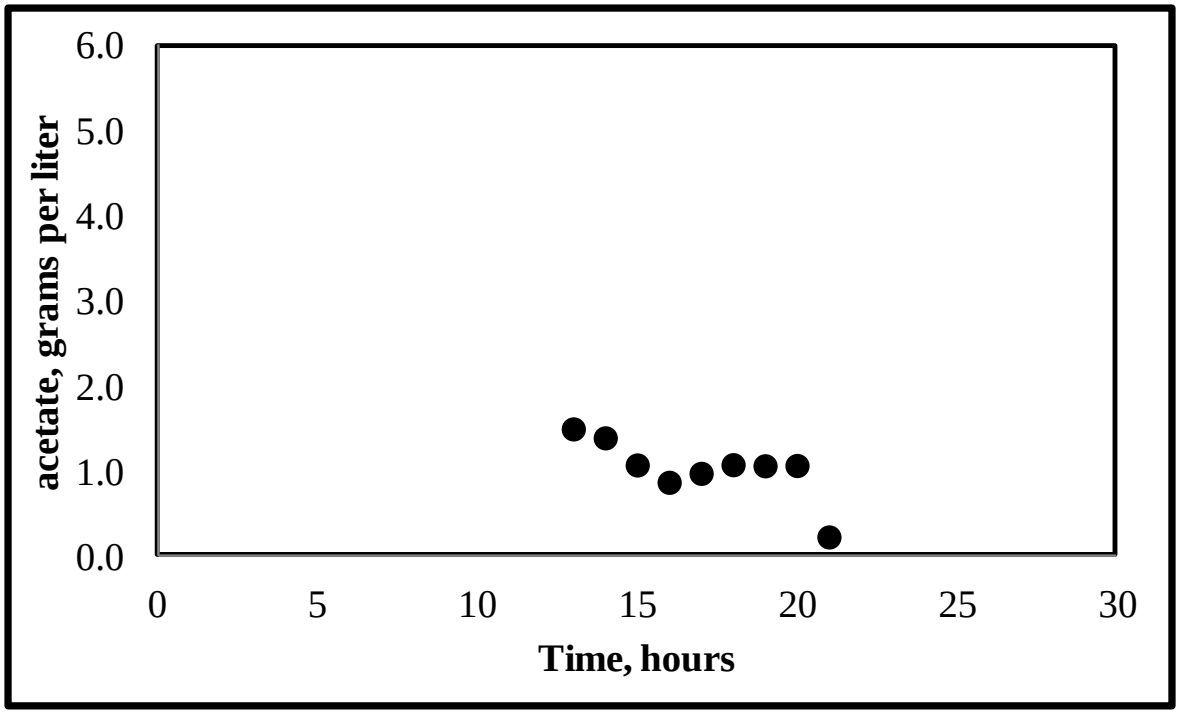

(b)

Figure 5-43. Carbon concentrations for glycerol-fed auto-induced cultures with lactose pulsed into system at 14 hours. (a) Lactose and glycerol concentrations; (b) acetic acid concentrations during fermentation.

As shown in Table 5-5, the final cell mass for auto-induced cultures with an extra pulse of lactose (and fed with glycerol) was extremely low compared to the cultures fed with glucose. However, the maximum amount of protein produced per gram of cell was practically the same. Though, the average amount for glycerol-fed cultures was slightly lower. The total amounts were also extremely different. Less than half of the total product for glucose-fed experiments was produced in glycerol-fed experiments. As stated above, this was due to the lack of cell growth during the cultivation process.

Table 5-5. Comparison of cell growth and protein production for auto-induced cultures with lactose pulsed into the reactor.

Feed	Average mg	Maximum mg	Average $Y_{P/X}$	Maximum $Y_{P/X}$	Final DCW
Glucose	301	358	13.9	16.3	33
Glycerol	148	177	12.1	16.4	19

5.4 Cost analysis

The cost of production is important to consider when comparing the different induction techniques. Table 5-6 summarizes the different induction techniques, feed types, and cost of producing GST-PTH-CBD. In calculating the final cost, the total amount of feed added to the reactor was tabulated. The mass of inducer was also calculated. Then, the total cost of the fermentation experiment was calculated based on these two variables. To find the cost per mg or cost per mg/g DCW, the total cost was divided by the respective number (either total mg produced or mg/g DCW produced, on average). The cost does not take into account any of the media components, since the components remained constant through the fed-batch fermentation experiments. The production cost also does not reflect the cost of pure oxygen, cooling water, or heating demands since the rate of usage of these materials are fairly constant between different experiments. Hence, the cost is based **only** on inducer and feed (type and volume added).

Table 5-6. Cost analysis of fed-batch fermentation experiments with respect to feed type, inducer, and the amount of protein produced.

Method	Feed	Cost per mg, $	Cost per mg/g DCW, $
Lactose 10 hrs after inoculation (st)	Glucose	0.042	0.58
Lactose 12 hrs after inoculation	Glucose	0.0073	0.24
Lactose at feed start	Glucose	0.0123	0.25
Lactose auto-induction	Glucose	0.0088	0.185
Lactose auto-induction with pulse	Glucose	0.0122	0.23
5 mM IPTG	Glucose	0.069	4.13
10 mM IPTG	Glucose	0.12	5.97
Lactose at feed start	Glycerol	0.017	0.31
Lactose auto-induction	Glycerol	0.017	0.36
Lactose auto-induction with pulse	Glycerol	0.055	0.67

As summarized in Table 5-6, **the IPTG-induced cultures cost over ten times the amount to produce 1 mg protein per g DCW** when compared to lactose-induced cultures. In the case of the IPTG-induced experiments, the cost of IPTG was the driving force. In other experiments, the amount of feed added to the reactor was what typically drove the cost high. Glycerol is more expensive to use as a feed source than glucose, but the feeding rates in glycerol-fed fermentations didn't reach as high of flow rates since the cultivations didn't last as long.

In considering the costs of manufacturing, it is important to compare the numbers with respect to grams of DCW because this takes into account the total amount of cells produced in the culture (i.e. the optical density or denseness of the culture). For example, the cost of production of protein using the saw-tooth feeding profile with lactose induction was high, not because of the amount of feed or the inducer type, but because the final cell density was high for the amount of total protein produced. Hence, the cost associated with the fermentation divided by a low mg/g DCW number leaves a resulting higher cost. On the other hand, the glucose-fed lactose-induced at 12 hours experiment cost half as much because the cost was divided by a higher mg/g DCW number. The fermentation with the lowest cost was the auto-induction glucose-fed experiment. This cultivation had a lower cell density, but a higher amount of protein was produced. Hence, the value of mg/g DCW was higher.

Since IPTG-induced experiments produced the most protein, but the cost was high, one can examine how many fermentation experiments would be necessary to complete to duplicate the amount of protein produced from IPTG using a different induction method. Table 5-7 shows how many fermentations are required using each method to produced 611 mg protein. This was the average amount produced from the 10 mM IPTG-induced experiments. Considering the cost

to make one milligram of protein (given in Table 5-6), it would be reasonable to perform multiple fermentations with different induction strategies for all other methods tested except the saw-tooth method and inducing the culture at feed start using glycerol as a feed source. Performing the required amount of these two experiments would push the cost per milligram higher than that for an IPTG-induced run. These costs are also presented in Table 5-7. It is also important to note that these costs reflect only the cost increase due to material usage. It does not take into account the increase in facility usage (air, oxygen, water, electricity, etc.) or the cost of labor (which would increase due to running multiple fermentation experiments).

Table 5-7. Number of fermentations required to achieve the same production as a single 10 mM IPTG-induced experiment.

Method	Feed	Average mg	Fermentations required	New cost per mg, $/mg
Lactose 11 hrs after inoculation (st)	Glucose	40.8	15	0.63
Lactose 12 hrs after inoculation	Glucose	327	1.9	0.014
Lactose at feed start	Glucose	192	3.2	0.039
Lactose auto-induction	Glucose	308	2.0	0.0176
Lactose auto-induction with pulse	Glucose	301	2.0	0.0244
5 mM IPTG	Glucose	542	1.1	0.0759
10 mM IPTG	Glucose	611	1.0	0.12
Lactose auto-induction	Glycerol	426	1.4	0.024
Lactose auto-induction with pulse	Glycerol	148	4.1	0.07
Lactose at feed start	Glycerol	244	2.5	0.14

Since a difference of up to $0.05 cents may not be a significant difference if the overall cost of production is high, additional calculations can be performed to incorporate other costs involved in production of the target proteins (media, centrifugation, labor, etc.). To compare costs associated with induction, the percent of total cost that is due to induction costs can be calculated and compared amongst the different methods. In order to perform these types of

calculations, a basis must be established. In this case, it is feasible to use one gram of protein as a basis for production. Using this basis and the total amount of PTH-CBD produced from each experiment, the number of fed-batch fermentations required to produce one gram of protein was calculated. It was also assumed that 100% recovery was achieved (after purification). The required number of fed-batch fermentations is given in Table 5-8.

Table 5-8. Requirement for fed-batch fermentations to produce one gram of protein.

Method	Feed	Average mg	Fermentations required
Lactose 11 hrs after inoculation (st)	Glucose	40.8	25
Lactose 12 hrs after inoculation	Glucose	327	3
Lactose at feed start	Glucose	192	5
Lactose auto-induction	Glucose	308	3
Lactose auto-induction with pulse	Glucose	301	3
5 mM IPTG	Glucose	542	2
10 mM IPTG	Glucose	611	2
Lactose auto-induction	Glycerol	426	2
Lactose auto-induction with pulse	Glycerol	148	7
Lactose at feed start	Glycerol	244	4

Other assumptions must be made in order to complete these calculations. The hands-on time for each fermentation experiment was assumed to be 8 hours. Hence, the total number of days for each method is the same as the fermentations required for the respective method. It was also assumed that there are 20 units available for use and these units are monitored for 350 days per year by one Ph.D. ($70K/year) and five BS-level technicians ($35K/year). Then, the total number of batch days is 7,000 and the total operating costs for the year in labor is $245K (to give $35/batch day).

For the centrifugation operating costs, it was assumed that two liters of culture broth can be spun down at a time and each spin cycle lasts for 90 minutes. The centrifuge has a 1/2 hp

motor and the cost for power is assumed to be $0.10 kWh. Hence, the cost of centrifugation for one spin cycle is $0.58. The cost of one liter of medium is $4.83 (making the medium in-house) and multiplying this number by the final volume for each fermentation experiment yields the total cost required for medium usage. The cost of feed and inducer was calculated using the same method as before, only this time they were multiplied by the number of required fermentations to produce one gram of product. Table 5-9 shows each method, the cost of labor, the cost of inducer, the total cost, and the percentage of the total cost that is due to the inducer. A complete table of calculations is given in Section 9.4.

Table 5-9. Cost breakdown for production of one gram of product.

Method	Feed	Total labor cost, $	Inducer cost, $	Total cost, $	Percent of cost due to inducer, %
Lactose 11 hrs after inoculation (st)	Glucose	875	23.75	1047.60	2
Lactose 12 hrs after inoculation	Glucose	105	2.85	128.30	2
Lactose at feed start	Glucose	175	4.75	213.20	2
Lactose auto-induction	Glucose	105	2.85	129.30	2
Lactose auto-induction with pulse	Glucose	105	5.70	132.20	4
5 mM IPTG	Glucose	70	69.50	155.60	45
10 mM IPTG	Glucose	70	139.00	225.30	62
Lactose auto-induction	Glycerol	70	1.90	95.20	2
Lactose auto-induction with pulse	Glycerol	245	13.30	338.70	4
Lactose at feed start	Glycerol	140	5.72	177.90	3

As shown in Table 5-9, the driving cost for most of the methods was labor. However, for the 10 mM IPTG-induced experiments, the driving cost was the cost of inducer (62% of all costs are from the inducer costs). For the 5 mM IPTG-induced experiments, the cost of labor and inducer were the same (45% of total cost comes from IPTG cost). For all of the lactose-induced

experiments, the percentage of cost due to inducer cost remained below 4%. Additionally, it is still feasible to perform multiple experiments using alternative induction techniques. All but two experiments (saw-tooth and lactose auto-induction with pulse and glycerol feed) cost less than the 10 mM IPTG-induced experiments. These costs reflect only the costs involved with the fermentation and production portion of the bioprocessing process. Downstream processing costs were not included in this cost analysis.

5.5 Summary of fermentation experiments

To recap all of the results from the fermentation experiments, please refer to Tables 5-10 and 5-11. Table 5-10 summarizes the final dry cell weights of each type of experiment. Clearly, IPTG-induced cultures achieved higher final cell masses than lactose-induced cultures. Also, there is a correlation between the (higher) concentration(s) of lactose put into the system and the lower numbers of cells achieved at the end of the cultivation. Similarly, if lactose was added prior to ten hours of elapsed cultivation time, the growth was stunted for glucose-fed cultures. Overall, glycerol-fed cultures also achieved lower cell masses.

Table 5-10. Summary of methods with final dry cell weights.

Method	Feed	DCW (grams)
Lactose 11 hrs after inoculation (st)	Glucose	50
Lactose 12 hrs after inoculation	Glucose	60
Lactose at feed start	Glucose	41
Lactose auto-induction	Glucose	43
Lactose auto-induction with pulse	Glucose	33
5 mM IPTG	Glucose	76
10 mM IPTG	Glucose	70
Lactose auto-induction	Glycerol	35
Lactose auto-induction with pulse	Glycerol	19
Lactose at feed start	Glycerol	19

Table 5-11 summarizes the protein numbers for each cultivation experiment. Even though the glycerol-fed cultures did not produce high cell densities, they excelled for protein expression. Glycerol-fed auto-induced cultures had the highest concentration of protein per gram DCW of the lactose-induced experiments. Of these experiments, they also had the highest total amount of protein, even though the cell mass was only 35 grams.

It is also interesting to note that multiple types of fermentation exhibited constant protein yield per gram DCW. One would expect the protein concentrations to change during the induction period, hence the optimization of induction routines with respect to timing. However, in this work, all but the following fermentations exhibited this constant yield: lactose auto-induction on glucose, lactose at feed start on glycerol, and lactose auto-induction with pulse on glycerol.

Table 5-11. Summary of protein production with respect to fermentation method. Glu and Gly refer to cultivations that were fed with glucose or glycerol, respectively.

Method	Feed	Avg mg	Max mg	Average $Y_{P/X}$	Maximum $Y_{P/X}$
Lactose 11 hrs after inoc (st)	Glu	40.8	44.9	2.97	3.23
Lactose 12 hrs after inoc	Glu	327	463	9.92	11.3
Lactose at feed start	Glu	192	220	9.44	10.9
Lactose auto-induction	Glu	308	369	11.4	14.6
Lactose auto-induction w/pulse	Glu	301	358	13.9	16.3
5 mM IPTG	Glu	542	629	9.06	9.72
10 mM IPTG	Glu	611	725	12.1	13.2
Lactose at feed start	Gly	244	308	13.7	16.2
Lactose auto-induction	Gly	426	522	20.2	22.0
Lactose auto-induction w/pulse	Gly	148	177	12.1	16.4

For a more visual comparison of growth outcomes, Figure 5-44 compares wet cell and dry cell weights of each fermentation experiment. Data is not shown for the un-induced experiments or for the glycerol-fed lactose induction at feed start due to the lack of a final cell pellet.

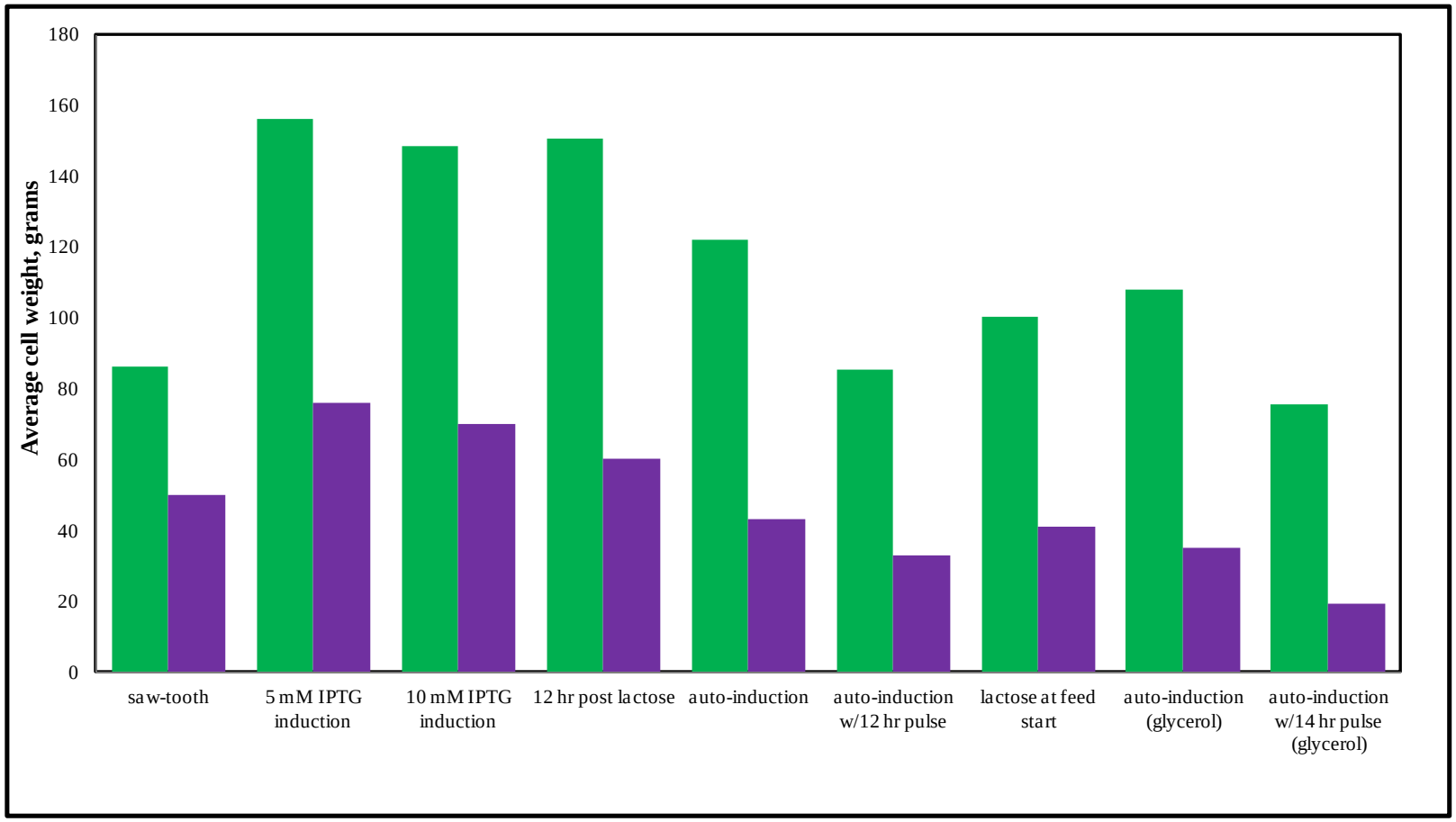

Figure 5-44. Comparison of average cell weights for different fed-batch induction techniques. The purple indicates the average dry cell weight for the given method; the green indicates the average wet cell weights for the different fermentation methods.

The analysis of carbohydrates led to some interesting insights into the fermentation system. First of all, glucose accumulation was much more extensive in induced experiments. Recall that for the un-induced experiments glucose accumulation did not occur until the very end of the fermentation experiment (24 hours after inoculation). For induced experiments, glucose accumulation began around 12 hours after inoculation in some cases. This shows that induction (protein expression) has a substantial effect on the uptake of glucose but not necessarily on the growth of the culture (in the IPTG-induced experiments). Also, in the case of the IPTG-induced experiments, glucose accumulated at higher amounts even though the growth for these cultures was better than those induced with lactose. For lactose-induced cultures, this indicates that less glucose must not be used only for increasing biomass and is used elsewhere in the system. Hence, lactose has an effect on how glucose is used, but not how glucose is taken up by the cells. If lactose was affecting glucose uptake rates, one would expect to witness higher concentrations of glucose in the supernatants. This was not the case. Additionally, the earlier on that lactose was introduced into the system, the lower the final dry cell weight of the culture was. For example, the results from the experiment in which lactose was introduced into the fermentation 12 hours after inoculation were similar to those from IPTG-induced experiments with respect to glucose accumulation and growth. When lactose was added when feed started, growth was similar to auto-induced cultures.

In an attempt to better describe the observation that lactose induction negatively affects cell growth when it is added earlier on during the fermentation experiment, the yield of biomass from glucose was calculated by plotting the total biomass versus the amount of feed consumed. Table 5-12 summarizes the results from these calculations. From the literature, it was expected that the yields from glycerol would be lower than the yields from glucose. Garcia-Arrazola et al.

(2005) found that biomass yield from glycerol was 0.39 g/g for their cultures. On the other hand, Murarka et al. (2005) found that biomass yields of *E.coli* K-12 and B strains from glycerol ranged from 0.03 to 0.055 g/g. The expected value for growth on glucose is 0.5 g cell/g glucose (refer to Section 2.3.3). However, it was not expected that the yield from the un-induced experiments was half as much as the reported value (the value that was used in the feed calculation).

Table 5-12. Yield of biomass from carbon source with respect to fermentation method.

Experiment	Feed type	$Y_{x/g}$ (g/g)
Un-induced control	Glucose	0.28
Lactose 11 hrs after inoculation (st)	Glucose	0.46
Lactose 12 hrs after inoculation	Glucose	0.23
Lactose at feed start	Glucose	0.12
Lactose auto-induction	Glucose	0.09
Lactose auto-induction with pulse	Glucose	0.03
5 mM IPTG	Glucose	0.18
10 mM IPTG	Glucose	0.12
Lactose auto-induction	Glycerol	0.08
Lactose auto-induction with pulse	Glycerol	0.04
Lactose at feed start	Glycerol	0.07

The yield of biomass from glucose in the saw-tooth experiment closely matched the pre-set yield of 0.5 g/g. This could be due to the fact that the culture in this experiment was completely substrate-limited. In the un-induced control experiments, the cultures were starved, but not to the point of the saw-tooth profile. As shown in the table for glucose-fed experiments, the earlier on lactose was added, the worse the yield. Also, the 10 mM IPTG-induced cultures had a lower average yield than the cultures induced with 5 mM IPTG. The timing of the addition of lactose in the glycerol-fed experiments did not have an effect on the yield of biomass from glycerol.

Prior to fed-batch fermentation experiments, it was thought that acetic acid would be inhibitory to growth due to the accumulation of the substrate in the media. As previously discussed, this is often an issue in fed-batch fermentations. However, under conditions where glucose accumulation occurred, acetic acid accumulation remained low. This characteristic of the different fermentations tested may mirror that that was witnessed by Shiloach et al. (1996) - BL21 does a decent job of self-regulating acetic acid accumulation by re-consuming the substrate. This phenomenon has been witnessed by others as well. Varma and Palsson (1994b) report on acetate re-consumption in the presence of glucose feed. They propose that high cell densities can result in the consumption of glucose and acetate simultaneously. This would account for the leveling-off of acetic acid concentration in the supernatant in many of the fermentation experiments. At some point during cultivation, the TCA cycle may become saturated due to the metabolism of glucose. After saturation, the amount of acetate produced (per cell) becomes steady. Due to the increase in the number of cells, one would expect that the acetate concentration in the system would increase. However, this was not seen, so perhaps BL21 does regulate acetate concentrations.

Recall that the glycerol feed contained the same molar concentrations of carbon as the glucose feed. In glycerol-fed experiments, the concentration of glycerol at the end of the experiment was extremely high. Even though the molar carbon content was the same, glycerol uptake was much slower, which resulted in lower dry cell weights and high concentrations of extracellular glycerol. It was expected that the slower uptake of glycerol would result in the inhibition of acetic acid production. This was also not the case, but glycerol feed was not utilized due to its ability to decrease the production of acetate. The production of acetate from glycerol was comparable to glucose-fed experiments and never exceeded 2 g/l.

As expected (due to the lift on catabolite repression), glycerol did have an effect on the uptake and consumption of lactose. For auto-induced cultures, lactose was absent at 15 hours after inoculation for the glycerol-fed culture. For the glucose-fed cultures, lactose was still present. Similarly, lactose was absent in the samples after 20 hours from the auto-induced cultures with a pulse and glycerol feed. In glucose-fed experiments, 4 g/l lactose still remained after 22 hours of cultivation. In all of the glycerol-fed experiments, lactose was depleted prior to the end of cultivation. This was not the case for the glucose-fed experiments.

5.6 Fine analysis of product

Remember from Section 5-1 that there was a significant amount of GST that was present as a degraded protein or truncated product in the cell lysate. This product ran at approximately 26 kDa on a SDS-PAGE gel (refer to Figure 5-8). From its reaction with the anti-bodies specific for GST, its appearance in the eluted portion of the product obtained from purification experiments, and mass spectrometry (MS) analysis, this product was confirmed as being GST. However, this product does not exist in this concentration in the fed-batch fermentation experiments. A similar band appeared at the same molecular weight, but this band was absent on the western blots performed. After this observation, the band was sent in for sequencing. The sequencing results revealed that the intense band at 26 kDa was β-lactamase. Figure 5-45 shows a gel that was used for densitometry with an intense band representing β-lactamase. The MS data indicates that of 47 tryptic fragments of GST, only one peak appears on the spectrum.

β-lactamase is present in gram-negative bacteria and accounts for its antibiotic resistance. It can hydrolyze ampicillin and related drugs by breaking apart the beta-lactam ring (Jacoby and Sutton, 1985). The concentration of β-lactamase in the lysates of samples from fed-batch

cultures remains steady throughout the fermentation. The expression of β-lactamase is typically constitutive - or continually expressed. It would be expected that this concentration would decrease due to both the breakdown of ampicillin during the process and to the increasing volume of the reactor. The increase in volume would assure that the cells come in contact with less antibiotic. However, if cells are under a stressed environment, expression of this protein may occur. Cultures in fed-batch fermentation may suffer from some of the stresses reported in Section 2.3. These stresses can influence changes in plasmid production, which in turn could cause over-expression of β-lactamase.

Additionally, it was reported that increased metabolic burden (from gene expression) can cause runaway plasmid replication (Camps, 2010). If so, then this would account for the increase in β-lactamase expression. However, one would also expect to see higher concentrations of product, as long as inducer is still present in the system. Since the same results were found for IPTG and lactose-induced systems, this must not be the case because IPTG cannot be metabolized by the cells.

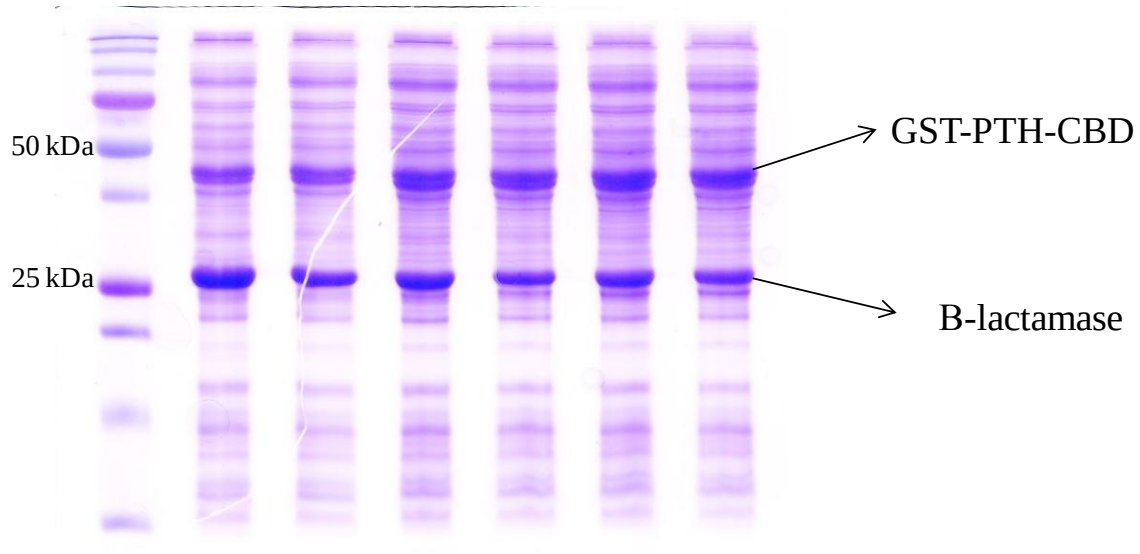

Figure 5-45. Sample SDS-PAGE gel showing β-lactamase.

According to Hong et al. (1992), using glycerol at a concentration of 50 g/l caused a 5-fold increase in recombinant β-lactamase in flask cultures. They do not see this increase without IPTG or with growth on glucose. While this is interesting and could be a cause for production on glycerol, this strong band is also seen in lysates from cells grown on glucose and in the absence of IPTG. Thus, glycerol feed must not be the cause for the appearance of a strong β-lactamase band.

5.7 Purification, activity analysis, and cleavage

Select lysates were purified using affinity purification techniques. A sample of a SDS-PAGE gel after purification is shown in Figure 5-46. Most of the product eluted in two aliquots (of 1 ml each). This occurred after two to three milliliters of elution buffer passed through the column (reference Figure 2-5 for the chromatogram). Also, the gel did not indicate that there was degraded GST in the lysate as the lower band representative of GST is absent. However, the western blot in Figure 5-47 showed these degraded bands.

From the following two figures, one can conclude that affinity chromatography with a GST-tag was a viable option for purification of the product.

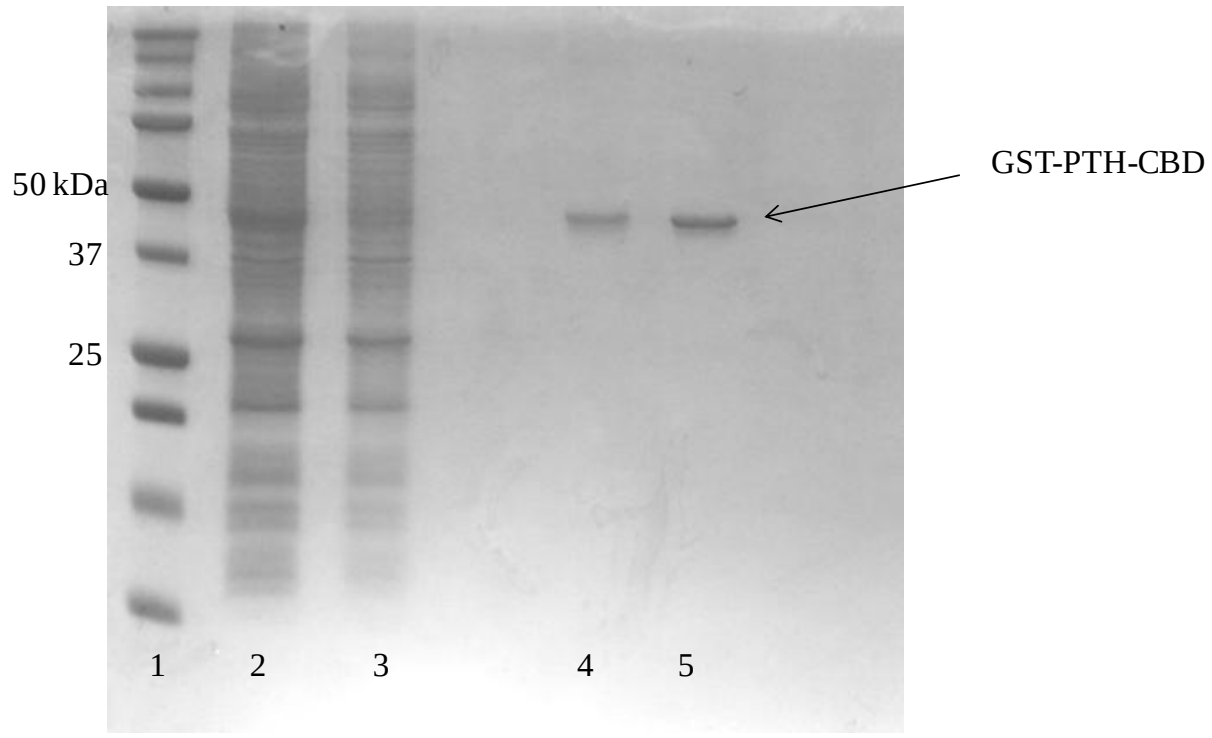

Figure 5-46. SDS-PAGE shows purity of fractions. Lane 1 - molecular weight marker; Lane 2 - lysate loaded to the column; Lane 3 - flow through: Lane 4 and 5- eluted fractions.

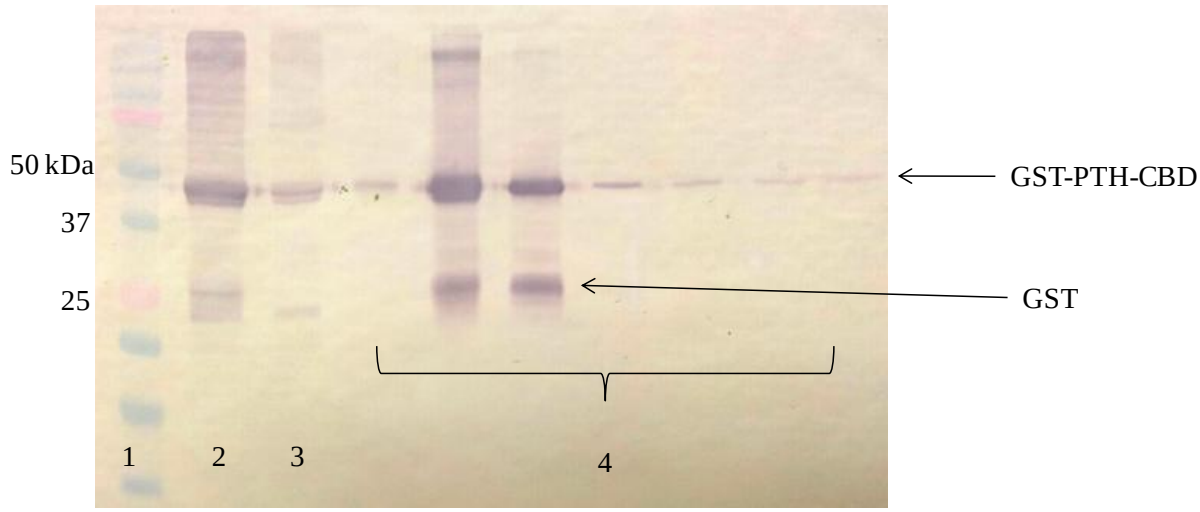

Figure 5-47. Western blot after purification shows some degraded product. This western blot correlates with the gel in Figure 5-46. Lane 1 - ladder marker; Lane 2 - lysate added to column; Lane 3 - flow through; Lanes indicated by 4 - eluted samples.

To check the collagen-binding activity of the collagen-binding domain, purified GST-PTH-CBD was incubated with collagen sheets. Equal amounts of green fluorescent protein and GST-PTH-CBD were incubated for a specified amount of time. As shown in Figure 5-48, the collagen sheet incubated with GST-PTH-CBD reacted with the visualization solution used in the western blotting protocol. This indicated that GST-PTH-CBD retained its collagen-binding activity and bound to the collagen sheet. On the other hand, little to no reaction occurred in the control samples. The slight coloration in these samples was due to the sensitivity of the visualization solution to light.

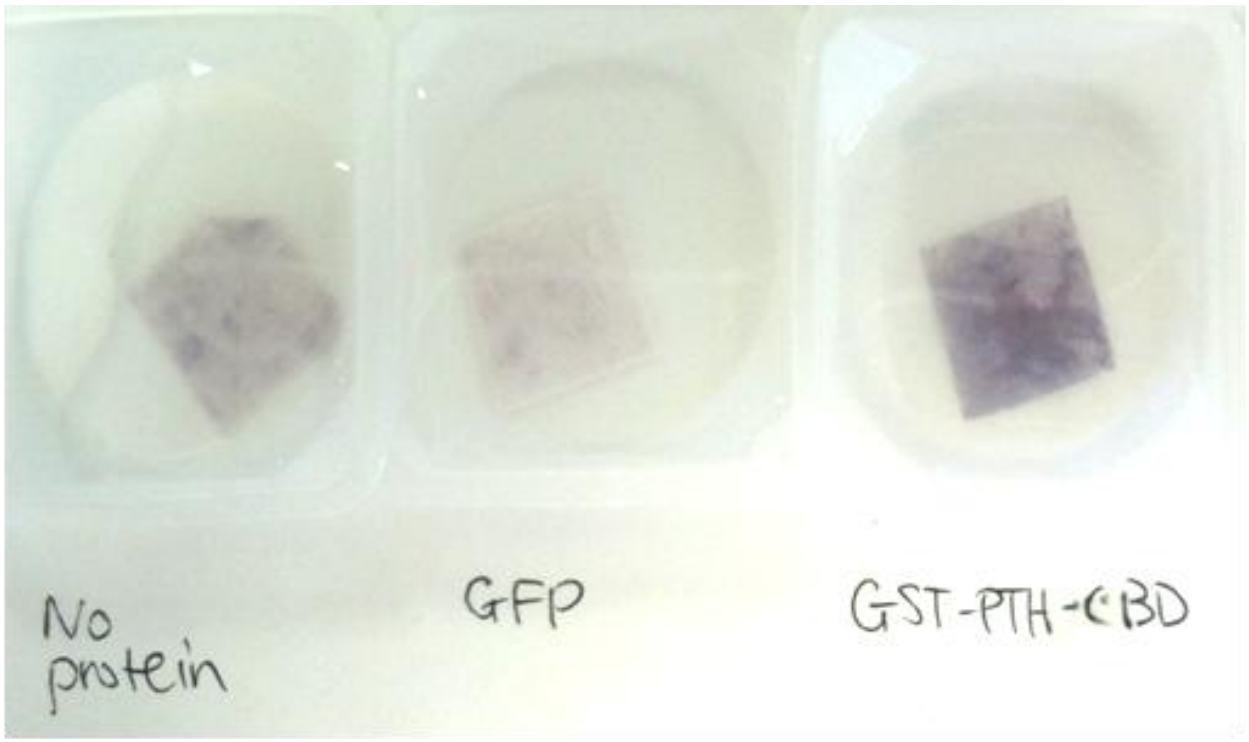

Figure 5-48. Activity analysis for GST-PTH-CBD using collagen binding sheets. There was an intense signal for GST-PTH-CBD on the collagen sheet, as indicated by the image on the far right.

In order to check cleavage of the tag, purified lysate was incubated overnight with Factor Xa. Cleavage must be performed prior to any testing of the activity of parathyroid hormone or

use of the target product. As shown in Figure 5-49, cleavage occurred. After incubation, the sample contained no 44 kDa protein, as indicated by the disappearance of the band that is in lanes 2 and 3. There was also the appearance of a very weak band at approximately 18 kDa with a band at approximately 20 kDa. The PTH-CBD portion of the protein runs between these two molecular weights. This region is indicated by the oval on the gel in Figure 5-49.

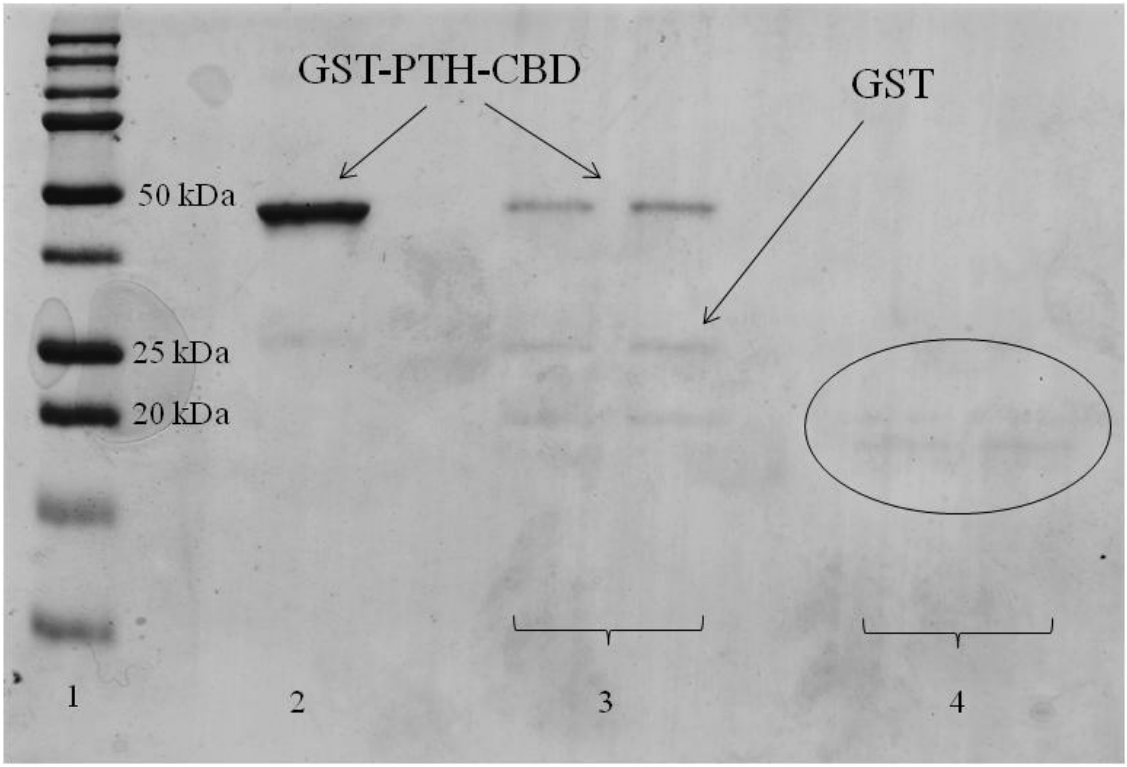

Figure 5-49. SDS-PAGE gel indicates cleavage of the GST tag using Factor Xa. Factor Xa shows up as two bands on reducing gel - 34 and 29 kDa. Lane 1 - Ladder marker; Lane 2 - purified lysate; Lane 3 - initial sample of purified lysate with Factor Xa (0 hr); Lane 4 - lysate after incubation with Factor Xa.

6. Simulations

6.1 Dynamic modeling

As observed in the protein profiles for most of the fermentation experiments, for this particular system the concentration of protein/g cell did not change with time (constant yield of product). In other words, the increase of total protein was directly proportional to the increase of cells in the system. The dynamic model presented in Section 2.5 that incorporates gene and mRNA concentrations will not work for this system because there is no change in protein concentration/g cell with respect to time for a fed-batch system. This modeling works for batch systems, but due to the extended length of fed-batch fermentation systems, this model will not work.

However, the dynamic model that relates feed, volume, biomass, acetate, glucose, and lactose is still applicable to fed-batch fermentations. As previously discussed, MATLAB was used for modeling this system of equations:

$$\frac{dF}{dt} = \mu F(t) \tag{6.1}$$

$$\frac{dV}{dt} = F(t) \tag{6.2}$$

$$\frac{dX}{dt} = \left(\mu - \frac{F(t)}{V(t)}\right) X \tag{6.3}$$

$$\frac{dA}{dt} = \left(\left(\frac{G}{G+K_A}\right)^{Kx} - (A_{cmax} \times \frac{A}{A+K_A})\right) X - \left(\frac{F(t)}{V(t)}\right) A \tag{6.4}$$

$$\frac{dG}{dt} = \left(\frac{F(t)}{V(t)}\right) * (G_F - G) - \left(\frac{qG_{max}}{1+\frac{A}{K_G}} \times \frac{G}{G+K_G}\right) X \tag{6.5}$$

$$\frac{dL}{dt} = \left(\frac{F(t)}{V(t)}\right) * \left(L_f - L\right) - \left(\frac{qL_{max}}{1+\frac{G}{K_L}} \times \frac{L}{L+K_L}\right) X \quad (6.6)$$

The following equations were examined as alternatives to the previous set of equations:

$$\frac{dA}{dt} = \frac{1}{Y_{\frac{A}{X}}} * \mu X - \left(\frac{F(t)}{V(t)}\right) A \quad (6.7)$$

$$\frac{dA}{dt} = \left(\frac{G}{G+K_A} - (A_{cmax} \times \frac{A}{A+K_A})\right) X - \left(\frac{F(t)}{V(t)}\right) A \quad (6.8)$$

$$\frac{dG}{dt} = \left(\frac{F(t)}{V(t)}\right) * (G_F - G) - \frac{1}{Y_{\frac{S}{X}}} * \mu X \quad (6.9)$$

$$\frac{dG}{dt} = \left(\frac{F(t)}{V(t)}\right) * (G_F - G) - \left(\frac{qG_{max} * G}{G+K_G}\right) X \quad (6.10)$$

$$\frac{dL}{dt} = \left(\frac{F(t)}{V(t)}\right) * \left(L_f - L\right) - \left(\frac{qL_{max} * L}{L+K_L}\right) X \quad (6.11)$$

Upon solving the model with the first set of equations (with K_G = 0.3, K_A = 0.25, K_L = 1.5, K_x = 2.1), the profiles for feed, volume, biomass, acetate, glucose, and lactose were plotted with the experimental values. As shown in Figure 6-1, the feed, volume, and biomass profiles using Equations 6.1 through 6.3 provided a good fit to the experimental data after the incorporation of a maintenance coefficient for the biomass profile. This coefficient is often incorporated to describe the fact that some carbon goes to maintaining cellular processes, not just to biomass formation. However, after minimization of the least squares difference and solving for the optimal saturation coefficients (previously described), the acetate, glucose, and lactose profiles were not a good match to the experimentally determined conditions. The resulting concentrations from the model for acetate and glucose were orders of magnitude higher than experimentally determined values. Making drastic changes in the saturation coefficients did not

affect the difference between the simulated values and the experimental values. While the final simulated values for lactose concentrations were a decent fit numerically, the slope for the consumption of lactose did not match that from the actual experiment. According to the model, as soon as lactose entered the system it began being consumed. Experimentally, as seen with diauxic growth, there is a lag phase after glucose is consumed for the cells to adjust to a secondary carbohydrate source. This model indicates that lactose was preferentially consumed over glucose, with no lag phase. As shown in Figure 6-1, glucose accumulated to values over 300 g/l, but lactose consumption began immediately after its introduction to the system.[***]

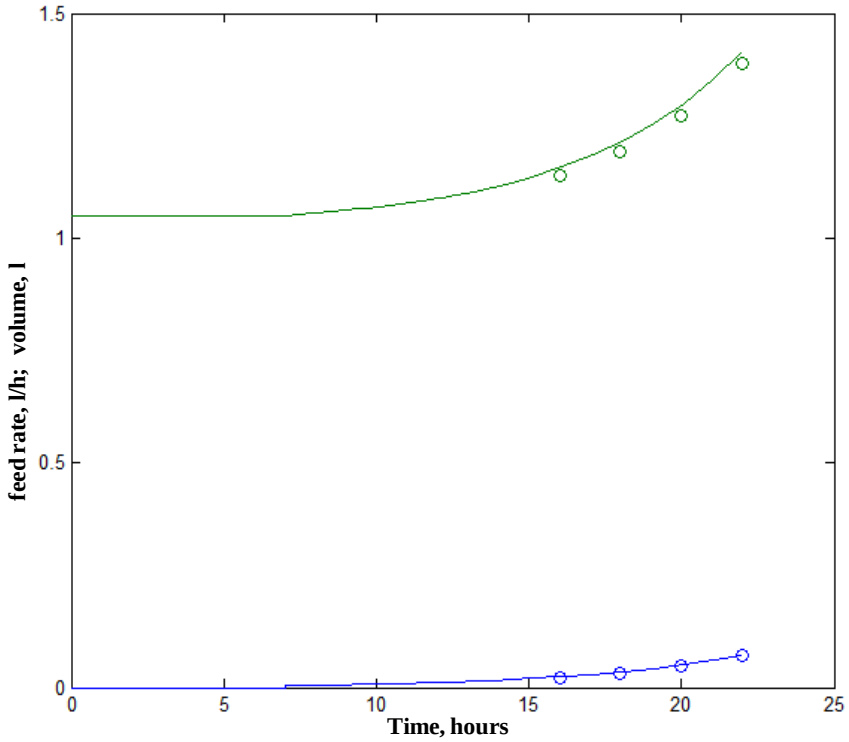

(a)

[***] For the remaining figures for the dynamic models, the open circles are representative of the experimental data points. The solid line is the simulated profile. Lastly, the arrows indicate the direction of the increase in the saturation coefficients, where applicable.

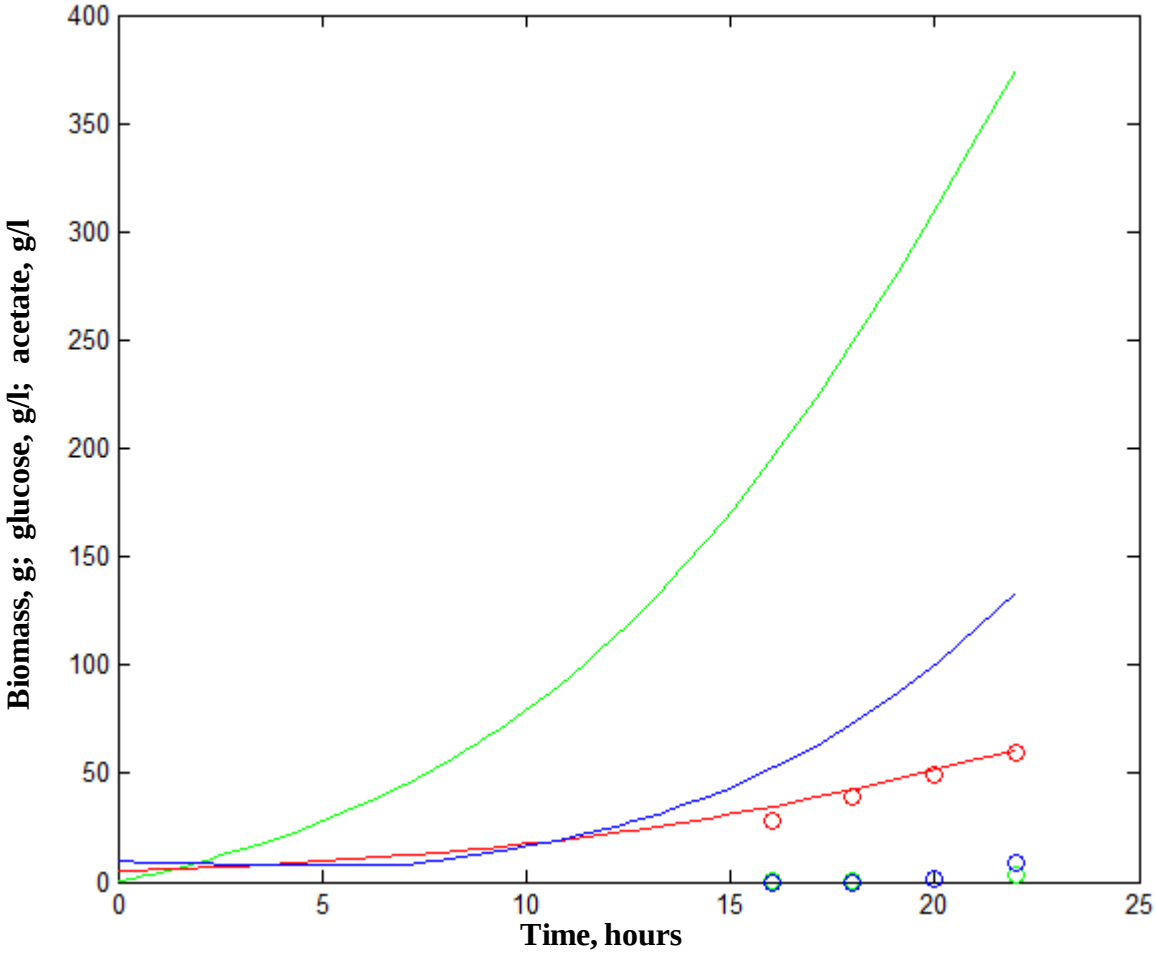
Biomass, g; glucose, g/l; acetate, g/l
Time, hours
0
50
100
150
200
250
300
350
400
0
5
10
15
20
25

(b)

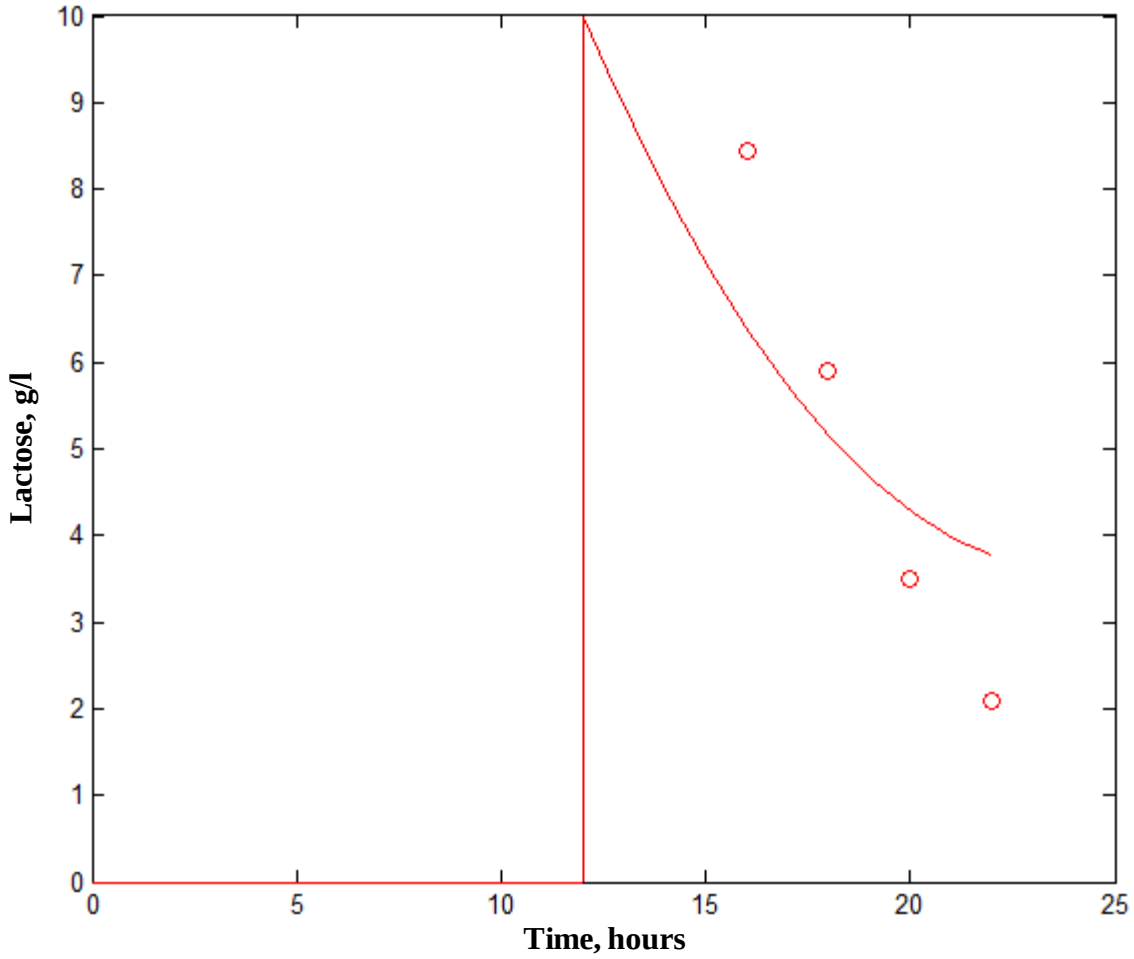

(c)

Figure 6-1. Simulated fermentation characteristics with experimental data. (a) Feed (l/hr) is shown in blue, volume (liters) is shown in green (open circles indicate the experimental data points); (b) Biomass (grams) is shown in red, glucose and acetate (g/l) are shown in blue and green, respectively with data; (c) Lactose concentrations (g/l) with open circles representing experimental data (pulsed into reactor at 12 hours).

It is clear that feed, volume, and biomass can be successfully simulated by manipulating the maintenance coefficient (depending on the experiment that is being simulated), but further examination of acetate, glucose, and lactose is required. To check this model with other types of fermentation experiments, the experimental data for the 5 mM IPTG-induced cultures was compared with the simulated values (for acetate and glucose). After fitting the feed, volume, and biomass, and after optimization of the saturation coefficients, the carbohydrate profiles were still orders of magnitude higher than the experimental values. Hence, the model did not properly convey the relationship between glucose, acetate, and lactose.

In an attempt to find a simulation that better describes the relationships between the carbohydrates, different combinations of equations were simulated where Equations 6.7 and 6.8 replaced Equation 6.4, Equations 6.9 and 6.10 replaced Equation 6.5, and Equation 6.11 replaced Equation 6.6. This resulted in 18 different permutations of the model where the equations for feed, volume, and biomass remained the same.

The first simulation tested the alternative lactose equation (Equation 6.11 for Equation 6.6). Figure 6-2 shows the profiles for acetate, glucose, and lactose after incorporation of the alternative equation.

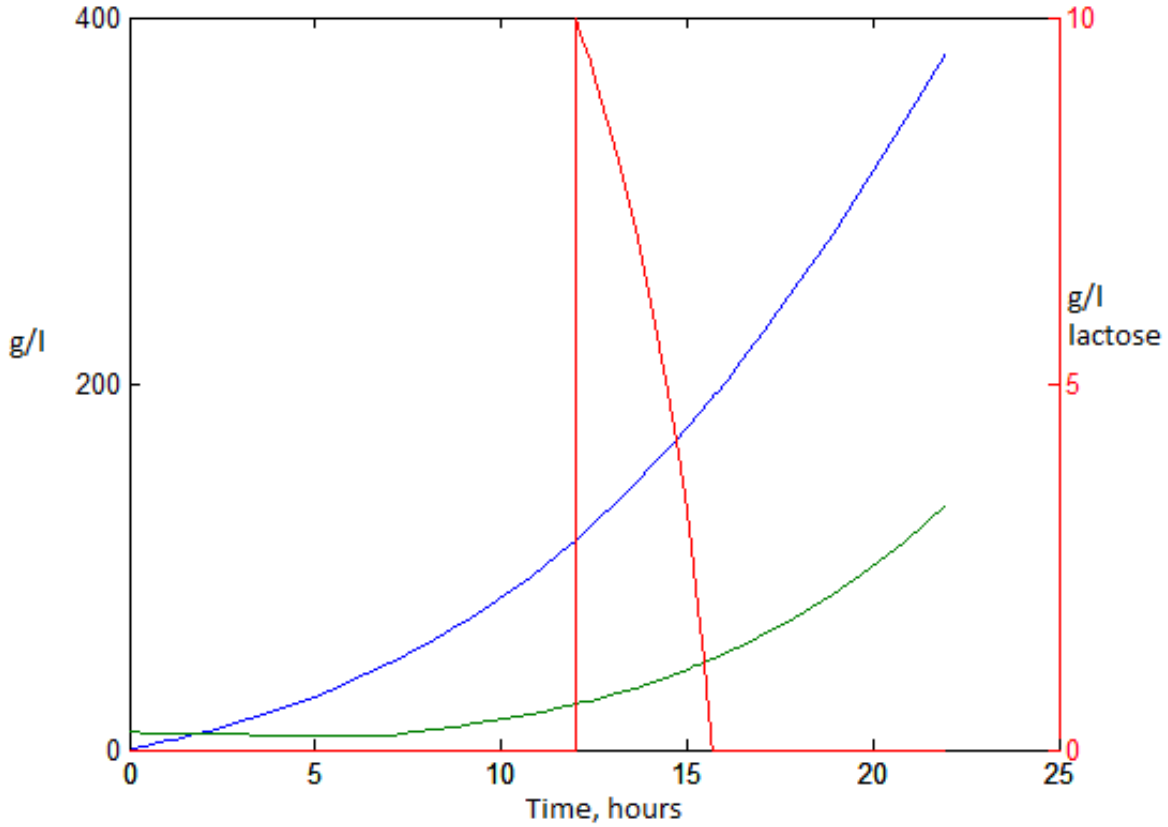

Figure 6-2. Simulation using alternative lactose equation. Lactose profile is shown in red; glucose profile is shown in green, and acetate profile is shown in blue. The sharp increase at 12 hours indicates that lactose has been added to the reactor.

This substitution did not aid in the fitting of lactose to experimental values. After 15 hours, lactose sharply declined while glucose steadily increased. Optimizing the saturation coefficient for lactose did not change the rate at which lactose was consumed. Hence, the model did not sufficiently describe the catabolite repression relationship that exists between glucose and lactose. One would not expect to see a decline in lactose concentration immediately after adding it to the system if glucose has accumulated to concentrations exceeding 100 g/l.

Simulations containing Equation 6.7 instead of Equation 6.4 resulted in acetate concentrations between 3000 and 6000 g/l depending on the optimized K_A value and the accompanying glucose equation. As a result, it was determined that Equation 6.7 would not be

sufficient at modeling the acetate profiles for the set of experiments performed for this dissertation. This observation was interesting because Equation 6.7 was so widely accepted in the literature (Mohseni et al., 2009; Roeva et al., 2007). However, the models used in the literature did not incorporate the addition of lactose to the system. Simulations containing 6.8 instead of 6.4 yielded no apparent difference in the projected acetate profiles after optimization of the saturation coefficients from the original model (the equations are the same if $K_x = 1$).

Since the modeling of acetate was unsuccessful and since acetate concentrations remained less than 2g/l for the majority of the experiments, the next simulations focused on modeling only glucose and lactose. Four different permutations of the simulation were tested with no acetate equation in the model (Equation 6.10 is equivalent to Equation 6.5 with no acetate, so there were only four permutations instead of six). The first of these permutations tested the original equations for glucose and lactose. The resultant profiles from this model are shown in Figure 6-3. Figure 6-3 (a) shows the results from examining the effect of changing the saturation coefficient for glucose only. Increasing K_G caused an increase in the rate at which glucose accumulated. Inversely, decreasing K_G caused an increase in glucose consumption during the batch phase of the fermentation. With this model (with no acetate equation), the overall glucose concentrations decreased so that they were no longer orders of magnitude higher than those that were experimentally determined. Figure 6-3 (b) shows the change in profiles with respect to changing the saturation coefficient of lactose. Changing K_L resulted in a change in the rate at which lactose is consumed. The general slope of the simulated lactose profile matched the slope of the consumption of lactose from experimentally determined data, and this slope is a better "fit" as the coefficient increases. Graph (c) of Figure 6-3 shows the profiles with optimized saturation coefficients. For these profiles, the glucose and lactose saturation

coefficients were 19 and 180 g/l, respectively. While these numbers provided a decent fit for predicting the final carbohydrate concentrations, the numbers cannot be experimentally described. Typically, the glucose saturation coefficient is on the order of 0.05 g/l and the lactose saturation coefficient was expected to be less than 10 g/l.

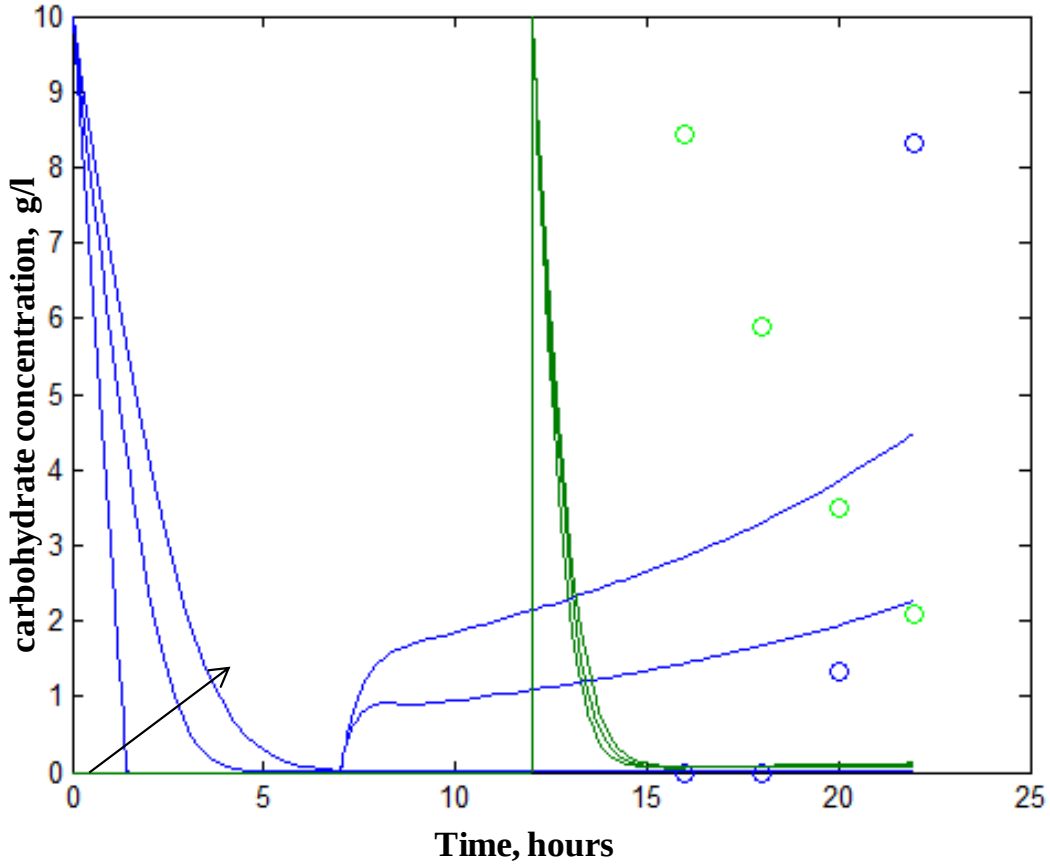

(a)

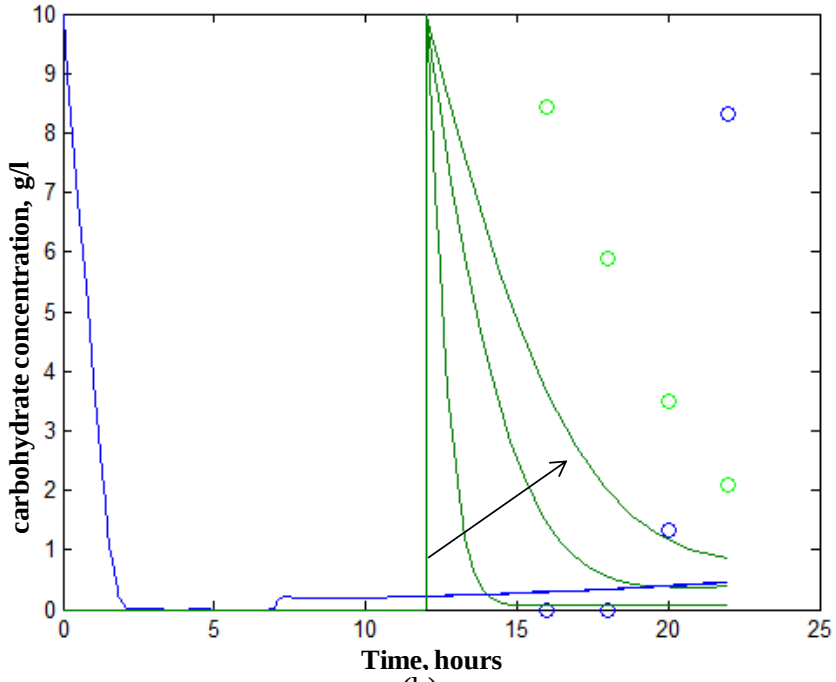

(b)

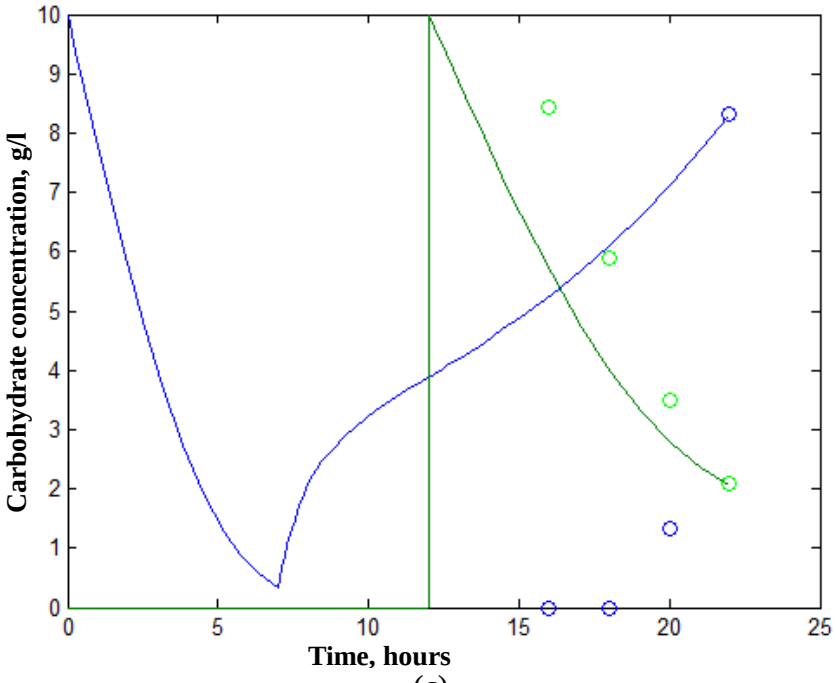

(c)

Figure 6-3. Simulation using original glucose and lactose equations without acetate equation. Lactose is given in green, glucose is given in blue. (a) Increase in glucose coefficient causes increase in final glucose numbers (K_G = 0.05, 1, 5); (b) Increase in saturation coefficient of lactose increases final simulated lactose values (K_L = 10, 50, 100, and 150); (c) "Optimized" saturation coefficients show match in final carbohydrate concentrations (K_G = 19 g/l, K_L = 180 g/l).

The second set of simulations without acetate utilized the original glucose equation with Equation 6.11 for lactose. Similar results for profiles were observed for this simulation as the one above. As shown in Figure 6-4 (a), the change in the saturation coefficient of glucose now has no effect on the lactose concentration due to the removal of glucose from the lactose equation – the carbohydrate equations are now decoupled. Like before, an increase in the saturation coefficient for glucose caused an increase in the final glucose concentration.

Similarly, an increase in K_L caused an increase in the final concentration of lactose (Figure 6-4 (b)). This was also previously observed. Lastly, the optimized profiles are shown in Figure 6-4 (c). The saturation coefficients for glucose and lactose are the same as the simulation using both of the original equations – 19 g/l and 180 g/l, respectively.

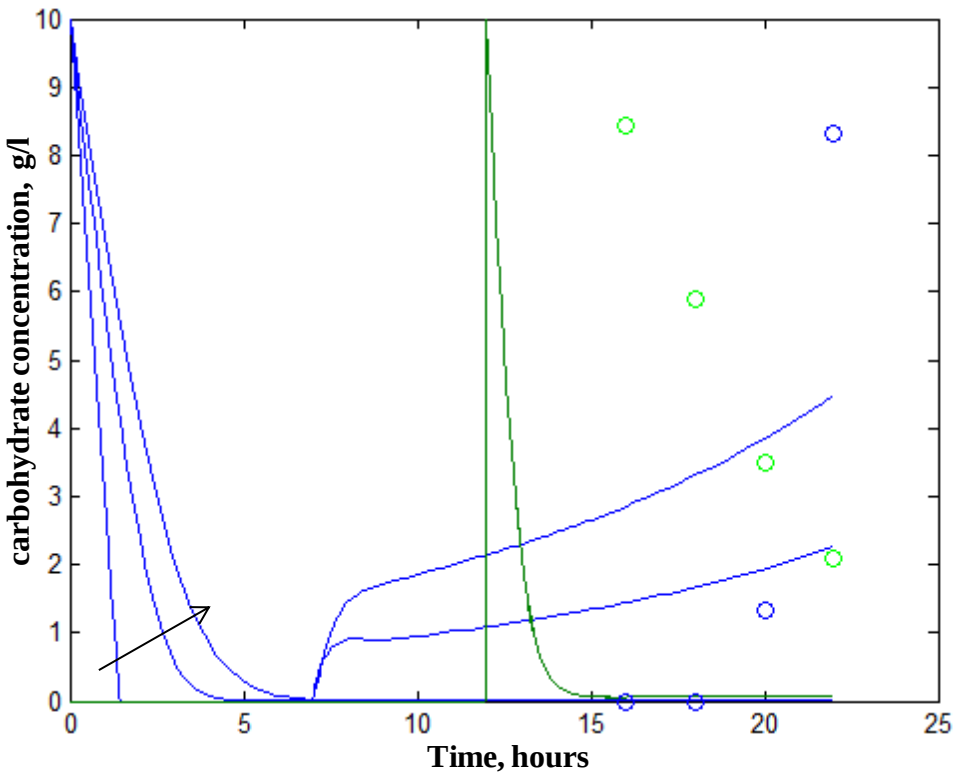

(a)

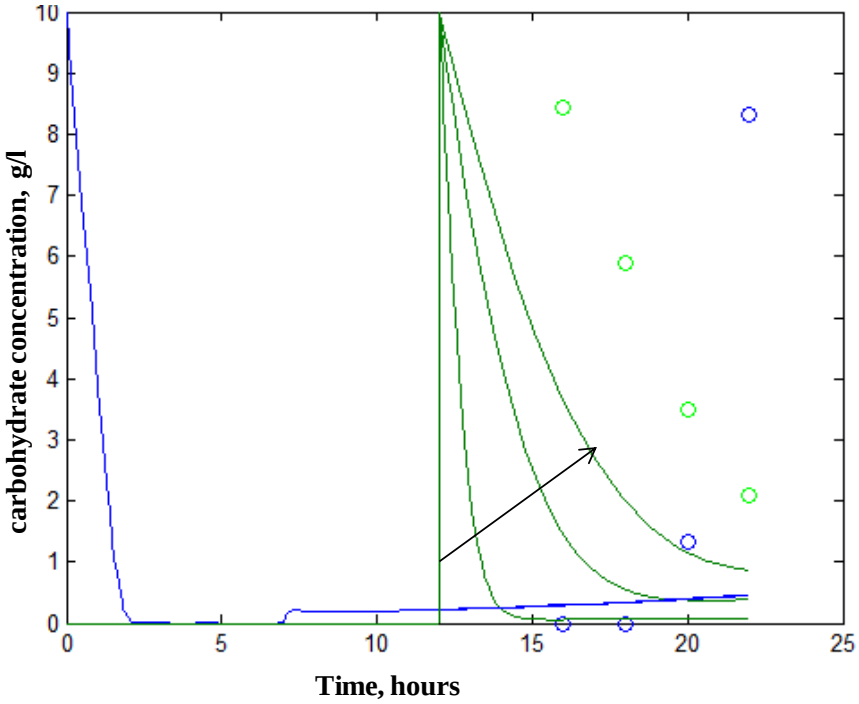

(b)

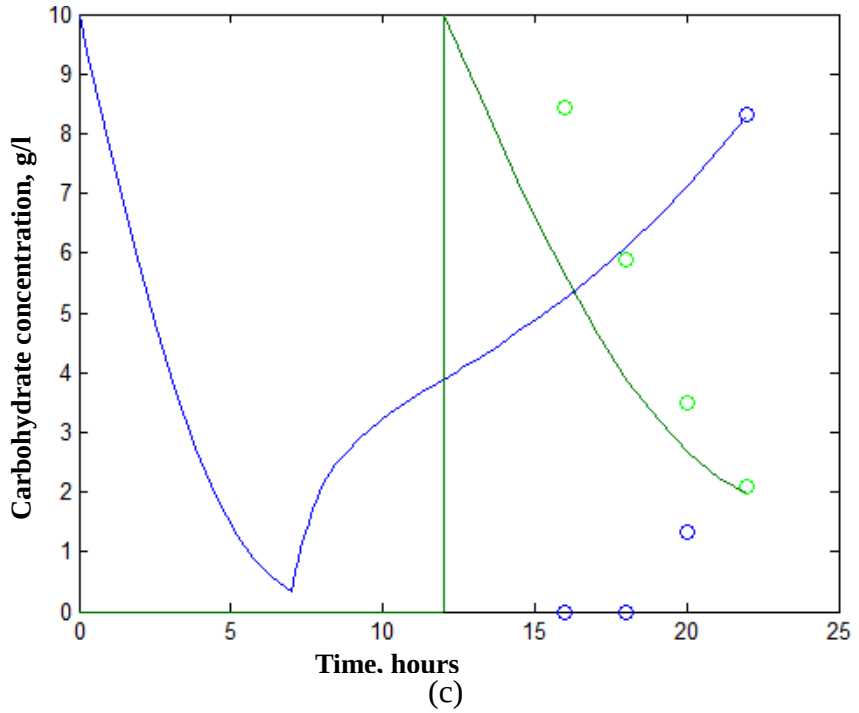

(c)

Figure 6-4. Simulation with original glucose equation and alternative lactose equation (without acetate). Lactose is given in green, glucose is given in blue. (a) Increase in glucose coefficient causes increase in final glucose numbers (K_G = 0.05, 1, 5); (b) Increase in saturation coefficient of lactose increases final simulated lactose values (K_L = 10, 50, 100, and 150); (c) "Optimized" saturation coefficients show match in final carbohydrate concentrations (K_G = 19 g/l, K_L = 180 g/l). Experimental data points are represented by the open circles.

After comparing the profiles in Figures 6-3 and 6-4, it is apparent that there was no significant difference between using the original lactose equation and the alterative equation (Equation 6.11) with the original glucose equation. The decoupling of the carbohydrates had little effect on the overall system. The next set of simulations examined the use of the alternative glucose equation (Equation 6.9).

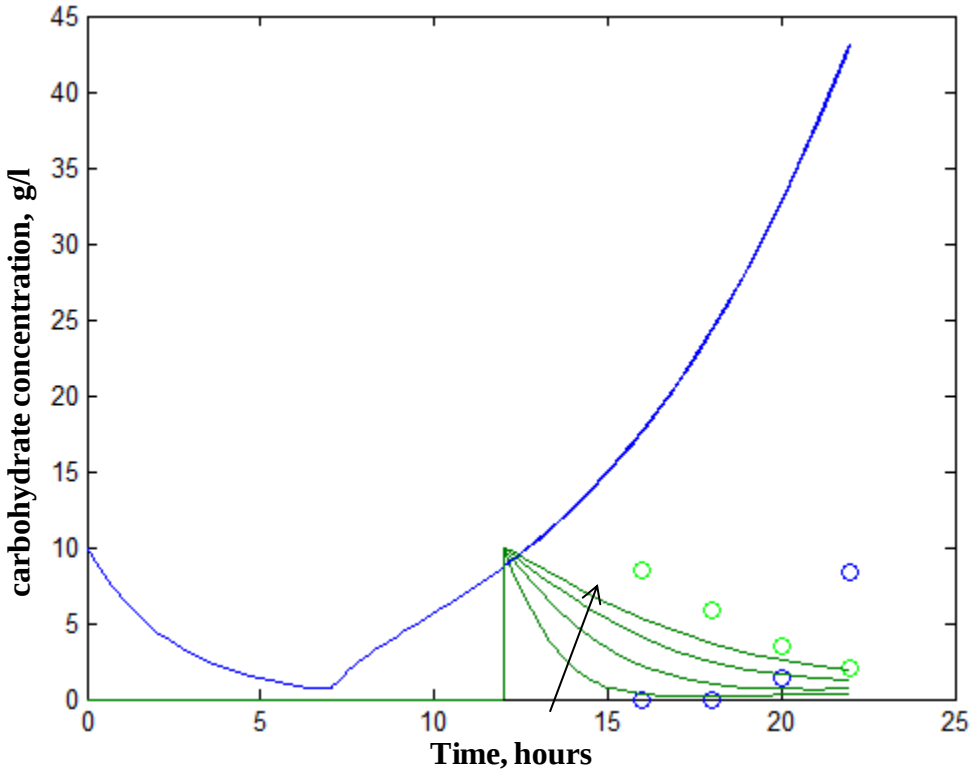

Figure 6-5. Simulation of alternative glucose and original lactose equations. Lactose is given in green; glucose is represented by blue.

As shown in Figure 6-5, the alternative glucose equation (Equation 6.9) coupled with the original lactose equation (Equation 6.6) was a worse fit for the representation of the experimental data. Since Equation 6.9 is used, unlike before, there were no parameters that could be changed to try to modify the profile. The lactose profile was still a decent fit for the experimental data and like before, increasing the coefficient for lactose caused an increase in the final lactose

concentration. However, the values of the coefficient in Figure 6-5 are 10, 50, 100, and 150. In order for the simulated lactose profile to be a decent fit, the coefficient had to exceed 150 g/l, which again does not have a physical meaning experimentally.

Due to the prevalence of Equation 6.9 in the literature, the lack of fitting between the glucose simulation and the experimental values is interesting to note here again. For this particular system, the relationship between carbohydrates appears to be unique. To finish off the possible permutations of the simulation, the last model utilized Equation 6.9 and Equation 6.11.

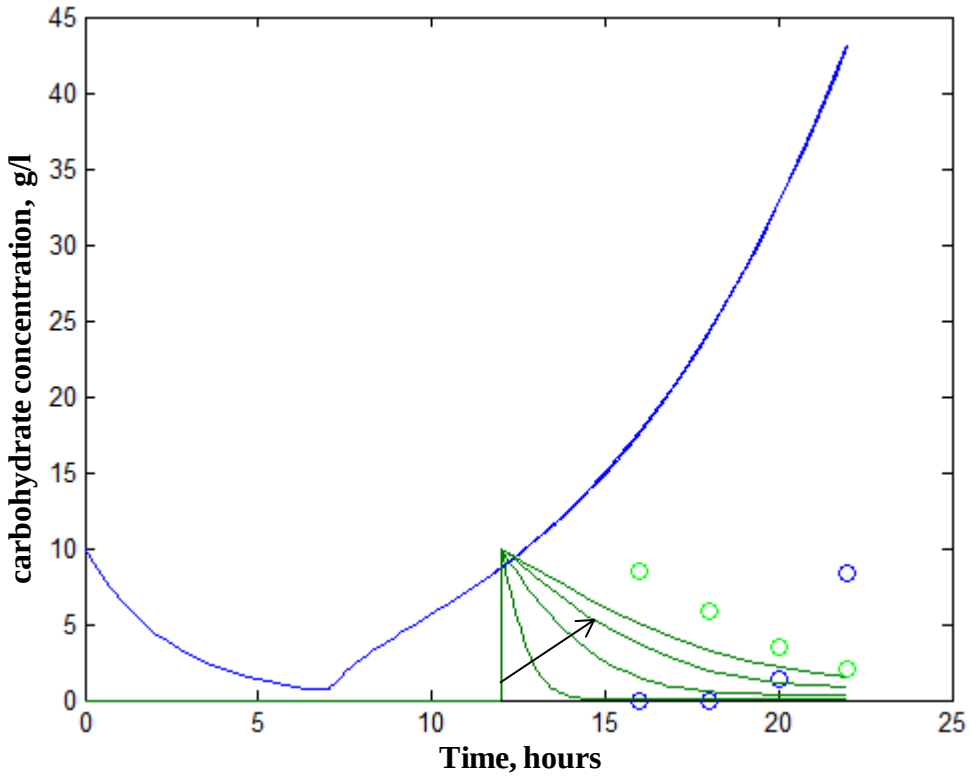

Figure 6-6. Simulation of the alternative glucose equation with the alternative lactose equation. Lactose is given in green; glucose is represented by blue.

The simulation utilizing Equations 6.9 and 6.11 (Figure 6-6) was not any different from the simulation represented by Figure 6-5. The only apparent difference was the final lactose concentration. The slope of both profiles in both simulations appeared to be the same.

The simulations using Equation 6.11 instead of Equation 6.6 maintained similar lactose profiles as before (with each type of equation), but glucose concentrations were high for simulations utilizing Equation 6.9 instead of Equation 6.5. Since Equation 6.9 takes into account only the constant consumption of glucose by cells, there were no parameters to change to try to achieve a better fit. Thus, the alternative glucose equation (prevalent in the literature) should not be considered for modeling the relationship between the carbohydrates within the context of this work (Mohseni et al., 2009; Roeva et al., 2007).

Although there is no apparent difference between the lactose equations when disregarding the presence of acetate, the original lactose equation (Equation 6.6) provided a better fit when simulations included the acetate equation (refer to Figures 6-1 and 6-2).

Overall, there is not enough information (taken from experiments or from the literature) to properly describe the relationship between the carbohydrates in the fed-batch fermentation systems that were examined. Recall that lactose affected the biomass production but not the glucose uptake rate. This observation is important in that the mass balance of carbon does not follow results that are typically found for fed-batch fermentation experiments. Apparently, the introduction of a third carbohydrate (lactose) interrupts the movement of carbon away from biomass production. The tracking of carbon may aid in filling the gaps for the dynamic modeling. This was performed using techniques consistent with metabolic flux analysis.

6.2 Metabolic flux analysis

The first step involved in solving the metabolic flux analysis model was to determine how the incorporation of the amino acids should occur. Using the experimental data (protein concentrations and cell mass) and the information about precursor demands (Holm's table), the requirement of amino acids was calculated. If the required concentration of amino acids did not exceed the concentration of amino acids that was present in the media, then these amino acids would actually feed into the flux system and not need to be produced from precursors. On the other hand, if the supplemented amino acids were exhausted after a certain amount of time, these amino acids would be formed from their metabolic precursors. Consider the 12 hour lactose-induced experimental as an example. At the 16 hour time point in the fermentation experiment, the dry cell weight and total protein produced was 28 grams and 0.248 grams, respectively. Using this data and the precursor demands (Tables 4-3 and 4-4), the consumption of the amino acids was estimated:

Table 6-1. Amino acids consumed by 16 hrs for the 12 hr lactose-induced fermentation experiment.

Amino acid	mmol/g cell	mmol/g protein	amount consumed (mmols)
Gly	0.582	0.706	16.47
Lys	0.326	0.706	9.30
Leu	0.428	0.82	12.19
Ser	0.205	0.478	5.86
Asp	0.229	0.615	6.56

As shown in Table 6-1, the estimated amino acid consumption exceeded 5 mmol by the first time point in the experiment. From this calculation, the initial model with the inclusion of the external amino acids was not necessary due to the lack of amino acids by the end of the experiment. For the examination of the change in fluxes, they were not considered to exist in an

external form (outside the cell in the media) and all amino acids for the metabolic flux analysis must be synthesized. They were not supplied from the culture broth at the fermentation times that were under investigation.

The data from the glucose-fed experiment with lactose induction at 12 hours was considered for the first simulation (this fermentation produced the highest biomass of all of the glucose-fed and lactose-induced experiments). The fluxes (shown in Figure 6-7) were normalized to the uptake of glucose (*r32*). Notice that upon normalization, the fluxes throughout the HMP pathway are high compared to the fluxes of carbon throughout the rest of the pathways examined. However, the rate of uptake of glucose is similar to the fluxes of carbon throughout the TCA cycle. Using the final concentrations to take a snap shot of the system using lactose induction at 12 hours with glucose feed pushed the carbon through the HMP pathway according to the metabolic flux analysis of the system. Additionally, using the final experimental concentrations do not allow for the intermediate concentrations to be zero (the sum of the fluxes at each intermediate component should be zero) after optimization. Also, the optimized biomass components are low compared to the intermediate fluxes using the final biomass concentration.

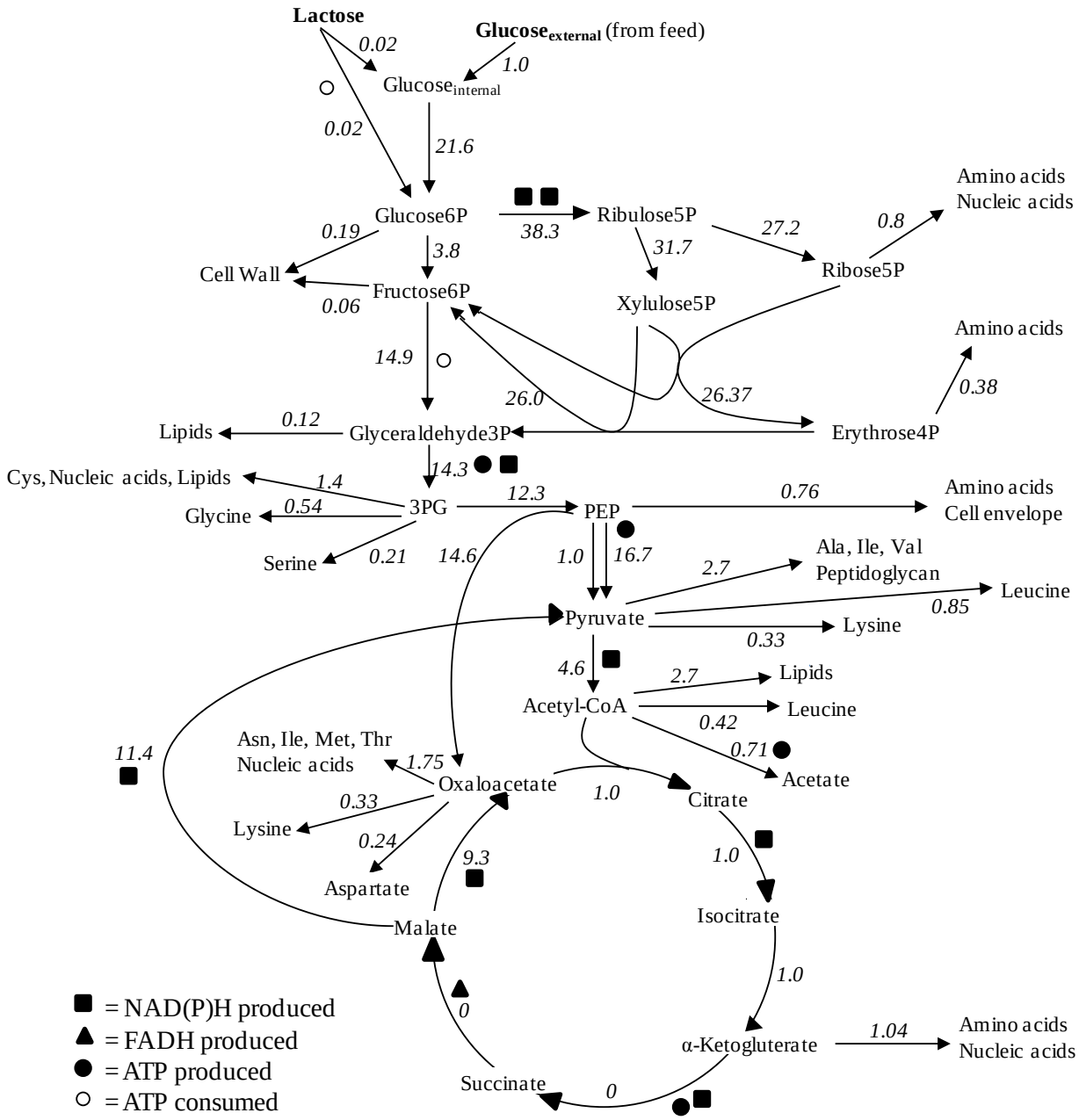

Figure 6-7. Simulated fluxes from 12 hour lactose-induced cultures with glucose feed.

In order to examine the fluxes for an experiment where the final biomass was lower but lactose, glucose, and acetate were still present in the system, the auto-induced culture with an additional lactose pulse was examined. Since all of the carbons were present at the end of the fermentation, the equations remained the same as those in the simulation for the 12 hour lactose-induced cultures. The major difference between these two simulations is the final dry cell weight.

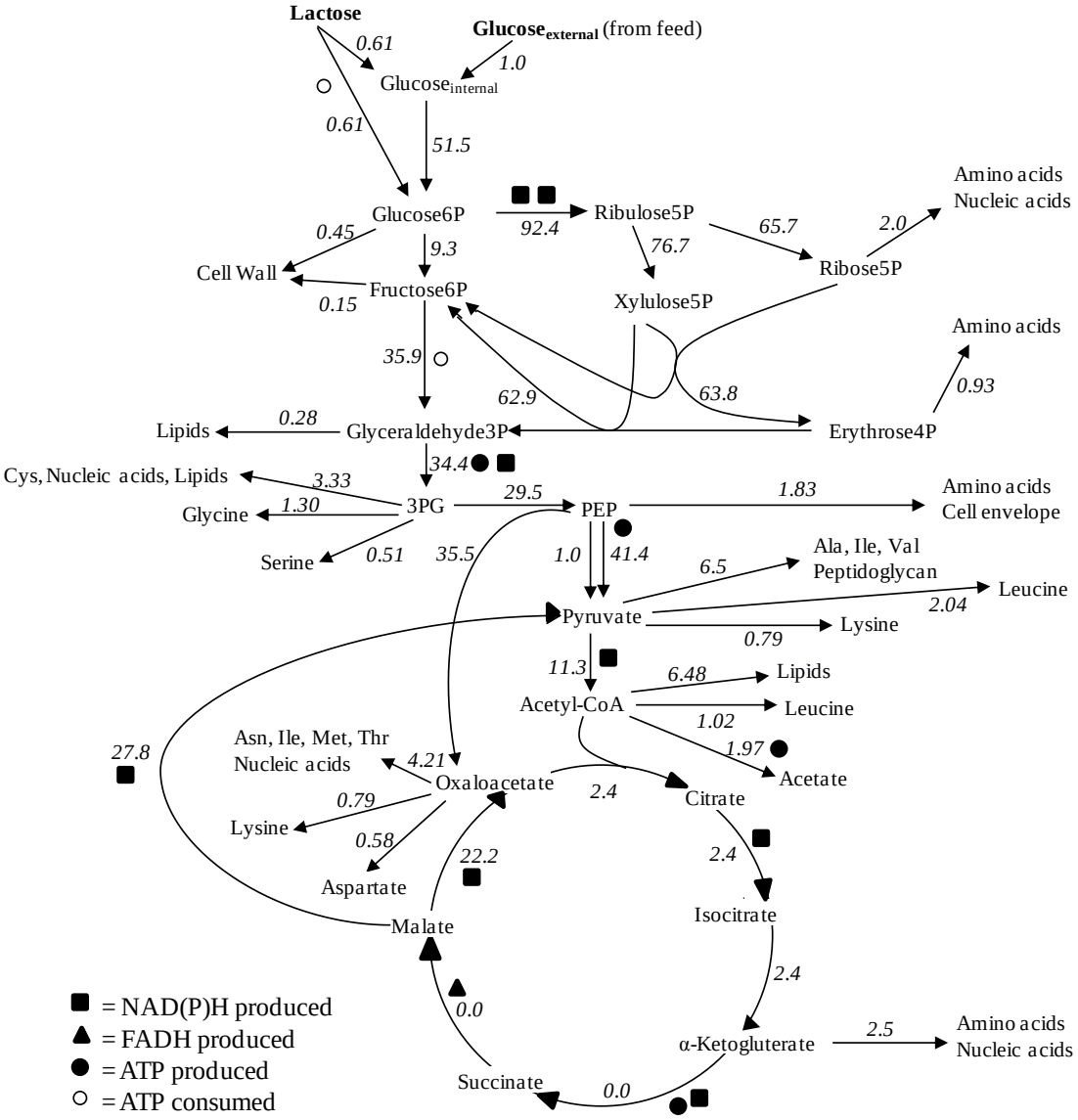

Figure 6-8. Simulated fluxes from auto-induced cultures with an additional pulse of lactose.

Compared to the fluxes for the 12 hour lactose-induced experiment, the biomass component fluxes are higher for this experiment. However, this is due to the fact that the uptake of glucose was significantly lower. Because of this, comparison of the fluxes between different experiments does not yield any information about the effects of the differences in biomass concentrations on metabolism. However, the non-normalized fluxes can be compared. Table 6-2 gives all of the fluxes for each experiment that was performed utilizing glucose feed. The glucose uptake rates can be compared, in addition to the fluxes used for synthesis of biomass components. It is important to note that these fluxes were calculated based on the final concentrations of carbons and biomass, so the resultant fluxes gave a final snapshot of the system as a whole. Also, the asterisked fluxes are the fluxes that were used in the optimization routine. As previously discussed, these fluxes contribute to the precursors for cell wall, amino acid, and nucleic acid synthesis.

Table 6-2. Simulated fluxes for each experiment with glucose feed. Each flux was normalized to the glucose uptake rate (r32). The pre-normalization uptake rate is also given at the bottom of the table (glu upt). The optimized fluxes are indicated by an asterisk.

r	12 hr lac induction	5 mm IPTG	10 mM IPTG	AI w/pulse	Lac at feed start	AI
1	21.60	15.56	16.84	51.55	54.86	69.53
2*	0.19	0.14	0.15	0.45	0.47	0.57
3	3.83	2.65	17.35	9.32	58.83	74.69
4	38.25	27.37	15.21	92.40	49.50	62.84
5	31.73	22.62	12.30	76.72	57.59	73.16
6	27.16	19.34	18.78	65.70	45.82	58.22
7*	0.83	0.62	0.67	2.01	2.12	2.57
8	26.37	18.74	18.13	63.81	43.85	55.73
9	26.00	18.47	10.03	62.93	67.66	85.97
10	14.86	10.63	16.52	35.87	37.63	97.13
11*	0.06	0.05	0.05	0.15	0.16	0.20
12*	0.12	0.09	0.09	0.28	0.30	0.36
13*	0.38	0.29	0.31	0.93	0.98	1.19
14*	1.38	1.04	1.12	3.34	3.53	4.29
15	14.32	10.46	38.84	34.37	142.67	142.78
16	12.28	8.93	37.19	29.51	137.61	136.41
17*	0.76	0.57	0.61	1.83	1.94	2.35
18	16.69	11.66	27.72	41.36	121.73	55.06
19*	2.70	2.02	2.18	6.50	6.88	8.35
20*	2.69	2.02	2.17	6.48	6.85	8.32
21	0.71	0.21	0.22	1.97	1.07	1.40
22	4.64	3.18	32.33	11.31	109.27	139.76
23	0.99	0.75	29.71	2.36	100.89	129.12
24	0.99	0.75	29.71	2.36	100.92	129.13
25	0.99	0.75	29.71	2.36	100.94	129.17
26*	1.04	0.78	0.84	2.50	2.64	3.21
27	0.00	0.00	28.91	0.00	98.48	126.07
28	0.00	0.00	28.91	0.00	98.48	126.07
29	9.28	6.66	21.03	22.17	73.26	92.49
30	14.56	10.35	31.30	35.49	155.28	146.63
31	11.35	7.93	24.94	27.84	68.89	87.20
32	0.98	1.01	1.02	1.01	1.02	1.02
33	0.02	0.00	0.00	0.61	0.00	0.00
34*	0.33	0.25	0.27	0.79	0.84	1.02
35*	0.85	0.63	0.68	2.04	2.16	2.62
36*	0.42	0.32	0.34	1.02	1.08	1.31
37*	0.24	0.18	0.20	0.58	0.62	0.75
38*	0.33	0.25	0.27	0.79	0.84	1.02
39*	1.75	1.31	1.41	4.22	4.46	5.41
40*	0.21	0.16	0.17	0.51	0.54	0.65
41*	0.54	0.40	0.43	1.30	1.37	1.66
gluc upt	0.21	0.28	0.26	0.11	0.13	0.05

The next step in the analysis of fluxes was to test the ability of the model to be predictive. Since the carbon and biomass concentrations are required in order to solve the model, this type of model is not predictive in the sense that it can predict final concentrations, but its accuracy can be checked using Euler's method. If the simulated concentrations match the experimental concentrations, then it is assumed that the model accurately predicted the intermediate fluxes. The first experiment that was modeled using a step-by-step analysis was the 12 hour lactose-induced experiment. The fluxes for this system are given in Table 6-3. Since the fluxes were used in calculating the final concentrations, they were not normalized to the glucose uptake rate.

Table 6-3. Fluxes between each time step for 12 hour lactose-induced experiment. Fluxes were not normalized to glucose uptake. The optimized fluxes are indicated by the asterisk.

r	$\Delta t_{16\text{-}18}$	$\Delta t_{18\text{-}20}$	$\Delta t_{20\text{-}22}$
1	4.54	4.67	4.32
2*	0.04	0.04	0.04
3	0.79	5.04	0.85
4	8.24	4.15	7.30
5	6.85	4.83	6.01
6	5.87	3.84	5.13
7*	0.17	0.17	0.17
8	5.70	3.68	4.96
9	5.62	5.68	4.88
10	3.15	5.45	3.00
11*	0.01	0.01	0.01
12*	0.02	0.02	0.02
13*	0.08	0.08	0.08
14*	0.29	0.29	0.29
15	2.96	11.21	3.19
16	2.53	10.78	2.76
17*	0.16	0.16	0.16
18	3.69	8.15	3.19
19*	0.57	0.57	0.57
20*	0.56	0.56	0.56

r	$\Delta t_{16\text{-}18}$	$\Delta t_{18\text{-}20}$	$\Delta t_{20\text{-}22}$
21	0.10	0.29	0.32
22	0.93	9.41	1.14
23	0.21	8.51	0.21
24	0.21	8.51	0.21
25	0.21	8.51	0.21
26*	0.22	0.22	0.22
27	0.00	8.30	0.00
28	0.00	8.30	0.00
29	1.98	5.81	1.72
30	3.17	8.13	2.79
31	2.49	7.18	2.11
32	0.00	0.10	0.47
33	0.06	0.05	0.03
34*	0.07	0.07	0.07
35*	0.18	0.18	0.18
36*	0.09	0.09	0.09
37*	0.05	0.05	0.05
38*	0.07	0.07	0.07
39*	0.37	0.37	0.37
40*	0.04	0.04	0.04
41*	0.11	0.11	0.11

To calculate the predicted concentration at the next time step, the initial concentration was used as described by Equation 4.16. The predicted concentrations for the 12 hour lactose-induced experiment are shown in Table 6-4. Since the simulated concentrations for glucose and acetate match the experimentally determined glucose and acetate concentrations, the model was able to accurately predict the intermediate fluxes involved in metabolism. The simulated concentrations for lactose were not as close of a match as those for glucose and acetate, but the simulated values gave a decent estimation of the experimental concentrations.

Table 6-4. Predicted (simulated) versus experimental concentrations for 12 hr lactose-induced experiment. Glu, ace, and lac refer to glucose, acetate, and lactose, respectively.

time	exp glu	exp ace	exp lac	sim glu	sim ace	sim lac
16	0	0.04	8.43	--	--	--
18	0	0.39	5.9	0	0.38	7.25
20	1.33	1.64	3.5	1.28	1.63	4.68
22	8.33	3.19	2.1	8.23	3.21	2.66

To check the ability of the model to predict the fluxes for other experiments, this process was repeated for the IPTG-induced experiments and the auto-induced experiment with an additional lactose pulse at 12 hours. In all instances, the model was able to accurately predict the intermediate fluxes. However, the prediction of the lactose concentrations were not as good as those for glucose and acetate in the experiment utilizing auto-induction with a lactose pulse. The carbon concentrations for both IPTG-induced experiments were accurately predicted using the fluxes. Table 6-5 gives the time step fluxes for both IPTG-induced experiments.

Table 6-5. Flux analysis for IPTG-induced experiments. The fluxes used in the optimization routine are indicated by the asterisk.

	5 mM IPTG induction					10 mM IPTG induction				
r	$\Delta t_{19\text{-}20}$	$\Delta t_{20\text{-}21}$	$\Delta t_{21\text{-}22}$	$\Delta t_{22\text{-}23}$	$\Delta t_{23\text{-}24}$	$\Delta t_{18\text{-}19}$	$\Delta t_{19\text{-}20}$	$\Delta t_{20\text{-}21}$	$\Delta t_{21\text{-}22}$	$\Delta t_{22\text{-}23}$
1	4.67	4.61	4.55	3.76	4.52	4.72	4.55	3.64	4.10	4.61
2*	0.04	0.04	0.04	0.04	0.04	0.04	0.04	0.04	0.04	0.04
3	5.03	4.95	4.86	3.28	4.82	1.22	0.77	0.62	0.69	1.20
4	4.25	4.19	4.10	3.50	4.07	8.17	8.15	5.85	7.01	7.91
5	3.74	4.87	4.76	2.66	4.72	9.73	6.76	4.71	5.75	6.72
6	5.16	3.87	3.78	3.91	3.75	3.16	5.79	3.99	4.90	5.73
7*	0.17	0.17	0.17	0.17	0.17	0.17	0.17	0.17	0.17	0.17
8	4.99	3.71	3.62	3.74	3.58	2.99	5.63	3.83	4.73	5.56
9	3.40	5.72	5.59	1.99	5.54	11.45	5.55	3.75	4.66	5.70
10	4.42	4.78	8.31	2.54	3.09	8.79	3.11	2.46	2.79	3.16
11*	0.01	0.01	0.01	0.01	0.01	0.01	0.01	0.01	0.01	0.01
12*	0.02	0.02	0.02	0.02	0.02	0.02	0.02	0.02	0.02	0.02
13*	0.08	0.08	0.08	0.08	0.08	0.08	0.08	0.08	0.08	0.08
14*	0.29	0.29	0.29	0.29	0.29	0.29	0.29	0.29	0.29	0.29
15	11.41	9.57	15.25	8.89	13.70	4.65	2.93	2.91	2.92	1.67
16	10.99	9.15	14.82	8.45	13.27	4.23	2.50	2.48	2.49	1.24
17*	0.16	0.16	0.16	0.16	0.16	0.16	0.16	0.16	0.16	0.16
18	7.37	8.50	8.75	5.40	10.72	6.56	3.53	2.25	2.89	3.63
19*	0.57	0.57	0.57	0.57	0.57	0.57	0.57	0.57	0.57	0.57
20*	0.56	0.56	0.56	0.56	0.56	0.56	0.56	0.56	0.56	0.56
21	0.05	0.04	0.04	0.01	0.03	0.07	0.07	0.00	0.03	0.05
22	9.38	9.22	9.04	6.15	8.92	1.74	0.90	0.85	0.87	1.73
23	8.70	8.56	8.38	5.51	8.26	1.05	0.21	0.21	0.21	1.06
24	8.70	8.56	8.38	5.51	8.27	1.05	0.21	0.21	0.21	1.06
25	8.70	8.56	8.38	5.51	8.26	1.05	0.21	0.21	0.21	1.06
26*	0.22	0.22	0.22	0.22	0.22	0.22	0.22	0.22	0.22	0.22
27	8.49	8.35	8.17	5.30	8.05	0.84	0.00	0.00	0.00	0.85
28	8.49	8.35	8.17	5.30	8.05	0.84	0.00	0.00	0.00	0.85
29	6.19	5.90	5.91	4.08	6.49	1.76	1.99	1.39	1.69	2.29
30	7.49	8.04	10.91	4.77	8.49	1.89	3.09	2.16	2.63	3.66
31	7.42	7.77	7.64	4.59	7.81	3.30	2.42	1.47	1.95	2.99
32	0.02	0.06	0.11	0.71	0.13	0.00	0.14	0.80	0.47	0.07
33	0.00	0.00	0.00	0.00	0.00	0.00	0.00	0.00	0.00	0.00
34*	0.07	0.07	0.07	0.07	0.07	0.07	0.07	0.07	0.07	0.07
35*	0.18	0.18	0.18	0.18	0.18	0.18	0.18	0.18	0.18	0.18
36*	0.09	0.09	0.09	0.09	0.09	0.09	0.09	0.09	0.09	0.09
37*	0.05	0.05	0.05	0.05	0.05	0.05	0.05	0.05	0.05	0.05
38*	0.07	0.07	0.07	0.07	0.07	0.07	0.07	0.07	0.07	0.07
39*	0.37	0.37	0.37	0.37	0.37	0.37	0.37	0.37	0.37	0.37
40*	0.04	0.04	0.04	0.04	0.04	0.04	0.04	0.04	0.04	0.04
41*	0.11	0.11	0.11	0.11	0.11	0.11	0.11	0.11	0.11	0.11

As shown in Table 6-5, the values for the fluxes that were contained in the optimization routine were the same for both IPTG-induced experiments. However, the model for the 5 mM IPTG-induced experiment indicated that more carbon moved through the TCA cycle than that for 10 mM IPTG-induction. On the other hand, the model for the 10 mM IPTG-induced experiments indicated that more carbon cycled through the HMP pathway than the model for the 5 mM IPTG-induced experiments. This was an interesting observation because the experimental results for the IPTG-induced fermentations were similar in nature. Glucose and acetate concentrations were basically the same for each experiment. The only (small) difference was the final biomass. Also, one would expect the fluxes through the HMP pathway to be higher for the 5 mM IPTG-induced experiments because the final biomass concentration was slightly higher. More cellular components are made from this system, but as previously discussed, the fluxes for the biomass components were the same for both models.

Table 6-6. Predicted versus experimentally determined carbon concentrations. (a) IPTG-induced experiments; (b) auto-induction with lactose pulse at 12 hours. Glu, ace, and lac refer to glucose, acetate, and lactose, respectively.

	5 mM IPTG induction				10 mM IPTG induction			
time	exp glu	sim glu	exp ace	sim ace	exp glu	sim glu	exp ace	sim ace
19	0.07	--	0.315	--	0.06	--	0.87	--
20	0.25	0.22	0.45	0.44	0.07	0.07	1.02	1.02
21	0.75	0.77	0.56	0.57	1.05	1.04	0.86	0.86
22	1.87	1.86	0.69	0.69	6.95	6.93	0.85	0.85
23	10.05	9.99	0.66	0.65	10.6	10.60	0.94	0.93
24	11.67	11.72	0.8	0.79	11.2	11.16	0.8	0.81

(a)

time	exp glu	sim glu	exp ace	sim ace	exp lac	sim lac
14	0	--	0.27	--	11.3	--
16	1.15	1.08	0.92	0.93	10.6	10.96
18	1.8	1.82	1.41	1.41	7.6	9.11
20	1.95	1.95	1.19	1.21	5.5	6.68
22	1.9	1.90	1.25	1.27	4.4	5.03

(b)

As previously discussed, the acetate and glucose concentrations were accurately predicted using metabolic flux analysis (Table 6-6). Even though the prediction for lactose was not as accurate, the predicted glucose and acetate concentrations were still very accurate for these experiments. Hence, the model was able to accurately predict the intermediate fluxes involved in glycolysis, the HMP pathway, and the TCA cycle when glucose is used as a feed source regardless of the type of inducer used.

Since the model accurately predicted fluxes for glucose-fed experiments, it was also used to predict the fluxes for glycerol-fed experiments. As discussed in Section 4-11, a few changes in the stoichiometric matrix were made in order to account for gluconeogenesis from glycerol feed. After making the changes, the system was solved for each glycerol-fed experiment using the final experimental concentrations. These fluxes are given in Table 6-7.

Table 6-7. Fluxes for each glycerol-fed experiment. Each flux was normalized to the glycerol uptake rate and the asterisked fluxes represent the fluxes that were used in the optimization routine. The glycerol uptake rate is also given at the bottom of the table (gly upt).

r	AI	AI w/pulse	15 g lac
1	0.00	0.02	0.00
2*	0.01	0.00	0.03
3	0.30	0.00	2.03
4	0.29	0.00	2.00
5	0.13	0.05	0.80
6	0.25	0.03	1.58
7*	0.04	0.02	0.12
8	0.14	0.03	0.98
9	0.16	0.04	1.04
10	0.00	0.07	0.00
11*	0.00	0.00	0.01
12*	0.01	0.00	0.02
13*	0.02	0.01	0.06
14*	0.07	0.03	0.21
15	1.26	0.98	2.98
16	1.16	0.94	2.66
17*	0.04	0.01	0.11
18	1.12	0.92	2.55
19*	0.13	0.05	0.40
20*	0.13	0.05	0.40
21	0.10	0.00	0.22
22	0.95	0.43	2.71

r	AI	AI w/pulse	15 g lac
23	0.70	0.37	2.04
24	0.70	0.37	2.04
25	0.70	0.37	2.04
26*	0.05	0.02	0.15
27	0.66	0.35	1.89
28	0.66	0.35	1.89
29	0.83	0.00	3.11
30	0.16	0.44	0.49
31	0.00	0.37	0.00
32	0.00	0.00	0.00
33	0.00	0.00	0.00
34*	0.02	0.01	0.05
35*	0.04	0.02	0.13
36*	0.02	0.01	0.06
37*	0.01	0.00	0.04
38*	0.02	0.01	0.05
39*	0.08	0.03	0.26
40*	0.01	0.00	0.03
41*	0.03	0.01	0.08
42	1	1	1
gly upt	4.632	11.65	1.48

Notice that using this final snapshot the production of cell wall and lipids from glucose 6-phosphate, fructose 6-phosphate, and glyceraldehyde 3-phosphate is zero (*r2*, *r11*, *r12*) for the auto-induced experiment with an additional pulse of lactose. This is disconcerting because the production of these components is required for cell growth. However, towards the end of this experiment, there was no additional growth because the stationary phase had been reached six hours prior to completion (see Figure 5-41). The lack of biomass production at the end of the experiment could account for the lack of flux towards the components that contribute to biomass.

Additionally, the cell wall components can be synthesized from peptidoglycan, of which there is a positive flux in Table 6-7 (Scheffers and Pinho, 2005).

Though it was not expected that the flux from glyceraldehydes 3-phosphate to fructose 6-phosphate would be zero, it is not an uncommon occurrence for glucose fed-experiments (Lee et al., 1997). This is also applicable for this glycerol-fed experiment since the fluxes have been reversed. The optimal way for glucose to be metabolized is through the HMP pathway because of the production of amino acids and nucleic acids that result from the processing of glucose through this pathway. As indicated by the model, the flow of carbon bypassed the backbone route in glycolysis and moved through the HMP pathway.

The same analysis was performed to check the accuracy of the model by comparing the simulated carbon concentrations with the concentrations that were experimentally determined. This analysis was performed on the auto-induced experiment and the experiment where 15 grams of lactose was added when the glycerol feeding started. Table 6-8 shows this analysis.

Table 6-8. Predicted versus experimental concentrations for glycerol-fed experiments. (a) Analysis for auto-induced experiments; (b) 15 grams of lactose at feed start analysis. Gly, ace, and lac refer to glycerol, acetate, and lactose, respectively.

time	exp gly	sim gly	exp ace	sim ace	exp lac	sim lac
13	0.22	--	0.07	--	0.24	--
15	0.39	0.24	0.20	0.20	0	0.12
17	9.84	0.43	0.27	0.27	0	0
19	26.88	10.34	0.47	0.47	0	0
21	53.30	27.68	0.72	0.72	0	0

(a)

time	exp gly	sim gly	exp ace	sim ace	exp lac	sim lac
13	0.09	--	0.07	--	3.50	--
14	0.13	0.09	0.09	0.09	1.88	2.66
15	1.42	0.28	0.32	0.32	0.98	1.45
16	4.68	1.82	0.11	0.11	0.39	0.70
17	12.57	5.64	0.36	0.36	0.02	0.18

(b)

These results were similar to those achieved for the glucose-fed experiments for the ability of the model to predict the lactose and acetate concentrations. However, the glycerol concentrations were not accurately predicted. Notice that for both glycerol-fed experiments, the predicted values actually predicted the experimental glycerol concentration at the previous time point. Consider the auto-induced case. The simulation predicted a glycerol concentration of 27 grams at the 21 hour time point. This is actually the experimentally determined concentration at the 19 hour time point. This trend followed for the other time points as well.

The lack of accuracy for the glycerol-fed experiments can be attributed to network errors. As previously discussed, the fluxes were reversed (all were reversible) to push carbon up through glycolysis and the HMP pathway to produce glucose 6-phosphate (gluconeogenesis). There could be an error in the underlying assumptions about the network. However, there is an additional network that allows for the production of glycogen under gluconeogenesis conditions. If the cells stored carbon as glycogen, this could account for the discrepancies between biomass and carbon uptake. The metabolic map that includes this network was given in Figure 4-8. The glycogen pathway is indicated by the dashed oval. This process also requires a molecule of ATP and it was assumed that glycogen comprised 1-5% of the cell's biomass.

After adjusting the stoichiometric matrix and the accumulation vector to account for the possibility of glycogen formation, the model was solved in the same way as before for the auto-induced experiment with glycerol feed. This was the only experiment where glycerol was used as a feed source and where lactose was depleted after the first time step. It was determined that adding the possibility of glycogen formation did not have an effect on the flux of glycerol through the network. The glycerol concentrations were still not accurately predicted by this model. Glycogen formation affected the fluxes involved in the HMP pathway and the TCA cycle, but did not affect the glycerol uptake rate. Table 6-9 shows the fluxes for glycerol uptake rate with the resulting predicted concentration in addition to what the flux would need to be in order to accurately predict the glycerol concentration that was achieved experimentally.

Table 6-9. Glycerol uptake rate required to accurately predict experimental data.

Time	*r42*, mM/gcell hr	Simulated concentration, g/l	Experimental concentration, g/l	*r42* to fit, mM/gcell hr	New simulated concentration, g/l
13→15	0.006	0.24	0.39	--	--
15→17	0.007	0.43	9.84	2.1	9.86
17→19	0.12	10.3	26.9	4.1	26.8
19→21	0.21	27.7	53.3	7.0	53.3

For the first time point there was still lactose present in the system and the predicted concentration for glycerol was close to the value that was experimentally determined so there was no change in uptake rate. However, for the next time point, the glycerol uptake rate must be 300 times higher than it actually was in order for the concentrations to match. For the third and fourth time points, the rate must increase by a factor of 34 and 33, respectively. Note that these calculations were performed assuming that the biomass concentration does not change. At this point, the odd relationship between low biomass concentrations and carbohydrate concentrations

comes to light. According to the model, with the given biomass concentrations, the glycerol concentrations remaining in the media should be much higher than they actually were.

The last calculation that was performed using the results from metabolic flux analysis was cellular yield from ATP in an attempt to further investigate the large differences in overall biomass yield. The fluxes that were involved in these calculations are given in Table 6-10 for all experiments using the un-regulated exponential feeding profile. The results from the calculations (refer to Equations 4.17 to 4.21) are given in Table 6-11.

Table 6-10. Fluxes used in yield of biomass from ATP calculations.

r	Description	12 hr lac induction	5 mm IPTG	10 mM IPTG	AI w/pulse	Lac at feed start	AI	Glycerol		
								AI	AI w/pulse	feed start
4	G6P to R5P	8.03	7.66	3.96	10.16	6.44	3.14	1.36	0.00	2.96
10	F6P to G3P	3.12	2.98	4.30	3.95	4.89	4.86	0.00	0.81	0.00
15	G3P to 3PG	3.01	2.93	10.10	3.78	18.55	7.14	5.84	11.36	4.41
18	PEP to Pyr	3.51	3.26	7.21	4.55	15.83	2.75	5.20	10.72	3.78
21	AcCoA to Acetate	0.15	0.06	0.06	0.22	0.14	0.07	0.48	0.00	0.32
22	Pyr to AcCoA	0.97	0.89	8.41	1.24	14.20	6.99	4.42	5.02	4.02
24	Cit to Iso	0.21	0.21	7.73	0.26	13.12	6.46	3.26	4.34	3.03
27	KG to Succ	0.00	0.00	7.52	0.00	12.80	6.30	3.04	4.11	2.80
28	Succ to Mal	0.00	0.00	7.52	0.00	12.80	6.30	3.04	4.11	2.80
29	Mal to OA	1.95	1.86	5.47	2.44	9.52	4.62	3.84	0.00	4.61
31	Mal to Pyr	2.38	2.22	6.48	3.06	8.96	4.36	0.00	4.36	0.00
33	Lac to G6P	0.00	0.00	0.00	0.07	0.00	0.00	0.00	0.01	0.00
42	Gly to G3P	0.00	0.00	0.00	0.00	0.00	0.00	4.63	11.65	1.48

Table 6-11. Contributions of energetics to ATP fluxes and biomass yield from ATP.

	12 hr lac induction	5 mm IPTG	10 mM IPTG	AI w/pulse	Lac at feed start	AI	Glycerol		
							AI	AI w pulse	15 g lac
FADH	0.0	0.0	7.5	0.0	12.8	6.3	3.0	4.1	2.8
NADPH	24.6	23.4	53.6	31.1	90.0	42.2	23.1	29.2	24.8
ATP	3.5	3.3	20.6	4.5	42.4	11.4	9.9	15.3	9.8
ATP total	35.5	33.7	96.8	45.0	170.5	71.7	42.6	56.8	44.5
D	0.19	0.19	0.19	0.24	0.30	0.14	0.03	0.05	0.12
Y cell/ATP	5.4	5.6	2.0	5.3	1.8	2.0	0.7	0.9	2.7
Biomass	60	76	70	33	41	43	35	19	19

Notice that the total amount of ATP produced for the 10 mM IPTG-induced and the lactose-induced at feed start experiments was very high compared to other experiments. Since biomass yield from ATP is inversely proportional to ATP production, their yields were lower. Also, the biomass yield from ATP for the glycerol-fed experiments were low (due to the low biomass concentrations. Next, the ratios of biomasses were compared to the ratios of biomass yield from ATP to see how closely these two are related. This analysis provided information as to why there were large differences in biomass production. If the ATP yield ratios match the biomass ratios, then the metabolic pathways that contribute to this difference can be identified.

As shown in Table 6-12, the ratios for a few of the experiments were practically the same, but for most they were different. For example, the ratios for the 5 mM IPTG-induced experiment and the 12 hr lactose-induced experiment were very similar (1.1 vs. 1.3), but the ratios for the 12 hr lactose-induced experiment to the auto-induced experiment with glycerol feed were very different (7.7 vs. 1.7). The highlighted ratios are those in which the percent error is less than or equal to 20%. (Refer to Section 9.9 for the complete table of percent error.) The differences can be accounted for by the total ATP fluxes in Table 6-11 (from the individual fluxes in Table 6-10).

Table 6-12. Ratios of ATP yield and biomass. Biomass ratios are given in parentheses. Ratios were calculated by diving the value for the experiments on the left hand side of the table (vertically arranged) by the value for the experiments given horizontally at the top of the table.

feed	experiment	12 hr lac	5 mM IPTG	10 mM IPTG	AI w/pulse	Lac at feed start	AI	Glycerol		
								AI	AI w/pulse	15 g lac
Glucose	12 hr lac	--	0.96 (0.8)	2.7 (0.85)	1.02 (1.82)	3 (1.46)	2.7 (1.4)	7.7 (1.7)	6 (3.2)	0.5 (3.2)
	5 mM IPTG	1.1 (1.3)	--	2.8 (1.09)	1.06 (2.3)	3.1 (1.85)	2.8 (1.8)	8 (2.2)	6.2 (4)	2.1 (4)
	10 mM IPTG	0.37 (0.86)	0.36 (0.92)	--	0.38 (2.12)	1.1 (1.7)	1 (1.63)	2.9 (2)	2.2 (3.7)	0.74 (3.7)
	AI w/pulse	0.98 (0.55)	0.95 (0.43)	0.95 (0.47)	--	2.9 (0.8)	2.7 (0.78)	7.6 (0.9)	5.9 (1.7)	2 (1.7)
	Lac at feed start	0.3 (0.68)	0.32 (0.54)	0.9 (0.56)	0.34 (1.24)	--	0.9 (0.95)	2.6 (1.2)	2 (1.7)	0.70 (1.7)
	AI	0.37 (0.72)	0.37 (0.46)	1 (0.61)	0.38 (1.3)	1.1 (1.3)	--	2.9 (1.2)	2.9 (2.3)	0.74 (2.3)
Glycerol	AI (gly)	0.13 (0.58)	0.13 (0.25)	0.35 (0.5)	0.13 (1.1)	0.39 (1.1)	0.35 (0.81)	--	0.8 (1.8)	0.3 (1.8)
	AI w/pulse (gly)	0.17 (0.32)	0.16 (0.25)	0.45 (0.27)	0.17 (0.58)	0.5 (0.58)	0.45 (0.44)	1.3 (0.54)	--	0.3 (1)
	15 g lac (gly)	0.5 (0.32)	0.48 (0.25)	1.35 (0.27)	0.51 (0.58)	1.5 (0.58)	1.4 (0.44)	3.9 (0.54)	3 (1)	--

Since there are only a few experiments in which the ATP yield ratios match the biomass ratios, the production of ATP cannot account for the discrepancies that were witnessed in the fermentation experiments for biomass production for all experiments. However, this analysis did provide insight into the pathways that are affected by different inducer and feed sources and how the changes in fluxes affect the overall ATP production.

After completing these simulations, it was determined that using step-by-step metabolic flux analysis (with Euler's method) can be used to accurately predict carbohydrate concentrations when glycerol is not the feed source, regardless of inducer type. The glycerol-fed experiments may not have worked due to the reversal of fluxes through the HMP pathway. This reversal completely changed the stoichiometric matrix and perhaps the dynamics of the model itself. However, the incorporation of lactose into the simulation was successful in that lactose uptake rates were calculated and predictions of experimental concentrations were fairly accurate.

7. Conclusions and recommendations

Overall, fed-batch fermentation is a viable option for production of GST-PTH-CBD and the methods developed here would work well with the production of other therapeutic fusion proteins. The media development method utilized in this dissertation can be adapted to the production of other proteins by examining their amino acid content and it is novel in the sense that all components remain defined in nature. The feeding profile developed in this dissertation would also work for fed-batch cultivations of other strains of *Escherichia coli*. However, the feeding profile should be modified if using a carbon substrate other than glucose. This would prevent the likely accumulation of other substrates, since glucose is taken up more rapidly by the cells that other carbon sources.

Additionally, in many of the experiments, it became apparent that lactose has an effect on the utilization of glucose. Growth became inhibited, but glucose uptake did not stop. This phenomenon could be further examined by using fed-batch fermentation with lactose induction for other systems that contain the *lac* operon. Insight into this particular relationship between carbohydrates and corresponding biomass production was lacking in the literature. In short, the following trends were observed for fed-batch fermentation experiments:

- Product yield from biomass remained constant for the duration of the fermentation for most experiments.
- Acetate concentrations remained well below inhibitory values, due to the design of the feeding profile.
- Lactose added earlier on negatively affected biomass yield and lactose was consumed regardless of the presence of glucose.

The following statements are brief recommendations for the fermentation experiments:

- To make the most cells, cultures should be induced with IPTG.
- To make the most product, cultures should be auto-induced and fed with glycerol.
- To make the most product with cost in mind, cultures should be auto-induced and fed with glycerol or auto-induced with an additional lactose pulse and fed with glucose.

Dynamic modeling for this system using the traditional types of equations did not work. The feed, volume, and biomass equations were a close fit to those experimentally observed. The final simulated lactose concentrations tracked with experimentally observed concentrations, but the slope of degradation was not a good fit. However, the simulation modeling the complete fermentation system was unable to accurately predict the glucose and acetate concentrations. It appears that under lactose induction, the relationship between the three carbohydrates for this expression system is unique.

Lastly, metabolic flux analysis was used to track the movement of carbon through metabolism in an attempt to identify the 'carbon sink' that was experimentally observed. This tool can be used to gain valuable insight into cellular metabolism with regards to the production of biomass using this particular construct. This type of modeling can be use to predict intermediate fluxes if some information is known about the external environment of the cell. Other systems using lactose as an inducer could be examined using metabolic flux analysis to further describe the relationship between carbohydrates and biomass production.

After a complete analysis of the data from metabolic flux analysis and the experiments, a final additional recommendation would be to examine the metabolism of a lac deficient strain. If lactose was used as an inducer, but it was unable to be metabolized, it may act more like IPTG in

the sense that growth is not affected. Then, the best of both cases would hold true - higher cell densities (as in the IPTG-induced experiments) with high protein yield from cells (as in the case of lactose-induced experiments).

8. References

Akesson, M., Hagander, P., & Axelsson, J. P. (2001) Avoiding acetate accumulation in *Escherichia coli* cultures using feedback control of glucose feeding. *Biotechnology and Bioengineering. 73*, 223-230.

Antoniewicz, M., Kranie, D., Laffend, L., Gozalez-Lergier, J., Kelleher, J., & Stephanopoulos, G. (2007) Metabolic flux analysis in a nonstationary system: Fed-batch fermentation of a high yielding strain of *E. coli* producing 1,3-propanediol. *Metabolic engineering. 9*, 277-292.

Aristidou, A., San, K., & Bennett, G. (1995) Metabolic engineering of *Escherichia coli* to enhance recombinant protein production through acetate reduction. *Biotechnol. Prog. 11*, 475-478.

Aucoin, M., McMurray-Beaulieu, V., Poulin, F., Boivin, E., Chen, J., Ardelean, F., Cloutier, M., Choi, Y., Miguez, C., & Jolicoeur, M. (2006) Identifying conditions for inducible protein production in *E. coli*: Combining a fed-batch and multiple induction approach. *Microbial Cell Factories. 5*, 27.

Babaeipour, V., Shojaosadati, S. A., Khalilzadeh, R., Maghsoudi, N., & Tabandeh, F. (2008) A proposed feeding strategy for the overproduction of recombinant proteins in *Escherichia coli. Biotechnology and applied biochemistry. 49*, 141.

Behme, S. (2009) Manufacturing of pharmaceutical proteins: From technology to economy. WILEY-VCH Verlag GmbH & Co, KGaA, Weinheim

Berrow, N., Bussow, K., Coutard, B., Diprose, J., Ekberg, M., Folkers, G. E., Levy, N., Lieu, V., Owens, R. J., Peleg, Y., Pinaglia, C., Quevillon-Cheruel, S., Salim, L., Scheich, C., Vincentelli, R., & Busso, D. (2006) Recombinant protein expression and solubility screening in *Escherchia coli*: A comparative study. *Biological Crystallography. 62*, 1218-1226.

Blommel, P. G., Becker, K., J., Duvnjak, P., & Fox, B. (2007) Enhanced bacterial protein expression during auto-induction obtained by alteration of *lac* Repressor dosage and medium composition. *Biotechnol. Prog. 23*, 585-598.

Camps, M. (2010) Modulation of ColE1-like plasmid replication for recombinant gene expression. *Recent patents on DNA & gene sequences. 4*, 58.

Carpenter, G., Stoscheck, C. M., & Soderquist, A. M. (1982) EPIDERMAL GROWTH FACTOR*. *Annals of the New York Academy of Sciences. 397*, 11-17.

Chassagnole, C., Noisommit-Rizzi, N., Schmid, J. W., Mauch, K., & Reuss, M. (2002) Dynamic modeling of the central carbon metabolism of *Escherichia coli. Biotechnology and bioengineering. 79*, 53-73.

Chen, Q., Bentley, W. E., & Weigand, W. A. (1995) Optimization for a recombinant *E. coli* fed-batch fermentation. *Applied Biochemistry and Biotechnology. 51/52*, 449-461.

Chen, W., Bailey, J., & Lee, S. (1991) Molecular design of expression systems: Comparison of different repressor control configurations using molecular mechanism models. *Biotech and Bioeng. 38*, 679-687.

Chen, W., Graham, C., & Ciccarelli, R. (1997) Automated fed-batch fermentation with feed-back controls based on dissolved oxygen (DO) and pH for production of DNA vaccines. *Journal of Industrial Microbiology & Biotechnology. 18*, 43-48.

Chen, W., Shi, C., Yi, S., Chen, B., Zhang, W., Fang, Z., Wei, Z., Jiang, S., Sun, X., Hou, X., Xiao, Z., Ye, G., & Dai, J. (2010) Bladder regeneration by collagen scaffolds with collagen binding human basic fibroblast growth factor. *The Journal of Urology. 183*, 2432-2439.

Cheng, B., Fournier, R., Relue, P., & Schisler, J. (2001) An experimental and theoretical study of the inhibition of *Escherichia coli lac* operon gene expression by antigene oligonucleotides. *Biotechnology and Bioengineering. 74*, 220-229.

Choi, J. H., Keum, K. C., & Lee, S. Y. (2006) Production of recombinant proteins by high cell density culture of *Escherichia coli. Chemical Engineering Science. 61*, 876-885.

Cockshott, A. R., & Bogle, I. D. L. (1999) Modelling the effects of glucose feeding on a recombinant *E. coli* fermentation. *Bioprocess Engineering. 20*, 83-90.

Covert, M. W., Schilling, C. H., & Palsson, B. (2001) Regulation of gene expression in flux balance models of metabolism. *Journal of theoretical biology. 213*, 73-88.

de Mare, L., Velut, S., Ledung, E., Cimander, C., Norrman, B., Nordberg Karlsson, E., Holst, O., & Hagander, P. (2005) A cultivation technique for *E. coli* fed-batch cultivations operating close to the maximum oxygen transfer capacity of the reactor. *Biotechnology Letters. 27*, 983-990.

De Mey, M., De Maeseneire, S., Soetaert, W., & Vandamme, E. (2007) Minimizing acetate formation in *E. coli* fermentations. *J Ind Microbiol Biotechnol. 34*, 689-700.

Donovan, R., Robinson, R., CW, & Glick, B. (1996) Review: Optimizing inducer and culture conditions for expression of foreign proteins under the control of the *lac* promoter. *Journal of Industrial Microbiology. 16*, 145-154.

Dubach, A., & Markl, H. (1992) Application of an extended kilman filter method for monitoring high cell density cultivation of *Escherichia coli. Journal of Fermentation and Bioengineering. 73*, 396-402.

Eiteman, M., & Altman, E. (2006) Overcoming acetate in *Escherichia coli* recombinant protein fermentations. *Trends in Biotechnology. 24*, 530-536.

Fan, D., Luo, Y., Mi, Y., Ma, X., & Shang, L. (2005) Characteristics of fed-batch cultures of recombinant *Escherichia coli* containing human-like collagen cDNA at different specific growth rates. *Biotechnology Letters. 27,* 865-870.

Faulkner, E., Barrett, M., Okor, S., Kieran, P., Casey, E., Paradisi, F., Engel, P., & Gennon, B. (2006) Use of fed-batch cultivation for achieving high cell densities for the pilot-scale production of a recombinant protein (phenylalanine dehydrogenase) in *Escherichia coli*. *Biotechnol. Prog. 22*, 889-897.

Ferrer-Miralles, N., Domingo-Espin, J., Corchero, J., Vazquez, E., & Villaverde, A. (2009) Microbial factories for recombinant pharmaceuticals. *Microbial Cell Factories. 8*, 17.

Fu, X., Tong, W., & Wei, D. (2005) Extracellular production of human parathyroid hormone as a thiooredoxin fusion form in *Escherichia coli* by chemical permeabilization combined with heat treatment. *Biotechnol Prog. 21*, 1429-1435.

Garcia-Arrazola, R., Siu, S. C., Chan, G., Buchanan, I., Doyle, B., Titchener-Hooker, N., & Baganz, F. (2005) Evaluation of a pH-stat feeding strategy on the production and recovery of fab' fragments from *E. coli*. *Biochemical Engineering Journal. 25*, 221-230.

Gombert, A. K., & Kilikian, B. V. (1998) Recombinant gene expression in *Escherichia coli* cultivation using lactose as an inducer. *Journal of Biotechnology. 60*, 47-54.

Grabski, A., Mehler, M., & Drott, D. (2005) The overnight express autoinduction system: High-density cell growth and protein expression while you sleep. *Nature Methods. 2*, 233-235.

Han, K., Lim, H. C., & Hong, J. (1992) Acetic acid formation in *Escherichia coli* fermentation. *Biotech and Bioneng. 39*, 663-671.

Hannachi Imen, E., Nakamura, M., Mie, M., & Kobatake, E. (2009) Construction of multifunctional proteins for tissue engineering: Epidermal growth factor with collagen binding and cell adhesive activities. *Journal of Biotechnology. 139*, 19-25.

Harder, M. P. F., Sanders, E. A., Wingender, E., & Deckwer, W. (1993) Studies on the production of human parathyroid hormone by recombinant *Escherichia coli*. *Appl Microbiol Biotechnol. 39*, 329-334.

Hoffman, B. J., Broadwater, J. A., Johnson, P., Harper, J., Fox, B. G., & Kenealy, W. R. (1995) Lactose fed-batch overexpression of recombinant metalloproteins in *Escherichia coli* BL21(DE3): Process control yielding high levels of metal-incorporated, soluble protein. *Protein expression and purification. 6*, 646-654.

Holms, W. H. (1986) The central metabolic pathways of *Escherichia coli*: Relationship between flux and control at a branch point, efficiency of conversion to biomass, and excretion of acetate. *Current Topics in Cellular Regulation. 28*, 59-105.

Hong, W. K., Kwon, S. J., & Kim, E. K. (1992) Effects of in-vitro protein stabilizers on the overproduction of recombinant beta-lactamase in *Escherichia coli*. *Biotechnol. Lett. 14*, 345-350.

Jacoby, G. A., & Sutton, L. (1985) Beta-lactamases and beta-lactam resistance in *Escherichia coli*. *Antimicrobial agents and chemotherapy. 28*, 703-705.

Jenzsch, M., Simutis, R., & Luebbert, A. (2006) Generic model control of the specific growth rate in recombinant *Escherichia coli* cultivations. *Journal of Biotechnology. 122*, 483-493.

Kauffman, K. J., Prakash, P., & Edwards, J. S. (2003) Advances in flux balance analysis. *Current opinion in biotechnology. 14*, 491-496.

Kayser, A., Weber, J., Volker, H., & Rinas, U. (2005) Metabolic flux analysis of *Escherichia coli* in glucose-limited continuous culture. I. growth-rate-dependent metabolic efficiency at steady state. *Microbiology. 151*, 693-706.

Kilikian, B., Suarez, I., Liria, C., & Gombert, A. K. (2000) Process strategies to improve heterologous protein production in *Escherichia coli* under lactose or IPTG induction. *Process Biochemistry. 35*, 1019-1025.

Kim, B. S., Lee, S. C., Lee, S. Y., Chang, Y. K., & Chang, H. N. (2004) High cell density fed-batch cultivation of *Escherichia coli* using exponential feeding combined with pH-stat. *Bioprocess Biosyst Eng. 26*, 147-150.

Kim, M., Elvin, C., Brownlee, A., & Lyons, R. (2007) High yield expression of recombinant pro-resilin: Lactose-induced fermentation in *E. coli* and facile purification. *Protein Expr. Purif. 52*, 230-236.

Kleman, G. L., Chalmers, J. J., Luli, G. W., & Strohl, W. R. (1991) A predictive and feedback control algorithm maintains a constant glucose concentration in fed-batch fermentations. *Applied and Environmental Microbiology. 57*, 910-917.

Kleman, G. L., & Strohl, W. R. (1994) Acetate metabolism by *Escherichia coli* in high-cell-density fermentation. *Applied and Environmental Microbiology. 60*, 3952-3958.

Koffas, M., Roberge, C., Lee, K., & Stephanopoulos, G. (1999) Metabolic engineering. *Annual Review of Biomedical Engineering. 1*, 535-557.

Korz, D. J., Rinas, U., Hellmuth, K., Sanders, E. A., & Deckwer, W. (1995) Simple fed-batch technique for high cell density cultivation of *Escherichia coli*. *Journal of Biotechnology. 39*, 59-65.

Kosinski, M. J., Rinas, U., & Bailey, J. E. (1992) Isopropyl-β-D-thiogalactopyranoside influences the metabolism of *Escherichia coli*. *Applied Microbiology and Biotechnology. 36*, 782-784.

Kotik, M., Kocanova, M., Maresova, H., & Kyslik, P. (2004) High-level expression of a fungal pyranose oxidase in high cell-density fed-batch cultivations of *Escherichia coli* using lactose as inducer. *Protein expression and purification. 36*, 61-69.

Kremling, A., Bettenbrock, K., Laube, B., Jahreis, K., Lengeler, J. W., & Gilles, E. D. (2001) The organization of metabolic reaction networks: application for diauxic growth on glucose and lactose. *Metab. Eng. 3*, 362-379.

Kweon, D., Han, N. S., Park, K., & Seo, J. (2001) Overproduction of phytolacca insularis protein in batch and fed-batch culture of recombinant *Escherichia coli. Process Biochemistry. 36*, 537-542.

Kwon, S., Kim, S., & Kim, E. (1996) Effects of glycerol on beta-lactamase production during high cell density cultivation of recombinant *Escherichia coli. Biotechnology progress. 12*, 205-208.

Lee, J., Goel, A., Ataai, M., & Domach, M. (1997) Supply-side analysis of growth of *bacillus subtilis* on glucose-citrate medium: Feasible network alternatives and yield optimality. *Applied and Environmental Microbiology. 63*, 710-718.

Lee, S. Y. (1996) High cell-density culture of *Escherichia coli. Trends in biotechnology. 14*, 98-105.

Levisauskas, D., & Tekoris, T. (2005) Model-based optimization of fed-batch fermentation processes using predetermined type feed-rate time profiles. A comparative study. *Information Technology and Control. 34*, 231-236.

Li, Z., Kessler, W., van den Heuvel, J., & Rinas, U. (2011) Simple defined autoinduction medium for high-level recombinant protein productino using T7-based *Escherichia coli* expression systems. *Appl Microbiol Biotechnol. 91*, 1203-1213.

Lin, Y. H., & Neubauer, P. (2000) Influence of controlled glucose oscillations on a fed-batch process of recombinant *Escherichia coli. Journal of Biotechnology. 79*, 27-37.

Liu, Q., Lin, J., Liu, M., Tao, X., Wei, D., Ma, X., & Yang, S. (2007) Large scale preparation of recombinant human parathyroid hormone 1–84 from *Escherichia coli. Protein expression and purification. 54*, 212-219.

Longobardi, G. P. (1994) Fed-batch versus batch fermentation. *Bioprocess Engineering. 10*, 185-194.

Macaloney, G., Hall, J. W., Rollins, M. J., Draper, I., Anderson, K. B., Preston, J., Thompson, B. G., & McNeil, B. (1997) The utility and performance of near-infra red spectroscopy in simultaneous monitoring of multiple components in a high cell density recombinant *Escherichia coli* production process. *Bioprocess Engineering. 17*, 157-167.

Matsushita, O., Jung, C., Minami, J., Katayama, S., Nishi, N., & Okabe, A. (1998) A study of the collagen-binding domain of a 116-kDa clostridium histolyticum collagenase*. *The Journal of Biological Chemistry. 273*, 3643-3648.

Meadows, A. L., Karnik, R., Lam, H., Forestell, S., & Snedecor, B. (2010) Application of dynamic flux balance analysis to an industrial *Escherichia coli* fermentation. *Metabolic engineering. 12*, 150-160.

Menzella, H., Ceccarelli, E., & Gramajo, H. (2003) Novel *Escherichia coli* strain allows efficient recombinant protein production using lactose as inducer. *Biotech and Bioneng. 82*, 809-817.

Mohseni, S., Babaeipour, V., & Vali, A. (2009) Design of sliding mode controller for the optimal control of fed-batch cultivation of recombinant *E.coli. Chemical Engineering Science. 64*, 4433-4441.

Murarka, A., Dharmadi, Y., Yazdani, S. S., & Gonzalez, R. (2008) Fermentative utilization of glycerol by *Escherichia coli* and its implications for the production of fuels and chemicals. *Applied and Environmental Microbiology. 74*, 1124-1135.

Namdev, P. K., Irwin, N., Thompson, B., & Gray, M. R. (1993) Effect of oxygen fluctuations on recombinant *Escherichia coli* fermentation. *Biotechnology and bioengineering. 41*, 666-670.

Neubauer, P., Hofmann, K., Holst, O., Mattiasson, B., & Kruschke, P. (1992) Maximizing the expression of a recombinant gene in *Escherichia coli* by manipulation of induction time using lactose as inducer. *Appl Microbiol Biotechnol. 36*, 739-744.

Neubauer, P., Häggström, L., & Enfors, S. (1995) Influence of substrate oscillations on acetate formation and growth yield in *Escherichia coli* glucose limited fed-batch cultivations. *Biotechnology and bioengineering. 47*, 139-146.

Nozomu, N., Matsushita, O., Yuube, K., Miyanaka, H., Okabe, A., & Wada, F. (1998) Collagen-binding growth factors: Production and characterization of functional fusion proteins having a collagen-binding domain. *Proceedings of the National Academy of Sciences of the United States of America. 95*, 7018-7023.

Panda, A. K., Khan, R. H., Mishra, S., Appa Rao, K. B. C., & Totey, S. M. (2000) Influences of yeast extract on specific cellular yield of ovine growth hormone during fed-batch fermentation of *E. coli. Bioprocess Engineering. 22*, 379-383.

Pramanik, J., & Keasling, J. D. (1997) Stoichiometric model of *Escherichia coli* metabolism: Incorporation of growth-rate dependent biomass composition and mechanistic energy requirements. *Biotech and Bioeng. 56*, 398-421.

Ramchuran, S., Holst, O., & Karlsson, E. (2005) Effect of postinduction nutrient feed composition and use of lactose as inducer during production of thermostable xylanase in

Escherchia coli glucose-limited fed-batch cultivations. *Journal of Bioscience and Bioengineering. 99*, 477-484.

Roeva, O., Pencheva, T., Tzonkov, S., Arndt, M., Hitzmann, B., Kleist, S., Miksch, G., & Friehs, K. (2007) Multiple model approach to modelling of *Escherichia coli* fed-batch cultivation extracellular production of bacterial phytase. *Electronic Journal of Biotechnology. 10*, 593-603.

Roeve, O., & Tzonkov, S. (2006) Modelling of *Escherichia coli* cultivations: Acetate inhibition in a fed-batch culture. *Bioautomation. 4*, 1-11.

Sakon, J., Gensure, R. C., & Matsushita, O. (2010) Fusion proteins of collagen-binding domain and parathyroid hormone. *20100129341*

Sandén, A. M., Prytz, I., Tubulekas, I., Förberg, C., Le, H., Hektor, A., Neubauer, P., Pragai, Z., Harwood, C., Ward, A., Picon, A., de Mattos, J. T., Postma, P., Farewell, A., Nyström, T., Reeh, S., Pedersen, S., & Larsson, G. (2003) Limiting factors in *Escherichia coli* fed-batch production of recombinant proteins. *Biotechnology and bioengineering. 81*, 158-166.

Santillan, M. (2008) Bistable behavior in a model of the *lac* operon in *Escherichia coli* with variable growth rate. *Biophysical Journal. 94*, 2065-2081.

Santillan, M., & Mackey, M. C. (2008) Quantitative approaches to the study of bistability in the *lac* operon of *Escherichia coli. J. R. Soc. Interface. 5*, S29-S39.

Sassenfeld, H. M. (1990) Engineering proteins for purification. *Trends in biotechnology. 8*, 88-93.

Sauer, U. (2006) Metabolic networks in motion: ^{13}C-based flux analysis. *Molecular Systems Biology. 14*, 1-10.

Sauer, U., Lasko, D. R., Fiaux, J., Hochuli, M., Glaser, R., Szyperski, T., Wüthrich, K., & Bailey, J. E. (1999) Metabolic flux ratio analysis of genetic and environmental modulations of *Escherichia coli* central carbon metabolism. *Journal of Bacteriology. 181*, 6679-6688.

Scheffers, D., & Pinho, M. G. (2005) Bacterial cell wall synthesis: New insights from localization studies. *Microbiology and molecular biology reviews. 69*, 585-607.

Shi, C., Chen, W., Zhao, Y., Chen, B., Xiao, Z., Wei, Z., Hou, X., Tang, J., Wang, Z., & Dai, J. (2011) Regeneration of full-thickness abdominal wall defects in rats using collagen scaffolds loaded with collagen-binding basic fibroblast growth factor. *Biomaterials. 32*, 753-759.

Shiloach, J., Kaufman, J., Guillard, A. S., & Fass, R. (1996) Effect of glucose supply strategy on acetate accumulation, growth, and recombinant protein production by *Escherichia coli*

BL21 ("lambda" DE3) and *escherichia coli* JM109. *Biotechnology and Bioengineering. 49*, 421-428.

Shiloach, J., & Fass, R. (2005) Growing *E. coli* to high cell density - A historical perspective on method development. *Biotechnology Advances. 23*, 345-357.

Shin, C. S., Hong, M. S., Bae, C. S., & Lee, J. (1997) Enhanced production of human mini-proinsulin in fed-batch cultures at high cell density of *Escherichia coli* BL21(DE3) [pET-3aT2M2]. *Biotechnology progress. 13*, 249-257.

Stephanopoulos, G. (1999) Metabolic fluxes and metabolic engineering. *Metabolic engineering. 1*, 1-11.

Studier, F. W. (2005) Protein production by auto-induction in high-density shaking cultures. *Protein expression and purification. 41*, 207-234.

Terpe, K. (2003) Overview of tag protein fusions: From molecular and biochemical fundamentals to commercial systems. *Applied Microbiology and Biotechnology. 60*, 523-533.

Ting, T., Thoma, G., Beitle, R., Davis, R., Perkins, R., Karim, K., & Liu, H. (2008) A simple substrate feeding strategy using a pH control trigger in fed-batch fermentation. *Applied Biochemistry and Biotechnology. 149*, 89-98.

Toyoshima, T., Matsushita, O., Minami, J., Nishi, N., Okabe, A., & Itano, T. (2001) Collagen-binding domain of a clostridium histolyticum collagenase exhibits a broad substrate spectrum both in vitro and in vivo. *Connect Tissue Res. 42*, 281-290.

Tripathi, N. K., Sathyaseelan, K., Jana, A. M., & Rao, P. V. L. (2009) High yield production of heterologous proteins with *Escherichia coli. Defence Science Journal. 59*, 137-146.

van Hoek, M. J. A., & Hogeweg, P. (2006) In silico evolved *lac* operons exhibit bistability for artificial inducers, but not for lactose. *Biophysical Journal. 91*, 2833-2843.

van Hoek, M. J. A., & Hogeweg, P. (2007) The effect of stochasticity on the *lac* operon: An evolutionary perspective. *PLoS Computational Biology. 3*, 1071-1082.

Varma, A., Boesch, B. W., & Palsson, B. O. (2004) Biochemical production capabilities of *Escherichia coli. Biotechnology and bioengineering. 42*, 59-73.

Varma, A., & Palsson, B. (1994a) Metabolic flux balancing: Basic concepts, scientific and practical use. *Nature Biotechnology. 12*, 994-998.

Varma, A., & Palsson, B. (1994b) Stoichiometric flux balance models quantitatively predit growth and metabolic by-product secretion in wild-type *Escherichia coli* W3110. *Applied and Environmental Microbiology. 10*, 3724-3731.

Wong, M., Wright, M., Woodley, J., & Lye, G. (2009) Enhanced recombinant protein synthesis in batch and fed-batch *Escherichia coli* fermentation based on removal of inhibitory acetate by electrodialysis. *J Chem Technol Biotechnol. 84*, 1284-1291.

Wong, P., Gladney, S., & Keasling, J. D. (1997) Mathematical model of the *lac* operon: Inducer exclusion, catabolite repression, and diauxic growth on glucose and lactose. *Biotechnol. Prog. 13*, 132-143.

Wong, H. H., Kim, Y. C., Lee, S. Y., & Chang, H. N. (1998) Effect of post-induction nutrient feeding strategies on the production of bioadhesive protein in *Escherichia coli. Biotechnology and bioengineering. 60*, 271-276.

Xu, B., Jahic, M., & Enfors, S. O. (2008) Modeling of overflow metabolism in batch and Fed-Batch cultures of *Escherichia coli. Biotechnology progress. 15*, 81-90.

Xu, J., Banerjee, A., Pan, S., & Li, Z. J. (2012) Galactose can be an inducer for production of therapeutic proteins by auto-induction using *E. coli* BL21 strains. *Protein expression and purification. 83*, 30-36.

Xue, W., Fan, D., Shang, L., Zhu, C., Ma, X., Zhu, X., & Yu, Y. (2010) Effects of acetic acid and its assimilation in fed-batch cultures of recombinant *Escherichia coli* containing human-like collagen cDNA. *Journal of Bioscience and Bioengineering. 109*, 257-261.

Yee, L., & Blanch, H. W. (1993) Recombinant trypsin production in high cell density fed-batch cultures in *Escherichia coli. Biotechnology and bioengineering. 41*, 781-790.

Zheng, Z., Yao, S., Zhan, X., & Lin, C. (2009) Improvement of hEGF production with enhanced cell division ability using dissolved oxygen responses to pulse addition of tryptone. *Biotechnology and Bioprocess Engineering. 14*, 52-59.

9. Appendix

9.1 Correlation for glucose concentration and absorbance for glucose hexokinase assay

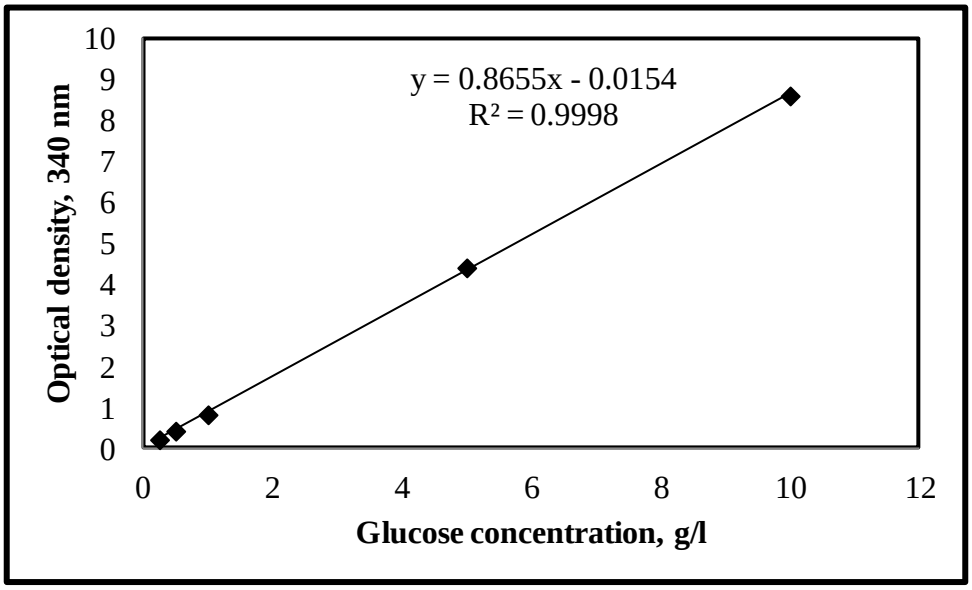

9.2 Correlation between cell mass and optical density with pellets washed 2x and dried at 60° C

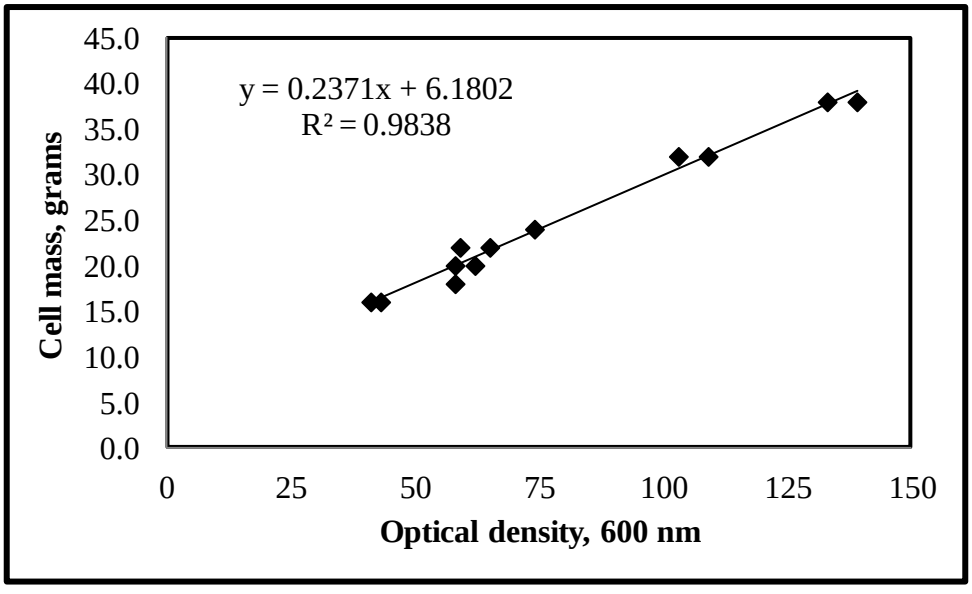

9.3 Retention times for substrates using HPLC Aminex 87N column with water as mobile phase

Substrate	Retention time (minutes)
Amino acid mix - 5mM	6.9
Mannose	7.3
Lactic	8.4
Lactose	8.9
glucose	11.2
Galactose	11.9
Xylose	12.1
Arabinose	12.97
Acetic acid	13.5
Ribose	14.37

9.4 Complete cost analysis calculations

Method	Feed	Reqd runs	total cost from labor, $	cost of feed per 1 run, $	total feed costs, $	cost of inducer per 1 run,	total inducer costs, $
Lactose 10 hrs after inoculation (st)	Glucose	25	875.00	0.78	19.51	0.95	23.75
Lactose 12 hrs after inoculation	Glucose	3	105.00	1.43	4.29	0.95	2.85
Lactose at feed start	Glucose	5	175.00	1.40	7.00	0.95	4.75
Lactose auto-induction	Glucose	3	105.00	1.75	5.25	0.95	2.85
Lactose auto-induction with pulse	Glucose	3	105.00	1.78	5.34	1.90	5.70
5 mM IPTG	Glucose	2	70.00	2.66	5.32	34.75	69.50
10 mM IPTG	Glucose	2	70.00	2.77	5.54	69.50	139.00
Lactose auto-induction	Glycerol	2	70.00	6.25	12.50	0.95	1.90
Lactose auto-induction with pulse	Glycerol	7	245.00	6.25	43.75	1.90	13.30
Lactose at feed start	Glycerol	4	140.00	2.78	11.12	1.43	5.72

Method	final volume of a single	final total volume, liters	spins required	centrifugation cost, $0.57/spin	cost of media, $4.83/liter	total costs, $	inducer costs/total costs
Lactose 10 hrs after inoculation (st)	1.2	30	15	8.55	120.75	1047.56	0.02
Lactose 12 hrs after inoculation	1.4	4.2	3	1.71	14.49	128.34	0.02
Lactose at feed start	1.4	7	4	2.28	24.15	213.18	0.02
Lactose auto-induction	1.5	4.5	3	1.71	14.49	129.30	0.02
Lactose auto-induction with pulse	1.5	4.5	3	1.71	14.49	132.24	0.04
5 mM IPTG	1.7	3.4	2	1.14	9.66	155.62	0.45
10 mM IPTG	1.6	3.2	2	1.14	9.66	225.34	0.62
Lactose auto-induction	1.4	2.8	2	1.14	9.66	95.20	0.02
Lactose auto-induction with pulse	1.4	9.8	5	2.85	33.81	338.71	0.04
Lactose at feed start	1.3	5.2	3	1.71	19.32	177.87	0.03

9.5 Reactions used for metabolic flux analysis

r1: Glucose + ATP → Glucose 6-phosphate + ADP + H^+
r2: Glucose 6-phosphate → Cell wall
r3: Glucose 6-phosphate → Fructose 6-phosphate
r4: Glucose 6-phosphate + 2 NADP + H_2O → Ribulose 5-phosphate + 2 NADPH + 2 H^+ + CO_2
r5: Ribulose 5-phosphate → Xylulose 5-phosphate
r6: Ribulose 5-phosphate → Ribose 5-phosphate
r7: Ribose 5-phosphate → AA + NA
r8: Xylulose 5-phosphate + Ribose 5-phosphate → Erythrose 4-phosphate
r9: Xylulose 5-phosphate + Erythrose 4-phosphate → Fructose 6-phosphate + Glyceraldehyde 3-phosphate
r10: Fructose 6-phosphate + ATP → 2 Glyceraldehyde 3-phosphate + ADP + H^+
r11: Fructose 6-phosphate → Cell wall
r12: Glyceraldehyde 3-phosphate → Lipids
r13: Erythrose 4-phosphate → AA
r14: 3-Phosphoglycerate → Cys + NA + Lipids
r15: Glyceraldehyde 3-phosphate + NAD^+ + P_i + ADP → 3-Phosphoglycerate (3PG) + NADH + ATP
r16: 3-Phosphoglycerate → Phosphoenolpyruvate (PEP) + H_2O
r17: Phosphoenolpyruvate → AA + Cell envelope
r18: Phosphoenolpyruvate + ADP + H^+→ Pyruvate + ATP
r19: Pyruvate → Ala, Ile, Val + Peptoglycan
r20: Acetyl-CoA → Lipids
r21: Acetyl-CoA + P_i + ADP → Acetate + ATP + CoA
r22: Pyruvate + NAD^+ + CoA-SH → NADH + H^+ + Acetyl-CoA + CO_2
r23: Acetyl-CoA + Oxaloacetate + H_2O → Citrate + CoA + H^+
r24: Citrate → Isocitrate
r25: Isocitrate + NADP → α-Ketoglutarate + NADPH + H^+ + CO_2
r26: α-Ketoglutarate → AA + NA
r27: α-Ketoglutarate → Succinate
r28: Succinate → Malate
r29: Malate → Oxaloacetate
r30: PEP + CO_2 + ATP → Oxaloacetate + ADP + P_i
r31: Malate + NAD → Pyruvate + NADH
r32: $Glucose_{external\ feed}$→$Glucose_{internal}$
r33: Lactose + ATP → Glucose 6-phosphate + ADP
r33: Galactose + ATP → Galactose 1-phosphate + ADP
r34: Pyruvate → Lysine
r35: Pyruvate → Leucine
r36: Acetyl-CoA → Leucine
r37: Oxaloacetate → Aspartate
r38: Oxaloacetate → Lysine
r39: Oxaloacetate → Asn, Ile, Met, Thr + NA
r40: 3-Phosphoglycerate → Serine
r41: 3-Phosphoglycerate → Glycine

r42: Glycerol + ATP → Glyceraldehyde 3-phosphate + ADP
r43: $Glucose_{internal}$ + ATP → Glycogen + ADP

9.6 Calculation of rho values for accumulation vector in MFA

r	precursor	component number	rho_P	rho_c_p	rho_c	rho_10%	rho_5%
8	R5P	x17	0.365	0.144	0.753	0.9195	0.90845
14	E4P	x18	1.003	0.361	0	0.4252	0.3931
18	PEP	x19	1.869	0.668	0.051	0.8392	0.77915
19	Pyruvate	x20	4.236	2.75	0.083	2.9814	2.9071
20	AcCoA	x21	0.82	0.428	2.5	2.967	2.9474
26	KG	x23	1.663	0.991	0.087	1.1447	1.1111
28	OA	x24	2.905	1.447	0.339	1.9322	1.8593
15	3PG	x25	1.275	0.874	0.616	1.5305	1.51045
13	Glyc3P	x26	0	0	0.129	0.129	0.129
12	F6P	x27	0	0	0.071	0.0709	0.0709
3	G6P	x28	0	0	0.205	0.205	0.205

The rho_10% and rho5% columns contains calculations based on a 10% or 5% production of target protein (from total protein pool), respectively.

9.7 MATLAB code for dynamic modeling

```
function [leastsqdiff, T,Y]=dynamic12hrindlactose(thekvalues,Tstar,Ystar2)

    %Tstar=xlsread('expdata.xlsx','12hrindlactose','A1:A5')
    %Ystar=xlsread('expdata.xlsx', '12hrindlactose','B1:G5')
    %k=[0.5; 0.5; 3; 1; 2]';fminsearch(@(k) mfile(k,Tstar,Ystar2),k)

    %constants
    constant(1) =   0.2;         %1/h
    constant(2) =   500;         %g/L substrate concentration in feed
    constant(3) =   5;           %cell mass at time of feed
    constant(4)=    1.05;        %volume at time of feed
    constant(5)=    1;           %oxygen used for glucose oxidation
    constant(6) =   0.15;        %g/gh, acetate reutilization
    constant(7) =   1.3;         %maximum uptake of glucose
    constant(8)=    0.04;        %maintenance
    constant(9) =   0.04;        %mol C/g carbon content in mol/g cell
    constant(10) =  1/30;        %mol C/g carbon content per gram of glucose
    constant(11) =  1.067;       %yield of acetate from oxygen
    constant(12) =  0.667;       %g/g yield of acetate on glucose
    constant(13) =  0.15;        %g/g yield of overflow cells on glucose
    constant(14) =  0.5;         %g/g yield of cells from glucose
    constant(15)=   1.067;       %yield of glucose from oxygen
    constant(16)=   0.51;        %aerobic yield coefficient
    constant(17)=   0.4;         %yield of cells from acetate
    constant(18)=   1.1;         %g/g cell/oxygen
    constant(19) =  10;          %amount of lactose added
    constant(20)=   1;           %maximum uptake of lactose

    %variables
    %thekvalues(1)= 1.5066;    %g/L fit to
    %thekvalues(2)= 1.075;    %g/L saturation constant for acetate
    %thekvalues(3)= .95;    %g/L  fit to data - eventually
    %thekvalues(4)= 0;    %g/l saturation constant for lactose
    %thekvalues(5)= 8.5915;   %the exponent on the qAg term

    initialconditions = [0.00 1.05 5.0 0 10.0 0];
    ODESolverOptions = odeset('NonNegative',[1 2 3 4 5 6]);

% First integrate system whilst there is no feed from zero to seven hours
% [T,Y]=ode23(@dynamicmodel,[0 7], initialconditions, ODESolverOptions);
% simulation data

[T,Y]=ode15s(@dynamicmodel,[0 7], initialconditions, ODESolverOptions);
        mn=size(Y);
        C1=0.006;
        C2=Y(mn(1),2);
        C3=Y(mn(1),3);
        C4=Y(mn(1),4);
        C5=Y(mn(1),5);
        C6=Y(mn(1),6);
        initialconditions2 = [C1 C2 C3 C4 C5 C6];
        mn=length(T);
```

```
        tiempo2=T(mn);

    %Second integration is from tiempo2 (about seven hours) to when
    %exponential actually starts, about 8.5 hours

[T2,Y2]=ode15s(@dynamicmodel,[tiempo2 8.5],
initialconditions2,ODESolverOptions);
        mn=size(Y2);
        C1=Y2(mn(1),1);
        C2=Y2(mn(1),2);
        C3=Y2(mn(1),3);
        C4=Y2(mn(1),4);
        C5=Y2(mn(1),5);
        C6=Y2(mn(1),6);
        initialconditions3 = [C1 C2 C3 C4 C5 C6];
        mn=length(T2);
        tiempo3=T2(mn);

    %Third integration is from tiempo3 during exponential

[T3,Y3]=ode15s(@dynamicmodel,[tiempo3 12], initialconditions3,
ODESolverOptions);
        mn=size(Y3);
        C1=Y3(mn(1),1);
        C2=Y3(mn(1),2);
        C3=Y3(mn(1),3);
        C4=Y3(mn(1),4);
        C5=Y3(mn(1),5);
        C6=10;
        initialconditions4=[C1 C2 C3 C4 C5 C6];
        mn=length(T3);
        tiempo4=T3(mn);

[T4,Y4]=ode15s(@dynamicmodel,[tiempo4,22], initialconditions4,
ODESolverOptions);
    compositeT=vertcat(T,T2,T3,T4);
    compositeY=vertcat(Y,Y2,Y3,Y4);

    T=compositeT;
    Y=compositeY;

    % use interpl to map T to Tstar
    % find the values in Y to pair with Ystar
    % difference matrix is then created

    Yinterp=simplesample(T4,Y4,Tstar,3);
    thekvalues
    Difference=abs((Ystar2-Yinterp)).^2

leastsqdiff=sum(Difference(:,1)+Difference(:,2)+Difference(:,3)+Difference(:,
4)+Difference(:,5)+Difference(:,6))
```

```
  function dy = dynamicmodel(t,y);
        dy = zeros(6,1); % a column vector

        %Feed equation
        if t<8.5
            dy(1)=0;
        else
            dy(1)=0.19*y(1)
        end

        %Volume equation
        dy(2)=y(1);

        %Biomass equation
        dy(3)=(.125-y(1)/y(2))*y(3);

        %Acetate equations
            if t<8.5
        dy(4)=0
            else
        qAg=(y(5)/(y(5)+thekvalues(2)))^thekvalues(5);
        qAc=constant(6)*(y(4)/(y(4)+thekvalues(2)));
        dy(4)=0.05*y(3)-qAc*y(3)-(y(1)/y(2))*y(4);
        end


       %Glucose equation; thekvalues3 = uptake of glucose when acetate is
      present;  thekvalues1 = saturation constant for glucose

        dy(5)=(y(1)/y(2))*(constant(2)-y(5))-y(5)/(y(5)+thekvalues(1)))*y(3);

        %lactose equation
        if t<12
            dy(6)=0;
        else
        dy(6)=y(1)/y(2)*(constant(19)-y(6))-
      (constant(20)/(1+(y(6)/thekvalues(4))))*
        (y(5)/(y(5)+thekvalues(4)))*y(3);
        end

    end
end
```

9.8 MATLAB code for metabolic flux analysis

```
function [objrates, fval, exitflag, output, lambda]=mfalinprogshort
%autoinduced with lactose and glycerol feed
%construct the stoichiometric matrix A

%Aeq(1,31)=1;
Aeq(1,32)=1;
Aeq(1,1)=-1;
Aeq(2,1)=1;
Aeq(2,32)=1;
Aeq(2,3)=-1;
Aeq(2,4)=-1;
Aeq(2,5)=-1;
Aeq(3,5)=1;
Aeq(3,6)=-1;
Aeq(3,7)=-1;
Aeq(4,7)=1;
Aeq(4,8)=-1;
Aeq(4,9)=-1;
Aeq(5,6)=1;
Aeq(5,9)=-1;
Aeq(5,10)=-1;
Aeq(6,4)=1;
Aeq(6,9)=1;
Aeq(6,10)=1;
Aeq(6,11)=-1;
Aeq(6,12)=-1;
Aeq(7,9)=1;
Aeq(7,14)=-1;
Aeq(7,10)=-1;
Aeq(8,11)=2;
Aeq(8,10)=1;
Aeq(8,13)=-1;
Aeq(8,16)=-1;
Aeq(8,34)=1;
Aeq(9,16)=1;
Aeq(9,17)=-1;
Aeq(9,15)=-1;
Aeq(10,17)=1;
Aeq(10,18)=-1;
Aeq(10,31)=-1;
Aeq(10,19)=-1;
Aeq(11,31)=1;
Aeq(11,19)=1;
Aeq(11,20)=-1;
Aeq(11,23)=-1;
Aeq(11,30)=-1;
Aeq(12,23)=1;
Aeq(12,21)=-1;
Aeq(12,22)=-1;
Aeq(12,24)=-1;
Aeq(13,24)=1;
Aeq(13,25)=-1;
Aeq(14,25)=1;
Aeq(14,26)=-1;
```

```
Aeq(15,26)=1;
Aeq(15,27)=-1;
Aeq(15,28)=-1;
Aeq(16,28)=1;
Aeq(16,30)=1;
Aeq(16,24)=-1;
Aeq(16,29)=-1;
Aeq(17,8)=1;
Aeq(18,14)=1;
Aeq(19,18)=1;
Aeq(20,20)=1;
Aeq(21,21)=1;
Aeq(22,22)=1;
Aeq(23,27)=1;
Aeq(24,29)=1;
Aeq(25,15)=1;
Aeq(26,13)=1;
Aeq(27,12)=1;
Aeq(28,3)=1;
Aeq(31,32)=2;
%Aeq(32,31)=1;
Aeq(33,5)=2;
Aeq(33,26)=1;

%for glycerol feed
Aeq(34,34)=1;

%Information for accumulation vector, X
%calculation of rho values are based on TP mass 10% of total protein mass

    D = 0.13;
    %Cglucose = 46.1;
    %Cacetate = 53.12;
    %Clactose = 6.1;
    %Caa = 0;
    biox = 28.5;
    rho8 = 0.9195;
    rho14 = 0.4252;
    rho18 = 0.8392;
    rho20 = 2.9814;
    rho21 = 2.97;
    rho27 = 1.1447;
    rho29 = 1.9322;
    rho15 = 1.5305;
    rho13 = 0.129;
    rho12 = 0.0709;
    rho3 = 0.205;
    rho_lys_pyr = 0.364;
    rho_leu_pyr = 0.9344;
    rho_leu_accoa = 0.4672;
    rho_lys_oa = 0.364;
    rho_asp_oa = 0.2671;
    rho_gly_3pg = 0.5944;
    rho_ser_3pg = 0.2323;
```

```
beq(1,1) = 0;
beq(2,1) = 0;
beq(3,1) = 0;
beq(4,1) = 0;
beq(5,1) = 0;
beq(6,1) = 0;
beq(7,1) = 0;
beq(8,1) = 0;
beq(9,1) = 0;
beq(10,1) = 0;
beq(11,1) = 0;
beq(12,1) = 0;
beq(13,1) = 0;
beq(14,1) = 0;
beq(15,1) = 0;
beq(16,1) = 0;
beq(17,1) = rho8*D;
beq(18,1) = rho14*D;
beq(19,1) = rho18*D;
beq(20,1) = rho20*D;
beq(21,1) = rho21*D;
beq(22,1) = 1.09/biox;
beq(23,1) = rho27*D;
beq(24,1) = rho29*D;
beq(25,1) = rho15*D;
beq(26,1) = rho13*D;
beq(27,1) = rho12*D;
beq(28,1) = rho3*D;
beq(31,1) = 0.35/biox;
beq(32,1) = 0/biox;
beq(33,1) = 18*D;

%With glycerol feed add the following:
Cglyc =204.4;
beq(34,1)=Cglyc*D/biox;

La=length(Aeq)
Lb=length(beq)

objective(1)=0;
objective(2)=0;
objective(3)=1;
objective(4)=0;
objective(5)=0;
objective(6)=0;
objective(7)=0;
objective(8)=1;
objective(9)=0;
objective(10)=0;
objective(11)=0;
objective(12)=1;
objective(13)=1;
objective(14)=1;
objective(15)=1;
objective(16)=0;
```

```
objective(17)=0;
objective(18)=1;
objective(19)=0;
objective(20)=1;
objective(21)=1;
objective(22)=0;
objective(23)=0;
objective(24)=0;
objective(25)=0;
objective(26)=0;
objective(27)=1;
objective(28)=0;
objective(29)=1;
objective(30)=0;
objective(31)=0;
objective(32)=0;
objective(33)=0;
objective(34)=0;

objective=transpose(objective);
objective=-1*objective;


A=[];
b=[];
lb=zeros(41);
ub=[];

[objrates,fval,exitflag, output, lambda]=linprog(objective,A,b,Aeq,beq,lb,ub)
```

9.9 Percent error for simulation versus experimental ratios (yield from ATP versus biomass). Highlighted cells are those with percent error less than or equal to 20%.

feed	experiment	12 hr lac	5 mM IPTG	10 mM IPTG	AI w/pulse	Lac at feed start	AI	Glycerol		
								AI	AI w/pulse	15 g lac
Glucose	12 hr lac	--	0.2	2.18	0.44	1.05	0.93	3.53	0.88	0.84
	5 mM IPTG	0.15	--	1.57	0.54	0.68	0.56	2.64	0.55	0.48
	10 mM IPTG	0.57	0.61	--	0.82	0.35	0.39	0.45	0.41	0.8
	AI w/pulse	0.78	1.21	1.02	--	2.63	2.46	7.44	2.47	0.18
	Lac at feed start	0.56	0.41	0.61	0.73	--	0.05	1.17	0.18	0.59
	AI	0.56	0.2	0.64	0.71	0.15	--	1.42	0.26	0.68
Glycerol	AI (gly)	0.78	0.48	0.3	0.88	0.65	0.57	--	0.56	0.83
	AI w/pulse (gly)	0.47	0.36	0.67	0.71	0.14	0.02	1.41	--	0.7
	15 g lac (gly)	0.56	0.92	4	0.12	1.59	2.18	6.22	2.00	--